UNIVERSIDADE DE LISBOA

FACULDADE DE FARMÁCIA

NEW INSIGHTS INTO THE STRUCTURE AND FUNCTION OF HUMAN PHENYLALANINE HYDROXYLASE:

INTERALLELIC COMPLEMENTATION, PROTEIN MISFOLDING AND MECHANISM OF CATALYTIC ACTIVATION

João Paulo Travassos Leandro

DOUTORAMENTO EM FARMÁCIA

(Bioquímica)

2011

UNIVERSIDADE DE LISBOA

FACULDADE DE FARMÁCIA

NEW INSIGHTS INTO THE STRUCTURE AND FUNCTION OF HUMAN PHENYLALANINE HYDROXYLASE:

INTERALLELIC COMPLEMENTATION, PROTEIN MISFOLDING AND MECHANISM OF CATALYTIC ACTIVATION

João Paulo Travassos Leandro

Promotors: Prof. Doutora Ana Paula Costa dos Santos Peralta Leandro

Prof. Doutora Maria Isabel Ginestal Tavares de Almeida

Prof. emeritus Torgeir Flatmark

DOUTORAMENTO EM FARMÁCIA

(Bioquímica)

2011

NEW INSIGHTS INTO THE STRUCTURE AND FUNCTION OF HUMAN PHENYLALANINE HYDROXYLASE: INTERALLELIC COMPLEMENTATION, PROTEIN MISFOLDING AND MECHANISM OF CATALYTIC ACTIVATION

UMA NOVA VISÃO SOBRE A ESTRUTURA E FUNÇÃO DA FENILALANINA HIDROXILASE HUMANA: COMPLEMENTAÇÃO INTERALÉLICA, MISFOLDING PROTEICO E MECANISMO DE ACTIVAÇÃO CATALÍTICA

Dissertação apresentada à Faculdade de Farmácia da Universidade de Lisboa, para prestação de provas de doutoramento em Farmácia, na especialidade de Bioquímica

João Paulo Travassos Leandro

Lisboa

2011

The studies presented in this thesis were performed at the Department of Biomedicine, University of Bergen under the supervision of Professor Torgeir Flatmark and at the Research Institute for Medicines and Pharmaceutical Sciences (iMed.UL), Faculty of Pharmacy, University of Lisbon under the supervision of Professor Ana Paula Costa dos Santos Peralta Leandro and Professor Maria Isabel Ginestal Tavares de Almeida.

João Paulo Travassos Leandro was the recipient of a Ph.D. fellowship (SFRH/BD/19024/2004) from Fundação para a Ciência e a Tecnologia, Lisbon, Portugal (co-funded by POCI 2010 and FSE).

De acordo com o disposto no ponto 1 do artigo nº 40 do Regulamento de Estudos Pós-Graduados da Universidade de Lisboa, deliberação nº 961/2003, publicado em Diário da República – II Série nº 153 – 5 de Julho de 2003, o Autor desta dissertação declara que participou na concepção e execução do trabalho experimental, interpretação dos resultados obtidos e redacção dos manuscriptos.

Ciência.Inovação 2010
Programa Operacional Ciência e Inovação 2010
MINISTÉRIO DA CIÊNCIA, TECNOLOGIA E ENSINO SUPERIOR
UNIÃO EUROPEIA
Fundo Social Europeu

Aos meus pais e irmãs.

To my parents and sisters.

Table of contents

Acknowledgements

First of all I would like to express my sincere gratitude to my supervisors Professor Paula Leandro, Professor Isabel Tavares de Almeida and Professor Torgeir Flatmark for their valuable guidance, support, enthusiasm and encouragement throughout these years.

I would also like to thank my co-authors Cátia Nascimento, Jaakko Saraste, Nina Simonsen, Anne Jorunn Stokka and Ole Andersen for an inspiring cooperation. Ali Sepulveda Munõz and Randi Svebak are specially thanked for their expert technical assistance.

Moreover, I would like to thank my friends and colleagues at the Faculty of Pharmacy and at the Department of Biomedicine for creating such a friendly environment and for their helpfulness and incentive.

Finally, I am very grateful to my friends and family for their unconditional support and love.

Summary

Phenylketonuria (PKU) is an autosomal recessive human inborn error of metabolism caused by dysfunction of the liver homotetrameric/homodimeric enzyme phenylalanine hydroxylase (hPAH), which results in increased levels of L-phenylalanine (L-Phe) in the blood and if untreated causes severe mental retardation. More than 550 mutations have been identified to date, with three quarters of PKU patients being compound heterozygous, leading to a high phenotypic diversity. Inconsistencies in some genotype-phenotype correlations with more severe phenotypes than the ones expected and lack of response to cofactor ((6*R*)-L-*erythro*-5,6,7,8-tetrahydrobiopterin (BH_4)) supplementation in patients with two known responsive mutations have raised the possibility of interallelic complementation (IC). We have shown that mutations involved in inconsistencies (I65T, R261Q, R270K and V338M) display a negative IC, with reduced enzymatic activity when mimicking the heteroallelic state of compound heterozygous PKU patients. Moreover, using wild-type and truncated mutants forms we were able to isolate an heterotetrameric hPAH form, WT/ΔN102-hPAH, that resulted from the assembly of two homodimers, since heterodimers did not form. This hybrid species revealed kinetic and regulatory properties that were influenced by interactions between the two homodimers within the heterotetramer.

Phenylketonuria is considered a protein misfolding disease with loss of function, as a large number of point mutations result in decreased stability, aggregation and accelerated protein degradation. The deleterious effects seem to particularly affect the *R*-domain of hPAH that contains an ACT module found in a large number of multimeric proteins with complex allosteric regulation. Here we have studied the effect of the missense mutation G46S in the *R*-domain that promotes self-association and fibril formation *in vitro*. The mutation seems to extend α-helix 1 and thus perturbs the α-β sandwich of the ACT module in the *R*-domain. We were able to modulate *in vitro* the mutant self-association process by chemical, pharmacological and molecular chaperones. The mutant G46S dimer also self-associates forming fibrils and an enhancement in the self-association was observed in the presence of WT dimer, due to hybrid formation (WT/G46S). However, only amorphous aggregates were observed and L-Phe binding precludes the self-association of the WT dimer, since the wild-type and mutant tetramer ↔

dimer equilibrium responds differently to the presence of L-Phe, thus explaining the phenotype of WT/G46S carriers, as none of the PKU heterozygous shows any clinical phenotype.

The *R*-domain of full-length hPAH is particularly unstable and when isolated it self-associates even in its WT form. This self-association was inhibited stereospecifically by L-Phe, pointing to a regulatory binding site that has been disputed over the years. It seems now evident that the isolated *R*-domain is able to bind L-Phe as we and other groups have observed, but the full-length enzyme has lost this ability with the simultaneously acquiring of complex regulatory mechanisms.

One of these regulatory mechanisms comprises the catalytic activation by the substrate. In the resting state hPAH is inhibited by the cofactor BH_4. Binding of L-Phe triggers a series of conformational changes that resulted in the activation of the enzyme. Crystal structures of hPAH with bound cofactor and substrate have revealed a large displacement of Tyr138 in a highly flexible loop, from a surface position to a partial buried position at the active site upon substrate binding. Here we have found an important functional role for Tyr138 displacement in positioning substrates for catalysis and in the L-Phe triggered conformational isomerization that results in catalytic activation of the enzyme.

Keywords: human phenylalanine hydroxylase; phenylketonuria; interallelic complementation; hybrid protein; misfolding; self-association; ACT domain; substrate activation.

Sumário

A fenilcetonúria (PKU; OMIM 261600) é uma doença autossómica recessiva do metabolismo, causada por uma deficiente actividade da enzima homotetramérica/homodimérica fenilalanina hidroxilase (hPAH; EC 1.14.16.1). A enzima existe maioritariamente nos hepatócitos, onde é responsável pela hidroxilação da L-fenilalanina (L-Phe) em L-tirosina (L-Tyr) na presença do cofactor (6*R*)-L-*eritro*-5,6,7,8-tetrahidrobiopterina (BH_4) e oxigénio. Nesta reacção ocorre simultaneamente a hidroxilação do cofactor, que posteriormente é regenerado pela acção da enzima dihidrobiopterina reductase. A fenilalanina hidroxilase é responsável pela homeostase da L-Phe, de forma a impedir o aumento dos níveis deste aminoácido, que são tóxicos para o cérebro, e simultaneamente evitar a sua completa depleção, comprometendo a síntese proteica. Deste modo, a enzima sofre uma regulação complexa, que envolve a activação catalítica pelo substrato L-Phe, com cooperatividade positiva e fosforilação do resíduo Ser16. A enzima é também regulada pelo cofactor BH_4, que provoca a sua inibição e estabilização num estado inactivo, na ausência de L-Phe.

Mais de 550 mutações foram identificadas no gene *PAH* humano, resultando em proteínas mutantes com baixa actividade e/ou estabilidade e consequente aparecimento da doença. Esta é caracterizada pelo aumento dos níveis de fenilalanina plasmática (hiperfenilalaninémia; HPA) e pela diminuição do teor de tirosina circulante. Na ausência de tratamento, a PKU resulta em atraso mental profundo. A terapêutica actual consiste na detecção da doença através do rastreio neonatal e na implementação imediata de uma dieta pobre em L-Phe, com controlo da tolerância ao aminoácido, a qual tem de ser mantida para a vida. Recentemente verificou-se que algumas mutações respondem à administração oral do cofactor BH_4 (suplementação com BH_4), especialmente as formas menos graves da doença, permitindo o aumento da actividade enzimática e consequente relaxamento da dieta. Este encontra-se já comercialmente disponível na forma sintética do isómero 6*R* do BH_4 (cloreto de sapropterina, Kuvan™).

Devido à heterogeneidade da doença, mais de 75% dos doentes são heterozigóticos compostos (portadores de duas diferentes mutações). Em alguns destes doentes foram verificadas inconsistências tanto ao nível da correlação genotipo-fenótipo do récem-nascido HPA, quer ao nível da resposta à suplementação com BH_4. A correlação genótipo/fenótipo bioquímico tem sido efectuada com base na actividade residual prevista (PRA), calculada pela média das

actividades determinadas *in vitro* de cada uma das proteínas mutantes associadas ao genótipo do doente. Em alguns doentes heterozigóticos compostos foram descritos fenótipos mais severos do que os previstos pela determinação da PRA. Particularmente, correlações genótipo-fenótipo em doentes HPA Portugueses envolvendo as mutações I65T, R261Q, R270K e V338M revelaram inconsistências.

No que diz respeito à suplementação com BH_4, alguns heterozigóticos compostos não revelaram uma resposta positiva ao tratamento, embora as duas mutações presentes no seu genótipo se encontrem descritas como respondendo ao BH_4 em doentes homozigóticos para as mesmas. Curiosamente, algumas dessas mutações estão relacionadas com as inconsistências detectadas ao nível de correlações genótipo-fenótipo (e.g. I65T e R261Q). De forma a explicar estas observações clínicas foi proposta a existência de fenómenos de complementação inter-alélica, a qual terá como base interacções entre as diferentes subunidades mutantes da enzima multimérica, originando uma proteína com menor actividade/estabilidade do que a prevista pela PRA (neste caso uma complementação inter-alélica negativa).

De forma a estudar este fenómeno desenvolvemos sistemas de expressão procariótica de forma a produzir e isolar os possíveis híbridos. Utilizando um sistema de expressão dupla foi possível reproduzir bioquimicamente a situação de um heterozigótico composto (tetrâmeros, heterotetrâmeros e dímeros) com as combinações das mutações descritas anteriormente. Todas estas mutações revelaram uma diminuição da actividade enzimática quando comparada com a prevista pela PRA, demonstrando a existência de fenómenos de complementação inter-alélica negativa. Com a utilização da forma selvagem (WT) e mutantes de deleção num sistema bicistrónico foi possível isolar pela primeira vez um híbrido da hPAH, neste caso um heterotetrâmero WT/ΔN102-hPAH. Nestes estudos, a existência de heterodímeros foi excluída, explicando o facto da hPAH selvagem ser isolada como tetrâmeros e dímeros, mas nunca como monómeros. O heterotetrâmero isolado apresenta propriedades cinéticas e reguladoras que demonstram a existência de interacções entre os dois dímeros na proteína híbrida. Estes resultados foram corroborados pela formação de heterotetrâmeros a partir de homodímeros pré-formados da forma selvagem e de um mutante com uma elevada propensão para agregar (WT/G46S). A presença do mutante leva à agregação da proteína WT, processo este dependente da presença de L-Phe, pois o equilíbrio entre as diferentes formas oligoméricas responde de forma diferente à presença do substrato.

A vasta maioria das mutações que afectam a proteína hPAH levam a uma diminuição da eficiência do *folding* proteico e/ou na redução da estabilidade da enzima, resultando na sua agregação e/ou rápida degradação. O domínio regulador da enzima revela uma reduzida estabilidade e o seu envolvimento no processo de *misfolding* tem sido evidenviado nos últimos anos. O estudo da mutação G46S, localizada no domínio regulador e que resulta na forma mais grave da doença, permitiu avaliar o processo de *misfolding* de um mutante envolvendo este domínio. Em estudos *in vitro*, a proteína mutante agrega, levando à formação de fibrilas. Este processo foi inibido parcialmente pela utilização de glicerol (chaperone químico), 3-amino-2-benzil-7-nitro-4-(2-quinolil)-1,2-dihidroisoquinolina-1-ona (um chaperone farmacológico recentemente proposto) e pelos chaperones moleculares Hsp70/Hsp40 e Hsp90.

O domínio regulador da hPAH apresenta um módulo ACT, que ocorre em várias enzimas multiméricas com complexos modos de regulação. Os módulos ACT formam normalmente dímeros e estão envolvidos na ligação de aminoácidos nas interfaces entre as duas subunidades. A instabilidade do domínio regulador da hPAH, onde não é possível existir a formação de dímeros entre os módulos ACT, foi também analisada pelo estudo deste na sua forma isolada. Curiosamente, tanto o domínio regulador mutante como o selvagem revelam tendência para agregar. No entanto, a agregação é inibida estereo-especificamente na forma selvagem pela fenilalanina, indicando que o domínio regulador na forma isolada consegue ligar o substrato, embora na enzima *full-length*, essa capacidade tenha sido perdida.

A ligação do substrato L-Phe ao sítio activo da enzima resulta num processo reversível de isomerização que ocorre numa escala de segundos a minutos. Este processo converte a enzima de um estado de baixa actividade/afinidade para um estado de alta actividade/afinidade, resultando na activação da enzima e na existência de cooperatividade positiva. Dado a inexistência da estrutura cristalográfica da enzima *full-length*, não foi possível até ao momento estabelecer o circuito de alterações conformacionais que levam à activação da enzima. No entanto, a existência de estruturas proteicas de formas truncadas do domínio catalítico da enzima em complexos binários (hPAH·(Fe(II)-cofactor) e ternários (hPAH·(Fe(II)-cofactor-substrato) permitiram verificar a existência de alterações conformacionais ao nível do domínio catalítico. Uma dessas alterações envolve o reposicionamento de um *loop* flexível da superfície da enzima para uma posição mais hidrofóbica no sítio activo da proteína. A maior alteração envolve o resíduo Tyr138, cuja cadeia lateral sofre uma deslocação de ~21 Å. De forma a compreender a função

desempenhada por este *loop* e em particular o papel desempenhado pela Tyr138, o resíduo foi mutado e o seu efeito avaliado ao nível do impacto na actividade enzimática e eficiência de *coupling* (co-hidroxilação de substrato e cofactor), bem como na isomerização da proteína. Estes resultados permitiram identificar que a Tyr138 desempenha um papel ao nível do reposicionamento dos substratos para catálise, mas sem afectar o *coupling* da reacção. No entanto, o resíduo Tyr138 também desempenha um papel regulador na isomerização conformacional desencadeada pela ligação do substrato no sítio activo, preenchendo mais uma lacuna no objectivo de compreender o processo de activação catalítica na fenilalanina hidroxilase humana.

Palavras-chave: fenilalanina hidroxilase humana, fenilcetónuria, complementação inter-alélica, proteínas híbridas, *misfolding*, polimerização, domínio ACT, activação catalítica.

List of publications

I. Leandro J., Nascimento C., Tavares de Almeida I., Leandro P. (2006) Co-expression of different subunits of human phenylalanine hydroxylase: evidence of negative interallelic complementation. *Biochim. Biophys. Acta, Mol. Basis Dis.* 1762, 544-550.

II. Leandro J., Leandro P., Flatmark T. (2011) Heterotetrameric forms of human phenylalanine hydroxylase: co-expression of wild-type and mutant forms in a bicistronic system. *Biochim. Biophys. Acta, Mol. Basis Dis.* 1812, 602-612.

III. Leandro J., Simonsen N., Saraste J., Leandro P., Flatmark T. (2011) Phenylketonuria as a protein *misfolding* disease: The mutation pG46S in phenylalanine hydroxylase promotes self-association and fibril formation. *Biochim. Biophys. Acta, Mol. Basis Dis.* 1812, 106-120.

IV. Leandro J., Saraste J., Leandro P., Flatmark T. (2011) Stereospecific binding of L-phenylalanine to the isolated regulatory domain of human phenylalanine hydroxylase. *Submitted.*

V. Stokka A.J., Leandro J., Andersen O.A., Leandro P., Flatmark T. (2011) Structure-function analysis of human phenylalanine hydroxylase – The functional role of Tyr138 in the flexible surface/active site loop. *Submitted.*

Related publications not include in the PhD thesis

VI. Nascimento C., Leandro J., Tavares de Almeida I., Leandro P. (2008) Modulation of the activity of newly synthesized human phenylalanine hydroxylase mutant proteins by low-molecular-weight compounds. *Protein J.* 27, 392-400.

VII. Nascimento C., Leandro J., Lino P.R., Ramos L., Almeida A.J., de Almeida I.T., Leandro P. (2010) Polyol additives modulate the *in vitro* stability and activity of

recombinant human phenylalanine hydroxylase. *Appl. Biochem. Biotechnol.* 162, 192-207.

Abbreviations

4a-OH-BH_4	tetrahydropterin-4a-carbinolamine
5-OH-Trp	5-hydroxy-tryptophan
6MPH_4	6-methyl-5,6,7,8-tetrahydropterin
6-PTPS	6-pyruvoyl-tetrahydropterin synthase
AAAH	aromatic amino acid hydroxylase
ADHD	attention-deficit/hyperactive disorder
BBB	blood-brain barrier
BH_2	L-*erythro*-7,8-dihydrobiopterin
BH_4	(6*R*)-L-*erythro*-5,6,7,8-tetrahydrobiopterin
C	catalytic
CePAH	*Caenorhabditis elegans* phenylalanine hydroxylase
CvPAH	*Chromobacterium violaceum* phenylalanine hydroxylase
DHFR	dihydrofolate reductase
DHPR	dihydropteridine reductase
DMPH_4	6,7-dimethyl-5,6,7,8-tetrahydropterin
DRP	L-DOPA-responsive dystonia
DTF	density functional theory
GI	gastrointestinal
GTP	guanosine triphosphate
GTP-CH	GTP cyclohydrolase
HPA	hyperphenylalaninemia
hPAH	human phenylalanine hydroxylase
hTH	human tyrosine hydroxylase
hTPH	human tryptophan hydroxylase
HXMS	hydrogen/deuterium exchange mass spectrometry
IARS	intrinsic autoregulatory sequence
IC	interallelic complementation
L-DOPA	L-3,4-dihydroxyphenylalanine
LNAA	large, neutral amino acid

L-Phe	L-phenylalanine
L-Trp	L-tryptophan
L-Tyr	L-tyrosine
MBP	maltose binding protein
MHP	mild hyperphenylalaninemia
NADH	nicotinamide adenine dinucleotide (reduced form)
n_H	hill coefficient
NLE	L-norleucine
O	oligomerization
PAH	phenylalanine hydroxylase
PAL	phenylalanine ammonia lyase
PCD	pterin-4a-carbinolamine dehydratase
PKA	cyclic AMP dependent protein kinase A
PKU	phenylketonuria
PRA	predicted residual activity
q-BH_2	quinonoid dihydrobiopterin
R	regulatory
rPAH	rat phenylalanine hydroxylase
rTH	rat tyrosine hydroxylase
SMBD	small molecule-binding domain
SNP	single nucleotide polymorphism
SPR	surface plasmon resonance
SR	sepiapterin reductase
TH	tyrosine hydroxylase
THA	3-(2-thienyl)-L-alanine
TMAO	trimethylamine *N*-oxide
TPH1	tryptophan hydroxylase 1
TPH2	tryptophan hydroxylase 2
WT	wild-type

Part I

General Introduction

1. The aromatic amino acid hydroxylase (AAAH) family

The aromatic amino acid hydroxylase (AAAHs) family comprises the structurally and functionally related enzymes phenylalanine hydroxylase (PAH; EC 1.14.16.1), tyrosine hydroxylase (TH; EC 1.14.16.2) and tryptophan hydroxylase 1 and 2 (TPH1 and TPH2, EC 1.14.16.4), that use the (6*R*)-L-*erythro*-5,6,7,8-tetrahydrobiopterin (BH_4) as cofactor. These enzymes are non-heme iron mono-oxygenases that *in vivo* catalyze the hydroxylation of the respective aromatic amino acid L-phenylalanine (L-Phe), L-tyrosine (L-Tyr) and L-tryptophan (L-Trp). The three enzymes share a high degree of sequence homology and domain organization, namely an N-terminal regulatory domain (*R*-domain), a catalytic core domain (*C*-domain) and a C-terminal oligomerization domain (*O*-domain) (Fig. 1). They also present an overall common catalytic mechanism involving the non-heme iron coordinated to a 2-His-1-carboxylate facial triad, the cofactor BH_4 and dioxygen (Kappock and Caradonna 1996; Fitzpatrick 1999; Flatmark and Stevens 1999; Fitzpatrick 2000; Fitzpatrick 2003; Teigen *et al.* 2007) (Fig. 2). The catalytic reaction involves the incorporation of one oxygen atom into the amino acid substrate, while the other oxygen atom is incorporated into the cofactor BH_4, yielding the corresponding hydroxylated amino acid and pterin 4a-carbinolamine (4a-OH-BH_4), respectively. Although BH_4 is usually referred to as a cofactor, it is in fact a co-substrate being hydroxylated during catalysis, and needs to be regenerated by other enzymes. The resulting compound 4a-OH-BH_4 has to be rapidly converted back to the reduced active form BH_4, since a spontaneous non-enzymatic conversion can occur (e.g. formation of primapterin) (Curtius *et al.* 1990; Davis *et al.* 1991). BH_4 recycling occurs through the BH_4-regeneration system which involves the enzyme pteridin 4a-carbinolamine dehydratase (PCD) and the NADH-dependent enzyme dihydropteridine reductase (DHPR), via the intermediate quinonoid dihydrobiopterin (q-BH_2). This compound can also isomerize to L-*erythro*-7,8-dihydrobiopterin (BH_2) which is converted back to BH_4 by dihydrofolate reductase (DHFR) (Kappock and Caradonna 1996) (Fig. 2).

BH_4 has a ubiquitous distribution in higher organisms, being an essential cofactor in several enzymatic reactions other than those involving AAAHs (Thöny *et al.* 2000). The pathway for the *de novo* synthesis of BH_4 from the precursor guanosine triphosphate (GTP) includes the enzymes GTP cyclohydrodrolase (GTP-CH), 6-pyruvoyl-tetrahydropterin synthase (6-PTPS) and sepiapterin reductase (SR) (Thöny *et al.* 2000) (Fig. 2).

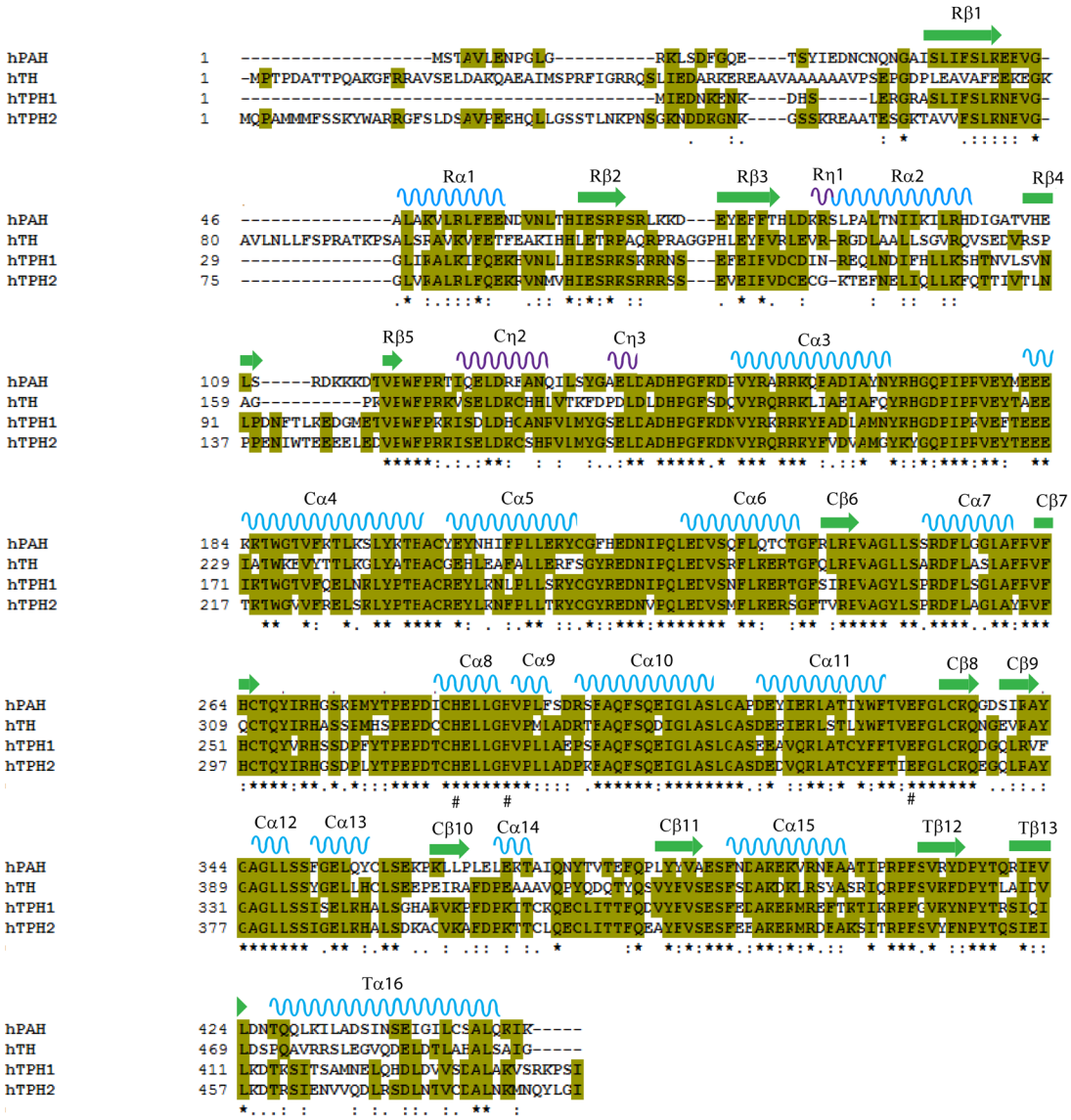

Figure 1. Sequence alignment of human phenylalanine hydroxylase (hPAH) (SWISS-PROT P00439), human tyrosine hydroxylase (hTH) isoform 2 (SWISS-PROT P07101-3), human tryptophan hydroxylase 1 (hTPH1) (SWISS-PROT P17752) and human tryptophan hydroxylase 2 (hTPH2) (SWISS-PROT Q8IWU9). The sequences were aligned using Clustal W and the figure was prepared using BioEdit (Hall 1999). The secondary structure assignment of hPAH is represented above the sequence and was obtained from the coordinates of the full-length PAH model constructed from rPAH (PDB ID: 1PHM) and hPAH (2PAH) crystal structures, and shown as α-helices (blue), 3/10-helices (purple) and β-strands (green). The symbols below the sequences correspond to clustal consensus results with asterisks indicating identity, and two dots or one dot denoting homolog properties, depending on the degree of similarity of the residues. Residues involved in iron coordination at the active site are marked with #.

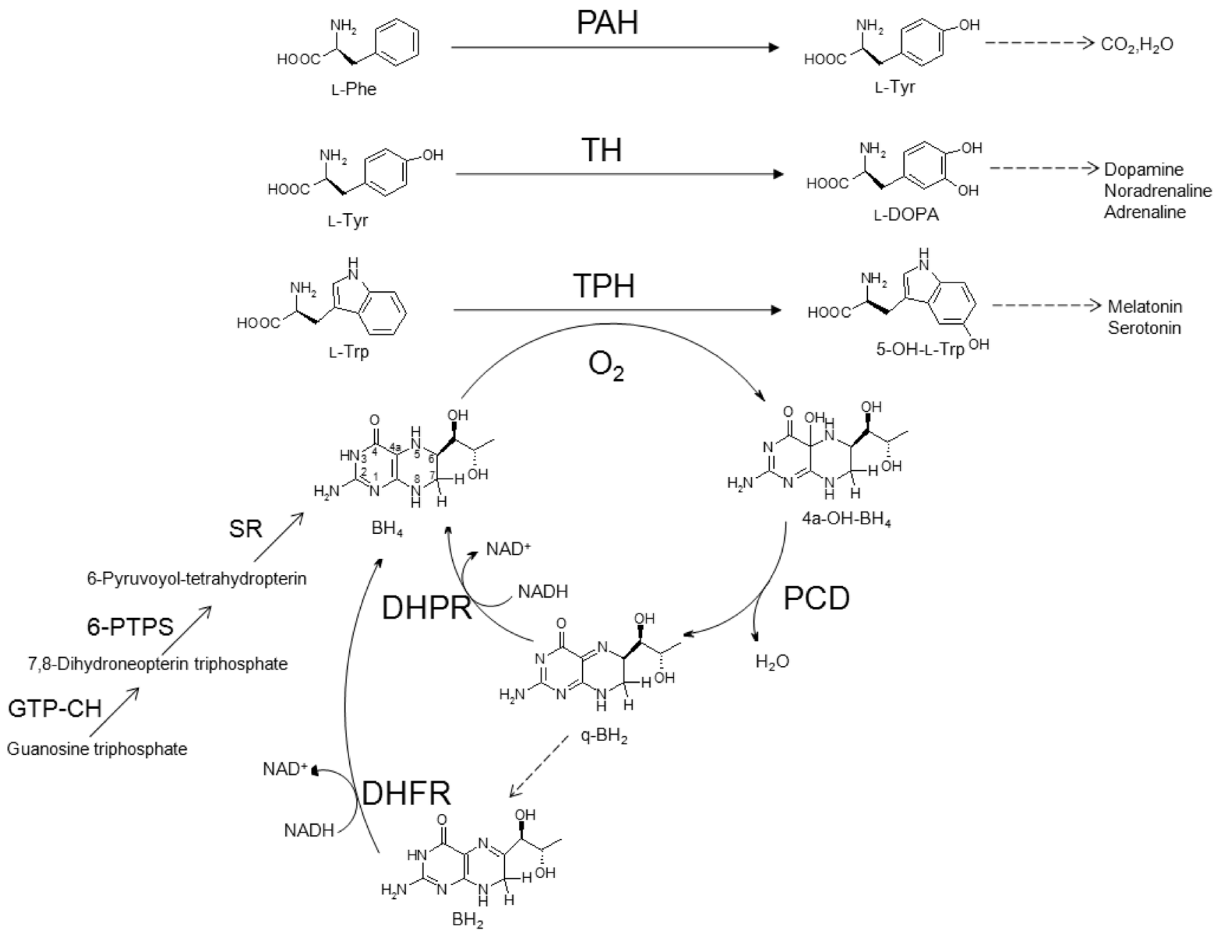

Figure 2. Overview of the BH_4-dependent aromatic amino acid hydroxylase system. Phenylalanine hydroxylase (PAH), tyrosine hydroxylase (TH) and tryptophan hydroxylase (TPH) catalyze the hydroxylation of the aromatic amino acids L-phenylalanine (L-Phe), L-tyrosine (L-Tyr) and L-tryptophan (L-Trp), respectively, using dioxygen and the cofactor (6*R*)-L-*erythro*-5,6,7,8-tetrahydrobiopterin (BH_4). The BH_4 biosynthetic and regeneration pathways are also shown. The regeneration system involves the dehydratation of tetrahydropterin-4a-carbinolamine (4a-OH-BH_4) by the enzyme pteridin 4a-carbinolamine dehydratase (PCD) and the conversion of the quinonoid dihydrobiopterin (q-BH_2) into BH_4, by the NADH-dependent enzyme dihydropteridine reductase (DHPR). The q-BH_2 form can alternatively isomerize to BH_2, which is reduced back to BH_4 by the enzyme dihydrofolate reductase (DHFR). The *de novo* BH_4 biosynthetic pathway from guanosine triphosphate involves the enzymes GTP cyclohydrolase (GTP-CH), 6-pyruvoyl-tetrahydropterin synthase (6-PTPS) and sepiapterin reductase (SR).

The AAAHs also display some distinct characteristics such as cellular localization, substrate specificity, regulation and cofactor structural preferences (Wang *et al.* 2002; Teigen *et al.* 2007). In contrast to the high degree of homology found in the catalytic core domain, the regulatory N-

terminal domains are highly variable in length and topology, reflecting different regulatory modes that are related to the specific function of the three enzymes (Hufton *et al.* 1995).

Phenylalanine hydroxylase (PAH) catalyzes the conversion of L-Phe into L-Tyr, the first and rate-limiting step in the catabolism of L-Phe in the liver (Fig. 2). A large number of mutations have been identified in the human *PAH* gene resulting in phenylketonuria (PKU) and hyperphenylalaninemia (HPA), the most common inborn error of metabolism (Surtees and Blau 2000). PAH is regulated positively by L-Phe and phosphorylation of Ser16 and negatively by BH_4 (Flatmark and Stevens 1999) (see Part I, sections 2 and 3).

Tyrosine hydroxylase (TH) catalyzes the hydroxylation of L-Tyr into L-3,4-dihydroxyphenylalanine (L-DOPA), the first step in the biosynthesis of cathecolamine neurotransmitters such as dopamine, noradrenaline and adrenaline (Fitzpatrick 1999; Flatmark and Stevens 1999) (Fig. 2). This reaction occurs in dopaminergic and noradrenergic neurons in the brain, in the peripheral sympathetic nervous system and in chromaffin cells in the adrenal medulla (Hufton *et al.* 1995; Kaufman 1995; Flatmark and Stevens 1999; Fitzpatrick 2000; Flatmark *et al.* 2002). The enzyme exists in at least four isoforms created by alternative splicing (Grima *et al.* 1987; Kaneda *et al.* 1987) and it is regulated essentially by feedback inhibition by catecholamines, phosphorylation at several serine residues in the *R*-domain (Kaufman 1995; Dunkley *et al.* 2004) and interaction with 14-3-3 proteins (Halskau Jr. *et al.* 2009). Additional regulatory mechanisms involve substrate inhibition (Quinsey *et al.* 1998) and negative cooperativity for the cofactor BH_4 (Flatmark *et al.* 1999).

Tryptophan hydroxylase (TPH) converts L-Trp into 5-hydroxytryptophan (5-OH-Trp), the first step of the biosynthesis of the neurotransmitter serotonin (5-hydroxytryptamine) and the hormone melatonin. Two individual isoforms with different properties and localization were identified (Walther *et al.* 2003). TPH1 is abundant in the peripheral tissues (e.g. gut, spleen and thymus) and pineal gland, whereas THP2, the central or neuronal form, is localized in the brain stem (Walther and Bader 2003; McKinney *et al.* 2005; Sakowski *et al.* 2006). The TPH enzyme is the less well understood member of the AAAHs family in terms of molecular, functional and regulatory properties. Nonetheless, TPH seems to be activated by phosphorylation and interaction with 14-3-3 proteins (Banik *et al.* 1997; Winge *et al.* 2008) and inhibited by catecholamines, but not by serotonin (Johansen *et al.* 1991; Martínez *et al.* 2001).

In contrast to PAH, few mutations have been identified in the genes encoding *TH*, *TPH*1 and *TPH*2 (Haavik *et al.* 2008). Nevertheless, dysfunction of human TH and TPH has been implicated in the pathogenesis of neurodegenerative and neuropsychiatric disorders (Haavik *et al.* 2008). TH mutant proteins are associated with autosomal recessive inherit forms of L-DOPA-responsive dystonia (DDR), juvenile parkinsonism and progressive infantile encephalopathy with L-DOPA-nonresponsive dystonia (Knappskog *et al.* 1995; Lüdecke *et al.* 1996; Haavik and Toska 1998; Ichinose *et al.* 1999; Swaans *et al.* 2000; Hoffmann *et al.* 2003; Kobayashi and Nagatsu 2005). Mutations and single nucleotide polymorphisms (SNPs) in the intronic and untranslated regions (UTRs) in the human *TPH* genes have been associated with psychiatric disorders like unipolar depression, bipolar disorder, suicidal behavior, attention-deficit/hyperactive disorder (ADHD) and anxiety (Boldrini *et al.* 2005; Sheehan *et al.* 2005; Zhang *et al.* 2005; Bach-Mizrachi *et al.* 2006; Li and He 2006b; Li and He 2006a; Chen *et al.* 2008; Cichon *et al.* 2008; McKinney *et al.* 2008; Porter *et al.* 2008). Additionally, impaired TPH1 enzyme activity has been implicated in disturbances of melatonin biosynthesis, sleep and immune system disorders, and gastrointestinal dysfunction (Ekwall *et al.* 1998; Walther and Bader 2003; Teigen *et al.* 2007).

2. Human phenylalanine hydroxylase (hPAH)

Human phenylalanine hydroxylase (hPAH) is a homotetrameric enzyme (in equilibrium with a dimeric form) with a polypeptide chain of 452 amino acids and a subunit molecular mass of ~52 kDa. Human PAH is a cytoplasmic enzyme present mainly in the liver (Kaufman 1971), but is also expressed in some extent in the kidney (Tessari *et al.* 1999; Møller *et al.* 2000) and epidermis (Schallreuter *et al.* 2005). Loss or severely reduced activity of hPAH has been shown to result in the metabolic disorder phenylketonuria (PKU), that if untreated will result in brain damage (see Part I, section 3).

2.1. The molecular genetics of hPAH

The human *PAH* gene is located on chromosome 12q23.2 (Woo *et al.* 1983; Lidksy *et al.* 1984; Scriver 2007) and consists of 13 exons spreading over 90 kb, representing 3% of the genomic sequence (Scriver *et al.* 2003), with introns varying from 1 to 20 kb (Kappock and Caradonna 1996). Only one hPAH isoform is produced. The 5′ UTR of h*PAH* gene lacks a proximal TATA box, but contains several consensus sequences for different response elements, suggesting that hPAH may be continuously expressed in the target tissues and multiple transcription factors may be involve in the regulation of its expression (Konecki *et al.* 1992).

2.2. The physiological function of hPAH

Human PAH is considered a catabolic enzyme due to its role in the degradation of L-Phe from food, contrasting to hTH and hTPH that are considered anabolic enzymes. However, hPAH also provides an endogenous source of L-Tyr to the organism by converting L-Phe, an essential amino acid that has to be include in the diet (Kalhan and Bier 2008), into L-Tyr which therefore is a non-essential amino acid.

The main pathway for disposal of L-Phe in a healthy human is the hydroxylation reaction catalyzed by hPAH, the initial and rate-limiting step in the complete catabolism of L-Phe to carbon dioxide and water. An alternative pathway for phenylalanine breakdown leads to the formation of toxic phenylketones. This pathway is initiated by transamination of phenylalanine to phenylpyruvate, followed by conversion of the latter compound to metabolites such as phenyllactate, phenylacetate and *o*-hydroxyphenylacetate, which are excreted in the urine (Kaufman 1999).

2.3. The structure of phenylalanine hydroxylase

2.3.1. The protomer and oligomeric forms of PAH

The first high resolution 3D structures of truncated forms of hPAH (Erlandsen *et al.* 1997) and rTH (Goodwill *et al.* 1997) were resolved in the 1990s, but until today no crystal structure has been obtained for the full-length mammalian PAH. So far, several crystal structures of truncated forms of hPAH in complex with ligands, such as adrenaline, noradrenaline, dopamine, L-DOPA, 3-(2-thienyl)-L-alanine (THA) and L-norleucine (NLE), have been described. However, from the determined structures only one (ΔC24-rPAH) includes the regulatory domain (Kobe *et al.* 1999), which has been difficult to study in all AAAHs. The structural studies together with site-directed mutagenesis and limited proteolysis have shown that the hPAH protomer is organized in a three domain structure: (i) a N-terminal regulatory domain (Ser2-Thr117); (ii) a catalytic domain (Val118-Phe410), enclosing the active site iron, the binding sites for substrate, cofactor and catecholamine inhibitors; and (iii) an oligomerization domain (Ser411-Lys452) containing motifs for dimerization and tetramerization (Fusetti *et al.* 1998; Flatmark and Stevens 1999; Kobe *et al.* 1999) (Fig. 3).

Human PAH exists in an equilibrium of homotetramers and homodimers, along with some higher oligomeric forms (Martínez *et al.* 1995; Bjørgo *et al.* 2001), while TH and TPH exist as homotetramers in solution (Kappock and Caradonna 1996; Flatmark and Stevens 1999). The tetramer is the high activity form of the enzyme, and reveals different properties when compared with the dimer, at the level of cooperativity, substrate affinity and activation (Martínez *et al.* 1995; Bjørgo *et al.* 2001). The hPAH tetramer ↔ dimer equilibrium is dependent on pH (Kappock *et al.* 1995) and L-Phe concentration (Martínez *et al.* 1995; Bjørgo *et al.* 2001). A decrease of pH and L-Phe binding to the enzyme shifts the equilibrium towards the tetrameric form.

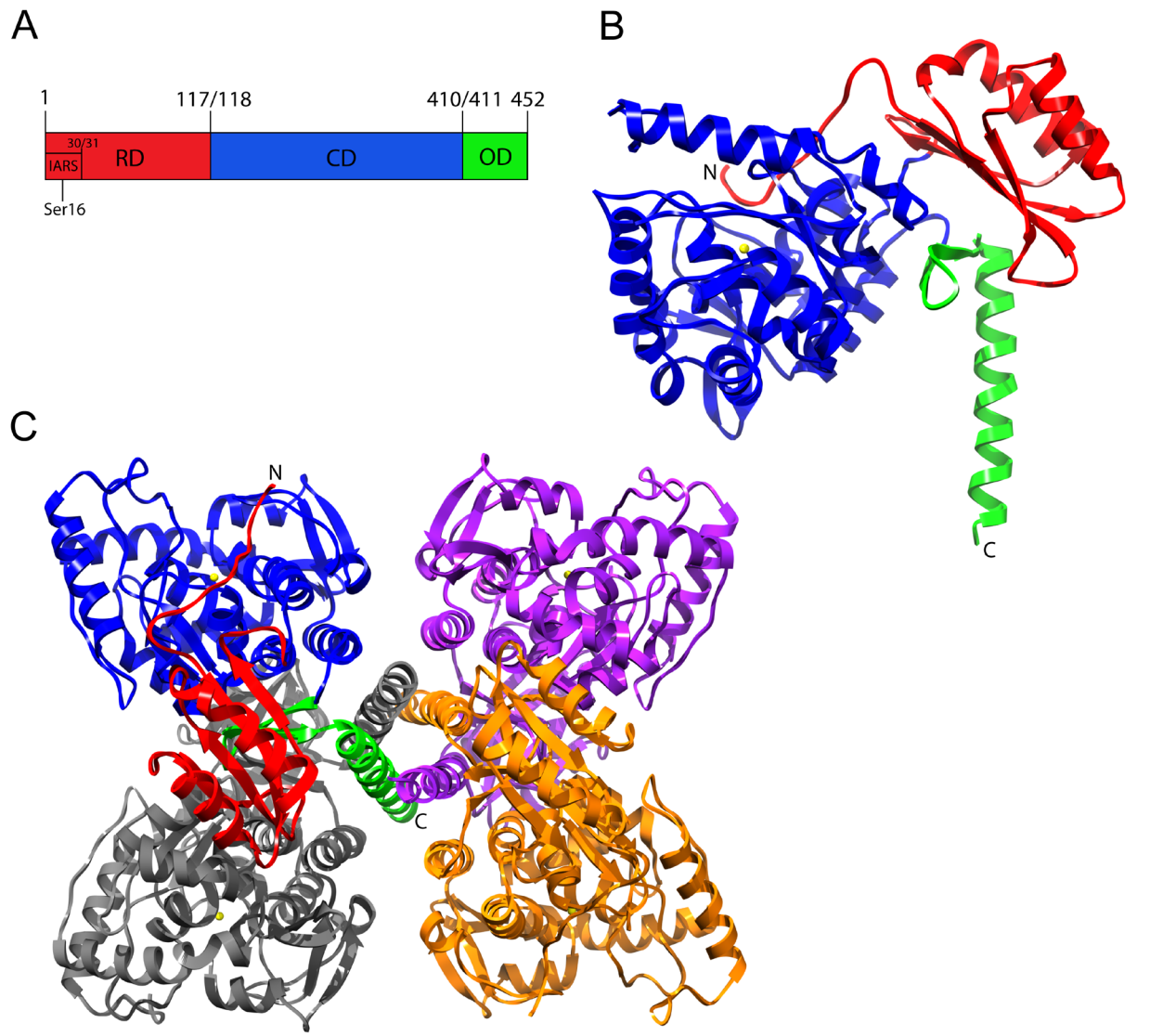

Figure 3. Domain organization and structure of hPAH. (A) Schematic representation of the functional domain structure of hPAH: regulatory domain (RD), catalytic domain (CD) and oligomerization domain (OD). The N-terminal intrinsic autoregulatory sequence (IARS) together with the Ser16 phosphorylation site is indicated. **(B and C)** Models of the full-length monomer **(B)** and tetramer **(C)** of hPAH generated by combining the crystal structure of a C-terminal truncated dimeric rPAH (ΔC24-rPAH, PDB ID: 2PHM) and the N-terminal truncated tetrameric hPAH (ΔN102-hPAH, PDB ID: 2PAH). The monomer in B is represented with the same color code as in the schematic representation in A, with the regulatory domain in red, the catalytic domain in blue and the oligomerization domain in green. One monomer in C is represented with the same color code as in B, while the other monomers are shown in gray, purple and orange. Iron atoms are shown as yellow spheres. Figures B and C were prepared using the program UCSF Chimera (Pettersen *et al.* 2004).

2.3.2. Structural and functional domains in PAH

2.3.2.1. The N-terminal regulatory domain

The regulatory domain of hPAH has a common $\alpha\beta$-sandwich, frequently observed in other regulatory domains of allosteric proteins, assembled from a $\beta\alpha\beta\beta\alpha\beta$-motif, and being classified as an ACT domain (see below) (Siltberg-Liberles and Martínez 2009), consisting of a four-stranded anti-parallel β-sheet flanked on one side by two α-helices (one α-helix and a combined 3/10- and α-helix) and on the other side by the catalytic domain (Kobe *et al.* 1999). This topology gives rise to a flexible structure, consistent with thermal denaturation studies that have shown that the *R*-domain unfolds at a lower temperature than the more compact *C*-domain (Thórólfsson *et al.* 2002).

While the *R*-domain core is located far from the active site in the *C*-domain, the N-terminal residues referred as the intrinsic autoregulatory sequence (IARS; residues 1-33) extends over the active site in the catalytic domain (Fig. 3B). The IARS forms a lid that partly controls the access of the solvent and substrates to the active site (Kobe *et al.* 1999; Kobe and Kemp 1999; Horne *et al.* 2002). The hinge bending region that separates the regulatory from the catalytic domain, around sequence 111-117, is involved in domain movements occurring upon activation by the substrate (Stokka *et al.* 2004; Li *et al.* 2010). The IARS also includes the phosphorylation site (Ser16), which is involved in the activation of the enzyme (see below, section 2.5.1).

The ACT domain (from aspartokinase, chorismate mutase and prephenate dehydrogenase, three proteins from the domain family) was first identified as a regulatory module found in a number of diverse proteins (Fig. 4) (Aravind and Koonin 1999). The ACT domain is a small molecule-binding domain (SMBD) with a high sequence divergence and evolutionary mobility (Anantharaman *et al.* 2001). ACT domains are usually found in allosteric proteins (e.g. *Escherichia coli* D-3-phosphoglycerate dehydrogenase) where they have a regulatory role, forming dimers (or higher-order oligomers) and binding small ligands (typically amino acids and pyrimidines) at their dimer interface (Aravind and Koonin 1999; Chipman and Shaanan 2001; Liberles *et al.* 2005; Grant 2006; Siltberg-Liberles and Martínez 2009).

The ACT domain in hPAH differs from the others archetypal ACT domain proteins by the fact that there are no contacts between the four ACT domains in the hPAH tetramer, and consequently no dimer interface is established (Flatmark and Stevens 1999; Kobe and Kemp 1999; Siltberg-Liberles and Martínez 2009). The putative L-Phe binding at the regulatory ACT

domain has therefore being challenged with evidence that the full-length hPAH enzyme is not able to bind L-Phe at the *R*-domain (Martínez *et al.* 1990; Martínez *et al.* 1991; Thórólfsson *et al.* 2002; Flydal *et al.* 2010), but the isolated *R*-domain seems to have the ability to bind the amino acid (Gjetting *et al.* 2001a; Li *et al.* 2011).

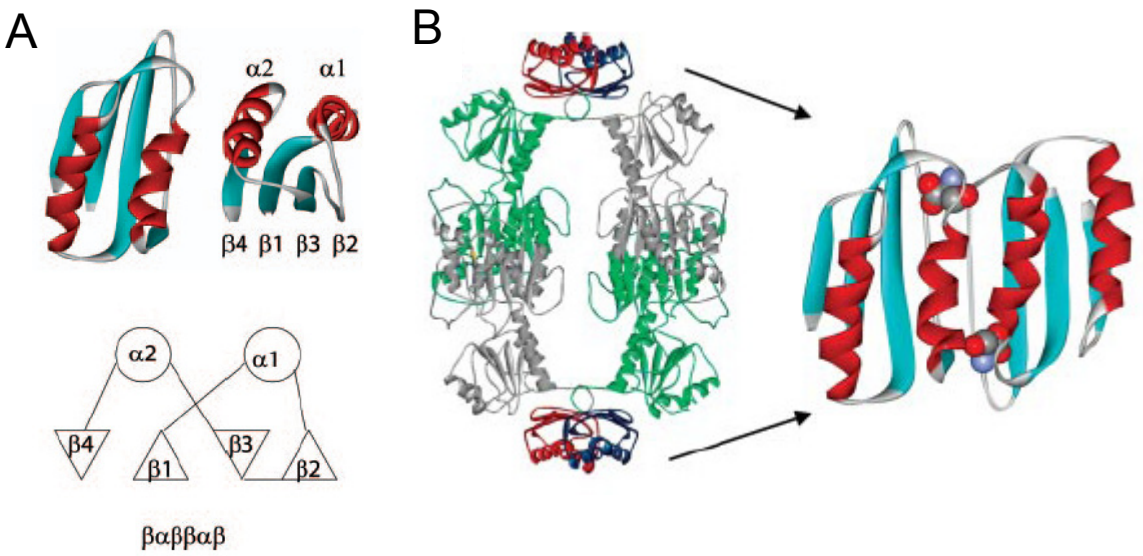

Figure 4. The prototypal ACT domain fold. (A) A single ACT domain from *E. coli* D-3-phosphoglycerate dehydrogenase displaying the *βαββαβ* motif. In the schematic representation below, the triangles pointing up or down indicate the direction of the strand in the *β* sheet, with numbers starting from the N-terminus. **(B)** The *E. coli* D-3-phosphoglycerate dehydrogenase tetramer (PDB ID: 1PSD), with the subunits in green and gray and ACT domains colored blue and red. The arrows indicate the location of the ACT domains in the structure, with the ligand (L-Ser) binding at the dimer interface in CPK format. Figure from Grant 2006.

2.3.2.2. The catalytic core domain

The catalytic domain of hPAH consists predominantly of *α*-helices. The domain has a basket-like organization with a total of 13 *α*-helices, two 3/10-helices, 6 short *β*-strands and loops of variable length connecting the secondary elements, with the catalytic iron at the bottom (Erlandsen *et al.* 1997). The active site is a 13 Å deep and 10 Å wide pocket. A 16 Å long and 8 Å wide channel connected to the active site pocket is most likely the entrance of solvent and ligands into the active site (Erlandsen *et al.* 1997). A 2-His-1-carboxylate facial triad motif anchored the catalytic mononuclear iron at the intersection of the channel and the active site pocket, 10 Å below the surface (Erlandsen *et al.* 1997), a structural motif that has been found in

other non-heme iron enzymes (Hegg and Que 1997; Lange and Que Jr. 1998; Que Jr. 2000; Koehntop *et al.* 2005). The active Fe(II) form in the binary cofactor complex displays an octahedral geometry interacting with the enzyme through His285 (N···2.12 Å), His290 (N···2.13 Å) and Glu330 (O···2.06 Å), and three water molecules (Fig. 5).

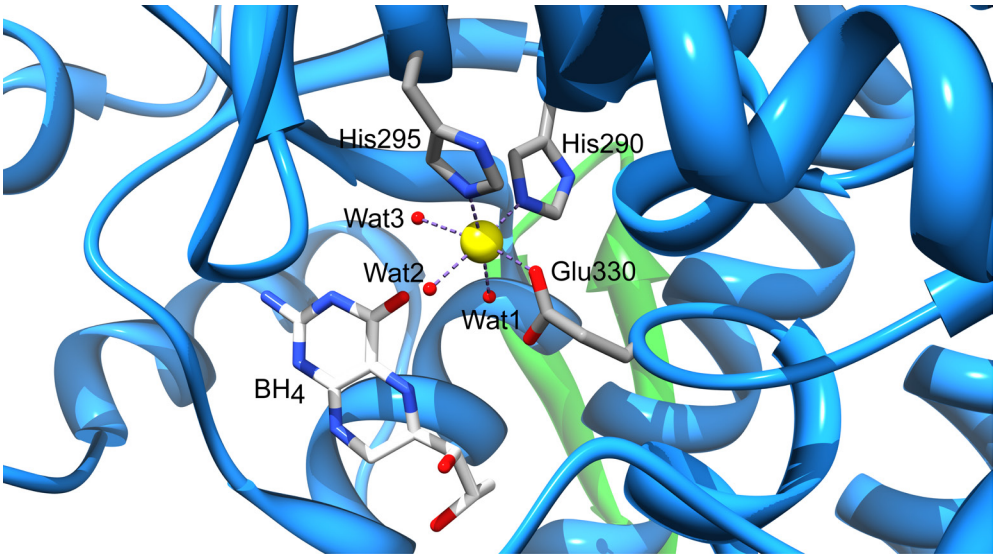

Figure 5. Close-up of the iron binding site in hPAH. The iron atom (Fe(II) form) is shown as a yellow sphere hexa-coordinated to His295, His290, Glu330 (in stick model) and three water molecules (Wat1, Wat2 and Wat3) represented as red spheres, in an octahedral geometry. The cofactor BH_4 is also represented in stick model. The catalytic domain is shown in blue and the oligomerization domain in green. The figure was prepared using the crystal structure of the binary cofactor complex (ΔN102/ΔC24-hPAH-Fe(II)·BH_4) (PDB ID: 1J8U) and the program UCSF Chimera (Pettersen *et al.* 2004).

The cofactor BH_4 binds at the active site, in the vicinity of the iron atom, where it makes stacking interactions with Phe254. The amino group at C2 and N3 hydrogen bonds with the carboxylic group of the conserved glutamate residue Glu286 (Teigen *et al.* 1999; Teigen *et al.* 2004). From the binary crystal structures (Erlandsen *et al.* 2000; Andersen *et al.* 2001; Andersen *et al.* 2002), BH_4 binds in the iron second coordination sphere, by an induced fit mechanism with the carbonyl oxygen (O4) located 3.67–4.18 Å from the iron. Local conformational changes as well as changes in the dihydroxypropyl side-chain were observed (Andersen *et al.* 2001). From the ternary crystal structures (Andersen *et al.* 2002; Andersen *et al.* 2003), the cofactor was found to bind closer to the iron, with the carbonyl oxygen distance to the iron ranging from 3.12–3.53 Å (Olsson *et al.* 2010b).

In the ternary crystal structures of substrate analogs, THA and NLE, the substrate was also found to bind in the second coordination sphere of the iron atom with the aromatic ring stacking against the imidazole group of the iron-bound His285 (Andersen *et al.* 2002; Andersen *et al.* 2003). The substrate was found to interact through hydrogen bonds to Arg270, Thr278 and Ser349, and water-mediate H-bonds to Tyr277, Ser350 and Glu353. Additionally hydrophobic interactions are observed with the phenyl group close to a cluster of aromatic amino acids (Phe331, Trp326) and Pro281 (Andersen *et al.* 2002).

Superposition of the binary and ternary complexes (Andersen *et al.* 2003) and studies of hydrogen/deuterium exchange mass spectrometry (HXMS) (Li *et al.* 2010) revealed that substrate binding results in structural changes at the catalytic domain, but also in the entire protomer, with a re-orientation of the regulatory and catalytic domains through hinge-bending regions (Stokka *et al.* 2004). A large displacement observed upon L-Phe binding was the refolding of a surface loop (residues 134-139) to a partially buried position at active site, with a backbone displacement of 9.6 Å for Tyr138 (Andersen *et al.* 2003).

2.3.2.3. The C-terminal oligomerization domain

The oligomerization domain consists of a dimerization (411-427) and a tetramerization (428-452) motifs. The dimerization motif consists of two β-strands (Tβ12 and Tβ13) held together by a loop (Figs. 1 and 3). The dimerization of the two protomers is mediated by van der Waals interactions and four H-bonds between the two loops. Additionally the two protomers interact across the dimerization interface with a buried area of 440 $Å^2$ (Erlandsen *et al.* 1997). The last 24 C-terminal amino acids (428-452) constitute the tetramerization motif, a 40 Å long α-helix (Tα16) (Fig.1). The helix is a conserved heptad repeat of hydrophobic residues and this leucine zipper plays an important role in the tetramerization domain swapping mechanism, where the helices from each monomer form an antiparallel coiled-coil structure in the middle of the tetramer (Fusetti *et al.* 1998). The hPAH tetramer is not completely symmetrical, and is considered a dimer of two conformationally dimers (Fusetti *et al.* 1998). The two dimers within the tetramer adopt a different relative orientation, due to rotation around the hinge region Asp425-Gln429 (at Thr427) that connects the dimerization and tetramerization motifs, followed by an another rotation around Gly442 in the C-terminal tetramerization helix (Fusetti *et al.* 1998).

2.4. The catalytic mechanism of L-Phe hydroxylation

The catalytic mechanism of hPAH, as well as all AAAHs, requires the substrate (L-Phe in hPAH), cofactor (co-substrate) BH_4, molecular dyoxygen as well as a non-heme iron in the ferrous form (Fe(II)) at the active site (Fisher *et al.* 1972; Gottschall *et al.* 1982). The PAH catalytic mechanism is not fully understood. In the monomeric bacterial *Chromobacterium violaceum* phenylalanine hydroxylase (CvPAH) the steady-state reaction mechanism was shown to be sequential and fully ordered with binding of pterin cofactor, L-Phe and finally dioxygen in consecutive order, prior to catalysis and release of any intermediate or product (Volner *et al.* 2003). In mammalian PAHs there is no consensus about the order of binding to form the quaternary complex (PAH-Fe(II)·BH_4·L-Phe·O_2), with different enzymes revealing different preferences for binding order (Fitzpatrick 2003; Costas *et al.* 2004).

The PAH catalytic mechanism can be divided in two parts: the first one involving the molecular oxygen activation by iron to form an iron-bound peroxopterin intermediate (Fe(II)–O–O–BH_4) and a second one where the oxygen-oxygen heterolytic bond cleavage leads to the formation of a oxyferryl (Fe(IV)=O) species which catalyzes the hydroxylation of L-Phe (Dix and Benkovic 1985; Dix *et al.* 1985; Feig and Lippard 1994; Kemsley *et al.* 1999; Fitzpatrick 2003; Eser *et al.* 2007; Pavon and Fitzpatrick 2009; Olsson *et al.* 2010a). A catalytic mechanism based on crystallographic studies of the ternary complex ΔN102/ΔC24-hPAH-Fe(II)·BH_4·THA (PDB ID: 1KW0) and modeling of dioxygen into the active site has been proposed (Andersen *et al.* 2002) (Fig. 6). In the resting state of PAH, the iron atom is in the ferric form (Fe(III)), which is reduced by BH_4 to the active ferrous form (Fe(II)) in a reaction independent of L-Phe (reductive activation of PAH) (Marota and Shiman 1984; Wallick *et al.* 1984; Shiman *et al.* 1994; Hagedoorn *et al.* 2001) (Fig. 6, Step 1).

The cofactor BH_4 binding at the active site of the pre-reduced enzyme results in a hexa-coordinated iron with three water molecules (Erlandsen *et al.* 2000; Andersen *et al.* 2001) (Fig. 6, Step 2). The direct binding of cofactor to iron during catalysis is still an open mechanistic question (Pember *et al.* 1987; Teigen *et al.* 1999; Teigen *et al.* 2005; Olsson *et al.* 2010a; Olsson *et al.* 2011). Subsequently, L-Phe binding to the binary complex results in a penta-coordinated square-pyramidal arrangement of the iron atom (Kemsley *et al.* 1999; Andersen *et al.* 2002), different from the hexa-coordinated octahedral geometry found in the unliganded ΔN102/ΔC24-

hPAH-Fe(III) or inactive binary ΔN102/ΔC24-hPAH-Fe(III)·BH_2 (Erlandsen *et al.* 2000) and active binary ΔN102/ΔC24-hPAH-Fe(II)·BH_4 complexes (Andersen *et al.* 2001).

The ternary complex formation results from the removal of two water molecules (Wat1 and Wat3), and in the re-orientation of Glu330, that becomes bidentate coordinated to the iron (Andersen *et al.* 2002) (Fig. 6, Step 3). These rearrangements create an available coordination position on the iron for dioxygen activation and the generation of the putative Fe(II)–O–O–BH_4 intermediate, with release of the last water molecule (Wat2) (Fig. 6, Step 4). Using density functional theory (DFT), the water dissociation process was shown to be remarkable facile in a gas-phase cluster model of the active site (ΔG = 1.5 kcal/mol) (Olsson *et al.* 2010a). A water-free first coordination sphere is also suggested from observations from electron paramagnetic resonance and ultraviolet-visible studies (Han *et al.* 2006). A less hydrophilic environment around the iron seems to stabilize the Fe(II)–O–O complex and reduce the risk of hydrogen peroxide formation, a mechanism that was also observed in other enzymes (Olsson *et al.* 2010a).

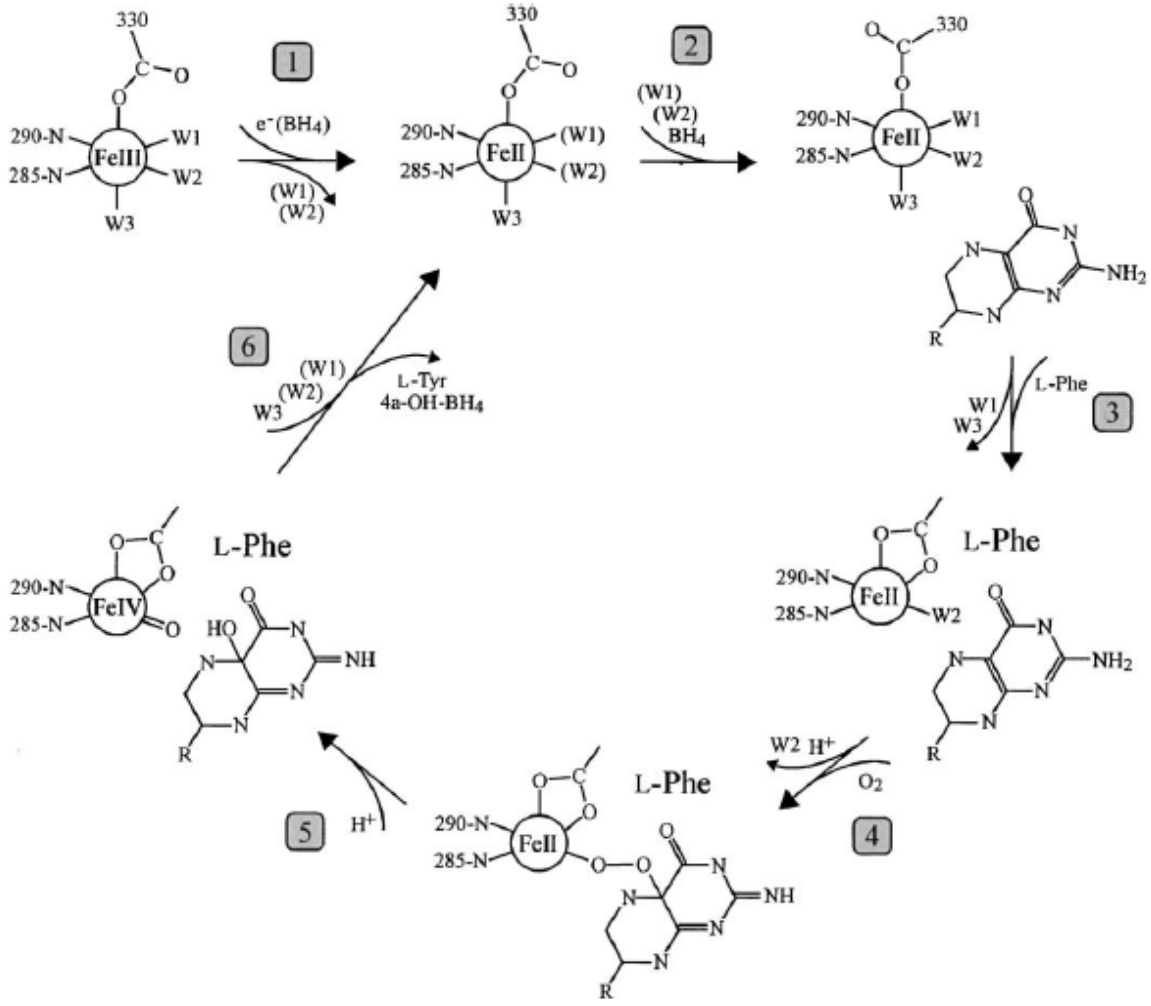

Figure 6. Proposed catalytic mechanism for the L-Phe hydroxylation by PAH. BH_4 reduces the Fe(III) form to the catalytic active Fe(II) form (Step 1). Reversible binding of BH_4 results in a hexa-coordinate Fe(II), with a change in the coordination of Glu330 and an increase in the electron density of water 1 and 2 (W1 and W2 in brackets) (Step 2). The reversible binding of L-Phe results in a highly distorted square pyramidal penta-coordinated Fe(II) with a bidentate coordination of Glu330 (Step 3). The reversible binding of dioxygen leads to the formation of the putative Fe(II)–O–O–BH_4 intermediate (Step 4), and heterolytic cleavage of the O–O bond leads to the formation of 4a-OH-BH_4 and a ferryl species, Fe(IV)=O (Step 5), which is responsible by the hydroxylation of L-Phe into L-Tyr, with subsequently released of the products (Step 6). Figure from Andersen *et al.* 2002.

The complete mechanism of dioxygen activation and the formation of Fe(II)–O–O–BH_4 intermediate still remain elusive (Costas *et al.* 2004; Abu-Omar *et al.* 2005). A stepwise binding has been proposed with three possible mechanisms: (i) an initial binding of dioxygen to Fe(II) forming an Fe(III)–O_2^- species that subsequently binds to BH_4 (metal catalyzed pathway); (ii)

dyoxygen binding to the cofactor forming a pterin hydroxyperoxide which then coordinates to the iron (metal-free pathway); or (iii) a concerted addition of dioxygen to both iron and cofactor (Costas *et al.* 2004; Abu-Omar *et al.* 2005). Heterolytic cleavage of the oxygen-oxygen bond of the Fe(II)–O–O complex resulting in the formation of the hydroxylated cofactor (4a-OH-BH_4) and a highly active oxygen intermediate Fe(IV)=O was proposed (Dix and Benkovic 1988; Bassan *et al.* 2003b; Bassan *et al.* 2003a; Fitzpatrick 2003; Eser and Fitzpatrick 2010) (Fig. 6, Step 5), that will ultimately hydroxylate the aromatic ring of L-Phe by an electrophilic aromatic substitution mechanism (Fig. 6, Step 6), returning the iron to the Fe(II) form (Pavon and Fitzpatrick 2006; Panay and Fitzpatrick 2008). Consequently, the dyoxygen atoms would be in fact incorporated into both substrate and cofactor (Dix and Benkovic 1988; Siegmund and Kaufman 1991). A high-spin Fe(IV) species have been directly observed in the TH catalytic reaction (Eser *et al.* 2007) and more recently in the catalytic cycle of a bacterial PAH (CvPAH) (Panay *et al.* 2011), which might correspond to the Fe(IV)=O intermediate. It has been proposed that 4a-OH-BH_4 will be released from the active site because this compound will present a decreased affinity due to the sp^3 configuration of the 4a position and to the bending in the pterin ring that impairs the stacking with Phe254 (Teigen *et al.* 1999). The release of the product (L-Tyr) may occur due to steric hindrance by Glu330 and Trp326 (Teigen *et al.* 1999; Andersen *et al.* 2002).

2.5. Regulatory properties of phenylalanine hydroxylase

Human PAH is tightly regulated in the human body in order to maintain the correct levels of L-Phe in the blood. High levels of L-Phe are toxic to the brain, while low levels can hamper protein synthesis, as hepatic levels of fully activated hPAH are enough to remove all L-Phe from the bloodstream within minutes (Shiman *et al.* 1982). *In vivo,* hPAH is regulated by three main mechanisms: (i) activation by substrate (Shiman and Gray 1980; Shiman *et al.* 1990), (ii) phosphorylation of Ser16 (Døskeland *et al.* 1996) and (iii) inhibition by the pterin cofactor (Shiman and Gray 1980; Xia *et al.* 1994). *In vitro*, hPAH can be artificially activated by chymotrypsin limited proteolysis (Iwaki *et al.* 1986), alkylation of the sulfhydryl group of Cys237 (Parniak and Kaufman 1981; Gibbs and Benkovic 1991) and interaction with ionic detergents, such as lysolecithin (Fisher and Kaufman 1973; Abita *et al.* 1984; Kaufman 1993). Removal of a N-terminal fragment by limited proteolysis activates the enzyme, and an

autoinhibitory effect by the *R*-domain was then proposed (Iwaki *et al.* 1986). The only available crystal structure of the regulatory PAH domain (dimeric ΔC24-rPAH) has confirmed the role of the *R*-domain, especially the N-terminal autoregulatory sequence (IARS) that partly covers the active site (Kobe *et al.* 1999). Studies on truncated forms of hPAH lacking part or the full *R*-domain and chimeric PAH with a *R*-domain from TH, all have shown that the enzyme is already in an activated state (Knappskog *et al.* 1996b; Daubner *et al.* 1997) and is not inhibited by the cofactor BH_4 (Jennings *et al.* 2001), properties that are not exhibited by the full-length enzyme.

2.5.1. Activation by substrate and phosphorylation

The substrate L-Phe is an allosteric activator of the hPAH enzyme, inducing conformational changes that result in two related effects (Kaufman 1993). The first one is associated with the activation of the enzyme. Preincubation with L-Phe results in a 5- to 6- fold activation of full-length hPAH (1.6-fold for the dimeric form) (Solstad and Flatmark 2000; Bjørgo *et al.* 2001), a process caused by conformational changes in the tetrameric/dimeric enzyme (Flatmark and Stevens 1999; Flatmark *et al.* 2001; Stokka and Flatmark 2003; Stokka *et al.* 2004; Li *et al.* 2010). Movements of the *R*-domain with displacement of the IARS seem to be involved, with an increased accessibility to the active site, as N-terminal truncated mutants are already in an activated state (Knappskog *et al.* 1996b; Stokka and Flatmark 2003). This L-Phe triggered activation is a slow (second-to-minutes) transition of the enzyme from a low activity, low affinity state "T"-state to a high activity "R"-state (Shiman and Gray 1980; Shiman *et al.* 1990), a characteristic of a hysteretic enzyme (Flatmark *et al.* 1999).

The second effect related to substrate binding is cooperativity. The full-length tetrameric form of hPAH binds the substrate L-Phe with positive cooperativity (the dimeric form does not display cooperativity), a major regulatory mechanism that involves all four monomers (Shiman and Gray 1980; Shiman *et al.* 1990; Bjørgo *et al.* 2001). Human PAH shows a non-hyperbolic (sigmoidal) dependence on substrate concentration for its equilibrium binding (Parniak and Kaufman 1981) and steady-state kinetics (Kaufman 1993). This process is thought to result from a homotropic cooperative mechanism triggered by L-Phe binding at the active site, consistent with only one L-Phe binding site per protomer, at least to elicit the positive cooperativity process (Martínez *et al.* 1990; Martínez *et al.* 1991; Martínez *et al.* 1993; Stokka and Flatmark 2003). The substrate L-Phe binds with an affinity ($S_{0.5}$) of ~150 μM for eukaryotic PAH and a Hill coefficient (n_H) of ~2

(Kaufman 1993; Teigen *et al.* 2007) and the physiological L-Phe level in healthy individuals is less than 120 μM (Pey and Martínez 2005; Blau *et al.* 2010b). The positive cooperative binding of L-Phe is considered to be physiologically important as a protection mechanism when the serum L-Phe concentration increases above normal levels. The mechanism allows L-Phe homeostasis in the blood by preventing HPA, but allowing a continuous supply of L-Tyr for protein synthesis (Kappock and Caradonna 1996; Olsson *et al.* 2010b). The activation and positive cooperativity mechanism of the full-length hPAH enzyme is a complex process that is still not completely understood.

Phosphorylation at Ser16 by the cyclic AMP dependent protein kinase A (PKA) is a post-translational modification that acts synergistically with L-Phe activation. The phosphorylated enzyme requires a lower L-Phe concentration for full catalytic activation while L-Phe levels increase the rate of phosphorylation by PKA (Døskeland *et al.* 1984; Phillips and Kaufman 1984; Kaufman 1993; Døskeland *et al.* 1996). In contrast, BH_4 reduces the rate of phosphorylation, but this inhibition is prevented in the presence of L-Phe (Døskeland *et al.* 1996). Phosphorylation seems to induce a local conformational change at Ser16 in the IARS, which facilitates the access of L-Phe to the active site (Miranda *et al.* 2002; Miranda *et al.* 2004).

2.5.2. Inhibition by cofactor

The cofactor BH_4 plays a role as co-substrate in the catalytic reaction, but has also a regulatory role in hPAH. BH_4 inhibits the enzyme by inducing a low-activity conformational state (the binary hPAH·BH_4 complex), inhibits L-Phe activation and reduces the rate of phosphorylation at Ser16 (Xia *et al.* 1994; Døskeland *et al.* 1996; Solstad *et al.* 2003; Teigen and Martínez 2003; Pey *et al.* 2004a; Pey *et al.* 2004b). The cofactor BH_4 inhibits hPAH in the absence of L-Phe (resting state) by protecting the enzyme from unfolding and degradation (Mitnaul and Shiman 1995), a stabilization process that plays a major role in the BH_4-responsive PKU (see below Section 3.2.1) (Martínez *et al.* 2008). The regulatory properties of the cofactor are dependent on the dihydroxypropyl side-chain at position C6 of the cofactor, as functional analogues such as 6-methyl-5,6,7,8-tetrahydropterin ($6MPH_4$) and 6,7-dimethyl-5,6,7,8-tetrahydropterin ($DMPH_4$) are able to substitute the natural cofactor in catalysis but do not induce the regulatory properties (Phillips and Kaufman 1984; Kaufman 1993; Kappock and Caradonna 1996; Pey *et al.* 2004b). The K_m value of PAH for BH_4 is in the range of 15–40 μM

(Olsson *et al.* 2010b). In a healthy individual the concentration of BH_4 in liver hepatocytes is approximately 5−10 μM (Pey and Martínez 2005) and hPAH subunit concentration is postulated to be equimolar. Therefore, the majority of hPAH is converted in the inactive but stable hPAH·BH_4 complex (Mitnaul and Shiman 1995), whose inhibitory effect is reversed by increasing levels of L-Phe in the blood. The BH_4 dependent activity of the non-activated enzyme is characterized by a Michaelis-Menten kinetics (Knappskog *et al.* 1996b), whereas the L-Phe activated form displays a positive cooperativity towards BH_4 binding (Gersting *et al.* 2010b).

2.6. Post-translational modifications in hPAH

The only known post-translational modifications to occur in hPAH *in vivo* are phosphorylation (discussed in the above section) and non-enzymatic deamidation of hPAH. The deamidation of labile amide groups of Asn (and Gln, although to a lesser degree) to Asp or L-isoaspartic acid, or to a lesser extent to D-isoaspartic acid, are in general related to mechanisms of aging and cellular turnover of proteins (Robinson *et al.* 1970; Robinson and Robinson 2001). The function of deamidation in hPAH is not completely clear, but a similar role is expected. Two-dimensional gel electrophoresis of different PAH preparations has revealed a microheterogeneity that corresponds to PAH forms with different degrees of deamidation (Solstad and Flatmark 2000). Asn32 in the *R*-domain and Asn376 in the *C*-domain were found to be the most determinant residues for the regulatory and functional differences observed in the deamidated proteins (Carvalho *et al.* 2003). Highly deamidated forms of hPAH are more susceptible to limited proteolysis, display an increased catalytic efficiency and substrate affinity (Solstad and Flatmark 2000).

Human PAH was also shown to be a substrate for the ubiquitin-conjugating enzyme system in an *in vitro* system (Døskeland and Flatmark 1996; Døskeland and Flatmark 2001), pointing to a degradation by the proteasome degradation machinery, at least to some extent. Turnover rates of hPAH have been reported to be approximately 8.4 h in cultured hepatoma cells (Baker and Shiman 1979) and *in vitro* cell-free coupled transcription-translation system (Waters *et al.* 1998a; Gámez *et al.* 2000). Several misfolding PKU mutations have been associated with increased protein turnover rates (Waters *et al.* 1998a; Waters *et al.* 1999; Gámez *et al.* 2000), and the degradation of the mutants might involve different proteolytic pathways (Waters 2003), including the ubiquitin-proteasome system.

3. Phenylketonuria (PKU)

Phenylketonuria (PKU; OMIM 216600) was the first inborn error of metabolism shown to be associated to neuropsychological symptoms. It was first described in 1934 by Dr. Asbjørn Følling following his studies of mentally retarded children who excreted phenylketonuric acid in their urine. Asbjørn Følling suggested that a metabolic anomaly with a pattern of an autosomal recessive genetic disease, apparently caused by an inherited defect in the metabolism of phenylalanine, was the cause of neuropsychological deficits (Følling 1934). In 1947 Jervis suggested that the metabolic error described by Følling was an inability to convert L-Phe into L-Tyr (Jervis 1947), and an hepatic system was soon thereafter discovered to be responsible for this conversion (Udenfriend and Cooper 1952), and the underlying cause pinned down to the deficient conversion of L-Phe to L-Tyr in the liver by phenylalanine hydroxylase (Jervis 1953). In the early 1950s, Dr. Horst Bickel successfully introduced a low-phenylalanine diet that resulted in reduced plasma L-Phe levels and disappearance of phenylpyruvic acid from urine, and also resulted in an improvement of physical development and behavior performance, (Bickel *et al.* 1953; Bickel *et al.* 1954; Armstrong and Tyler 1955; Woolf *et al.* 1955) if started within the first weeks of life (Bickel *et al.* 1954; Armstrong and Low 1957; Clader 1957). In the 1960s Robert Guthrie introduced a simple blood screening method for detection of high levels of plasma L-Phe in newborns (the Guthrie test) (Guthrie and Susi 1963).

3.1. PKU mutations and clinical outcome

Phenylketonuria is caused by a deficiency of the hepatic phenylalanine hydroxylase enzyme, due to mutations in the *PAH* gene. The failure to metabolize L-Phe results in its accumulation in blood and toxic levels in the brain. In untreated PKU, the high levels of L-Phe together with the presence of phenylketones (formed from the transaminase pathway) give rise to neurotoxicity and results in severe mental retardation or impaired cognitive development, growth abnormalities and behavioral difficulties (Scriver and Kaufman 2001; Blau *et al.* 2010b; Feillet *et al.* 2010; Mazur *et al.* 2010). Additional symptoms can include microcephaly, eczematous rash, autism, ADHD symptoms, agoraphobia, seizures and motor dysfunction (Waisbren and Levy 1991; Arnold *et al.* 1998; Antshel and Waisbren 2003; Baieli *et al.* 2003; Blau *et al.* 2010b; Mazur *et al.* 2010).

PKU is inherited in an autosomal recessive fashion, when both alleles are mutated. At present, more than 550 disease-causing mutations in the *PAH* gene have been identified and registered in the Human PAH Mutation Knowledgebase (hPAHdb; *www.pahdb.mcgill.ca/*) (Hoang *et al.* 1996; Scriver *et al.* 2003; Scriver 2007). The current spectrum of PKU mutations consists of ~60% missense mutations; ~13% deletions; ~11% splice mutations; ~6% silent mutations; ~5% nonsense mutations and ~2% insertions. Mutations have been identified in all 13 exons, but the majority are found in the 3′-half of the gene, namely between exon 5 and 12 (Waters *et al.* 1998b). Due to the large number of mutations, most of the patients (approximately 75%) are heteroallelic for *PAH* mutations being classified as compound heterozygous (Scriver and Waters 1999)

In Caucasians the frequency of PKU is approximately 1 per 10,000 but this value can fluctuate by geographical region and among ethnic groups (Blau *et al.* 2010b). Although the majority of the HPA cases resulted from mutations in the *PAH* gene, approximately 1–2% of HPA resulted from mutations in genes coding for the enzymes involved in the *de novo* synthesis of BH_4 from GTP and in the regeneration system of BH_4 (Part I, section 1) (HPA secondary to BH_4 deficiency) (Thöny and Blau 2006; Blau *et al.* 2010b). Differential diagnosis of PKU *versus* BH_4 deficiency is carried out by blood or urinary pterin analyses or blood DHPR activity (Blau *et al.* 2003).

Expression and characterization analyses of several PAH missense mutations in complementary *in vitro* systems (for review, see the PAH Mutation Analysis Consortium database) (Hoang *et al.* 1996) and computational studies have identified at least three main groups of enzymatic phenotypes which differ in their kinetic behaviour and/or stability, i.e. (i) structurally stable mutations with altered kinetic properties, e.g. mutations at residues involved in substrate (L-Phe) or the pterin cofactor (BH_4) binding; (ii) mutations with normal or almost normal kinetic properties, but reduced stability both *in vitro* and *in vivo*; and (iii) mutations affecting both kinetic and stability properties of the enzyme (Knappskog *et al.* 1996a; Flatmark *et al.* 1997; Bjørgo *et al.* 1998; Waters *et al.* 1998a; Waters *et al.* 1999; Waters *et al.* 2000; Gjetting *et al.* 2001b; Waters 2003; Pey *et al.* 2007; Gersting *et al.* 2008). From these studies it emerged that a decrease in protein stability is the main molecular pathogenic mechanism (Pey *et al.* 2007), with PKU being considered a protein misfolded disease (Gregersen *et al.* 2001; Gregersen 2006; Gregersen *et al.* 2006; Martínez *et al.* 2008).

The *PAH* gene mutations lead to a wide spectrum of clinical and biochemical phenotypes with different degrees of severity, ranging from classical or severe PKU (reduced or no enzymatic activity), to mild PKU and mild HPA (considerable hPAH activity). The classification of PKU severity is based on blood phenylalanine concentration before treatment and/or dietary Phe intake tolerance, at five years of age, in order to maintain L-Phe plasmatic levels below 360 μM. The classic PKU form is associated with blood Phe concentrations above 1200 μM before treatment and a dietary Phe tolerance of less than 20 mg/kg of body weight; mild PKU is linked with blood Phe concentrations between 600-1200 μM and a dietary Phe tolerance between 20-25 mg/kg of body weight; and mild HPA (MHP) is associated with blood Phe concentrations between 120-600 μM, when the patient is on a normal diet and a dietary Phe tolerance greater than 25 mg/kg of body weight (Güttler and Guldberg 1994; Blau 2010; Blau *et al.* 2010b; Feillet *et al.* 2010). It must be emphasized that the blood Phe concentration in a healthy person varies from 50–110 μM. Individuals with mild HPA have a much lower risk of impaired cognitive development in the absence of treatment, although some might have decreased executive functioning (Gassió *et al.* 2005).

Elevated levels of blood L-Phe are associated with neuropsychological impairment, especially in the first years of life through several mechanisms, particularly dysmyelination and dopamine and serotonin depletion (Fig. 7) (Surtees and Blau 2000; Gassió *et al.* 2005; Feillet *et al.* 2010). HPA has been shown to cause white-matter lesions and increase myelin turnover, with delayed or reduced myelination in children and loss of myelin in adults. However, the causal link between dysmyelination and neuropsychological deficit has not been clearly demonstrated (Blau *et al.* 2010b; Feillet *et al.* 2010). Nonetheless, a relation between the white-matter abnormalities in PKU patients and neuropsychological impairment was established (Huttenlocher 2000; Anderson *et al.* 2007).

Hyperphenylalaninemia also affects the neurotransmitters function in the brain, due to depletion of L-Tyr levels. The L-Phe transport across the blood brain barrier (BBB) is mediated by the L-amino acid transporter 1 (LAT1). This carrier is also responsible for the transport of the two other large, neutral amino acids (LNAA), L-Tyr (precursor of dopamine and noradrenaline) and L-Trp (precursor of serotonin) (Part I, section 1) (Pietz *et al.* 1999). Therefore, L-Phe competes with the other aromatic amino acids for their transport into the brain. Consequently, in PKU patients the supply of L-Tyr and L-Trp for protein synthesis (Kalsner *et al.* 2001; Hoeksma

et al. 2009) as well as the level of essential neurotransmitters can be dramatically reduced (van Spronsen *et al.* 2009).

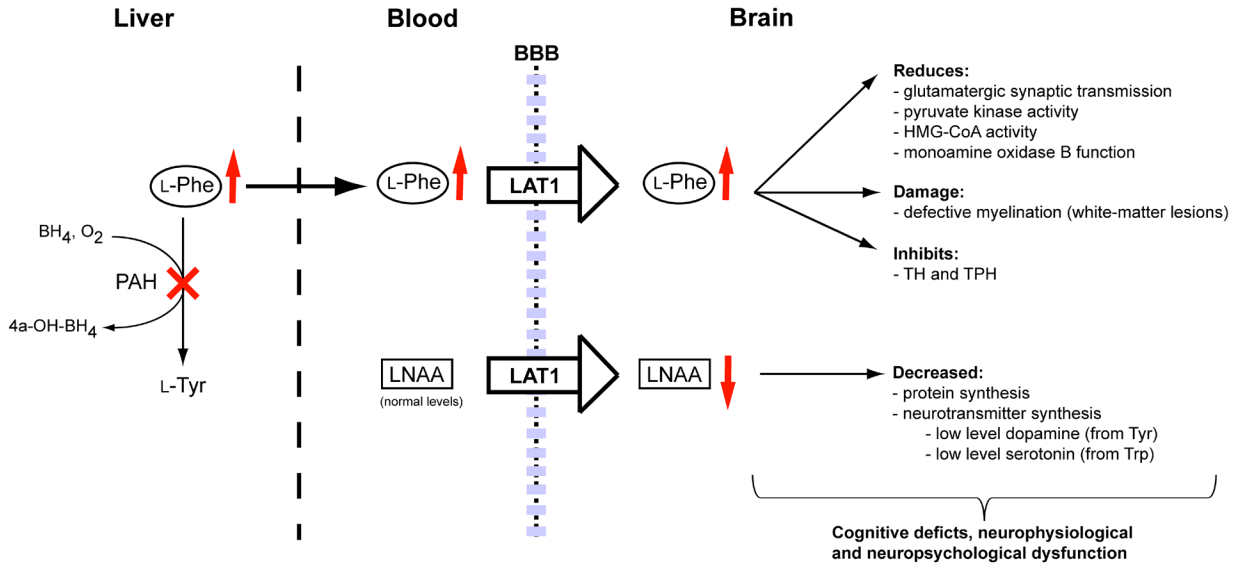

Figure 7. Potential mechanisms of neurocognitive impairment by hyperphenylalaninemia (HPA). BBB indicates blood-brain barrier; L-Phe, L-phenylalanine; BH4, (6*R*)-L-*erythro*-5,6,7,8-tetrahydrobiopterin; 4a-OH-BH_4, tetrahydropterin-4a-carbinolamine; L-Tyr, L-tyrosine; LNAA, large, neutral amino acid; LAT1, L-amino acid transporter 1; HMG-CoA, 3-hydroxy-3-methylglutaryl-coenzyme; TH, tyrosine hydroxylase; TPH, tryptophan hydroxylase; L-Trp, L-tryptophan. Adapted from Feillet *et al.* 2010.

Other possible mechanisms involved in brain function impairment include disturbed glutamatergic synaptic transmission (Martynyuk *et al.* 2005), cholesterol biosynthetic pathway (through a moderately inhibition of the 3-hydroxy-3-methylglutaryl-coenzyme (HMG-CoA) (Shefer *et al.* 2000), glucose metabolism (inhibition of pyruvate kinase) (Hörster *et al.* 2006; Wasserstein *et al.* 2006) and reduced function of the monoamine oxidase B as a modifying gene (Ghozlan *et al.* 2004). DNA damage and oxidative stress may also play a role on PKU pathogenesis (Sitta *et al.* 2006; Sitta *et al.* 2009).

In recent years, the importance of blood phenylalanine variability has been a topic of major discussion. It has been proposed that not only the mean lifetime blood L-Phe level, but also the degree of fluctuation of L-Phe concentration during long-term dietary management could be of clinical importance, affecting the cognitive outcome (Burgard *et al.* 1996; Arnold *et al.* 1998;

Anastasoaie *et al.* 2008). Thus, in addition to maintain average L-Phe levels, the stability of blood L-Phe over time (homeostasis) might be an important goal in the treatment strategy (Blau *et al.* 2010b).

Another important health concern related to PKU pathogenesis is the relation between prenatal L-Phe exposure and the offspring outcome. Women with PKU that have discontinue the Phe-free diet and become pregnant may develop maternal PKU. When maternal L-Phe concentrations are above 360 μM, normally defined as the critical threshold, the fetus is exposed to teratogenic concentrations of the amino acid (Koch *et al.* 2003a; Waisbren and Azen 2003; Widaman and Azen 2003). In that case, newborns may manifest severe mental retardation, microcephaly, developmental delay, facial dysmorphisms, low birth weight and congenital heart disease (Lenke and Levy 1980; Levy and Waisbren 1983; Hoeks *et al.* 2009; Blau 2010). Therefore, in PKU women maintenance of maternal blood L-Phe levels within a range of 100–250 μM and minimization of L-Phe variation, before conception and during pregnancy is essential to achieve the best possible offspring outcome (Maillot *et al.* 2008).

3.2. The treatment of PKU

The main treatment goals for PKU are to maintain L-Phe concentration within safe limits (120–360 μM and 120–240 μM for pregnant PKU women) to prevent the onset or aggravation of neuropsychological symptoms and to ensure a normal growth and healthy life throughout adulthood (Giovannini *et al.* 2007).

At present, the routine detection of hyperphenylalaninemia by Neonatal Screening Programs (the Guthrie test or modern systems based in tandem mass spectrometry) leads to the identification of PKU patients within the first days of life, allowing that a low L-Phe diet can be started early, and thus avoiding the development of severe clinical symptoms (Smith *et al.* 1990). Nowadays, this low-protein diet, supplemented with L-Phe-free mixture of amino acids, vitamins, minerals and other nutrients remains the most effective treatment for PKU (Giovannini *et al.* 2007; Blau *et al.* 2010b).

A strict dietary control management is recommend in early childhood, and although it can be relaxed in older children and adults, a life-long management is currently recommend to avoid any harmful neurological effects (Blau 2010). However, the compliance to this life-long restriction diet is difficult, and usually it erodes as patients get older, with up to 75% of PKU

patients becoming essentially non-adherent in adulthood (Koch *et al.* 2002; Walter *et al.* 2002; Walter and White 2004; Blau *et al.* 2010b). Although an early reduction of L-Phe concentration can avoid the most serious deleterious effects, if there is a poor metabolic control of the L-Phe levels over time, it can result in persistent consequences such as lower intelligence quotient, impair executive function (e.g. planning, working memory, information processing, problem solving, sustained attention, abstract reasoning), delayed speech and behavioral problems (National Institutes of Health Consensus Development Panel 2001; Huijbregts *et al.* 2002; Arnold *et al.* 2004; Leuzzi *et al.* 2004; Channon *et al.* 2007; VanZutphen *et al.* 2007; Albrecht *et al.* 2009; Blau 2010). A discontinuation of the dietary treatment in early-treated adults can also result in vitamin deficiencies, osteoporosis, neurological and psychological decline, including spastic paresis, late-onset epilepsy, ataxia, tremor and problems such as neuroses, depression and anxiety (Hoeks *et al.* 2009; Blau 2010). The absence of a clear management of PKU in adult patients, together with inconsistencies in the definition of the mild HPA phenotype and management discrepancies between countries can also contribute to a long-term outcome less than optimal in PKU patients (Ahring *et al.* 2009; Blau *et al.* 2010a; Feillet *et al.* 2010).

Although compliance with a restrictive Phe-free diet prevents most of the harmful effects of PKU, it may lead to insufficiencies of essential nutrients (such as tyrosine, iron, trace elements or long-chain polyunsaturated fatty acids), and abnormal energy supply, due to reduced intake of carbohydrates and fats (Przyrembel and Bremer 2000; Acosta *et al.* 2004). The clinical manifestation of these nutritional deficits comprise decrease bone density, overweight and growth retardation (Przyrembel and Bremer 2000; Acosta *et al.* 2003; Koletzko *et al.* 2007; Modan-Moses *et al.* 2007). The strict L-Phe diet has also been associated with selenium and coenzyme Q10 deficiencies that may alter the antioxidant status, especially with increase patient age (van Bakel *et al.* 2000; Artuch *et al.* 2004). Therefore, in the last years new approaches to substitute or alleviate the restrictive L-Phe-free diet and improve clinical outcomes are emerging. Recent developments include: BH_4 or large neutral amino acid supplementation, glycomacropeptide as protein source, enzyme therapy (replacement and substitution), gene therapy (Sarkissian *et al.* 2009) and repopulation of hepatic PAH activity by liver cell transplantation (Harding 2008). Among these strategies the cofactor BH_4 supplementation is already successfully used in the treatment of a large number of PKU patients (see below, section 3.2.1) (Levy *et al.* 2007).

The glycomacropeptide is a protein derivative from cheese whey that in its purified form is naturally free of aromatic amino acids, but is rich in other essential amino acids (Etzel 2004; Laclair *et al.* 2009). This protein could be a useful adjunct to the low-Phe diet, when in a purified form and when supplemented with the missing limiting amino acids. Glycomacropeptide is therefore an alternative source of dietary protein, improving the dietary compliance and metabolic control in PKU patients (Lim *et al.* 2007; Ney *et al.* 2009; van Calcar *et al.* 2009).

The supplementation with large neutral amino acids is a strategy based on the fact that LNAAs compete and inhibit the L-Phe transport across the blood-brain barrier (section 3.1) and L-Phe uptake via intestinal absorption at the gastrointestinal tract, with cationic amino acids also inhibiting the uptake (Matalon *et al.* 2003; Matalon *et al.* 2006). LNAAs have been shown to significantly reduce blood (Matalon *et al.* 2006; Matalon *et al.* 2007) and brain L-Phe levels (Pietz *et al.* 1999), and to increase blood L-Tyr and L-Trp concentration (Koch *et al.* 2003b), improving the executive functioning (Schindeler *et al.* 2007). Long-term studies of the efficacy and safety of LNAAs supplementation are still necessary, but their use in off-diet and non-compliant diet patients seems recommend (Rocha and Martel 2009).

Enzyme substitution therapy with the plant derived phenylalanine ammonia lyase (PAL, E. C. 4.3.1.5) is an additional approach to treat PKU that is currently in phase II clinical trials (ClinicalTrials.gov 2010). PAL is a stable L-Phe degrading enzyme from plants and yeasts that unlike PAH does not require a cofactor. However, L-Tyr is not a product of PAL catalytic reaction where phenylalanine is converted to metabolically insignificant amounts of ammonia and trans-cinnamic acid, a harmless metabolite converted to benzoic acid and excreted in urine as hippurate (Sarkissian *et al.* 1999). Nevertheless, the first PAL formulations presented a very short half-life and were highly immunogenic in parenteral therapy (Gámez *et al.* 2005; Ikeda *et al.* 2005). To overcome these problems pegylated forms of PAL were developed (Sarkissian *et al.* 2008) and the results from subcutaneous administration phase I clinical trials demonstrated a reduction of ~60% of the mean blood L-Phe level without serious adverse effects (BioMarin Pharmaceutical Inc. 2009). An oral formulation of PAL is also under evaluation (Kang *et al.* 2010).

Enzyme replacement therapy with recombinant wild-type human phenylalanine hydroxylase is another alternative to treat PKU. In this case no L-Tyr supplementation would be required. The major drawbacks of the therapy are the difficulty to obtain a stable form of hPAH for

formulation and the cofactor requirement (Gámez *et al.* 2004; Kim *et al.* 2004). Studies involving hPAH fusions proteins to HIV-transactivator of transcription peptide and human hepatocyte growth factor, to target the enzyme specifically to the liver are also under way (Eavri and Lorberboum-Galski 2007).

The PKU somatic gene therapy requires the use of DNA-based gene transfer methodologies in order to replace the mutant gene by a functional *PAH* gene in the liver, consequently restoring hPAH enzymatic activity. Several reports using viral and non-viral delivery gene systems in murine PKU models have shown to correct the HPA phenotype (Harding 2008; Jung *et al.* 2008; Rebuffat *et al.* 2010; Yagi *et al.* 2011). An alternative strategy of gene therapy includes the expression of *PAH* gene in a heterologous tissue (e.g. skeletal muscle), with enzymes from the BH_4 biosynthetic pathway (Ding *et al.* 2008). Another complementary gene therapy approach involves transplantation of cells with a complete PAH hydroxylase system (Harding 2008). However, all these gene therapy approaches are still far from reaching clinical use.

3.2.1. The BH_4-responsive mutations

A significant number of PKU mutations result in phenotypes that are responsive to pharmacologic administration of the cofactor BH_4 (Zurflüh *et al.* 2008). Treatment of those patients with exogenous BH_4 results in an increased hepatic activity of hPAH and decreased hyperphenylalaninemia, opening a new strategy in PKU treatment and management (Kure *et al.* 1999; Muntau *et al.* 2002; Fiege and Blau 2007; Zurflüh *et al.* 2008; Blau *et al.* 2009). Mild PKU mutations, with considerable residual activity, are more likely to respond to BH_4 intake while non-responders, usually classic PKU, present two inactive alleles (Bernegger and Blau 2002; Muntau *et al.* 2002). Although BH_4-responsiveness can in some cases be predicted from the presence of specific mutations, it seems that the full genotype is more important. A database that contains the current list of BH_4-responsive genotypes can be found at *http://www.bh4.org*. Nonetheless, in PKU management the genotype should always be combined with a tetrahydrobiopterin-loading test followed by a 1 to 4-week trial of sapropterin dihydrochloride, a commercial formulation of BH_4, and the dose adjusted according to the response (Blau *et al.* 2009; Karačić *et al.* 2009; Feillet *et al.* 2010). In Europe, BH_4 is given orally to newborns at 20 mg/kg bodyweight per day (48-h loading test) and the blood L-Phe concentration measured at 0, 8, 16 and 24 h after the load (Blau *et al.* 2009; Blau *et al.* 2010a). BH_4-reponsiveness is normally

defined as an observed reduction of blood L-Phe of at least 30% (Bernegger and Blau 2002; Fiege and Blau 2007). A drastically L-Phe reduction (>85%) usually indicates a deficiency in the recycling and biosynthesis of the cofactor and a non-responder usually shows a reduction of less than 20% (Blau 2008; Blau *et al.* 2010b).

The molecular basis of BH_4-reponsiveness are multifactorial (Blau and Erlandsen 2004), but the main mechanisms appear to involve the correction of catalytic defects (decreased affinity for cofactor) and a natural chaperone effect with the stabilization of the mutant protein against misfolding/aggregation/degradation (Erlandsen *et al.* 2004; Pey *et al.* 2004a; Scavelli *et al.* 2005; Aguado *et al.* 2006; Gersting *et al.* 2010a).

The commercial form of the natural BH_4, sapropterin dihydrochloride (Kuvan™, BioMarin Pharmaceutical Inc, CA, USA), a soluble tablet formulation, has passed the clinical trials with approximately 20–50% of PKU patients reaching a reduction of >30% of blood L-Phe level (Burton *et al.* 2007; Levy *et al.* 2007; Blau *et al.* 2009; Trefz *et al.* 2009a). The overall frequency of BH_4-responsiveness is estimated to be ~50–60%, based on genetic allelic data (Zurflüh *et al.* 2008; Blau 2010). Sapropterin dihydrochloride was approved by the US Food and Drug Administration (FDA), European Medicines Agency (EMEA) and in Japan. In Europe it is indicate for the treatment of HPA in adult patients and PKU children (>4 years old) or BH_4 deficiency (Blau *et al.* 2009). The most frequent side effects are mild and include: upper respiratory tract infection, headache, vomiting, pharyngo-laryngeal pain, nasopharyngitis and diarrhea (Levy *et al.* 2007; Lee *et al.* 2008). Sapropterin dihydrochloride can provide a good L-Phe control in some patients, increasing their dietary L-Phe tolerance and opening the possibility to make adjustments towards a less restrictive diet (Blau 2010). However, data related to neurocognitive outcomes in long-term BH_4 treated patients is still scarce (Gassió *et al.* 2010).

3.2.2. Natural, chemical and pharmacological chaperones in PKU treatment

Several human genetic diseases are misfolding diseases caused by defects in protein folding or trafficking that results in the accumulation or degradation of the proteins by cellular protein quality control systems (Gregersen *et al.* 2006). This group of proteins is a likely candidate to new therapeutic strategies using small chemical compounds such as cofactors, protein inhibitors, osmolytes and ligands, the so called natural/chemical/pharmacological chaperones, in order to rescue the misfolded unstable mutant protein from degradation (loss of function) or aggregation

(gain of function), and thereby restoring protein function (Cohen and Kelly 2003; Kolter and Wendeler 2003; Loo and Clarke 2007; Leandro and Gomes 2008). The use of these compounds have been evaluated in several human diseases including neurodegenerative and metabolic disorders (Leandro and Gomes 2008), e.g. several pharmacological chaperones are already in clinical evaluation for treatment of some lysosomal storage diseases as Gaucher, Fabry and Pompe disease (Parenti 2009).

In PKU a large number of the identified missense mutations result in misfolded proteins and increased protein turnover, with PKU being considered a conformational disease with loss of function due to decrease conformational stability (Pey *et al.* 2007; Gersting *et al.* 2008). Natural chaperoning in PKU with cofactor BH_4 is an already approved treatment for a subset of PKU mutations (see section above). Chemical chaperoning of hPAH with osmolytes (glycerol, trimethylamine *N*-oxide (TMAO), mannitol) has been shown to increase the catalytic activity and stability of the wild-type and mutant forms of the protein (Leandro *et al.* 2001; Nascimento *et al.* 2008; Nascimento *et al.* 2010), opening new perspectives to the identification of low-molecular-weight compounds that increase enzyme activity/stability, which may also be useful in future enzyme replacement therapy formulation. Recently, a screening of over 1000 pharmacological agents has identified small-molecule binders that efficiently enhanced the thermal stability of wild-type and misfolded mutant forms, significantly increased the activity and steady-state PAH protein levels in transiently transfected cells and raised the PAH activity in mouse liver (Pey *et al.* 2008). Similar studies were extended to other AAAHs, namely tyrosine hydroxylase and tryptophan hydroxylase 2, with promising results (Calvo *et al.* 2010). These studies open a potential treatment strategy for PKU and other AAAHs related diseases by pharmacological chaperoning.

3.3. Interallelic complementation

A unique property of homo-oligomeric enzymes associated with human genetic disorders is their potential ability to exhibit interallelic complementation (IC), a phenomenon that occurs when a multimeric protein is formed from subunits produced by different mutant alleles of a gene, and particular combinations of two alleles, at a given *locus*, produce a less (positive IC) or a more (negative IC) severe phenotype than their homoallelic counterparts. IC is observed in homomeric enzymes where the protomers exhibit interactions resulting in hybrid proteins with

functional or stability properties deviating significantly from the average of the parental enzymes.

Interallelic complementation has been implicated in several human diseases (Veitia 2009), including neurodegenerative disorders such as familial amyloid polyneuropathy (Hammarström *et al.* 2003; Keetch *et al.* 2005), cancer (Nicholls *et al.* 2002; Dridi *et al.* 2003; Dong *et al.* 2007; Lee and Sabapathy 2008) and metabolic disorders such as, argininosuccinic aciduria (McInnes *et al.* 1984; Howell *et al.* 1998; Yu *et al.* 2001), erythropoietic protoporphyria (Ohgari *et al.* 2005), galactosemia (Elsevier and Fridovich-Keil 1996; Christacos and Fridovich-Keil 2002) and PKU (Kaufman *et al.* 1975).

In PKU the IC phenomenon was first pointed out in 1975, when Kaufman and Max (Kaufman *et al.* 1975) observed deviations from proportionality in PAH activity of parents of PKU patients (obligate heterozygous). They introduced the term negative interallelic complementation to illustrate the negative effects of protein-protein interactions occurring between the mutant subunits in the tetrameric hPAH enzyme. Additional clinical evidence lending support to a negative IC in some compound heterozygous PKU patients has been obtained from genotype-phenotype correlations studies, where some patients present a more severe phenotype than the anticipated by the predicted residual activity (PRA), based on *in vitro* assays of recombinant proteins (Burgard *et al.* 1996; Kayaalp *et al.* 1997; Guldberg *et al.* 1998; Rivera *et al.* 2000), and from clinical data of BH_4-loading tests where some patients displayed an absence or only a partial response to BH_4, although carrying two BH_4-responsive alleles (Karačić *et al.* 2009; Trefz *et al.* 2009b). Interactions between different hPAH protomers have been demonstrated by the yeast two-hybrid system (Waters *et al.* 2001), but the molecular mechanism of negative IC and its role in PKU pathogenesis is still far from being solved.

4. References

Abita J. P., Parniak M. and Kaufman S. (1984) The activation of rat liver phenylalanine hydroxylase by limited proteolysis, lysolecithin, and tocopherol phosphate. Changes in conformation and catalytic properties. *J. Biol. Chem.* 259: 14560-14566.

Abu-Omar M. M., Loaiza A. and Hontzeas N. (2005) Reaction mechanisms of mononuclear non-heme iron oxygenases. *Chem. Rev.* 105: 2227-2252.

Acosta P. B., Yannicelli S., Singh R., Mofidi S., Steiner R., DeVincentis E., Jurecki E., Bernstein L., Gleason S., Chetty M. and Rouse B. (2003) Nutrient intakes and physical growth of children with phenylketonuria undergoing nutrition therapy. *J. Am. Diet. Assoc.* 103: 1167-1173.

Acosta P. B., Yannicelli S., Singh R. H., Elsas II L. J., Mofidi S. and Steiner R. D. (2004) Iron status of children with phenylketonuria undergoing nutrition therapy assessed by transferrin receptors. *Genet. Med.* 6: 96-101.

Aguado C., Pérez B., Ugarte M. and Desviat L. R. (2006) Analysis of the effect of tetrahydrobiopterin on *PAH* gene expression in hepatoma cells. *FEBS Lett.* 580: 1697-1701.

Ahring K., Bélanger-Quintana A., Dokoupil K., Gokmen Ozel H., Lammardo A. M., MacDonald A., Motzfeldt K., Nowacka M., Robert M. and van Rijn M. (2009) Dietary management practices in phenylketonuria across European centres. *Clin. Nutr.* 28: 231-236.

Albrecht J., Garbade S. F. and Burgard P. (2009) Neuropsychological speed tests and blood phenylalanine levels in patients with phenylketonuria: a meta-analysis. *Neurosci. Biobehav. Rev.* 33: 414-421.

Anantharaman V., Koonin E. V. and Aravind L. (2001) Regulatory potential, phyletic distribution and evolution of ancient, intracellular small-molecule-binding domains. *J. Mol. Biol.* 307: 1271-1292.

Anastasoaie V., Kurzius L., Forbes P. and Waisbren S. (2008) Stability of blood phenylalanine levels and IQ in children with phenylketonuria. *Mol. Genet. Metab.* 95: 17-20.

Andersen O. A., Flatmark T. and Hough E. (2001) High resolution crystal structures of the catalytic domain of human phenylalanine hydroxylase in its catalytically active Fe(II) form and binary complex with tetrahydrobiopterin. *J. Mol. Biol.* 314: 279-291.

Andersen O. A., Flatmark T. and Hough E. (2002) Crystal structure of the ternary complex of the catalytic domain of human phenylalanine hydroxylase with tetrahydrobiopterin and 3-(2-thienyl)-L-alanine, and its implications for the mechanism of catalysis and substrate activation. *J. Mol. Biol.* 320: 1095-1108.

Andersen O. A., Stokka A. J., Flatmark T. and Hough E. (2003) 2.0 Å resolution crystal structures of the ternary complexes of human phenylalanine hydroxylase catalytic domain with tetrahydrobiopterin and 3-(2-thienyl)-L-alanine or L-norleucine: substrate specificity and molecular motions related to substrate binding. *J. Mol. Biol.* 333: 747-757.

Anderson P. J., Wood S. J., Francis D. E., Coleman L., Anderson V. and Boneh A. (2007) Are neuropsychological impairments in children with early-treated phenylketonuria (PKU) related to white matter abnormalities or elevated phenylalanine levels? *Dev. Neuropsychol.* 32: 645-668.

Antshel K. M. and Waisbren S. E. (2003) Developmental timing of exposure to elevated levels of phenylalanine is associated with ADHD symptom expression. *J. Abnorm. Child Psychol.* 31: 565-574.

Aravind L. and Koonin E. V. (1999) Gleaning non-trivial structural, functional and evolutionary information about proteins by iterative database searches. *J. Mol. Biol.* 287: 1023-1040.

Armstrong M. D. and Tyler F. H. (1955) Studies on phenylketonuria. I. Restricted phenylalanine intake in phenylketonuria. *J. Clin. Invest.* 34: 565-580.

Armstrong M. D. and Low N. L. (1957) Phenylketonuria VIII. Relation between age, serum phenylalanine level, and phenylpyruvic acid excretion. *Proc. Soc. Exp. Biol. Med.* 94: 142-146.

Arnold G. L., Kramer B. M., Kirby R. S., Plumeau P. B., Blakely E. M., Sanger Cregan L. S. and Davidson P. W. (1998) Factors affecting cognitive, motor, behavioral and executive functioning in children with phenylketonuria. *Acta Paediatr.* 87: 565-570.

Arnold G. L., Vladutiu C. J., Orlowski C. C., Blakely E. M. and DeLuca J. (2004) Prevalence of stimulant use for attentional dysfunction in children with phenylketonuria. *J. Inherit. Metab. Dis.* 27: 137-143.

Artuch R., Colomé C., Sierra C., Brandi N., Lambruschini N., Campistol J., Ugarte D. and Vilaseca M. A. (2004) A longitudinal study of antioxidant status in phenylketonuric patients. *Clin. Biochem.* 37: 198-203.

Bach-Mizrachi H., Underwood M. D., Kassir S. A., Bakalian M. J., Sibille E., Tamir H., Mann J. J. and Arango V. (2006) Neuronal tryptophan hydroxylase mRNA expression in the human dorsal and median raphe nuclei: major depression and suicide. *Neuropsychopharmacology* 31: 814-824.

Baieli S., Pavone L., Meli C., Fiumara A. and Coleman M. (2003) Autism and phenylketonuria. *J. Autism Dev. Disord.* 33: 201-204.

Baker R. E. and Shiman R. (1979) Measurement of phenylalanine hydroxylase turnover in cultured hepatoma cells. *J. Biol. Chem.* 254: 9633-9639.

Banik U., Wang G. A., Wagner P. D. and Kaufman S. (1997) Interaction of phosphorylated tryptophan hydroxylase with 14-3-3 proteins. *J. Biol. Chem.* 272: 26219-26225.

Bassan A., Blomberg M. R. and Siegbahn P. E. (2003a) Mechanism of aromatic hydroxylation by an activated FeIV=O core in tetrahydrobiopterin-dependent hydroxylases. *Chem. Eur. J.* 9: 4055-4067.

Bassan A., Blomberg M. R. and Siegbahn P. E. (2003b) Mechanism of dioxygen cleavage in tetrahydrobiopterin-dependent amino acid hydroxylases. *Chem. Eur. J.* 9: 106-115.

Bernegger C. and Blau N. (2002) High frequency of tetrahydrobiopterin-responsiveness among hyperphenylalaninemias: a study of 1,919 patients observed from 1988 to 2002. *Mol. Genet. Metab.* 77: 304-313.

Bickel H., Gerrard J. and Hickmans E. M. (1953) Influence of phenylalanine intake on phenylketonuria. *Lancet* 262: 812-813.

Bickel H., Gerrard J. and Hickmans E. M. (1954) The influence of phenylalanine intake on the chemistry and behaviour of a phenyl-ketonuric child. *Acta Paediatr.* 43: 64-77.

BioMarin Pharmaceutical Inc. (2009). "Results From Phase 1 Clinical Study of PEG-PAL in PKU and Update on Phase 2 Clinical Study." Retrieved January 18, 2011, from http://phx.corporate-ir.net/phoenix.zhtml?c=106657&p=irol-newsArticle&ID=1297622&highlight=.

Bjørgo E., Knappskog P. M., Martínez A., Stevens R. C. and Flatmark T. (1998) Partial characterization and three-dimensional-structural localization of eight mutations in exon 7 of the human phenylalanine hydroxylase gene associated with phenylketonuria. *Eur. J. Biochem.* 257: 1-10.

Bjørgo E., de Carvalho R. M. and Flatmark T. (2001) A comparison of kinetic and regulatory properties of the tetrameric and dimeric forms of wild-type and Thr427→Pro mutant human phenylalanine hydroxylase: contribution of the flexible hinge region Asp425-Gln429 to the tetramerization and cooperative substrate binding. *Eur. J. Biochem.* 268: 997-1005.

Blau N., Bonafé L. and Blaskovics M., Disorders of phenylalanine and tetrahydrobiopterin metabolism, in: N. Blau, M. Duran, M. Blaskovics and K. M. Gibson (Eds.) Physician's Guide to the Laboratory Diagnosis of Metabolic Diseases, Springer, Heidelberg, 2003, pp. 89-106.

Blau N. and Erlandsen H. (2004) The metabolic and molecular bases of tetrahydrobiopterin-responsive phenylalanine hydroxylase deficiency. *Mol. Genet. Metab.* 82: 101-111.

Blau N. (2008) Defining tetrahydrobiopterin (BH_4)-responsiveness in PKU. *J. Inherit. Metab. Dis.* 31: 2-3.

Blau N., Bélanger-Quintana A., Demirkol M., Feillet F., Giovannini M., MacDonald A., Trefz F. K. and van Spronsen F. J. (2009) Optimizing the use of sapropterin (BH_4) in the management of phenylketonuria. *Mol. Genet. Metab.* 96: 158-163.

Blau N. (2010) Sapropterin dihydrochloride for phenylketonuria and tetrahydrobiopterin deficiency. *Expert Rev. Endocrinol. Metab.* 5: 483-494.

Blau N., Bélanger-Quintana A., Demirkol M., Feillet F., Giovannini M., MacDonald A., Trefz F. K. and van Spronsen F. (2010a) Management of phenylketonuria in Europe: survey results from 19 countries. *Mol. Genet. Metab.* 99: 109-115.

Blau N., van Spronsen F. J. and Levy H. L. (2010b) Phenylketonuria. *Lancet* 376: 1417-1427.

Boldrini M., Underwood M. D., Mann J. J. and Arango V. (2005) More tryptophan hydroxylase in the brainstem dorsal raphe nucleus in depressed suicides. *Brain Res.* 1041: 19-28.

Burgard P., Rupp A., Konecki D. S., Trefz F. K., Schmidt H. and Lichter-Konecki U. (1996) Phenylalanine hydroxylase genotypes, predicted residual enzyme activity and phenotypic parameters of diagnosis and treatment of phenylketonuria. *Eur. J. Pediatr.* 155 Suppl 1: S11-15.

Burton B. K., Grange D. K., Milanowski A., Vockley G., Feillet F., Crombez E. A., Abadie V., Harding C. O., Cederbaum S., Dobbelaere D., Smith A. and Dorenbaum A. (2007) The response of patients with phenylketonuria and elevated serum phenylalanine to treatment with oral sapropterin dihydrochloride (6R-tetrahydrobiopterin): a phase II, multicentre, open-label, screening study. *J. Inherit. Metab. Dis.* 30: 700-707.

Calvo A. C., Scherer T., Pey A. L., Ying M., Winge I., McKinney J., Haavik J., Thöny B. and Martínez A. (2010) Effect of pharmacological chaperones on brain tyrosine hydroxylase and tryptophan hydroxylase 2. *J. Neurochem.* 114: 853-863.

Carvalho R. N., Solstad T., Bjørgo E., Barroso J. F. and Flatmark T. (2003) Deamidations in recombinant human phenylalanine hydroxylase. Identification of labile asparagine residues and functional characterization of Asn → Asp mutant forms. *J. Biol. Chem.* 278: 15142-15152.

Channon S., Goodman G., Zlotowitz S., Mockler C. and Lee P. J. (2007) Effects of dietary management of phenylketonuria on long-term cognitive outcome. *Arch. Dis. Child.* 92: 213-218.

Chen C., Glatt S. J. and Tsuang M. T. (2008) The tryptophan hydroxylase gene influences risk for bipolar disorder but not major depressive disorder: results of meta-analyses. *Bipolar Disord.* 10: 816-821.

Chipman D. M. and Shaanan B. (2001) The ACT domain family. *Curr. Opin. Struct. Biol.* 11: 694-700.

Christacos N. C. and Fridovich-Keil J. L. (2002) Impact of patient mutations on heterodimer formation and function in human galactose-1-P uridylyltransferase. *Mol. Genet. Metab.* 76: 319-326.

Cichon S., Winge I., Mattheisen M., Georgi A., Karpushova A., Freudenberg J., Freudenberg-Hua Y., Babadjanova G., Van Den Bogaert A., Abramova L. I., Kapiletti S., Knappskog P. M., McKinney J., Maier W., Jamra R. A., Schulze T. G., Schumacher J., Propping P., Rietschel M., Haavik J. and Nöthen M. M. (2008) Brain-specific tryptophan hydroxylase 2 (TPH2): a functional Pro206Ser substitution and variation in the 5'-region are associated with bipolar affective disorder. *Hum. Mol. Genet.* 17: 87-97.

Clader D. E. (1957) Accelerated intellectual growth and personality development as seen in phenylketonuric subjects during medical treatment. *Am. J. Ment. Defic.* 62: 538-542.

ClinicalTrials.gov. (2010). "Dose-Finding Study to Evaluate the Safety, Efficacy, and Tolerability of Multiple Doses of rAvPAL-PEG in Subjects With Phenylketonuria (PKU)." Retrieved January 18, 2011, from http://www.clinicaltrials.gov/ct2/show/NCT00925054?term=pal-001&rank=1.

Cohen F. E. and Kelly J. W. (2003) Therapeutic approaches to protein-misfolding diseases. *Nature* 426: 905-909.

Costas M., Mehn M. P., Jensen M. P. and Que L., Jr. (2004) Dioxygen activation at mononuclear nonheme iron active sites: enzymes, models, and intermediates. *Chem. Rev.* 104: 939-986.

Curtius H. C., Matasovic A., Schoedon G., Kuster T., Guibaud P., Giudici T. and Blau N. (1990) 7-Substituted pterins. A new class of mammalian pteridines. *J. Biol. Chem.* 265: 3923-3930.

Daubner S. C., Hillas P. J. and Fitzpatrick P. F. (1997) Characterization of chimeric pterin-dependent hydroxylases: contributions of the regulatory domains of tyrosine and phenylalanine hydroxylase to substrate specificity. *Biochemistry* 36: 11574-11582.

Davis M. D., Kaufman S. and Milstien S. (1991) Conversion of 6-substituted tetrahydropterins to 7-isomers via phenylalanine hydroxylase-generated intermediates. *Proc. Natl. Acad. Sci. U. S. A.* 88: 385-389.

Ding Z., Harding C. O., Rebuffat A., Elzaouk L., Wolff J. A. and Thöny B. (2008) Correction of murine PKU following AAV-mediated intramuscular expression of a complete phenylalanine hydroxylating system. *Mol. Ther.* 16: 673-681.

Dix T. A. and Benkovic S. J. (1985) Mechanism of "uncoupled" tetrahydropterin oxidation by phenylalanine hydroxylase. *Biochemistry* 24: 5839-5846.

Dix T. A., Bollag G. E., Domanico P. L. and Benkovic S. J. (1985) Phenylalanine hydroxylase: absolute configuration and source of oxygen of the 4a-hydroxytetrahydropterin species. *Biochemistry* 24: 2955-2958.

Dix T. A. and Benkovic S. J. (1988) Mechanism of oxygen activation by pteridine-dependent monooxygenases. *Acc. Chem. Res.* 21: 101–107.

Dong P., Tada M., Hamada J., Nakamura A., Moriuchi T. and Sakuragi N. (2007) p53 dominant-negative mutant R273H promotes invasion and migration of human endometrial cancer HHUA cells. *Clin. Exp. Metastasis* 24: 471-483.

Døskeland A. P., Døskeland S. O., Øgreid D. and Flatmark T. (1984) The effect of ligands of phenylalanine 4-monooxygenase on the cAMP-dependent phosphorylation of the enzyme. *J. Biol. Chem.* 259: 11242-11248.

Døskeland A. P. and Flatmark T. (1996) Recombinant human phenylalanine hydroxylase is a substrate for the ubiquitin-conjugating enzyme system. *Biochem. J.* 319: 941-945.

Døskeland A. P., Martínez A., Knappskog P. M. and Flatmark T. (1996) Phosphorylation of recombinant human phenylalanine hydroxylase: effect on catalytic activity, substrate activation and protection against non-specific cleavage of the fusion protein by restriction protease. *Biochem. J.* 313: 409-414.

Døskeland A. P. and Flatmark T. (2001) Conjugation of phenylalanine hydroxylase with polyubiquitin chains catalysed by rat liver enzymes. *Biochim. Biophys. Acta* 1547: 379-386.

Dridi W., Fetni R., Lavoie J., Poupon M. F. and Drouin R. (2003) The dominant-negative effect of p53 mutants and p21 induction in tetraploid G1 arrest depends on the type of p53 mutation and the nature of the stimulus. *Cancer Genet. Cytogenet.* 143: 39-49.

Dunkley P. R., Bobrovskaya L., Graham M. E., von Nagy-Felsobuki E. I. and Dickson P. W. (2004) Tyrosine hydroxylase phosphorylation: regulation and consequences. *J. Neurochem.* 91: 1025-1043.

Eavri R. and Lorberboum-Galski H. (2007) A novel approach for enzyme replacement therapy. The use of phenylalanine hydroxylase-based fusion proteins for the treatment of phenylketonuria. *J. Biol. Chem.* 282: 23402-23409.

Ekwall O., Hedstrand H., Grimelius L., Haavik J., Perheentupa J., Gustafsson J., Husebye E., Kämpe O. and Rorsman F. (1998) Identification of tryptophan hydroxylase as an intestinal autoantigen. *Lancet* 352: 279-283.

Elsevier J. P. and Fridovich-Keil J. L. (1996) The Q188R mutation in human galactose-1-phosphate uridylyltransferase acts as a partial dominant negative. *J. Biol. Chem.* 271: 32002-32007.

Erlandsen H., Fusetti F., Martínez A., Hough E., Flatmark T. and Stevens R. C. (1997) Crystal structure of the catalytic domain of human phenylalanine hydroxylase reveals the structural basis for phenylketonuria. *Nat. Struct. Biol.* 4: 995-1000.

Erlandsen H., Bjørgo E., Flatmark T. and Stevens R. C. (2000) Crystal structure and site-specific mutagenesis of pterin-bound human phenylalanine hydroxylase. *Biochemistry* 39: 2208-2217.

Erlandsen H., Pey A. L., Gámez A., Pérez B., Desviat L. R., Aguado C., Koch R., Surendran S., Tyring S., Matalon R., Scriver C. R., Ugarte M., Martínez A. and Stevens R. C. (2004) Correction of kinetic and stability defects by tetrahydrobiopterin in phenylketonuria patients with certain phenylalanine hydroxylase mutations. *Proc. Natl. Acad. Sci. U. S. A.* 101: 16903-16908.

Eser B. E., Barr E. W., Frantom P. A., Saleh L., Bollinger J. M., Jr., Krebs C. and Fitzpatrick P. F. (2007) Direct spectroscopic evidence for a high-spin Fe(IV) intermediate in tyrosine hydroxylase. *J. Am. Chem. Soc.* 129: 11334-11335.

Eser B. E. and Fitzpatrick P. F. (2010) Measurement of intrinsic rate constants in the tyrosine hydroxylase reaction. *Biochemistry* 49: 645-652.

Etzel M. R. (2004) Manufacture and use of dairy protein fractions. *J. Nutr.* 134: 996S-1002S.

Feig A. L. and Lippard S. J. (1994) Reactions of non-heme iron(II) centers with dioxygen in biology and chemistry. *Chem. Rev.* 94: 759–805.

Feillet F., van Spronsen F. J., MacDonald A., Trefz F. K., Demirkol M., Giovannini M., Bélanger-Quintana A. and Blau N. (2010) Challenges and pitfalls in the management of phenylketonuria. *Pediatrics* 126: 333-341.

Fiege B. and Blau N. (2007) Assessment of tetrahydrobiopterin (BH_4) responsiveness in phenylketonuria. *J. Pediatr.* 150: 627-630.

Fisher D. B., Kirkwood R. and Kaufman S. (1972) Rat liver phenylalanine hydroxylase, an iron enzyme. *J. Biol. Chem.* 247: 5161-5167.

Fisher D. B. and Kaufman S. (1973) The stimulation of rat liver phenylalanine hydroxylase by lysolecithin and chymotrypsin. *J. Biol. Chem.* 248: 4345-4353.

Fitzpatrick P. F. (1999) Tetrahydropterin-dependent amino acid hydroxylases. *Annu. Rev. Biochem.* 68: 355-381.

Fitzpatrick P. F. (2000) The aromatic amino acid hydroxylases. *Adv. Enzymol. Relat. Areas Mol. Biol.* 74: 235-294.

Fitzpatrick P. F. (2003) Mechanism of aromatic amino acid hydroxylation. *Biochemistry* 42: 14083-14091.

Flatmark T., Knappskog P. M., Bjørgo E. and Martínez A., Molecular characterization of disease related mutant forms of human phenylalanine hydroxylase and tyrosine hydroxylase, in: W. Pfleiderer and H. Rokos (Eds.), Chemistry and biology of pteridines and folates, vol. 8, Blackwell Science, Berlin, 1997, pp. 503-508.

Flatmark T., Almås B., Knappskog P. M., Berge S. V., Svebak R. M., Chehin R., Muga A. and Martínez A. (1999) Tyrosine hydroxylase binds tetrahydrobiopterin cofactor with negative cooperativity, as shown by kinetic analyses and surface plasmon resonance detection. *Eur. J. Biochem.* 262: 840-849.

Flatmark T. and Stevens R. C. (1999) Structural insight into the aromatic amino acid hydroxylases and their disease-related mutant forms. *Chem. Rev.* 99: 2137-2160.

Flatmark T., Stokka A. J. and Berge S. V. (2001) Use of surface plasmon resonance for real-time measurements of the global conformational transition in human phenylalanine hydroxylase in response to substrate binding and catalytic activation. *Anal. Biochem.* 294: 95-101.

Flatmark T., Almås B. and Ziegler M. G. (2002) Catecholamine metabolism: an update on key biosynthetic enzymes and vesicular monoamine transporters. *Ann. N. Y. Acad. Sci.* 971: 69-75.

Flydal M. I., Mohn T. C., Pey A. L., Siltberg-Liberles J., Teigen K. and Martínez A. (2010) Superstoichiometric binding of L-Phe to phenylalanine hydroxylase from *Caenorhabditis elegans*: evolutionary implications. *Amino Acids* (*In press*), doi:10.1007/s00726-010-0611-6.

Følling A. (1934) Über ausscheidung von phenylbrenztraubensäure in den harn als stoffwechselanomalie in verbindung mit imbezillität. *Hoppe-Seylers Z. Physiol. Chem.* 277: 169-176.

Fusetti F., Erlandsen H., Flatmark T. and Stevens R. C. (1998) Structure of tetrameric human phenylalanine hydroxylase and its implications for phenylketonuria. *J. Biol. Chem.* 273: 16962-16967.

Gámez A., Pérez B., Ugarte M. and Desviat L. R. (2000) Expression analysis of phenylketonuria mutations. Effect on folding and stability of the phenylalanine hydroxylase protein. *J. Biol. Chem.* 275: 29737-29742.

Gámez A., Wang L., Straub M., Patch M. G. and Stevens R. C. (2004) Toward PKU enzyme replacement therapy: PEGylation with activity retention for three forms of recombinant phenylalanine hydroxylase. *Mol. Ther.* 9: 124-129.

Gámez A., Sarkissian C. N., Wang L., Kim W., Straub M., Patch M. G., Chen L., Striepeke S., Fitzpatrick P., Lemontt J. F., O'Neill C., Scriver C. R. and Stevens R. C. (2005) Development of pegylated forms of recombinant *Rhodosporidium toruloides* phenylalanine ammonia-lyase for the treatment of classical phenylketonuria. *Mol. Ther.* 11: 986-989.

Gassió R., Artuch R., Vilaseca M. A., Fusté E., Boix C., Sans A. and Campistol J. (2005) Cognitive functions in classic phenylketonuria and mild hyperphenylalaninaemia: experience in a paediatric population. *Dev. Med. Child Neurol.* 47: 443-448.

Gassió R., Vilaseca M. A., Lambruschini N., Boix C., Fusté M. E. and Campistol J. (2010) Cognitive functions in patients with phenylketonuria in long-term treatment with tetrahydrobiopterin. *Mol. Genet. Metab.* 99 Suppl 1: S75-78.

Gersting S. W., Kemter K. F., Staudigl M., Messing D. D., Danecka M. K., Lagler F. B., Sommerhoff C. P., Roscher A. A. and Muntau A. C. (2008) Loss of function in phenylketonuria is caused by impaired molecular motions and conformational instability. *Am. J. Hum. Genet.* 83: 5-17.

Gersting S. W., Lagler F. B., Eichinger A., Kemter K. F., Danecka M. K., Messing D. D., Staudigl M., Domdey K. A., Zsifkovits C., Fingerhut R., Glossmann H., Roscher A. A. and Muntau A. C. (2010a) Pah^{enu1} is a mouse model for tetrahydrobiopterin-responsive phenylalanine hydroxylase deficiency and promotes analysis of the pharmacological chaperone mechanism *in vivo*. *Hum. Mol. Genet.* 19: 2039-2049.

Gersting S. W., Staudigl M., Truger M. S., Messing D. D., Danecka M. K., Sommerhoff C. P., Kemter K. F. and Muntau A. C. (2010b) Activation of phenylalanine hydroxylase induces positive cooperativity toward the natural cofactor. *J. Biol. Chem.* 285: 30686-30697.

Ghozlan A., Varoquaux O. and Abadie V. (2004) Is monoamine oxydase-B a modifying gene and phenylethylamine a harmful compound in phenylketonuria? *Mol. Genet. Metab.* 83: 337-340.

Gibbs B. S. and Benkovic S. J. (1991) Affinity labeling of the active site and the reactive sulfhydryl associated with activation of rat liver phenylalanine hydroxylase. *Biochemistry* 30: 6795-6802.

Giovannini M., Verduci E., Salvatici E., Fiori L. and Riva E. (2007) Phenylketonuria: dietary and therapeutic challenges. *J. Inherit. Metab. Dis.* 30: 145-152.

Gjetting T., Petersen M., Guldberg P. and Güttler F. (2001a) Missense mutations in the N-terminal domain of human phenylalanine hydroxylase interfere with binding of regulatory phenylalanine. *Am. J. Hum. Genet.* 68: 1353-1360.

Gjetting T., Petersen M., Guldberg P. and Güttler F. (2001b) *In vitro* expression of 34 naturally occurring mutant variants of phenylalanine hydroxylase: correlation with metabolic phenotypes and susceptibility toward protein aggregation. *Mol. Genet. Metab.* 72: 132-143.

Goodwill K. E., Sabatier C., Marks C., Raag R., Fitzpatrick P. F. and Stevens R. C. (1997) Crystal structure of tyrosine hydroxylase at 2.3 Å and its implications for inherited neurodegenerative diseases. *Nat. Struct. Biol.* 4: 578-585.

Gottschall D. W., Dietrich R. F., Benkovic S. J. and Shiman R. (1982) Phenylalanine hydroxylase. Correlation of the iron content with activity and the preparation and reconstitution of the apoenzyme. *J. Biol. Chem.* 257: 845-849.

Grant G. A. (2006) The ACT domain: a small molecule binding domain and its role as a common regulatory element. *J. Biol. Chem.* 281: 33825-33829.

Gregersen N., Bross P., Andresen B. S., Pedersen C. B., Corydon T. J. and Bolund L. (2001) The role of chaperone-assisted folding and quality control in inborn errors of metabolism: protein folding disorders. *J. Inherit. Metab. Dis.* 24: 189-212.

Gregersen N. (2006) Protein misfolding disorders: pathogenesis and intervention. *J. Inherit. Metab. Dis.* 29: 456-470.

Gregersen N., Bross P., Vang S. and Christensen J. H. (2006) Protein misfolding and human disease. *Annu. Rev. Genomics Hum. Genet.* 7: 103-124.

Grima B., Lamouroux A., Boni C., Julien J. F., Javoy-Agid F. and Mallet J. (1987) A single human gene encoding multiple tyrosine hydroxylases with different predicted functional characteristics. *Nature* 326: 707-711.

Güttler F. and Guldberg P. (1994) Mutations in the phenylalanine hydroxylase gene: genetic determinants for the phenotypic variability of hyperphenylalaninemia. *Acta Paediatr. Suppl.* 407: 49-56.

Guldberg P., Rey F., Zschocke J., Romano V., François B., Michiels L., Ullrich K., Hoffmann G. F., Burgard P., Schmidt H., Meli C., Riva E., Dianzani I., Ponzone A., Rey J. and Güttler F. (1998) A European multicenter study of phenylalanine hydroxylase deficiency: classification of 105 mutations and a general system for genotype-based prediction of metabolic phenotype. *Am. J. Hum. Genet.* 63: 71-79.

Guthrie R. and Susi A. (1963) A simple phenylalanine method for detecting phenylketonuria in large populations of newborn infants. *Pediatrics* 32: 338-343.

Haavik J. and Toska K. (1998) Tyrosine hydroxylase and Parkinson's disease. *Mol. Neurobiol.* 16: 285-309.

Haavik J., Blau N. and Thöny B. (2008) Mutations in human monoamine-related neurotransmitter pathway genes. *Hum. Mutat.* 29: 891-902.

Hagedoorn P. L., Schmidt P. P., Andersson K. K., Hagen W. R., Flatmark T. and Martínez A. (2001) The effect of substrate, dihydrobiopterin, and dopamine on the EPR spectroscopic properties and the midpoint potential of the catalytic iron in recombinant human phenylalanine hydroxylase. *J. Biol. Chem.* 276: 22850-22856.

Hall T. A. (1999) BioEdit: a user-friendly biological sequence alignment editor and analysis program for Windows 95/98/NT. *Nucl. Acids Symp. Ser.* 41: 95-98.

Halskau Jr. O., Ying M., Baumann A., Kleppe R., Rodriguez-Larrea D., Almås B., Haavik J. and Martínez A. (2009) Three-way interaction between 14-3-3 proteins, the N-terminal region of tyrosine hydroxylase, and negatively charged membranes. *J. Biol. Chem.* 284: 32758-32769.

Hammarström P., Wiseman R. L., Powers E. T. and Kelly J. W. (2003) Prevention of transthyretin amyloid disease by changing protein misfolding energetics. *Science* 299: 713-716.

Han A. Y., Lee A. Q. and Abu-Omar M. M. (2006) EPR and UV-vis studies of the nitric oxide adducts of bacterial phenylalanine hydroxylase: effects of cofactor and substrate on the iron environment. *Inorg. Chem.* 45: 4277-4283.

Harding C. (2008) Progress toward cell-directed therapy for phenylketonuria. *Clin. Genet.* 74: 97-104.

Hegg E. L. and Que L., Jr. (1997) The 2-His-1-carboxylate facial triad - an emerging structural motif in mononuclear non-heme iron(II) enzymes. *Eur. J. Biochem.* 250: 625-629.

Hoang L., Byck S., Prevost L. and Scriver C. R. (1996) PAH Mutation Analysis Consortium Database: a database for disease-producing and other allelic variation at the human PAH locus. *Nucleic Acids Res.* 24: 127-131.

Hoeks M. P., den Heijer M. and Janssen M. C. (2009) Adult issues in phenylketonuria. *Neth. J. Med.* 67: 2-7.

Hoeksma M., Reijngoud D. J., Pruim J., de Valk H. W., Paans A. M. and van Spronsen F. J. (2009) Phenylketonuria: High plasma phenylalanine decreases cerebral protein synthesis. *Mol. Genet. Metab.* 96: 177-182.

Hoffmann G. F., Assmann B., Bräutigam C., Dionisi-Vici C., Häussler M., de Klerk J. B., Naumann M., Steenbergen-Spanjers G. C., Strassburg H. M. and Wevers R. A. (2003) Tyrosine hydroxylase deficiency causes progressive encephalopathy and dopa-nonresponsive dystonia. *Ann. Neurol.* 54 Suppl 6: S56-65.

Horne J., Jennings I. G., Teh T., Gooley P. R. and Kobe B. (2002) Structural characterization of the N-terminal autoregulatory sequence of phenylalanine hydroxylase. *Protein Sci.* 11: 2041-2047.

Hörster F., Schwab M. A., Sauer S. W., Pietz J., Hoffmann G. F., Okun J. G., Kölker S. and Kins S. (2006) Phenylalanine reduces synaptic density in mixed cortical cultures from mice. *Pediatr. Res.* 59: 544-548.

Howell P. L., Turner M. A., Christodoulou J., Walker D. C., Craig H. J., Simard L. R., Ploder L. and McInnes R. R. (1998) Intragenic complementation at the argininosuccinate lyase locus: reconstruction of the active site. *J. Inherit. Metab. Dis.* 21 Suppl 1: 72-85.

Hufton S. E., Jennings I. G. and Cotton R. G. (1995) Structure and function of the aromatic amino acid hydroxylases. *Biochem. J.* 311: 353-366.

Huijbregts S. C., de Sonneville L. M., van Spronsen F. J., Licht R. and Sergeant J. A. (2002) The neuropsychological profile of early and continuously treated phenylketonuria: orienting, vigilance, and maintenance *versus* manipulation-functions of working memory. *Neurosci. Biobehav. Rev.* 26: 697-712.

Huttenlocher P. R. (2000) The neuropathology of phenylketonuria: human and animal studies. *Eur. J. Pediatr.* 159 Suppl 2: S102-106.

Ichinose H., Suzuki T., Inagaki H., Ohye T. and Nagatsu T. (1999) Molecular genetics of dopa-responsive dystonia. *Biol. Chem.* 380: 1355-1364.

Ikeda K., Schiltz E., Fujii T., Takahashi M., Mitsui K., Kodera Y., Matsushima A., Inada Y., Schulz G. E. and Nishimura H. (2005) Phenylalanine ammonia-lyase modified with polyethylene glycol: potential therapeutic agent for phenylketonuria. *Amino Acids* 29: 283-287.

Iwaki M., Phillips R. S. and Kaufman S. (1986) Proteolytic modification of the amino-terminal and carboxyl-terminal regions of rat hepatic phenylalanine hydroxylase. *J. Biol. Chem.* 261: 2051-2056.

Jennings I. G., Teh T. and Kobe B. (2001) Essential role of the N-terminal autoregulatory sequence in the regulation of phenylalanine hydroxylase. *FEBS Lett.* 488: 196-200.

Jervis G. A. (1947) Studies on phenylpyruvic oligophrenia: the position of the metabolic error. *J. Biol. Chem.* 169: 651-656.

Jervis G. A. (1953) Phenylpyruvic oligophrenia deficiency of phenylalanine-oxidizing system. *Proc. Soc. Exp. Biol. Med.* 82: 514-515.

Johansen P. A., Wolf W. A. and Kuhn D. M. (1991) Inhibition of tryptophan hydroxylase by benserazide and other catechols. *Biochem. Pharmacol.* 41: 625-628.

Jung S. C., Park J. W., Oh H. J., Choi J. O., Seo K. I., Park E. S. and Park H. Y. (2008) Protective effect of recombinant adeno-associated virus 2/8-mediated gene therapy from the maternal hyperphenylalaninemia in offsprings of a mouse model of phenylketonuria. *J. Korean Med. Sci.* 23: 877-883.

Kalhan S. C. and Bier D. M. (2008) Protein and amino acid metabolism in the human newborn. *Annu. Rev. Nutr.* 28: 389-410.

Kalsner L. R., Rohr F. J., Strauss K. A., Korson M. S. and Levy H. L. (2001) Tyrosine supplementation in phenylketonuria: diurnal blood tyrosine levels and presumptive brain influx of tyrosine and other large neutral amino acids. *J. Pediatr.* 139: 421-427.

Kaneda N., Kobayashi K., Ichinose H., Kishi F., Nakazawa A., Kurosawa Y., Fujita K. and Nagatsu T. (1987) Isolation of a novel cDNA clone for human tyrosine hydroxylase: alternative RNA splicing produces four kinds of mRNA from a single gene. *Biochem. Biophys. Res. Commun.* 146: 971-975.

Kang T. S., Wang L., Sarkissian C. N., Gámez A., Scriver C. R. and Stevens R. C. (2010) Converting an injectable protein therapeutic into an oral form: phenylalanine ammonia lyase for phenylketonuria. *Mol. Genet. Metab.* 99: 4-9.

Kappock T. J., Harkins P. C., Friedenberg S. and Caradonna J. P. (1995) Spectroscopic and kinetic properties of unphosphorylated rat hepatic phenylalanine hydroxylase expressed in *Escherichia coli*. Comparison of resting and activated states. *J. Biol. Chem.* 270: 30532-30544.

Kappock T. J. and Caradonna J. P. (1996) Pterin-dependent amino acid hydroxylases. *Chem. Rev.* 96: 2659-2756.

Karačić I., Meili D., Sarnavka V., Heintz C., Thöny B., Ramadža D. P., Fumić K., Mardešić D., Barić I. and Blau N. (2009) Genotype-predicted tetrahydrobiopterin (BH_4)-responsiveness and molecular genetics in Croatian patients with phenylalanine hydroxylase (PAH) deficiency. *Mol. Genet. Metab.* 97: 165-171.

Kaufman S. (1971) The phenylalanine hydroxylating system from mammalian liver. *Adv. Enzymol. Relat. Areas Mol. Biol.* 35: 245-319.

Kaufman S., Max E. E. and Kang E. S. (1975) Phenylalanine hydroxylase activity in liver biopsies from hyperphenylalaninemia heterozygotes: deviation from proportionality with gene dosage. *Pediatr. Res.* 9: 632-634.

Kaufman S. (1993) The phenylalanine hydroxylating system. *Adv. Enzymol. Relat. Areas Mol. Biol.* 67: 77-264.

Kaufman S. (1995) Tyrosine hydroxylase. *Adv. Enzymol. Relat. Areas Mol. Biol.* 70: 103-220.

Kaufman S. (1999) A model of human phenylalanine metabolism in normal subjects and in phenylketonuric patients. *Proc. Natl. Acad. Sci. U. S. A.* 96: 3160-3164.

Kayaalp E., Treacy E., Waters P. J., Byck S., Nowacki P. and Scriver C. R. (1997) Human phenylalanine hydroxylase mutations and hyperphenylalaninemia phenotypes: a metanalysis of genotype-phenotype correlations. *Am. J. Hum. Genet.* 61: 1309-1317.

Keetch C. A., Bromley E. H., McCammon M. G., Wang N., Christodoulou J. and Robinson C. V. (2005) L55P transthyretin accelerates subunit exchange and leads to rapid formation of hybrid tetramers. *J. Biol. Chem.* 280: 41667-41674.

Kemsley J. N., Mitić N., Zaleski K. L., Caradonna J. P. and Solomon E. I. (1999) Circular dichroism and magnetic circular dichroism spectroscopy of the catalytically competent ferrous active site of phenylalanine hydroxylase and its interaction with pterin cofactor. *J. Am. Chem. Soc.* 121: 1528-1536.

Kim W., Erlandsen H., Surendran S., Stevens R. C., Gámez A., Michols-Matalon K., Tyring S. K. and Matalon R. (2004) Trends in enzyme therapy for phenylketonuria. *Mol. Ther.* 10: 220-224.

Knappskog P. M., Flatmark T., Mallet J., Lüdecke B. and Bartholomé K. (1995) Recessively inherited L-DOPA-responsive dystonia caused by a point mutation (Q381K) in the tyrosine hydroxylase gene. *Hum. Mol. Genet.* 4: 1209-1212.

Knappskog P. M., Eiken H. G., Martínez A., Bruland O., Apold J. and Flatmark T. (1996a) PKU mutation (D143G) associated with an apparent high residual enzyme activity: expression of a kinetic variant form of phenylalanine hydroxylase in three different systems. *Hum. Mutat.* 8: 236-246.

Knappskog P. M., Flatmark T., Aarden J. M., Haavik J. and Martínez A. (1996b) Structure/function relationships in human phenylalanine hydroxylase. Effect of terminal deletions on the oligomerization, activation and cooperativity of substrate binding to the enzyme. *Eur. J. Biochem.* 242: 813-821.

Kobayashi K. and Nagatsu T. (2005) Molecular genetics of tyrosine 3-monooxygenase and inherited diseases. *Biochem. Biophys. Res. Commun.* 338: 267-270.

Kobe B., Jennings I. G., House C. M., Michell B. J., Goodwill K. E., Santarsiero B. D., Stevens R. C., Cotton R. G. and Kemp B. E. (1999) Structural basis of autoregulation of phenylalanine hydroxylase. *Nat. Struct. Biol.* 6: 442-448.

Kobe B. and Kemp B. E. (1999) Active site-directed protein regulation. *Nature* 402: 373-376.

Koch R., Burton B., Hoganson G., Peterson R., Rhead W., Rouse B., Scott R., Wolff J., Stern A. M., Güttler F., Nelson M., de la Cruz F., Coldwell J., Erbe R., Geraghty M. T., Shear C., Thomas J. and Azen C. (2002) Phenylketonuria in adulthood: a collaborative study. *J. Inherit. Metab. Dis.* 25: 333-346.

Koch R., Hanley W., Levy H., Matalon K., Matalon R., Rouse B., Trefz F., Güttler F., Azen C., Platt L., Waisbren S., Widaman K., Ning J., Friedman E. G. and de la Cruz F. (2003a) The maternal phenylketonuria international study: 1984-2002. *Pediatrics* 112: 1523-1529.

Koch R., Moseley K. D., Yano S., Nelson Jr. M. and Moats R. A. (2003b) Large neutral amino acid therapy and phenylketonuria: a promising approach to treatment. *Mol. Genet. Metab.* 79: 110-113.

Koehntop K. D., Emerson J. P. and Que Jr. L. (2005) The 2-His-1-carboxylate facial triad: a versatile platform for dioxygen activation by mononuclear non-heme iron(II) enzymes. *J. Biol. Inorg. Chem.* 10: 87-93.

Koletzko B., Sauerwald T., Demmelmair H., Herzog M., von Schenck U., Böhles H., Wendel U. and Seidel J. (2007) Dietary long-chain polyunsaturated fatty acid supplementation in infants with phenylketonuria: a randomized controlled trial. *J. Inherit. Metab. Dis.* 30: 326-332.

Kolter T. and Wendeler M. (2003) Chemical chaperones - a new concept in drug research. *Chembiochem* 4: 260-264.

Konecki D. S., Wang Y., Trefz F. K., Lichter-Konecki U. and Woo S. L. (1992) Structural characterization of the 5' regions of the human phenylalanine hydroxylase gene. *Biochemistry* 31: 8363-8368.

Kure S., Hou D. C., Ohura T., Iwamoto H., Suzuki S., Sugiyama N., Sakamoto O., Fujii K., Matsubara Y. and Narisawa K. (1999) Tetrahydrobiopterin-responsive phenylalanine hydroxylase deficiency. *J. Pediatr.* 135: 375-378.

Laclair C. E., Ney D. M., MacLeod E. L. and Etzel M. R. (2009) Purification and use of glycomacropeptide for nutritional management of phenylketonuria. *J. Food Sci.* 74: E199-206.

Lange S. J. and Que Jr. L. (1998) Oxygen activating nonheme iron enzymes. *Curr. Opin. Chem. Biol.* 2: 159-172.

Leandro P., Lechner M. C., Tavares de Almeida I. and Konecki D. (2001) Glycerol increases the yield and activity of human phenylalanine hydroxylase mutant enzymes produced in a prokaryotic expression system. *Mol. Genet. Metab.* 73: 173-178.

Leandro P. and Gomes C. M. (2008) Protein misfolding in conformational disorders: rescue of folding defects and chemical chaperoning. *Mini-Rev. Med. Chem.* 8: 901-911.

Lee M. K. and Sabapathy K. (2008) The R246S hot-spot p53 mutant exerts dominant-negative effects in embryonic stem cells *in vitro* and *in vivo*. *J. Cell Sci.* 121: 1899-1906.

Lee P., Treacy E. P., Crombez E., Wasserstein M., Waber L., Wolff J., Wendel U., Dorenbaum A., Bebchuk J., Christ-Schmidt H., Seashore M., Giovannini M., Burton B. K. and Morris A. A. (2008) Safety and efficacy of 22 weeks of treatment with sapropterin dihydrochloride in patients with phenylketonuria. *Am. J. Med. Genet. A* 146: 2851-2859.

Lenke R. R. and Levy H. L. (1980) Maternal phenylketonuria and hyperphenylalaninemia. An international survey of the outcome of untreated and treated pregnancies. *N. Engl. J. Med.* 303: 1202-1208.

Leuzzi V., Pansini M., Sechi E., Chiarotti F., Carducci C., Levi G. and Antonozzi I. (2004) Executive function impairment in early-treated PKU subjects with normal mental development. *J. Inherit. Metab. Dis.* 27: 115-125.

Levy H. L. and Waisbren S. E. (1983) Effects of untreated maternal phenylketonuria and hyperphenylalaninemia on the fetus. *N. Engl. J. Med.* 309: 1269-1274.

Levy H. L., Milanowski A., Chakrapani A., Cleary M., Lee P., Trefz F. K., Whitley C. B., Feillet F., Feigenbaum A. S., Bebchuk J. D., Christ-Schmidt H. and Dorenbaum A. (2007) Efficacy of sapropterin dihydrochloride (tetrahydrobiopterin, 6*R*-BH_4) for reduction of phenylalanine concentration in patients with phenylketonuria: a phase III randomised placebo-controlled study. *Lancet* 370: 504-510.

Li D. and He L. (2006a) Further clarification of the contribution of the tryptophan hydroxylase (*TPH*) gene to suicidal behavior using systematic allelic and genotypic meta-analyses. *Hum. Genet.* 119: 233-240.

Li D. and He L. (2006b) Meta-analysis shows association between the tryptophan hydroxylase (*TPH*) gene and schizophrenia. *Hum. Genet.* 120: 22-30.

Li J., Dangott L. J. and Fitzpatrick P. F. (2010) Regulation of phenylalanine hydroxylase: conformational changes upon phenylalanine binding detected by hydrogen/deuterium exchange and mass spectrometry. *Biochemistry* 49: 3327-3335.

Li J., Ilangovan U., Daubner S. C., Hinck A. P. and Fitzpatrick P. F. (2011) Direct evidence for a phenylalanine site in the regulatory domain of phenylalanine hydroxylase. *Arch. Biochem. Biophys.* 505: 250-255.

Liberles J. S., Thórólfsson M. and Martínez A. (2005) Allosteric mechanisms in ACT domain containing enzymes involved in amino acid metabolism. *Amino Acids* 28: 1-12.

Lidksy A. S., Robson K. J., Thirumalachary C., Barker P. E., Ruddle F. H. and Woo S. L. (1984) The PKU locus in man is on chromosome 12. *Am. J. Hum. Genet.* 36: 527-533.

Lim K., van Calcar S. C., Nelson K. L., Gleason S. T. and Ney D. M. (2007) Acceptable low-phenylalanine foods and beverages can be made with glycomacropeptide from cheese whey for individuals with PKU. *Mol. Genet. Metab.* 92: 176-178.

Loo T. W. and Clarke D. M. (2007) Chemical and pharmacological chaperones as new therapeutic agents. *Expert. Rev. Mol. Med.* 9: 1-18.

Lüdecke B., Knappskog P. M., Clayton P. T., Surtees R. A., Clelland J. D., Heales S. J., Brand M. P., Bartholomé K. and Flatmark T. (1996) Recessively inherited L-DOPA-responsive parkinsonism in infancy caused by a point mutation (L205P) in the tyrosine hydroxylase gene. *Hum. Mol. Genet.* 5: 1023-1028.

Maillot F., Lilburn M., Baudin J., Morley D. W. and Lee P. J. (2008) Factors influencing outcomes in the offspring of mothers with phenylketonuria during pregnancy: the importance of variation in maternal blood phenylalanine. *Am. J. Clin. Nutr.* 88: 700-705.

Marota J. J. and Shiman R. (1984) Stoichiometric reduction of phenylalanine hydroxylase by its cofactor: a requirement for enzymatic activity. *Biochemistry* 23: 1303-1311.

Martínez A., Haavik J. and Flatmark T. (1990) Cooperative homotropic interaction of L-noradrenaline with the catalytic site of phenylalanine 4-monooxygenase. *Eur. J. Biochem.* 193: 211-219.

Martínez A., Andersson K. K., Haavik J. and Flatmark T. (1991) EPR and ^{1}H-NMR spectroscopic studies on the paramagnetic iron at the active site of phenylalanine hydroxylase and its interaction with substrates and inhibitors. *Eur. J. Biochem.* 198: 675-682.

Martínez A., Olafsdottir S. and Flatmark T. (1993) The cooperative binding of phenylalanine to phenylalanine 4-monooxygenase studied by ^{1}H-NMR paramagnetic relaxation. Changes in water accessibility to the iron at the active site upon substrate binding. *Eur. J. Biochem.* 211: 259-266.

Martínez A., Knappskog P. M., Olafsdottir S., Døskeland A. P., Eiken H. G., Svebak R. M., Bozzini M., Apold J. and Flatmark T. (1995) Expression of recombinant human phenylalanine hydroxylase as fusion protein in *Escherichia coli* circumvents proteolytic degradation by host cell proteases. Isolation and characterization of the wild-type enzyme. *Biochem. J.* 306: 589-597.

Martínez A., Knappskog P. M. and Haavik J. (2001) A structural approach into human tryptophan hydroxylase and its implications for the regulation of serotonin biosynthesis. *Curr. Med. Chem.* 8: 1077-1091.

Martínez A., Calvo A. C., Teigen K. and Pey A. L. (2008) Rescuing proteins of low kinetic stability by chaperones and natural ligands phenylketonuria, a case study. *Prog. Mol. Biol. Transl. Sci.* 83: 89-134.

Martynyuk A. E., Glushakov A. V., Sumners C., Laipis P. J., Dennis D. M. and Seubert C. N. (2005) Impaired glutamatergic synaptic transmission in the PKU brain. *Mol. Genet. Metab.* 86 Suppl 1: S34-42.

Matalon R., Surendran S., Matalon K. M., Tyring S., Quast M., Jinga W., Ezell E. and Szucs S. (2003) Future role of large neutral amino acids in transport of phenylalanine into the brain. *Pediatrics* 112: 1570-1574.

Matalon R., Michals-Matalon K., Bhatia G., Grechanina E., Novikov P., McDonald J. D., Grady J., Tyring S. K. and Güttler F. (2006) Large neutral amino acids in the treatment of phenylketonuria (PKU). *J. Inherit. Metab. Dis.* 29: 732-738.

Matalon R., Michals-Matalon K., Bhatia G., Burlina A. B., Burlina A. P., Braga C., Fiori L., Giovannini M., Grechanina E., Novikov P., Grady J., Tyring S. K. and Güttler F. (2007) Double blind placebo control trial

of large neutral amino acids in treatment of PKU: effect on blood phenylalanine. *J. Inherit. Metab. Dis.* 30: 153-158.

Mazur A., Jarochowicz S., Sykut-Cegielska J., Gradowska W., Kwolek A. and Oltarzewski M. (2010) Evaluation of somatic development in adult patients with previously undiagnosed and/or untreated phenylketonuria. *Med. Princ. Pract.* 19: 46-50.

McInnes R. R., Shih V. and Chilton S. (1984) Interallelic complementation in an inborn error of metabolism: genetic heterogeneity in argininosuccinate lyase deficiency. *Proc. Natl. Acad. Sci. U. S. A.* 81: 4480-4484.

McKinney J., Knappskog P. M. and Haavik J. (2005) Different properties of the central and peripheral forms of human tryptophan hydroxylase. *J. Neurochem.* 92: 311-320.

McKinney J., Johansson S., Halmøy A., Dramsdahl M., Winge I., Knappskog P. M. and Haavik J. (2008) A loss-of-function mutation in tryptophan hydroxylase 2 segregating with attention-deficit/hyperactivity disorder. *Mol. Psychiatry* 13: 365-367.

Miranda F. F., Teigen K., Thórólfsson M., Svebak R. M., Knappskog P. M., Flatmark T. and Martínez A. (2002) Phosphorylation and mutations of Ser(16) in human phenylalanine hydroxylase. Kinetic and structural effects. *J. Biol. Chem.* 277: 40937-40943.

Miranda F. F., Thórólfsson M., Teigen K., Sanchez-Ruiz J. M. and Martínez A. (2004) Structural and stability effects of phosphorylation: Localized structural changes in phenylalanine hydroxylase. *Protein Sci.* 13: 1219-1226.

Mitnaul L. J. and Shiman R. (1995) Coordinate regulation of tetrahydrobiopterin turnover and phenylalanine hydroxylase activity in rat liver cells. *Proc. Natl. Acad. Sci. U. S. A.* 92: 885-889.

Modan-Moses D., Vered I., Schwartz G., Anikster Y., Abraham S., Segev R. and Efrati O. (2007) Peak bone mass in patients with phenylketonuria. *J. Inherit. Metab. Dis.* 30: 202-208.

Møller N., Meek S., Bigelow M., Andrews J. and Nair K. S. (2000) The kidney is an important site for *in vivo* phenylalanine-to-tyrosine conversion in adult humans: A metabolic role of the kidney. *Proc. Natl. Acad. Sci. U. S. A.* 97: 1242-1246.

Muntau A. C., Röschinger W., Habich M., Demmelmair H., Hoffmann B., Sommerhoff C. P. and Roscher A. A. (2002) Tetrahydrobiopterin as an alternative treatment for mild phenylketonuria. *N. Engl. J. Med.* 347: 2122-2132.

Nascimento C., Leandro J., Tavares de Almeida I. and Leandro P. (2008) Modulation of the activity of newly synthesized human phenylalanine hydroxylase mutant proteins by low-molecular-weight compounds. *Protein J.* 27: 392-400.

Nascimento C., Leandro J., Lino P. R., Ramos L., Almeida A. J., de Almeida I. T. and Leandro P. (2010) Polyol additives modulate the *in vitro* stability and activity of recombinant human phenylalanine hydroxylase. *Appl. Biochem. Biotechnol.* 162: 192-207.

National Institutes of Health Consensus Development Panel (2001) National Institutes of Health Consensus Development Conference Statement: phenylketonuria: screening and management, October 16-18, 2000. *Pediatrics* 108: 972-982.

Ney D. M., Gleason S. T., van Calcar S. C., MacLeod E. L., Nelson K. L., Etzel M. R., Rice G. M. and Wolff J. A. (2009) Nutritional management of PKU with glycomacropeptide from cheese whey. *J. Inherit. Metab. Dis.* 32: 32-39.

Nicholls C. D., McLure K. G., Shields M. A. and Lee P. W. (2002) Biogenesis of p53 involves cotranslational dimerization of monomers and posttranslational dimerization of dimers. Implications on the dominant negative effect. *J. Biol. Chem.* 277: 12937-12945.

Ohgari Y., Sawamoto M., Yamamoto M., Kohno H. and Taketani S. (2005) Ferrochelatase consisting of wild-type and mutated subunits from patients with a dominant-inherited disease, erythropoietic protoporphyria, is an active but unstable dimer. *Hum. Mol. Genet.* 14: 327-334.

Olsson E., Martínez A., Teigen K. and Jensen V. R. (2010a) Water dissociation and dioxygen binding in phenylalanine hydroxylase. *Eur. J. Inorg. Chem.* 2010: 351-356.

Olsson E., Teigen K., Martínez A. and Jensen V. R. (2010b) The aromatic amino acid hydroxylase mechanism: a perspective from computational chemistry. *Adv. Inorg. Chem.* 62: 437-500.

Olsson E., Martínez A., Teigen K. and Jensen V. R. (2011) Formation of the iron-oxo hydroxylating species in the catalytic cycle of aromatic amino acid hydroxylases. *Chemistry (In press)*, doi:10.1002/chem.201002910.

Panay A. J. and Fitzpatrick P. F. (2008) Kinetic isotope effects on aromatic and benzylic hydroxylation by *Chromobacterium violaceum* phenylalanine hydroxylase as probes of chemical mechanism and reactivity. *Biochemistry* 47: 11118-11124.

Panay A. J., Lee M., Krebs C., Bollinger J. M. and Fitzpatrick P. F. (2011) Evidence for a high spin Fe(IV) species in the catalytic cycle of a bacterial phenylalanine hydroxylase. *Biochemistry (In press),* doi:10.1021/bi1019868.

Parenti G. (2009) Treating lysosomal storage diseases with pharmacological chaperones: from concept to clinics. *EMBO Mol. Med.* 1: 268-279.

Parniak M. A. and Kaufman S. (1981) Rat liver phenylalanine hydroxylase. Activation by sulfhydryl modification. *J. Biol. Chem.* 256: 6876-6882.

Pavon J. A. and Fitzpatrick P. F. (2006) Insights into the catalytic mechanisms of phenylalanine and tryptophan hydroxylase from kinetic isotope effects on aromatic hydroxylation. *Biochemistry* 45: 11030-11037.

Pavon J. A. and Fitzpatrick P. F. (2009) Demonstration of a peroxide shunt in the tetrahydropterin-dependent aromatic amino acid monooxygenases. *J. Am. Chem. Soc.* 131: 4582-4583.

Pember S. O., Benkovic S. J., Villafranca J. J., Pasenkiewicz-Gierula M. and Antholine W. E. (1987) Adduct formation between the cupric site of phenylalanine hydroxylase from *Chromobacterium violaceum* and 6,7-dimethyltetrahydropterin. *Biochemistry* 26: 4477-4483.

Pettersen E. F., Goddard T. D., Huang C. C., Couch G. S., Greenblatt D. M., Meng E. C. and Ferrin T. E. (2004) UCSF Chimera - a visualization system for exploratory research and analysis. *J. Comput. Chem.* 25: 1605-1612.

Pey A. L., Pérez B., Desviat L. R., Martínez M. A., Aguado C., Erlandsen H., Gámez A., Stevens R. C., Thórólfsson M., Ugarte M. and Martínez A. (2004a) Mechanisms underlying responsiveness to tetrahydrobiopterin in mild phenylketonuria mutations. *Hum. Mutat.* 24: 388-399.

Pey A. L., Thórólfsson M., Teigen K., Ugarte M. and Martínez A. (2004b) Thermodynamic characterization of the binding of tetrahydropterins to phenylalanine hydroxylase. *J. Am. Chem. Soc.* 126: 13670-13678.

Pey A. L. and Martínez A. (2005) The activity of wild-type and mutant phenylalanine hydroxylase and its regulation by phenylalanine and tetrahydrobiopterin at physiological and pathological concentrations: an isothermal titration calorimetry study. *Mol. Genet. Metab.* 86 Suppl 1: S43-53.

Pey A. L., Stricher F., Serrano L. and Martínez A. (2007) Predicted effects of missense mutations on native-state stability account for phenotypic outcome in phenylketonuria, a paradigm of misfolding diseases. *Am. J. Hum. Genet.* 81: 1006-1024.

Pey A. L., Ying M., Cremades N., Velazquez-Campoy A., Scherer T., Thöny B., Sancho J. and Martínez A. (2008) Identification of pharmacological chaperones as potential therapeutic agents to treat phenylketonuria. *J. Clin. Invest.* 118: 2858-2867.

Phillips R. S. and Kaufman S. (1984) Ligand effects on the phosphorylation state of hepatic phenylalanine hydroxylase. *J. Biol. Chem.* 259: 2474-2479.

Pietz J., Kreis R., Rupp A., Mayatepek E., Rating D., Boesch C. and Bremer H. J. (1999) Large neutral amino acids block phenylalanine transport into brain tissue in patients with phenylketonuria. *J. Clin. Invest.* 103: 1169-1178.

Porter R. J., Mulder R. T., Joyce P. R., Miller A. L. and Kennedy M. (2008) Tryptophan hydroxylase gene (*TPH1*) and peripheral tryptophan levels in depression. *J. Affect. Disord.* 109: 209-212.

Przyrembel H. and Bremer H. J. (2000) Nutrition, physical growth, and bone density in treated phenylketonuria. *Eur. J. Pediatr.* 159 Suppl 2: S129-135.

Que Jr. L. (2000) One motif - many different reactions. *Nat. Struct. Biol.* 7: 182-184.

Quinsey N. S., Luong A. Q. and Dickson P. W. (1998) Mutational analysis of substrate inhibition in tyrosine hydroxylase. *J. Neurochem.* 71: 2132-2138.

Rebuffat A., Harding C. O., Ding Z. and Thöny B. (2010) Comparison of adeno-associated virus pseudotype 1, 2, and 8 vectors administered by intramuscular injection in the treatment of murine phenylketonuria. *Hum. Gene Ther.* 21: 463-477.

Rivera I., Cabral A., Almeida M., Leandro P., Carmona C., Eusébio F., Tasso T., Vilarinho L., Martins E., Lechner M. C., de Almeida I. T., Konecki D. S. and Lichter-Konecki U. (2000) The correlation of genotype and phenotype in Portuguese hyperphenylalaninemic patients. *Mol. Genet. Metab.* 69: 195-203.

Robinson A. B., McKerrow J. H. and Cary P. (1970) Controlled deamidation of peptides and proteins: an experimental hazard and a possible biological timer. *Proc. Natl. Acad. Sci. U. S. A.* 66: 753-757.

Robinson N. E. and Robinson A. B. (2001) Molecular clocks. *Proc. Natl. Acad. Sci. U. S. A.* 98: 944-949.

Rocha J. C. and Martel F. (2009) Large neutral amino acids supplementation in phenylketonuric patients. *J. Inherit. Metab. Dis.* 32: 472-480.

Sakowski S. A., Geddes T. J., Thomas D. M., Levi E., Hatfield J. S. and Kuhn D. M. (2006) Differential tissue distribution of tryptophan hydroxylase isoforms 1 and 2 as revealed with monospecific antibodies. *Brain Res.* 1085: 11-18.

Sarkissian C. N., Shao Z., Blain F., Peevers R., Su H., Heft R., Chang T. M. and Scriver C. R. (1999) A different approach to treatment of phenylketonuria: phenylalanine degradation with recombinant phenylalanine ammonia lyase. *Proc. Natl. Acad. Sci. U. S. A.* 96: 2339-2344.

Sarkissian C. N., Gámez A., Wang L., Charbonneau M., Fitzpatrick P., Lemontt J. F., Zhao B., Vellard M., Bell S. M., Henschell C., Lambert A., Tsuruda L., Stevens R. C. and Scriver C. R. (2008) Preclinical evaluation of multiple species of PEGylated recombinant phenylalanine ammonia lyase for the treatment of phenylketonuria. *Proc. Natl. Acad. Sci. U. S. A.* 105: 20894-20899.

Sarkissian C. N., Gámez A. and Scriver C. R. (2009) What we know that could influence future treatment of phenylketonuria. *J. Inherit. Metab. Dis.* 32: 3-9.

Scavelli R., Ding Z., Blau N., Haavik J., Martínez A. and Thöny B. (2005) Stimulation of hepatic phenylalanine hydroxylase activity but not *Pah*-mRNA expression upon oral loading of tetrahydrobiopterin in normal mice. *Mol. Genet. Metab.* 86 Suppl 1: S153-155.

Schallreuter K. U., Chavan B., Rokos H., Hibberts N., Panske A. and Wood J. M. (2005) Decreased phenylalanine uptake and turnover in patients with vitiligo. *Mol. Genet. Metab.* 86 Suppl 1: S27-33.

Schindeler S., Ghosh-Jerath S., Thompson S., Rocca A., Joy P., Kemp A., Rae C., Green K., Wilcken B. and Christodoulou J. (2007) The effects of large neutral amino acid supplements in PKU: an MRS and neuropsychological study. *Mol. Genet. Metab.* 91: 48-54.

Scriver C. R. and Waters P. J. (1999) Monogenic traits are not simple: lessons from phenylketonuria. *Trends Genet.* 15: 267-272.

Scriver C. R. and Kaufman S., Hyperphenylalaninemia: Phenylalanine Hydroxylase Deficiency, in: C. R. Scriver, A. L. Beaudet, D. Valle and W. S. Sly (Eds.) The Metabolic and Molecular Bases of Inherited Disease, McGraw-Hill, New York, 2001, pp. 1667-1724.

Scriver C. R., Hurtubise M., Konecki D., Phommarinh M., Prevost L., Erlandsen H., Stevens R., Waters P. J., Ryan S., McDonald D. and Sarkissian C. (2003) PAHdb 2003: what a locus-specific knowledgebase can do. *Hum. Mutat.* 21: 333-344.

Scriver C. R. (2007) The *PAH* gene, phenylketonuria, and a paradigm shift. *Hum. Mutat.* 28: 831-845.

Sheehan K., Lowe N., Kirley A., Mullins C., Fitzgerald M., Gill M. and Hawi Z. (2005) Tryptophan hydroxylase 2 (*TPH2*) gene variants associated with ADHD. *Mol. Psychiatry* 10: 944-949.

Shefer S., Tint G. S., Jean-Guillaume D., Daikhin E., Kendler A., Nguyen L. B., Yudkoff M. and Dyer C. A. (2000) Is there a relationship between 3-hydroxy-3-methylglutaryl coenzyme a reductase activity and forebrain pathology in the PKU mouse? *J. Neurosci. Res.* 61: 549-563.

Shiman R. and Gray D. W. (1980) Substrate activation of phenylalanine hydroxylase. A kinetic characterization. *J. Biol. Chem.* 255: 4793-4800.

Shiman R., Mortimore G. E., Schworer C. M. and Gray D. W. (1982) Regulation of phenylalanine hydroxylase activity by phenylalanine *in vivo*, *in vitro*, and in perfused rat liver. *J. Biol. Chem.* 257: 11213-11216.

Shiman R., Jones S. H. and Gray D. W. (1990) Mechanism of phenylalanine regulation of phenylalanine hydroxylase. *J. Biol. Chem.* 265: 11633-11642.

Shiman R., Xia T., Hill M. A. and Gray D. W. (1994) Regulation of rat liver phenylalanine hydroxylase. II. Substrate binding and the role of activation in the control of enzymatic activity. *J. Biol. Chem.* 269: 24647-24656.

Siegmund H. U. and Kaufman S. (1991) Hydroxylation of 4-methylphenylalanine by rat liver phenylalanine hydroxylase. *J. Biol. Chem.* 266: 2903-2910.

Siltberg-Liberles J. and Martínez A. (2009) Searching distant homologs of the regulatory ACT domain in phenylalanine hydroxylase. *Amino Acids* 36: 235-249.

Sitta A., Barschak A. G., Deon M., Terroso T., Pires R., Giugliani R., Dutra-Filho C. S., Wajner M. and Vargas C. R. (2006) Investigation of oxidative stress parameters in treated phenylketonuric patients. *Metab. Brain Dis.* 21: 287-296.

Sitta A., Manfredini V., Biasi L., Treméa R., Schwartz I. V., Wajner M. and Vargas C. R. (2009) Evidence that DNA damage is associated to phenylalanine blood levels in leukocytes from phenylketonuric patients. *Mutat. Res.* 679: 13-16.

Smith I., Beasley M. G. and Ades A. E. (1990) Intelligence and quality of dietary treatment in phenylketonuria. *Arch. Dis. Child.* 65: 472-478.

Solstad T. and Flatmark T. (2000) Microheterogeneity of recombinant human phenylalanine hydroxylase as a result of nonenzymatic deamidations of labile amide containing amino acids. Effects on catalytic and stability properties. *Eur. J. Biochem.* 267: 6302-6310.

Solstad T., Stokka A. J., Andersen O. A. and Flatmark T. (2003) Studies on the regulatory properties of the pterin cofactor and dopamine bound at the active site of human phenylalanine hydroxylase. *Eur. J. Biochem.* 270: 981-990.

Stokka A. J. and Flatmark T. (2003) Substrate-induced conformational transition in human phenylalanine hydroxylase as studied by surface plasmon resonance analyses: the effect of terminal deletions, substrate analogues and phosphorylation. *Biochem. J.* 369: 509-518.

Stokka A. J., Carvalho R. N., Barroso J. F. and Flatmark T. (2004) Probing the role of crystallographically defined/predicted hinge-bending regions in the substrate-induced global conformational transition and catalytic activation of human phenylalanine hydroxylase by single-site mutagenesis. *J. Biol. Chem.* 279: 26571-26580.

Surtees R. and Blau N. (2000) The neurochemistry of phenylketonuria. *Eur. J. Pediatr.* 159 Suppl 2: S109-113.

Swaans R. J., Rondot P., Renier W. O., Van Den Heuvel L. P., Steenbergen-Spanjers G. C. and Wevers R. A. (2000) Four novel mutations in the tyrosine hydroxylase gene in patients with infantile parkinsonism. *Ann. Hum. Genet.* 64: 25-31.

Teigen K., Froystein N. Å. and Martínez A. (1999) The structural basis of the recognition of phenylalanine and pterin cofactors by phenylalanine hydroxylase: implications for the catalytic mechanism. *J. Mol. Biol.* 294: 807-823.

Teigen K. and Martínez A. (2003) Probing cofactor specificity in phenylalanine hydroxylase by molecular dynamics simulations. *J. Biomol. Struct. Dyn.* 20: 733-740.

Teigen K., Dao K. K., McKinney J. A., Gorren A. C., Mayer B., Frøystein N. Å., Haavik J. and Martínez A. (2004) Tetrahydrobiopterin binding to aromatic amino acid hydroxylases. Ligand recognition and specificity. *J. Med. Chem.* 47: 5962-5971.

Teigen K., Jensen V. R. and Martínez A. (2005) The reaction mechanism of phenylalanine hydroxylase - a question of coordination. *Pteridines* 16: 27-34.

Teigen K., McKinney J. A., Haavik J. and Martínez A. (2007) Selectivity and affinity determinants for ligand binding to the aromatic amino acid hydroxylases. *Curr. Med. Chem.* 14: 455-467.

Tessari P., Deferrari G., Robaudo C., Vettore M., Pastorino N., De Biasi L. and Garibotto G. (1999) Phenylalanine hydroxylation across the kidney in humans rapid communication. *Kidney Int.* 56: 2168-2172.

Thöny B., Auerbach G. and Blau N. (2000) Tetrahydrobiopterin biosynthesis, regeneration and functions. *Biochem. J.* 347: 1-16.

Thöny B. and Blau N. (2006) Mutations in the BH_4-metabolizing genes GTP cyclohydrolase I, 6-pyruvoyl-tetrahydropterin synthase, sepiapterin reductase, carbinolamine-4a-dehydratase, and dihydropteridine reductase. *Hum. Mutat.* 27: 870-878.

Thórólfsson M., Ibarra-Molero B., Fojan P., Petersen S. B., Sanchez-Ruiz J. M. and Martínez A. (2002) L-phenylalanine binding and domain organization in human phenylalanine hydroxylase: a differential scanning calorimetry study. *Biochemistry* 41: 7573-7585.

Trefz F. K., Burton B. K., Longo N., Casanova M. M., Gruskin D. J., Dorenbaum A., Kakkis E. D., Crombez E. A., Grange D. K., Harmatz P., Lipson M. H., Milanowski A., Randolph L. M., Vockley J., Whitley C. B., Wolff J. A., Bebchuk J., Christ-Schmidt H. and Hennermann J. B. (2009a) Efficacy of sapropterin dihydrochloride in increasing phenylalanine tolerance in children with phenylketonuria: a phase III, randomized, double-blind, placebo-controlled study. *J. Pediatr.* 154: 700-707.

Trefz F. K., Scheible D., Götz H. and Frauendienst-Egger G. (2009b) Significance of genotype in tetrahydrobiopterin-responsive phenylketonuria. *J. Inherit. Metab. Dis.* 32: 22-26.

Udenfriend S. and Cooper J. R. (1952) The enzymatic conversion of phenylalanine to tyrosine. *J. Biol. Chem.* 194: 503-511.

van Bakel M. M., Printzen G., Wermuth B. and Wiesmann U. N. (2000) Antioxidant and thyroid hormone status in selenium-deficient phenylketonuric and hyperphenylalaninemic patients. *Am. J. Clin. Nutr.* 72: 976-981.

van Calcar S. C., MacLeod E. L., Gleason S. T., Etzel M. R., Clayton M. K., Wolff J. A. and Ney D. M. (2009) Improved nutritional management of phenylketonuria by using a diet containing glycomacropeptide compared with amino acids. *Am. J. Clin. Nutr.* 89: 1068-1077.

van Spronsen F. J., Hoeksma M. and Reijngoud D. J. (2009) Brain dysfunction in phenylketonuria: is phenylalanine toxicity the only possible cause? *J. Inherit. Metab. Dis.* 32: 46-51.

VanZutphen K. H., Packman W., Sporri L., Needham M. C., Morgan C., Weisiger K. and Packman S. (2007) Executive functioning in children and adolescents with phenylketonuria. *Clin. Genet.* 72: 13-18.

Veitia R. A. (2009) Dominant negative factors in health and disease. *J. Pathol.* 218: 409-418.

Volner A., Zoidakis J. and Abu-Omar M. M. (2003) Order of substrate binding in bacterial phenylalanine hydroxylase and its mechanistic implication for pterin-dependent oxygenases. *J. Biol. Inorg. Chem.* 8: 121-128.

Waisbren S. E. and Levy H. L. (1991) Agoraphobia in phenylketonuria. *J. Inherit. Metab. Dis.* 14: 755-764.

Waisbren S. E. and Azen C. (2003) Cognitive and behavioral development in maternal phenylketonuria offspring. *Pediatrics* 112: 1544-1547.

Wallick D. E., Bloom L. M., Gaffney B. J. and Benkovic S. J. (1984) Reductive activation of phenylalanine hydroxylase and its effect on the redox state of the non-heme iron. *Biochemistry* 23: 1295-1302.

Walter J. H., White F. J., Hall S. K., MacDonald A., Rylance G., Boneh A., Francis D. E., Shortland G. J., Schmidt M. and Vail A. (2002) How practical are recommendations for dietary control in phenylketonuria? *Lancet* 360: 55-57.

Walter J. H. and White F. J. (2004) Blood phenylalanine control in adolescents with phenylketonuria. *Int. J. Adolesc. Med. Health* 16: 41-45.

Walther D. J. and Bader M. (2003) A unique central tryptophan hydroxylase isoform. *Biochem. Pharmacol.* 66: 1673-1680.

Walther D. J., Peter J. U., Bashammakh S., Hörtnagl H., Voits M., Fink H. and Bader M. (2003) Synthesis of serotonin by a second tryptophan hydroxylase isoform. *Science* 299: 76.

Wang L., Erlandsen H., Haavik J., Knappskog P. M. and Stevens R. C. (2002) Three-dimensional structure of human tryptophan hydroxylase and its implications for the biosynthesis of the neurotransmitters serotonin and melatonin. *Biochemistry* 41: 12569-12574.

Wasserstein M. P., Snyderman S. E., Sansaricq C. and Buchsbaum M. S. (2006) Cerebral glucose metabolism in adults with early treated classic phenylketonuria. *Mol. Genet. Metab.* 87: 272-277.

Waters P. J., Parniak M. A., Hewson A. S. and Scriver C. R. (1998a) Alterations in protein aggregation and degradation due to mild and severe missense mutations (A104D, R157N) in the human phenylalanine hydroxylase gene (*PAH*). *Hum. Mutat.* 12: 344-354.

Waters P. J., Parniak M. A., Nowacki P. and Scriver C. R. (1998b) *In vitro* expression analysis of mutations in phenylalanine hydroxylase: linking genotype to phenotype and structure to function. *Hum. Mutat.* 11: 4-17.

Waters P. J., Parniak M. A., Akerman B. R., Jones A. O. and Scriver C. R. (1999) Missense mutations in the phenylalanine hydroxylase gene (*PAH*) can cause accelerated proteolytic turnover of PAH enzyme: a mechanism underlying phenylketonuria. *J. Inherit. Metab. Dis.* 22: 208-212.

Waters P. J., Parniak M. A., Akerman B. R. and Scriver C. R. (2000) Characterization of phenylketonuria missense substitutions, distant from the phenylalanine hydroxylase active site, illustrates a paradigm for mechanism and potential modulation of phenotype. *Mol. Genet. Metab.* 69: 101-110.

Waters P. J., Scriver C. R. and Parniak M. A. (2001) Homomeric and heteromeric interactions between wild-type and mutant phenylalanine hydroxylase subunits: evaluation of two-hybrid approaches for functional analysis of mutations causing hyperphenylalaninemia. *Mol. Genet. Metab.* 73: 230-238.

Waters P. J. (2003) How *PAH* gene mutations cause hyper-phenylalaninemia and why mechanism matters: insights from *in vitro* expression. *Hum. Mutat.* 21: 357-369.

Widaman K. F. and Azen C. (2003) Relation of prenatal phenylalanine exposure to infant and childhood cognitive outcomes: results from the International Maternal PKU Collaborative Study. *Pediatrics* 112: 1537-1543.

Winge I., McKinney J. A., Ying M., D'Santos C. S., Kleppe R., Knappskog P. M. and Haavik J. (2008) Activation and stabilization of human tryptophan hydroxylase 2 by phosphorylation and 14-3-3 binding. *Biochem. J.* 410: 195-204.

Woo S. L., Lidsky A. S., Güttler F., Chandra T. and Robson K. J. (1983) Cloned human phenylalanine hydroxylase gene allows prenatal diagnosis and carrier detection of classical phenylketonuria. *Nature* 306: 151-155.

Woolf L. I., Griffiths R. and Moncrieff A. (1955) Treatment of phenylketonuria with a diet low in phenylalanine. *Br. Med. J.* 1: 57-64.

Xia T., Gray D. W. and Shiman R. (1994) Regulation of rat liver phenylalanine hydroxylase. III. Control of catalysis by (6*R*)-tetrahydrobiopterin and phenylalanine. *J. Biol. Chem.* 269: 24657-24665.

Yagi H., Ogura T., Mizukami H., Urabe M., Hamada H., Yoshikawa H., Ozawa K. and Kume A. (2011) Complete restoration of phenylalanine oxidation in phenylketonuria mouse by a self-complementary adeno-associated virus vector. *J. Gene Med.* 13: 114-122.

Yu B., Thompson G. D., Yip P., Howell P. L. and Davidson A. R. (2001) Mechanisms for intragenic complementation at the human argininosuccinate lyase locus. *Biochemistry* 40: 15581-15590.

Zhang X., Gainetdinov R. R., Beaulieu J. M., Sotnikova T. D., Burch L. H., Williams R. B., Schwartz D. A., Krishnan K. R. and Caron M. G. (2005) Loss-of-function mutation in tryptophan hydroxylase-2 identified in unipolar major depression. *Neuron* 45: 11-16.

Zurflüh M. R., Zschocke J., Lindner M., Feillet F., Chery C., Burlina A., Stevens R. C., Thöny B. and Blau N. (2008) Molecular genetics of tetrahydrobiopterin-responsive phenylalanine hydroxylase deficiency. *Hum. Mutat.* 29: 167-175.

Part II

Aims of the Study

Since the first report in 1934, by Asbjørn Følling, PKU has been the subject of extensive research. However, beyond the knowledge accumulated along these years there are still diverse aspects that have remained largely overlooked and others that owing to the increase awareness of their importance demand a more thoroughly study. In this perspective, the main goal of this thesis was to further elucidate those aspects, namely the phenomenon of interallelic complementation (IC) (Part III); the study of misfolding mutants involving the *R*-domain of phenylalanine hydroxylase (Part IV) and the identification of the structure-function role of amino acids residues in catalysis and catalytic activation of hPAH, particularly those localized in the highly flexible loop 131-155 (Part V).

The negative interallelic complementation phenomenon in PKU was first proposed by Seymour Kaufman in 1975. Although the majority of PKU patients are compound heterozygous (~75%) with a high genotypic heterogeneity (>550 mutations identified to date), raising the importance of IC in PKU pathogenesis, this phenomenon has been largely neglected. The first experimental evidence lending support to a negative interallelic complementation in some compound heterozygous PKU patients had been obtained from the first metanalysis of genotype-phenotype correlation studies and more recently from inconsistencies observed in the treatment with cofactor BH_4. Therefore, due to the increase understanding that the characterization of the interactions between wild-type and mutant protomers and between different mutant protomers is clinically relevant, as they will contribute to a better understanding of the metabolic phenotype in PKU/HPA patients and BH_4-responsiveness and will also be essential in the development of new emerging therapies (e.g. pharmacological chaperones), in Part III of this work the molecular basis of interallelic complementation in human phenylalanine hydroxylase was addressed.

Interactions between different hPAH protomers have been demonstrated by the yeast two-hybrid system. However, the molecular mechanism of interallelic complementation and its role in PKU pathogenesis remained elusive since heteromeric forms of hPAH have never been isolated and characterized biochemically. The conventional expressions studies of recombinant hPAH initiated in the 1990s led to the characterization of more than 100 hPAH mutant forms in the homoallelic state. Nevertheless, they did not allow the characterization of heteroallelic states. Hence, our first aim was the development of a dual vector prokaryotic expression system producing two different hPAH subunits, mimicking the natural heteroallelic state in heterozygous or in compound heterozygous patients (Part III, section 1; **Paper I**). The mutations

analyzed, namely the I65T, R261Q, R270K and V388M, were selected due to the observed inconsistencies in genotype-phenotype correlation studies of Portuguese hyperphenylalaninemic compound heterozygous patients and thus likely candidates of negative IC. Albeit the produced recombinant proteins resembled the heteroallelic state observed in compound heterozygous, with mixed populations of hetero-/homo-oligomers (i.e. homo-oligomer-1 + homo-oligomer-2 + hetero-oligomer-1/2) in addition to some dimers, the expression system did not allowed the isolation of individual hetero-oligomeric species. Therefore, our next challenge was the development of a bicistronic system (Part III, section 2; **Paper II)** to express wild-type and truncated forms of hPAH, allowing the isolation of pure heteromeric forms and to answer to some fundamental questions related to the assembly of hybrid forms (existence of hetero-tetramers and/or hetero-dimers), and the formation of heteromeric species with different functional domains.

Phenylketonuria is considered a protein misfolding disease with loss of function. Human PAH has a small margin of stability and a high frequency of misfolding hPAH mutations are associated with PKU/HPA, resulting in enzymes with a propensity to self-associate and to form higher-order oligomers (when overexpressed in prokaryotic systems) and to be rapidly degraded (when expressed in eukaryotic cells). This group of mutations does not directly affect the catalytic function, but impairs molecular motions involved in regulatory processes, substrate and cofactor binding and oligomerization assembly. Particularly the N-terminal regulatory domain (*R*-domain) seems to play a crucial role in the instability and misfolding of the protein. Therefore, we aimed to comprehensively study *in vitro* the missense mutation G46S in the *R*-domain of hPAH, associated with the severe form of PKU, which is rapidly degraded when expressed in HEK293 cells (Part IV, section 1, **Paper III**). The experimental approach with the putative maltose binding protein (MBP) as fusion partner allowed the recovery of the mutant in a metastable conformational state, and cleavage of fusion protein enabled the study of the molecular mechanism of the self-association and the structural properties of the higher-order oligomers, as well as the effect of molecular/chemical/pharmacological chaperones. We also aimed to extend the studies of this misfolded mutant and the wild-type (WT) to truncated forms of the *R*-domain (residues 2-120). These forms were analyzed (Part IV, section 2; **Paper IV**) using a similar experimental approach, and the WT *R*-domain self-association propensity was

further explored in terms of the controversial allosteric regulatory binding site for L-phenylalanine in the *R*-domain of hPAH.

The substrate L-Phe triggered activation of hPAH, a key regulatory property of the enzyme, is characterized by a reversible transition from a low activity/affinity state (T-state) to a high activity/affinity state (R-state). There is no crystal structure of the full-length enzyme, but high-resolution structures of a truncated dimeric form of the binary cofactor complex (ΔN102/ΔC24-hPAH-Fe(II)·BH_4) and ternary cofactor-substrate analog complex (ΔN102/ΔC24-hPAH-Fe(II)·BH_4·THA) have provided insights into the roles of active site residues and conformational changes in substrate recognition and catalysis, leading to the proposal of a catalytic mechanism for PAH. Moreover, these structures have revealed that substrate binding triggers a conformational isomerization, including a Cα displacement of ~10 Å for Tyr138 and ~21 Å of its side-chain hydroxyl group from a surface position in a flexible loop to a partially buried position within a hydrophobic core at the active site. In the closely related rTH, a homologous flexible loop seems to be involved in the rate-limiting step of the TH reaction. In hPAH the functional importance of the L-Phe-induced displacement observed for the flexible surface loop (conserved in mammalian PAHs) and relocation of the Y138 hydroxyl group was addressed experimentally (Part V, section 1, **Paper V**), by mutation of the residue (Y138F/A/E/K) in the dimeric catalytic core domain (ΔN102/ΔC24-hPAH) and in the full-length tetrameric hPAH.

Part III

Interallelic Complementation in human Phenylalanine Hydroxylase

1. Co-expression of different subunits of human phenylalanine hydroxylase: Evidence of negative interallelic complementation

João Leandro, Cátia Nascimento, Isabel Tavares de Almeida, Paula Leandro

Biochimica et Biophysica Acta (Molecular Basis of Disease), 1762 (2006) 544–550.

Available online at www.sciencedirect.com
SCIENCE DIRECT
Biochimica et Biophysica Acta 1762 (2006) 544–550
BIOCHIMICA ET BIOPHYSICA ACTA
BBA
http://www.elsevier.com/locate/bba

Co-expression of different subunits of human phenylalanine hydroxylase: Evidence of negative interallelic complementation

João Leandro, Cátia Nascimento, Isabel Tavares de Almeida, Paula Leandro *

Unidade de Biologia Molecular e Biopatologia Experimental, Centro de Patogénese Molecular, Faculdade de Farmácia da Universidade de Lisboa, Av. Prof. Gama Pinto, 1649-003 Lisboa, Portugal

Received 28 November 2005; received in revised form 1 February 2006; accepted 3 February 2006
Available online 28 February 2006

Abstract

To study the interaction between two different subunits of the heteromeric human phenylalanine hydroxylase (hPAH), present in hyperphenylalaninemic (HPA) compound heterozygous patients, heteroallelic hPAH enzymes were produced. A dual vector expression system was used (PRO™ Bacterial Expression System) in which each mutant subunit was expressed from a separate compatible vector, with different epitope tags, in a single bacterial host. Experimental conditions were selected in order that each plasmid produced equivalent levels of mutant subunits. In this study, we demonstrated that both subunits were expressed and that the purified heteroallelic enzymes, were catalytically active. As expected, the produced proteins displayed enzymatic activities levels lower than the predicted catalytic activity, calculated by averaging in vitro PAH activities from both alleles, and were strongly dependent on the proteins subunit composition. The obtained data suggest that interactions between the studied hPAH subunits, namely the I65T, R261Q, R270K and V388M, and the wild-type protein occurred. As postulated, this phenomenon could be a source of phenotypic variation in genetic diseases involving multimeric proteins.

Keywords: Heteroallelic human phenylalanine hydroxylase; Dual expression system; Interallelic complementation

1. Introduction

Human phenylalanine hydroxylase (hPAH; E.C. 1.14.16.1) is a homotetrameric non-heme iron dependent enzyme that hydroxylates phenylalanine (L-Phe) to tyrosine (L-Tyr). In man, hPAH dysfunction leads to phenylketonuria (PKU; OMIM 261600) and related forms of hyperphenylalaninemia (HPA) [1]. The enzymatic phenotype of this recessive metabolic disease results from the combined expression of the two mutant alleles. Most HPA patients are heteroallelic for PAH mutations being classified as compound heterozygous [2].

There is now considerable direct evidence indicating that it is possible to establish genotype/phenotype correlations [3,4] in the homoallelic state and in most cases of functional hemizygous patients (resulting from the combination with a "null" allele that completely abolishes PAH activity) [5]. However, in the heteroallelic state inconsistencies exist between the observed metabolic phenotype and the "predicted residual activity" (PRA) [6], as calculated from the mean of the monoallelic in vitro PAH enzyme activities for each mutation comprising the genotype [3]. In these patients, the presence of several mutations, namely the I65T, R261Q and V388M mutations, associated either among each other or with other mutations gives rise to more severe phenotypes than those anticipated by the PRA [6]. This phenomenon was already known since 1975 when Kaufman and Max [7] observed, in parents of PKU patients (obligate heterozygous), a deviation from proportionality in the determined PAH activity. These authors introduced the term negative interallelic complementation to illustrate the protein–protein interactions occurring between the subunits of the multimeric hPAH enzyme.

Recently, using a yeast two-hybrid approach [8,9], it was demonstrated that the wild-type hPAH subunits interact with different hPAH mutant subunits, thus, indicating the production of heteromeric PAH enzymes. However, a central question

* Corresponding author. Tel.: +351 217946400; fax: +351 217946491.
E-mail address: aleandro@ff.ul.pt (P. Leandro).

0925-4439/$ - see front matter © 2006 Elsevier B.V. All rights reserved.
doi:10.1016/j.bbadis.2006.02.001

remains concerning the enzymatic activity of the postulated produced hybrid hPAH proteins. Till now, the use of conventional expression systems had never allowed to test for the hypothesis of a negative impact of a particular mutation on the activity of a heteromeric hPAH, since in these systems, a single mutant allele is expressed, thus, producing a homoallelic protein phenotype.

Using a dual vector expression strategy, for the co-production of two mutant hPAH subunits, we were able to mimic the natural heteroallelic state occurring in heterozygous individuals and compound heterozygous patients. Two different subunits were simultaneously produced in equivalent amounts in the same bacterial host, using two different plasmids (PRO™ Bacterial Expression System). The studied mutations included the I65T, R261Q, R270K and V388M mutant forms, which contribute mostly for the observed genotype/phenotype inconsistencies in the Portuguese PKU population [10].

The determined enzymatic activities showed that when co-expressed the produced mutant enzymes presented lower catalytic activities than the predicted by individual expression of the mutant subunits. The obtained results were in full accordance with the postulated phenomenon of negative interallelic complementation.

2. Material and methods

2.1. Materials

The PRO™ Bacterial Expression System was from Clontech (Clontech Laboratories, Palo Alto, USA). The synthetic cofactor 6-methyl-tetrahydropterin (6-MPH$_4$), L-Phe, HEPES and dithiothreitol (DTT) were from Sigma Chemical Co (St. Louis, USA). Catalase was purchased from Roche Diagnostics GmbH (Mannheim, Germany). All reagents were of analytical grade.

2.2. Construction of recombinant dual expression vectors

The PRO™ Bacterial Expression System comprises two expression vectors developed by Lutz and Bujard [11], namely the pPROLar and pPROTet. These vectors present different replication origins, a Myc epitope (–Glu–Gln–Lys–Leu–Ile–Ser–Glu–Glu–Asp–Leu–) and encode resistance to different antibiotics such that only cells expressing both vectors would be resistant to both kanamycin (pPROLar) and chloramphenicol (pPROTet). The pPROLar vector contains the $P_{lac/ara-1}$ promoter, induced by isopropylthio-β-D-galactoside (IPTG) and arabinose (Ara), and the pPROTet vector includes the $P_{LtetO-1}$ promoter, induced in response to anhydrotetracycline (aTc). A recombinant-deficient host (DH5αPRO; Clontech Laboratories, Palo Alto, USA) was used to minimize recombination between plasmids.

The original vectors were subjected to Site Directed Mutagenesis (Quikchange II; Stratagene, La Jolla, USA) in order to introduce a 6xHis purification tag (Table 1). Moreover, the pPROLar Myc-tag was removed and the Xpress epitope (–Asp–Leu–Tyr–Asp–Asp–Asp–Asp–Lys–) was introduced. The pPROLar–XPress–His and pPROTet–Myc–His expression vectors were obtained. The enterokinase (EK) recognition sequence was maintained just before the hPAH coding sequence in order to be possible to remove the 6xHis tag. However, the EK treatment it is not necessary, since we have demonstrated previously that these tags did not interfere with the activity of the recombinant protein [12].

For prokaryotic expression the coding sequence of hPAH [13] (GenBank accession U49897) was introduced in the BamHI site of pPROLar–XPress–His and pPROTet–Myc–His expression vectors, in frame with the start codon. Using the mutagenic oligonucleotides described in Table 1, the studied mutations were introduced by Site Directed Mutagenesis (Quikchange II). The obtained constructs were sequenced to confirm the introduction of the desired modifications and were used to transform competent DH5αPRO cells. Propagation of pPROTet–Myc–His constructs was performed in LB plates supplemented with spectinomycin (50 μg/ml, final concentration) and chloramphenicol (34 μg/ml, final concentration). The pPROLar–XPress–His constructs were propagated in LB plates supplemented with spectinomycin and kanamycin (both at 50 μg/ml, final concentration).

The strategy to achieve dual vector expression was to transform *E. coli* host cells simultaneously with two different hPAH subunits, each cloned in a different vector. To select the co-expressed constructs, LB plates supplemented with spectinomycin, kanamycin (both at 50 μg/ml final concentration) and chloramphenicol (34 μg/ml, final concentration) were used.

2.3. Co-expression of recombinant hPAH subunits

The protein expression was initially optimised, for each system individually, by testing the optimal inducers concentration and induction time. Final concentrations of aTc from 1 to 100 ng/ml were used for induction of pPROTet–Myc–His constructs. The pPROLar–XPress –His constructs were assayed for induction with a constant IPTG concentration (1 mM) and variable amounts of arabinose in the culture medium (0 to 0.2%). Kinetic induction studies were performed with an incubation period of 12 hours, with samples collected at 0, 1, 2, 3, 4, 5 and 12 hours after induction.

For the co-production of two different 6xHis–hPAH subunits, fresh overnight cultures were diluted 1:100 in LB medium containing 34 μg/ml of chloramphenicol, 50 μg/ml of spectinomycin and 50 μg/ml of kanamycin. Cells were grown at 37 °C with expression induced by addition of the optimised amounts of IPTG, arabinose and aTc when the A_{600} was about 0.6. Simultaneously 0.1 mM ferrous ammonium sulfate (Fe^{2+}) was added to the culture. Induction was performed for a period determined to maximize the prokaryotic expression of the heteroallelic hPAH enzyme forms under investigation.

Table 1
Oligonucleotides used for site directed mutagenesis

Primers	Position[a]	Sequence (5′–3′)
6xHis–tag F	pPROTet 96–131; pROLar 122–158	AGAAAGGTACCCATGGGTCATCATCATCATCATCATGAACAGAAACTGATCAGC
6xHis–tagR		GCTGATCAGTTTCTGTTCATGATGATGATGATGATGACCCATGGGTACCTTTCT
I65T-F	cDNA 183–203	CTAGATTCAGTGTGGGTCAGG
I65T-R		CCTGACCCACACTGAATCTAG
R261Q-F	cDNA 772–792	GTGGAAGACTTGGAAGGCCAG
R261-R		CTGGCCTTCCAAGTCTTCCAC
V388M-F	cDNA 1152–1172	CTCTCTGCCATGTAATACAGG
V388M-R		CCTGTATTACATGGCAGAGAG
R270K-F	cDNA 799–819	CAGTACATGAAACATGGATCC
R270K-R		GGATCCATGTTTGATGTACTG

[a] Nucleotide positions refer to Konecki-Kwok PAH cDNA (PAH Mutation Analysis Consortium Database; http://www.mcgill.ca/pahdb). Nucleotide mismatch positions are underlined.

Bacterial pellets were obtained by centrifugation at 4000×g for 10 min at 4 °C. The pellets (stored at −20 °C until used) were resuspended (40%, w/v) in lysis buffer (50 mM potassium phosphate; 300 mM NaCl, pH 7.8; 10% glycerol) containing 1 mM phenylmethanesulphonyl fluoride (PMSF) and 1 mg/ml lysozyme. After a 30 min incubation at 4 °C, cells were disrupted by passage through a Carver Press (Model C, from F.S. Carver Inc., Wabash, IN, USA) at 4000 psi. The crude extract was then centrifuged at 10,000×g at 4 °C for 20 min. The concentrations of imidazole and β-mercaptoethanol (β-ME) in the supernatants were adjusted to 10 mM and processed immediately.

The recombinant 6xHis–hPAH proteins expressed from the pPROLar–XPress–His and pPROTet–Myc–His vectors were designated 6xHis–hPAH$_{Lar}$ and 6xHis–hPAH$_{Tet}$, respectively. Expression of heteroallelic proteins was always carried out with both possible combinations (e.g. wt$_{Lar}$/V388M$_{Tet}$ and wt$_{Tet}$/V388M$_{Lar}$).

2.4. Purification and analysis of recombinant proteins

The presence of the 6xHis tag allowed the purification of the recombinant protein by IMAC using a Ni-chelating resin (Ni-NTA-Resin; Qiagen, Valencia, USA), as previously described [12]. Aliquots of the purified enzyme samples were analysed by SDS-PAGE (10% gel) after Coomassie brilliant blue R staining. Western immuno-analysis was performed according to standard methods [14] using the anti-Myc or the anti-Xpress as the primary antibodies (Invitrogen; Carlsbad, USA) and the anti-mouse IgG-HRP (Cell Signalling; Beverly, USA) as the secondary antibody. Protein concentrations were determined by the method of Bradford [15] using bovine serum albumin (BSA) as standard. Protein purity was assessed by densitometric scanning of destained gels or membrane blots followed by analysis using the Gel-Pro Analyzer (version 2.0) software (Media Cybernetics).

2.5. Assay of enzymatic activity

Enzyme assays were performed with the purified fusion proteins, essentially as described by Martinez et al [16] with some minor modifications [12]. The PAH activity was assayed using the synthetic cofactor 6-methyl-tetrahydropterin (6-MPH$_4$) and the substrate (L-Phe) at final concentrations of 500 μM and 1 mM, respectively. All stages of protein purification, analysis and enzyme assays were performed without intervening freeze–thaw cycles.

2.6. Cleavage of the fusion peptide

The leader fusion peptide 6xHis was excised from the recombinant fusion protein by cleavage with EK (Invitrogen, Carlsbad, USA). In this assay 50 μg of purified enzyme were incubated with 1 U of EK in 50 mM Tris–HCl pH 8.0, 1 mM $CaCl_2$ (ratio EK: fusion protein about 1:30) for 5 h at 4 °C.

3. Results

The wild-type and mutant hPAH cDNAs were cloned into the pPROLar–XPress–His and pPROTet–Myc–His expression vectors. Western Blot analysis of crude cell lysates revealed the presence of a single fusion protein band with a molecular mass of about 55 kDa. Assuming a molecular mass of 3 kDa for the fusion peptide [12] the 52-kDa protein corresponds to the expected full-length hPAH wild-type or mutant forms [17,18].

Expression conditions, including inducers concentration and induction time, were analysed in order to achieve equimolecular levels of each subunit comprising the hPAH heteroallelic state. Regulation of wild-type hPAH expression from the $P_{LtetO-1}$ and $P_{lac/ara-1}$ promoters showed that the highest and equivalent protein levels were reached using 100 ng/ml of aTc, for the pPROTet–Myc–His construct, and 0.2% arabinose/1 mM IPTG for the pPROLar–Xpress–His construct (Fig. 1). Using the above inducers concentration maximum yields of recombinant proteins were obtained between 4 and 5 h, for the wild-type form and at 4 h induction for the studied mutant forms (Fig. 2). After these time points, a decrease in the protein production was observed. Based on these observations, a 4-h induction time was chosen to produce the wild-type and the mutant recombinant 6xHis–hPAH proteins.

After IMAC purification the 6xHis hPAHwt protein presented, for both expression vectors, 95% purity. Similar to the results obtained with other expression systems [12,19] the recombinant mutant forms showed lower purity grades, namely 75–80% for the I65T, R261Q and V388M (pPROLar–XPress–His and pPROTet–Myc–His constructs). The R270K$_{Lar}$ protein was produced almost to homogeneity, whereas the R270K$_{Tet}$ mutant protein (Fig. 3) presented only 60% purity. In addition to a main band of full-length hPAH (55 kDa), a minor band of higher molecular mass was observed for the R270K$_{Tet}$ mutant form (Fig. 3). However, Western blot analysis showed that this band did not represent immunoreactive hPAH protein (results not shown).

The 6xHis fusion peptide was efficiently cleaved from the recombinant enzymes (EK digestion), yielding a protein with a MW of about 52 kDa (results not shown).

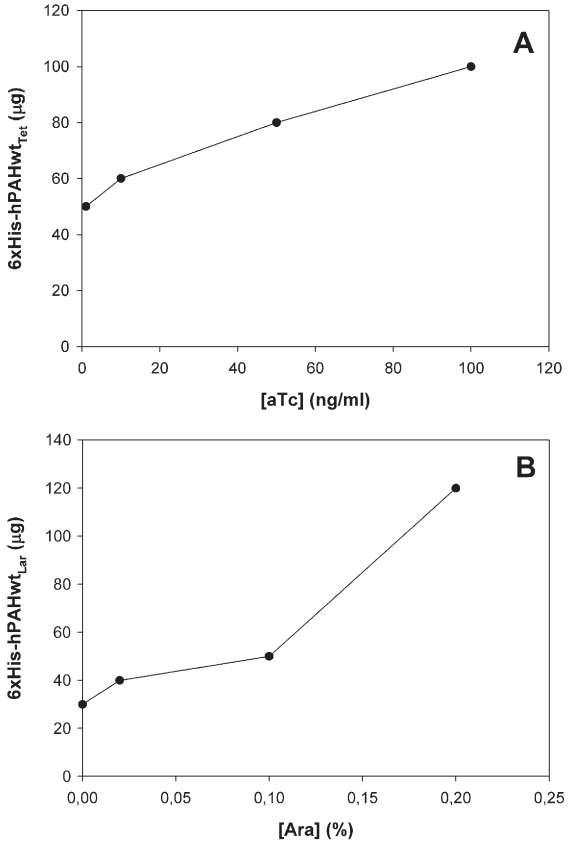

Fig. 1. Regulation of wild-type 6xHis–hPAH expression from the $P_{LtetO-1}$ (A) and $P_{Lac/ara-1}$ (B) promoters. Assays were performed with 500 ml of growth medium and 4-h incubation. Each value represents the mean of two independent analysis. Arabinose induction was performed with a constant 1 mM IPTG concentration.

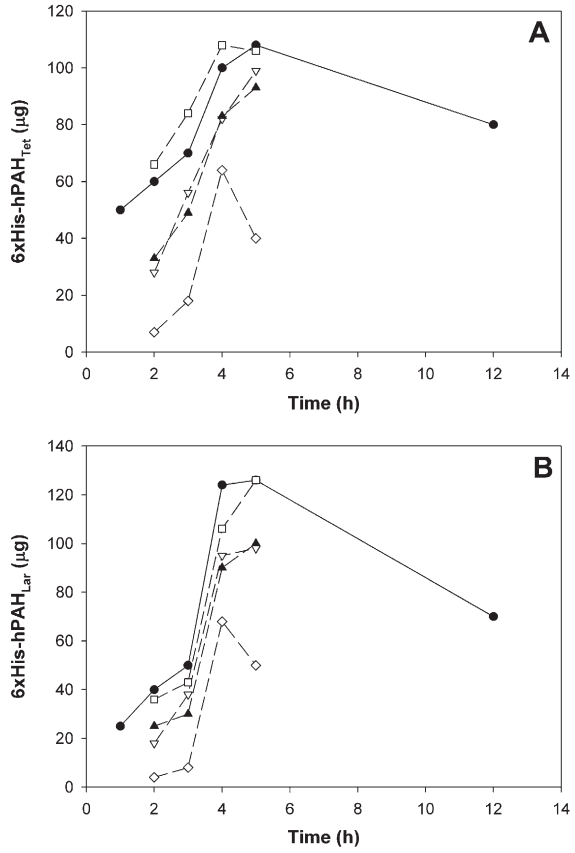

Fig. 2. Expression of wild-type and mutant 6xHis–hPAH enzymes encoded by the recombinant vectors pPROTet–Myc–His (A) and pPROLar–XPress–His (B), along time induction, using the optimized inducers concentrations. (●) hPAH wt; (□) R261Q mutant form; (▽) I65T mutant form; (▲) V388M mutant form; (◊) R270K mutant form. Each value represents the mean of two independent experiments.

Co-production of two different subunits was demonstrated by Western blot analysis of the purified recombinant proteins, using the anti-Myc and the anti-Xpress antibodies. The presence of the two subunits possessing both epitopes is illustrated in Fig. 4 for the co-produced 6xHis–hPAHwt$_{Tet}$/V388M$_{Lar}$.

In order to perform a comparative analysis, the enzymatic activities of the homomeric forms of 6xHis hPAH proteins were also determined (Table 2). When assayed at standard conditions (1 mM L-Phe and 500 µM 6-MPH$_4$), the wild-type form revealed a catalytic activity of 5818 nmol Tyr min^{-1} mg^{-1}. The

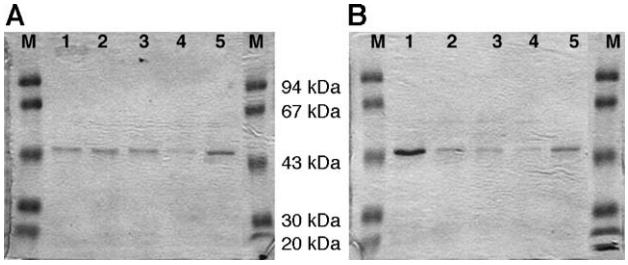

Fig. 3. SDS-PAGE analysis of hPAH mutant forms expressed from recombinant vectors pPROLar–XPress–His (A) and pPROTet–Myc–His (B). (M) Molecular weight marker; (1–4) 6xHis–hPAH recombinant forms of R261Q (1); I65T (2); V388M (3) R270K (4) and; wild-type (5).

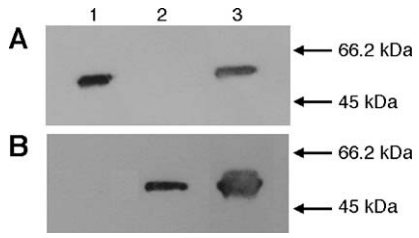

Fig. 4. Western blotting analysis of purified (1) 6xHis–hPAHwt$_{Tet}$ (Myc epitope); (2) 6xHis–hPAH V388M$_{Lar}$ (Xpress epitope) and (3) co-produced 6xHis–hPAHwt$_{Tet}$/6xHis–hPAH V388M$_{Lar}$ protein (Myc and Xpress epitope). Immunodetection using the anti-Myc (A) and anti-Xpress (B) antibodies (see text for details).

purified homomeric R270K protein exhibited only 2.1% (121 nmol Tyr min^{-1} mg^{-1}) of residual activity, whereas mutations I65T, R261Q and V388M presented 26.5% (1539 nmol Tyr min^{-1} mg^{-1}), 27.6% (1603 nmol Tyr min^{-1} mg^{-1}) and 27% (1569 nmol Tyr min^{-1} mg^{-1}) respectively, of the activity of the native enzyme.

The subunits of the co-produced 6xHis hPAH proteins were expressed alternatively by each of the vectors and their enzymatic activities were determined. The obtained values were compared (Student's *t* test) in order to determine if their difference were statistically significant (Table 2).

As shown in Table 2, the enzymatic activities of the purified co-produced mutant proteins were always lower than the PRA. The R270K/R261Q protein presented an experimental activity 21% lower than the PRA. For the V388M/I65T, V388M/R261Q and I65T/R261Q we could observe a similar effect in the decrease of the enzymatic activity (38, 35 and 28%, respectively). Proteins produced by co-expressing the R270K and V388M alleles showed the higher activity decrease (88%), while the R270K/I65T co-produced protein presented an experimental activity 52% lower than the PRA. The hPAHwt/V338M protein, mimicking a heterozygous condition, also presented a residual activity (38.5%) lower than the PRA (63.5%).

4. Discussion

Interallelic complementation is a phenomenon that occurs when a hybrid protein is expressed from two different mutated alleles of a gene. When compared to the predicted residual activity the produced heteromeric protein could present a higher (positive complementation) or lower (negative complementation) catalytic activity.

The observation that some PKU patients present a more severe phenotype than the predicted [6] suggests that the resulting heterotetrameric enzyme activity should be lower than the predicted value, determined from the independent enzyme activities of the respective homomeric mutant proteins. To give an explanation for this phenomenon the occurrence of a negative interallelic complementation mechanism has been evoked. While interactions of different subunits of a hybrid hPAH protein were already proven to occur [8,9], the enzymatic activities of such heteromeric proteins had never been determined.

In order to co-produce two different subunits of a heteroallelic hPAH phenotype, a prokaryotic dual vector co-

Table 2
Enzymatic activities of homoallelic and heteroallelic 6xHis hPAH recombinant proteins produced by simultaneous expression of two subunits

PAH sub-unit composition	Specific activity [a] (nmol Tyr min^{-1} mg^{-1})	Residual enzyme activity [b] (%)	PRA [c] (%)	Observed decrease (%)
$hPAHwt_{Lar}/hPAHwt_{Tet}$	5818±82.7 (100%)		–	–
$I65T_{Lar}/I65T_{Tet}$	1539±42.4 (26.5%)		–	–
$R261Q_{Lar}/R261Q_{Tet}$	1603±49.5 (27.6%)		–	–
$R270K_{Lar}/R270K_{Tet}$	121±18.4 (2.1%)		–	–
$V388M_{Lar}/V388M_{Tet}$	1569±41.0 (27.0%)		–	–
$V388M_{Lar}/hPAHwt_{Tet}$	2336 (40%)	38.5	63.5	39
$V388M_{Tet}/hPAHwt_{Lar}$	2200 (37%)			
	(*P* n.d.)			
$V388M_{Lar}/I65T_{Tet}$	918±49.0 (15.8%)	16.5	26.7	38
$V388M_{Tet}/I65T_{Lar}$	1003±20.8 (17.2%)			
	(*P*>0.05)			
$V388M_{Lar}/R261Q_{Tet}$	1062±34.9 (18.2%)	17.6	27.3	35
$V388M_{Tet}/R261Q_{Lar}$	987±35.5 (17.0%)			
	(*P*>0.05)			
$V388M_{Lar}/R270K_{Tet}$	118±7.4 (2.03%)	1.77	14.4	88
$V388M_{Tet}/R270K_{Lar}$	88±15.6 (1.51%)			
	(*P*>0.05)			
$R270K_{Lar}/I65T_{Tet}$	474±6.0 (8.15%)	6.91	14.3	52
$R270K_{Tet}/I65T_{Lar}$	330±10.5 (5.67%)			
	(*P*<0.001)			
$R270K_{Lar}/R261Q_{Tet}$	676±10.5 (11.6%)	11.8	14.8	21
$R270K_{Tet}/R261Q_{Lar}$	691±8.3 (11.9%)			
	(*P*>0.1)			
$I65T_{Lar}/R261Q_{Tet}$	1185±15.9 (20.4%)	19.4	27.0	28
$I65T_{Tet}/R261Q_{Lar}$	1075±20.5 (18.5%)			
	(*P*<0.01)			

[a] Values are means ± standard deviation determined from three independent experiments, except for the $V388M_{Lar}/hPAHwt_{Tet}$ and $V388M_{Tet}/hPAHwt_{Lar}$ constructs (two experiments); Statistical analysis compared subunits produced from different expression vectors; statistical significance (*P* value) was determined using the Student's *t* test; values in parenthesis refer to % of activity relative to the wild-type form (residual activity).

[b] Mean of residual enzyme activity determined for both constructs.

[c] (PRA) Predicted enzymatic activity, calculated by averaging the experimental enzymatic activities of the corresponding homomeric proteins. (n.d.) not determined.

expression system (PRO system) was used. The different modes of promoter regulation allowed us to control independently the expression of the two cloned alleles. Actually, the use of 100 ng/ml of aTc (pPROTet–Myc–His constructs) and 0.2% arabinose/1 mM IPTG (pPROLar–XPress–His constructs) produced similar quantities of each different protein (Fig. 1). This fact represents one of the greatest advantages of the dual vector system when compared to the bicistronic system [20].

We first studied each expression vector individually in order to confirm that they were suitable for the production of catalytically active PAH enzyme. The use of pPROLar–XPress–His and pPROTet–Myc–His expression vectors allowed the purification of the full-length recombinant 6xHis–hPAH proteins (55 kDa), with purity grades ranging from 60 to 95%. The resulting mutant homoallelic forms presented relative enzymatic activities (Table 2) similar to those obtained previously, using the pTrcHis prokaryotic expression system [12,19].

The presence of different epitopes in the constructs (Myc and Xpress) allowed us to confirm the presence of both subunits in the coexpressing assays. As shown by Western blot analysis (Fig. 4), cotransformation with the different pPROLar–XPress–His and pPROTet–Myc–His constructs into the *E. coli* strain DH5αPRO resulted in the production of similar levels of the two different subunits of the co-produced $hPAHwt_{Tet}/V388M_{Lar}$ protein.

In order to prove that the determined enzymatic activities of the co-produced proteins were independent of the vector used to express the studied allele, each hPAH subunit, comprising the heteroallelic state, was always synthesized in the two possible combinations (Table 2). The obtained enzymatic activities were not significantly different (*P*>0.05), except for the R270K/I65T (*P*<0.001) and R261Q/I65T (*P*<0.01) proteins. In these two co-produced proteins the determined *P* value (<0.05) could not be explained neither by the presence of a particular subunit, namely the I65T subunit as it was not observed for the co-produced V388M/I65T mutant protein, nor by an higher expression level of one of the vectors. Moreover, the same range of residual activity was calculated (Table 2) for the R270K/I65T combinations (8.1 and 5.67%) and for the R261Q/I65T combinations (18.5 and 20.4%). Therefore, any of the construct combinations could be used to study the interallelic complementation phenomenon.

We could demonstrate for the heteroallelic mutant proteins, a decrease in the enzymatic activity when compared to the predicted residual activity (PRA). These values, ranging from 88% (V388M/R270K) to 21% (R270K/R261Q), reflect a negative interaction between the studied mutant subunits.

Furthermore, we can conclude that the subunit interactions are strongly dependent on the nature of the mutant proteins present. Among these, the R270K subunit presented a higher negative effect, particularly over the V388M subunit. It has been postulated that reduced stability is likely the most important attribute for the association of the R270K mutation with PKU in vivo [19]. Therefore, the observed drastic effect of this mutant subunit could be related to an altered protein oligomerisation.

Each subunit of the tetrameric hPAH comprises a N-terminal regulatory domain (Ser2–Ser110), a catalytic domain (Ser110–Ser411) a dimerisation motif (Ser411–Thr427) and a C-terminal tetramerisation domain (Glu428–Lys452) [21]. The regulatory domain from one subunit establishes contacts with the catalytic domain of the other subunit in the dimer. The tetramers are considered to be a dimer of dimers in which the subunits in one dimer contact the subunits in the adjacent dimer only via the α-helical tetramerisation motif. As none of the studied mutations affect the hPAH tetramerisation domain (I65T and R261Q are dimer interface mutations) [22,23] probably they will affect the existing interactions between the subunit interfaces and not directly the tetrameric unit assembly. As a consequence, the enzymatic function could be directly affected as the studied mutations could interfere with the necessary conformational changes occurring at the dimer interface upon activation by L-Phe [24]. We could also admit that they result in quaternary structures relatively less stable. In this regard, the dual expression system described herein will allow the study of the oligomerisation pattern of the produced proteins as well as their enzymatic properties (studies in course). It must be noted that albeit there is now a high-resolution structure available for the hPAH enzyme, there is still no direct proof of subunit interaction or a clear insight into the possible structural basis of any such interaction.

In conclusion, from our observations, it seems clear that a phenomenon of negative interallelic complementation exists between the studied hPAH subunits, mimicking heterozygous and heterozygous compound patients. Furthermore, it appears likely that this phenomenon could be a general source of phenotypic variation in genetic diseases involving multimeric proteins. Such interactions must be considered in any attempt to establish genotype/phenotype correlations in patients affected by such disorders.

Acknowledgements

This study was supported by grants from the Fundação para a Ciência e Tecnologia: PECS/C/SAU/34/95; POCTI/MGI/40844/2001, SFRH/BD/10.807/2002 (to Cátia Nascimento) and SFRH/BD/19024/2004 (to João Leandro). We are grateful to Dr. David Konecki for helpful suggestions in the choice of the dual expression system.

References

[1] C.R. Scriver, S. Kaufman, R.C. Eisensmith, S.L.C. Woo, The hyperphenylalaninemias, in: C.R. Scriver, A.L. Beaudet, W.S. Sly, D. Valle (Eds.), The Metabolic and Molecular Bases of Inherited Disease, McGraw-Hill, New York, 1995, pp. 1015–1075.

[2] C.R. Scriver, P.J. Waters, Monogenic traits are not simple, Trends Genet. 15 (1999) 267–272.

[3] Y. Okano, R.C. Eisensmith, F. Guttler, U. Lichter-Konecki, D.S. Konecki, F.K. Trefz, M. Dasovich, T. Wang, K. Henriksen, C. Lou, S.L.C. Woo, Molecular basis of phenotypic heterogeneity in phenylketonuria, N. Engl. J. Med. 324 (1991) 1232–1238.

[4] U. Lichter-Konecki, A. Rupp, D.S. Konecki, F.K. Trefz, H. Schmidt, P. Burgard, Relation between phenylalanine hydroxylase genotypes and sphenotypic parameters of diagnosis and treatment of hyperphenylalaninemic disorders, J. Inherit. Metab. Dis. 17 (1994) 362–365.

[5] P. Guldberg, I. Mikkelsen, F.F. Henriksen, H.C. Lou, F. Guttler, In vivo assessment of mutations in the phenylalanine hydroxylase gene by phenylalanine loading: characterization of seven common mutations, Eur. J. Pediatr. 154 (1995) 551–556.

[6] E. Kayaalp, E. Treacy, P.J. Waters, S. Byck, P. Nowacki, C.R. Scriver, Human phenylalanine hydroxylase mutations and hyperphenylalaninemia phenotypes: a metanalysis of genotype–phenotype correlations, Am. J. Hum. Genet. 61 (1997) 1309–1317.

[7] S. Kaufman, E.E. Max, Phenylalanine hydroxylase activity in liver biopsies from hyperphenylalaninemia heterozygotes: deviation from proportionality with gene dosage, Pediatr. Res. 9 (1975) 632–634.

[8] P.J. Waters, C.R. Scriver, M.A. Parniak, Homomeric and heteromeric interactions between wild-type and mutant phenylalanine hydroxylase subunits: evaluation of two-hybrid approaches for functional analysis of mutations causing hyperphenylalaninemia, Mol. Genet. Metab. 73 (2001) 230–238.

[9] B. Perez, L.R. Desviat, M. Ugarte, Analysis of defective subunit interactions using the two-hybrid system, Methods Mol. Biol. 232 (2003) 245–256.

[10] I. Rivera, A. Cabral, M. Almeida, P. Leandro, C. Carmona, F. Eusébio, T. Tasso, L. Vilarinho, E. Martins, M.C. Lecnher, I.T. de Almeida, D.S. Konecki, U. Lichter-Konecki, The correlation of genotype and phenotype in Portuguese hyperphenylalaninemia patients, Mol. Genet. Metal. 69 (2000) 195–220.

[11] R. Lutz, H. Bujard, Independent and tight regulation of transcriptional units in *Escherichia coli* via the LacR/O, the TetR/O and AraC/I1-I2 regulatory elements, Nucleic Acids Res. 25 (1997) 1203–1210.

[12] P. Leandro, I. Rivera, M.C. Lechner, I. Tavares de Almeida, D.S. Konecki, The V388M mutation results in a kinetic variant form of phenylalanine hydroxylase, Mol. Genet. Metab. 69 (2000) 204–212.

[13] S.C. Kwock, F.D. Ledley, A.G. DiLella, K.J. Robson, S.L.C. Woo, Nucleotide sequence of a full-length complementary DNA clone and aminoacid sequence of phenylalanine hydroxylase, Biochemistry 24 (1985) 556–561.

[14] F.M. Ausubel, R. Brent, R.E. Kingston, D.D. Moore, J.G. Seidman, J.A. Smith, K. Struhl, Current Protocols in Molecular Biology, John Wiley and Sons, New York, 1994.

[15] M.M. Bradford, A rapid and sensitive method for the quantitation of microgram quantities of protein utilizing the principle of protein-dye binding, Anal. Biochem. 72 (1976) 248–254.

[16] A. Martinez, P.M. Knappskog, S. Olafsdottir, A.P. Doskeland, H.G. Eiken, R.M. Svebak, M. Bozzini, J. Apold, T. Flatmark, Expression of recombinant phenylalanine hydroxylase as a fusion protein in Escherichia coli circumvents proteolytic degradation by host cell proteases, Biochem. J. 306 (1995) 589–597.

[17] S.C. Smith, B.E. Kemp, W.J. McAdam, J.F.B. Mercer, R.G.H. Cotton, Two apparent molecular weight forms of human and monkey phenylalanine hydroxylase are due to phosphorylation, J. Biol. Chem. 259 (1984) 11284–11289.

[18] S.L.C. Woo, S.S Gillam, L.I. Woolf, The isolation and properties of phenylalanine hydroxylase from human liver, Biochem. J. 139 (1974) 741–749.

[19] P. Leandro, I. Rivera, M.C. Lechner, D.S. Konecki, I. Tavares de Almeida, Prokaryotic expression analysis of I269L and R270K

mutations of the phenylalanine hydroxylase gene, Gene Funct. Dis. 1 (2001) 46–50.
[20] P. Rucker, F.M. Torti, S.V. Torti, Recombinant ferritin: modulation of subunit stoichiometry in bacterial expression systems, Protein Eng. 10 (1997) 967–973.
[21] M. Thorolfsson, B. Ibarra-Molero, P. Fojan, S.B. Peterson, J.M. Sanchez-Ruiz, A. Martinez, L-Phenylanine binding and domain organization in human phenylalanine hydroxylase: a differential scanning calorimetry study, Biochemistry 41 (2002) 7573–7585.
[22] H. Erlandsen, R.C. Stevens, The structural basis of phenylketonuria, Mol. Genet. Metab. 68 (1999) 103–125.
[23] H. Erlandsen, E. Bjørgo, T. Flatmark, R.C. Stevens, Crystal structure and site-specific mutagenesis of pterin-bound human phenylalanine hydroxylase, Biochemistry 39 (2000) 2208–2217.
[24] I.G. Jennings, R.G.H. Cotton, B. Kobe, Structural interpretation of mutations in phenylalanine hydroxylase protein aids in identifying genotype–phenotype correlations in phenylketonuria, Eur. J. Hum. Genet. 8 (2000) 683–696.

2. Heterotetrameric forms of human phenylalanine hydroxylase: Co-expression of wild-type and mutant forms in a bicistronic system

João Leandro, Paula Leandro, Torgeir Flatmark

Biochimica et Biophysica Acta (Molecular Basis of Disease), 1812 (2011) 602–612.

Biochimica et Biophysica Acta 1812 (2011) 602–612

Contents lists available at ScienceDirect

Biochimica et Biophysica Acta

journal homepage: www.elsevier.com/locate/bbadis

Heterotetrameric forms of human phenylalanine hydroxylase: Co-expression of wild-type and mutant forms in a bicistronic system

João Leandro [a,b,*], Paula Leandro [b], Torgeir Flatmark [a]

[a] Department of Biomedicine, University of Bergen, Jonas Lies vei 91, N-5009 Bergen, Norway
[b] Metabolism and Genetics Group, Research Institute for Medicines and Pharmaceutical Sciences (iMed.UL), Faculty of Pharmacy, University of Lisbon, Av. Prof. Gama Pinto, 1649–003 Lisbon, Portugal

ARTICLE INFO

Article history:
Received 15 October 2010
Received in revised form 19 January 2011
Accepted 3 February 2011
Available online 17 Febraury 2011

Keywords:
Phenylketonuria
Human phenylalanine hydroxylase
Interallelic complementation
Bicistronic system
Hybrid protein
Heteroallelic protein

ABSTRACT

Hybrid forms of human phenylalanine hydroxylase (hPAH) mutants have been found to present catalytic activities lower than predicted from the individual recombinant forms, indicating that interallelic complementation could be a major determinant of the metabolic phenotype of compound heterozygous phenylketonuric (PKU) patients. To provide a molecular explanation for interallelic complementation we have here developed a bicistronic expression system and a purification strategy to obtain isolated hPAH heteromeric forms. On co-expression of WT-hPAH (~50% tetramer; ~10% dimer) and the N- and C-terminally truncated form ΔN102/ΔC24-hPAH (~80% dimer) no heterodimers were recovered. Moreover, by co-expression of WT-hPAH and the N-terminally truncated form ΔN102-hPAH (~95% tetramer), heterotetramers, as a result of an assembly of two different homodimers, were isolated. The recovered (WT)/(ΔN102)-hPAH heterotetramers revealed a catalytic activity deviating significantly from that calculated by averaging the respective recombinant homotetrameric forms. The heterotetramer assembly also results in conformational changes in the WT-hPAH protomer, as detected by trypsin limited proteolysis. The finding that the presence of two homodimers with different kinetic parameters influences the properties of the resulting heterotetrameric protein indicates that the dimers exhibit interactions which are transmitted across the assembled tetramer. The bicistronic expression system developed here allowed the isolation of hybrid forms that exhibit negative interallelic complementation, and may represent a model system for studying the molecular pathogenic mechanisms of *PAH* gene mutations in compound heterozygous PKU patients, providing the rationale to understand the observed inconsistencies both in genotype/phenotype correlations and in the response to BH_4 supplementation.

1. Introduction

Human phenylalanine hydroxylase (hPAH, human phenylalanine 4-monooxygenase, EC 1.14.16.1), is a non-heme iron enzyme that catalyzes the hydroxylation of L-phenylalanine (L-Phe) to L-tyrosine (L-Tyr) in the presence of the cofactor (6*R*)-L-*erythro*-5,6,7,8-tetrahydrobiopterin (BH_4) and dioxygen, the rate-limiting step in L-Phe catabolism [1]. hPAH is a homotetrameric/homodimeric protein with the protomer organized into three functional domains: a regulatory N-terminal domain (residues 1–117) containing the phosphorylation site (Ser16) and an autoregulatory sequence (ARS, residues 1–33); a catalytic core domain (residues 118–411); and a C-terminal region (residues 412–452) including the dimerization and tetramerization motifs [1,2]. The tetramer is a dimer of two conformationally different dimers, related by a 2-fold noncrystallographic symmetry axis [3]. It is activated 5- to 6-fold on preincubation with L-Phe, reveals a positive kinetic cooperativity with respect to L-Phe and Michaelis–Menten kinetics with BH_4 for the non-preactivated enzyme [4] and BH_4-dependent positive cooperativity for the preactivated form [5].

Mutations in hPAH causing lost or impaired activity of the enzyme are associated with the autosomal recessively inherited disease phenylketonuria (PKU, OMIM 261600), the most frequent disorder of amino acid metabolism [6], with a high genotypic heterogeneity (more than 500 different *PAH* gene mutations identified to date; http://www.pahdb.mcgill.ca [7]). If untreated, PKU patients present neurological damages due to the increased levels of L-Phe in body fluids [8], and life-long dietary restriction of L-Phe remains the most effective treatment for PKU [9]. Some PKU patients respond to oral ingestion of the pterin cofactor (BH_4) by a reduction in blood L-Phe concentration (BH_4-responsive) and therefore, presently BH_4 is accepted as a novel therapeutic approach. However, it has been

Abbreviations: 6His, hexahistidyl tag; BH_4, (6*R*)-L-*erythro*-5,6,7,8-tetrahydrobiopterin; hPAH, human phenylalanine hydroxylase; IC, interallelic complementation; IPTG, isopropyl-β-D-thio-galactoside; L-Phe, L-phenylalanine; MBP, maltose binding protein; PKU, phenylketonuria; PRA, predicted residual activity; WT, wild-type

* Corresponding author at: Metabolism and Genetics Group, iMed.UL, Faculty of Pharmacy, University of Lisbon, Av. Prof. Gama Pinto, 1649–003 Lisbon, Portugal. Tel.: +351 217946400; fax: +351 217946491.
E-mail address: jptleandro@ff.ul.pt (J. Leandro).

0925-4439/$ – see front matter © 2011 Elsevier B.V. All rights reserved.
doi:10.1016/j.bbadis.2011.02.001

shown that the full genotype determines the BH_4-responsive phenotype [10–12].

A unique property of homomeric enzymes associated with human genetic disorders is their potential ability to exhibit interallelic complementation (IC), a phenomenon that occurs in heteroallelic states when particular combinations of two different alleles, at a given *locus*, produce a less (positive IC) or a more (negative IC) severe phenotype than their homoallelic counterparts. IC is observed in homomeric enzymes where the protomers exhibit interactions resulting in hybrid proteins with functional or stability properties significantly different from the average of the parental enzymes. The phenomenon is proposed to contribute to the phenotypic diversity of several human diseases including metabolic disorders such as PKU [13,14], argininosuccinic aciduria [15–17], erythropoietic protoporphyria [18] and galactosemia [19,20], neurodegenerative disorders such as familial amyloid polyneuropathy [21,22] and cancer [23,24]. Interallelic complementation is assumed to be of particular importance in PKU since ~75% of PKU patients are compound heterozygous, encoding two different mutant hPAH protomers [25]. Experimental evidence lending support to a negative IC in some compound heterozygous PKU patients has been obtained by the observations that the patients present: (i) a more severe metabolic phenotype than that anticipated by the predicted residual activity (PRA) based on *in vitro* assays of recombinant proteins [26–28], and (ii) an absence or only a partial response to BH_4, although carrying two BH_4-responsive alleles [29]. Interactions between different hPAH protomers have been demonstrated by three different experimental strategies, i.e. *in vitro* formation of heterotetramers from different dimers [30], the yeast two-hybrid system [31] and a dual vector prokaryotic expression system producing two different hPAH subunits mimicking the natural heteroallelic state in heterozygous or in compound heterozygous patients [14]. However, the molecular mechanism of negative IC and its role in PKU pathogenesis is far from being solved since heterotetrameric forms of hPAH have only been demonstrated *in vitro* [30], but never isolated and characterized biochemically.

In order to provide some insight into the assembly process of heteroallelic hPAH proteins and their non-additive gene dosage effect, truncated forms of the protein (ΔN102-hPAH and ΔN102/ΔC24-hPAH) were co-expressed with WT-hPAH, and the heteromeric forms characterized biochemically. To isolate the recombinant heteromeric proteins in high yield and purity a bicistronic expression system was developed, presenting the different protomers as fusion proteins with the chaperone maltose binding protein (MBP) [30,32] and different affinity purification tags (calmodulin binding peptide (CBP), hexahistidyl peptide (6His) and StrepII peptide). The affinity isolated heteromeric species were characterized by their steady-state kinetic properties and susceptibility to limited proteolysis.

2. Materials and methods

2.1. Materials

The DNA primers used for mutagenesis were provided by Eurogentec (Seraing, Belgium) and the restriction endonucleases were from New England Biolabs (USA). *Escherichia coli* BL21(DE3) and the prokaryotic expression vector pETDuet-1 were obtained from Novagen (Merck KGaA, Darmstadt, Germany). The restriction protease factor Xa was obtained from Protein Engineering Technology ApS (Aarhus, Denmark). SDS molecular mass standard was delivered by Bio-Rad and the pterin cofactor (6*R*)-L-*erythro*-5,6,7,8-tetrahydrobiopterin (BH_4) was obtained from Schircks Laboratories (Jona, Switzerland). Trypsin and trypsin inhibitor were delivered by Sigma-Aldrich (St. Louis, MO, USA).

2.2. Construction of the bicistronic expression vectors

The calmodulin binding peptide (later replaced by the StrepII sequence) and the hexahistidyl peptide (6His; HHHHHH) were firstly selected to produce different N-terminal tagged recombinant proteins using the bicistronic expression vector pETDuet-1. This vector contains two multiple cloning sites (MCS1 and MCS2), each preceded by a T7 promoter/*lac* operator and a ribosome binding site. A T7 terminator sequence is located at 3′ of the MCS2.

The strategy to construct the bicistronic expression vector is depicted in Supplementary Fig. S1. The sequence coding for the calmodulin binding peptide (CBP; KRRWKKNFIAVSAANRFKKISSSGAL) together with a *Pme*I restriction sequence were introduced 5′ to the MBP coding sequence by three steps of site-directed mutagenesis using the pMAL-hPAH vector as a template [33] and primers CBP1st-F/CBP1st-R, CBP2nd-F/CBP2nd-R and CBP3rd-F/CBP3rd-R (Table 1). The resulting vector pMAL-CBP-MBP-pep$_{(Xa)}$-WT-hPAH was double digested with *Pme*I/*Sbf*I. The isolated expression cassette was blunted with T4 DNA polymerase, according to standard procedures, and cloned into the MCS1 of pETDuet-1 vector which had been previously digested with *Nco*I, blunted and dephosphorylated with calf intestinal alkaline phosphatase (CIP), thus generating the expression vector pETDuet-1-CBP-MBP-pep$_{(Xa)}$-WT-hPAH.

In order to replace the CBP tag by the StrepII tag (WSHPQFEK), two steps of site-directed mutagenesis were performed using the pETDuet-1-CBP-MBP-pep$_{(Xa)}$-WT-hPAH as template and primers STRII-F/STRII-R and CBPDel-F/CBPDel-R (Table 1). In the obtained construct (pETDuet-1-StrepII-MBP-pep$_{(Xa)}$-WT-hPAH) a new T7 terminator was introduced 3′ to MCS1, by site-directed mutagenesis, using primers CRET7-F/CRET7-R (Table 1).

To create the bicistronic expression construct the sequence coding for the 6His tag and the *Pme*I restriction sequence were previously introduced 5′ to the MBP coding sequence by site-directed mutagenesis, using pMAL-MBP-pep$_{(Xa)}$-ΔN102-hPAH or pMAL-MBP-pep$_{(Xa)}$-ΔN102/ΔC24-hPAH constructs as templates [34] and primers HisF/HisR (Table 1). The expression cassette was isolated, after *Pme*I/*Sbf*I double digestion, blunt-ended and cloned into the MCS2 of pETDuet-1-StrepII-MBP-pep$_{(Xa)}$-WT-hPAH vector which had been previously digested with *Eco*RV (MCS2), blunt-ended and dephosphorylated. The pETDuet-1-[StrepII-MBP-pep$_{(Xa)}$-WT-hPAH/6His-MBP-pep$_{(Xa)}$-ΔN102-hPAH] and pETDuet-1-[StrepII-MBP-pep$_{(Xa)}$-WT-hPAH/6His-MBP-pep$_{(Xa)}$-ΔN102/ΔC24-hPAH] bicistronic constructs were obtained (Fig. 1). Site-directed mutagenesis reactions were always performed using the Quikchange® II XL system (Stratagene, La Jolla, CA, USA) and the authenticity of mutagenesis reactions and cloning was always verified by DNA sequencing using the BigDye® Terminator v3.1 Cycle Sequencing Kit (Applied Biosystems) in an ABI 3730xl DNA Analyzer (Applied Biosystems). All the expression constructs present a cleavage site for factor Xa (IEGR) between the N-terminal fusion protein and the hPAH sequence.

2.3. Expression and purification of recombinant hPAH

E. coli BL21(DE3) competent cells were transformed with the pETDuet-1-[StrepII-MBP-pep$_{(Xa)}$-hPAH$_1$/6His-MBP-pep$_{(Xa)}$-hPAH$_2$] (hPAH$_1$: WT-hPAH; hPAH$_2$: ΔN102-hPAH or ΔN102/ΔC24-hPAH) expression vectors and grown in LB medium, supplemented with 50 μg·mL^{-1} ampicillin and 0.2% glucose, at 37 °C. Protein expression was induced with 1 mM isopropyl thio-β-D-galactoside (IPTG), when the A_{600} was about 0.8. Ferrous ammonium sulfate, at 0.2 mM, was added simultaneously with IPTG and 3 h after induction. After 8 h incubation, at 28 °C, bacteria were harvested and the pellets stored at −20 °C until use. To rule out homologous recombination, plasmid integrity was checked. To purify the recombinant enzymes, cells were resuspended in lysis buffer

Table 1
Oligonucleotides used for site-directed mutagenesis.

Template	Primers[a]	Sequence (5′→3′)[b]
pMAL-hPAH$_{wt}$	CBP1st F	CCAACAAGGACCATAGATTATG**GTTTAAACTTAAGCGACGATGGAAAAAGA**AAAATCGAAGAAGGTAAACTGG
	CBP1st R	CCAGTTTACCTTCTTCGATTTT**TCTTTTTCCATCGTCGCTTAAGTTTAAAC**CATAATCTATGGTCCTTGTTGG
pMAL-CBP1-hPAH$_{wt}$	CBP2nd F	CTTAAGCGACGATGGAAAAAGA**ATTTCATAGCCGTCTCAGCAGCCAACCGC**AAAATCGAAGAAGGTAAACTGG
	CBP2nd R	CCAGTTTACCTTCTTCGATTTT**GCGGTTGGCTGCTGAGACGGCTATGAAAT**TCTTTTTCCATCGTCGCTTAAG
pMAL-CBP2-hPAH$_{wt}$	CBP3rd F	GCCGTCTCAGCAGCCAACCGC**TTTAAGAAAATCTCATCCTCCGGGGCACTT**AAAATCGAAGAAGGTAAACTGG
	CBP3rd R	CCAGTTTACCTTCTTCGATTTT**AAGTGCCCCGGAGGATGAGATTTTCTTAAA**GCGGTTGGCTGCTGAGACGGC
pETDuet-1-CBP-hPAH$_{wt}$	STRII F	GAAAATCTCATCCTCCGGGGCACTT**GCTAGCTGGAGCCACCCGCAGTTCGAAAAAGGCAGC**AAAATCGAAGAAGGTAAACTGG
	STRII R	CCAGTTTACCTTCTTCGATTTT**GCTGCCTTTTTCGAACTGCGGGTGGCTCCAGCTAGC**AAGTGCCCCGGAGGATGAGATTTTC
pETDuet-1-CBP-STRII-hPAH$_{wt}$	CBPDel F	CAATTCCCCTCTAGAAATAATTTTGTTTAACTTTAAGAAGGAGATATACCATGGCTAGCTGGAGCCACCCGCAGTTCGAAAAA GGCAGCAAAATCGAAGAAGG
	CBPDel R	CCTTCTTCGATTTTGCTGCCTTTTTCGAACTGCGGGTGGCTCCAGCTAGCCATGGTATATCTCCTTCTTAAAGTTAAACAAAAT TATTTCTAGAGGGGAATTG
pETDuet-1-STRII-hPAH$_{wt}$	CRET7T F	GCAGGTCGACAAGCTTGCGGCCGCATAATGCTT**CTAGCATAACCCCTTGGGGCCTCTAAACGGGTCTTGAGGGGTTTTTTG** AAGTCGAACAGAAAGTAATCGTATTGTACACG
	CRET7T R	CGTGTACAATACGATTACTTTCTGTTCGACTT**CAAAAAACCCCTCAAGACCCGTTTAGAGGCCCCAAGGGGTTATGCTAG** AAGCATTATGCGGCCGCAAGCTTGTCGACCTGC
pMAL-hPAH$_{\Delta N102}$ and pMAL-hPAH$_{\Delta N102/\Delta C24}$	HIS F	CCAACAAGGACCATAGATTATG**GTTTAAACCATCACCATCACCATCAC**AAAATCGAAGAAGGTAAACTGG
	HIS R	CCAGTTTACCTTCTTCGATTTT**GTGATGGTGATGGTGATGGTTTAAAC**CATAATCTATGGTCCTTGTTGG

[a] F—forward, R—reverse.
[b] Mismatch nucleotides are shown in boldface; nucleotides used to create new restrictions sites are underlined.

(10 mM Tris–HCl, 200 mM NaCl, 0.5 μg·mL^{-1} pepstatin, pH 7.25) supplemented with 1× Complete Protease Inhibitor Cocktail (Roche Applied Science) and disrupted by passage through a *French Press*. The presence of the MBP tag, in both hPAH subunits, allowed the purification of the fusion proteins using an amylose resin (New England Biolabs), previously equilibrated with 15 mM Na–Hepes, 200 mM NaCl, and 1 mM EDTA, pH 7.4. Recombinant proteins were eluted with 10 mM maltose [33].

The tetramers and dimers were isolated by size-exclusion chromatography (SEC), using a HiLoad Superdex 200 HR column (1.6 cm × 60 cm, Amersham Biosciences) and a mobile phase containing 20 mM Na–Hepes, 200 mM NaCl, pH 7.0 (SEC buffer) pumped at a flow rate of 0.38 mL·min^{-1}. The relative molecular mass of the different oligomeric forms was estimated from a calibration curve obtained with the following standard proteins: aprotinin (6.5 kDa), ribonuclease A (13.7 kDa), carbonic anhydrase (29 kDa), ovalbumin (43 kDa), BSA (66 and 132 kDa), conalbumin (75 kDa), aldolase (158 kDa), ferritin (440 kDa) and thyroglobulin (669 kDa). Blue Dextran 2000 and AMP were used to determine the void volume (V_0 = 45.2 mL) and the total exclusion volume (V_T = 115.5 mL) of the column, respectively. All purification steps were carried out at 4 °C. The relative amounts of the different oligomeric states were calculated by deconvolution of the obtained chromatograms using the PeakFit software (Systat Software Inc). Protein concentration was estimated by the Bradford method [35] using bovine serum albumin (BSA) as the standard.

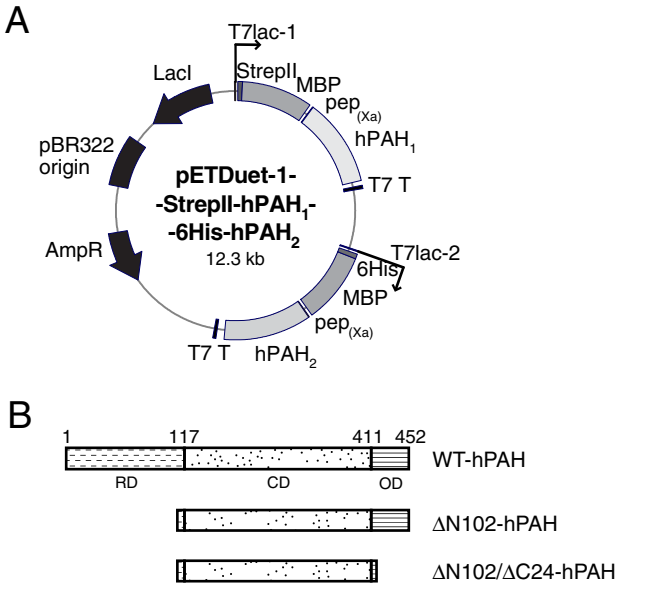

Fig. 1. Schematic representation of the bicistronic expression construct and the hPAH polypeptide chains used to study interallelic complementation. (A) pETDuet-1 expression construct carrying two expression cassettes each under the control of a T7 *lac* promoter (T7lac-1 and T7lac-2) and presenting a T7 polymerase termination site (T7T); the hPAH$_1$ polypeptide chain is expressed as a fusion protein with the StrepII tag (StrepII) and the maltose binding protein (MBP) and the hPAH$_2$ polypeptide chain is expressed as a fusion protein with the hexahistidyl tag (6His) and MBP; pep$_{(Xa)}$ represents the sequence encoding the factor Xa protease cleavage site. (B) Schematic illustration of the structure of wild-type (WT-hPAH) and truncated forms (ΔN102-hPAH and ΔN102/ΔC24-hPAH) of hPAH with the regulatory (RD), catalytic (CD) and oligomerization (OD) domains represented; the residue number of the last amino acid in each domain is indicated.

2.4. Isolation of hybrid proteins

The tetrameric or dimeric fractions obtained from SEC were applied to a Ni-chelating resin (Ni–NTA, Qiagen, Valencia, CA), pre-equilibrated in SEC buffer containing 10 mM imidazole, and stirred for 1 h at 4 °C. The flow-through was collected (Fraction 1: StrepII-MBP-hPAH$_1$ homomeric proteins) and the resin was washed with SEC buffer containing 20 mM imidazole, followed by a SEC buffer washing step containing 50 mM imidazole. The fusion proteins were eluted with SEC buffer containing 150 mM imidazole (Fraction 2: 6His-MBP-hPAH$_2$ homomeric and StrepII-MBP-hPAH$_1$/6His-MBP-hPAH$_2$ heteromeric proteins).

Fraction 2 was then applied to a Strep-Tactin resin (Strep-Tactin Superflow high capacity, IBA, Göttingen, Germany) and stirred for 1 h at 4 °C. The flow-through was collected (Fraction 3: 6His-MBP-hPAH$_2$ homomeric proteins) and the resin was washed with SEC buffer. The hybrid proteins were eluted with SEC buffer containing 2.5 mM desthiobiotin (Fraction 4: StrepII-MBP-hPAH$_1$/6His-MBP-hPAH$_2$ heteromeric proteins).

The fusion proteins obtained in Fractions 1, 3 and 4 were cleaved for 4 h at 4 °C by factor Xa (Protein Engineering Technology ApS), using a protease to substrate ratio of 1:30 (by mass), and applied to a second column of amylose resin, to remove MBP, followed by removal of factor Xa protease using the Xa Removal Resin (QIAGEN). The homomeric hPAH$_1$ and hPAH$_2$ and the heteromeric hPAH$_1$/hPAH$_2$ forms were then obtained.

Protein purity was analyzed by SDS-PAGE on 10% (w/v) polyacrylamide gels. The gels were stained by 0.1% (w/v) Coomassie Brilliant Blue R250 (Bio-Rad) in 50% (v/v) methanol and 10% (v/v) acetic acid. Stained gels were scanned using VersaDoc 4000 (Bio-Rad) and the protein bands were quantified using the Quantity One 1-D Analysis Software (Bio-Rad).

2.5. Assay of enzymatic activity

The hPAH activity was assayed essentially as described [33], using 0.1 $mg \cdot mL^{-1}$ of catalase and an enzyme activation step by prior incubation (5 min) with L-Phe. BSA, at 0.5% (w/v), was included in the reaction mixture to stabilize the diluted purified hPAH preparations. The amount of L-Tyr formed after 1 min was measured by HPLC and fluorimetric detection [36]. The steady-state kinetic data were analyzed by nonlinear regression analysis using the SigmaPlot® Technical Graphing Software and the modified Hill equation of LiCata and Allewel [37] for cooperative substrate binding as well as substrate inhibition [38]. In order to study the effect of preincubation with L-Phe on the specific activity, 1 mM L-Phe was added together with 75 μM BH_4 at the initiation of the hydroxylation reaction. In this case a 3 min time course was then followed.

2.6. Limited proteolysis with trypsin

Limited proteolysis of WT, ΔN102 and (WT)/(DN102)-hPAH tetrameric forms was performed at 25 °C in 20 mM Na–Hepes, 200 mM NaCl, pH 7.0 and a protease to hPAH ratio of 1:200 (by mass) in the absence or presence of 1 mM L-Phe. The final protein concentration was 0.3 $mg \cdot mL^{-1}$. At timed intervals (0–60 min) aliquots of the reaction were mixed with soybean trypsin inhibitor (at 1:1.5 (by mass) protease to inhibitor ratio) and subjected to SDS-PAGE analysis. Gels were stained by Coomassie brilliant blue and the band corresponding to the full-length protein was quantified by densitometry.

3. Results

3.1. Co-expression of hybrid hPAH proteins using a bicistronic expression system

Using a dual vector expression system encoding two different epitopes (Myc and Xpress) we have previously shown the presence of assembled hybrid hPAH proteins presenting a catalytic activity lower than the PRA [14]. In theory five different tetrameric species would be formed, from the combination of two different co-expressed hPAH subunits ($hPAH_1$:$hPAH_2$), in the following ratios: 0:4, 1:3, 2:2, 3:1 and 4:0. However, by performing a cross-linking reaction of the co-expressed Myc-WT-hPAH and Xpress-WT-hPAH prior to the co-immunoprecipitation step, heterotetramers but not heterodimers were detected in the immunoblots (R. Almeida, J. Leandro et al., personal communication). The absence of heterodimers indicates that the heterotetrameric species 1:3 and 3:1 ($hPAH_1$:$hPAH_2$) would not be formed and only the heterotetrameric $2hPAH_1$:$2hPAH_2$ will be expected, as represented in Fig. 2. Nevertheless, using the described dual expression system [14], the low yields of obtained hybrid

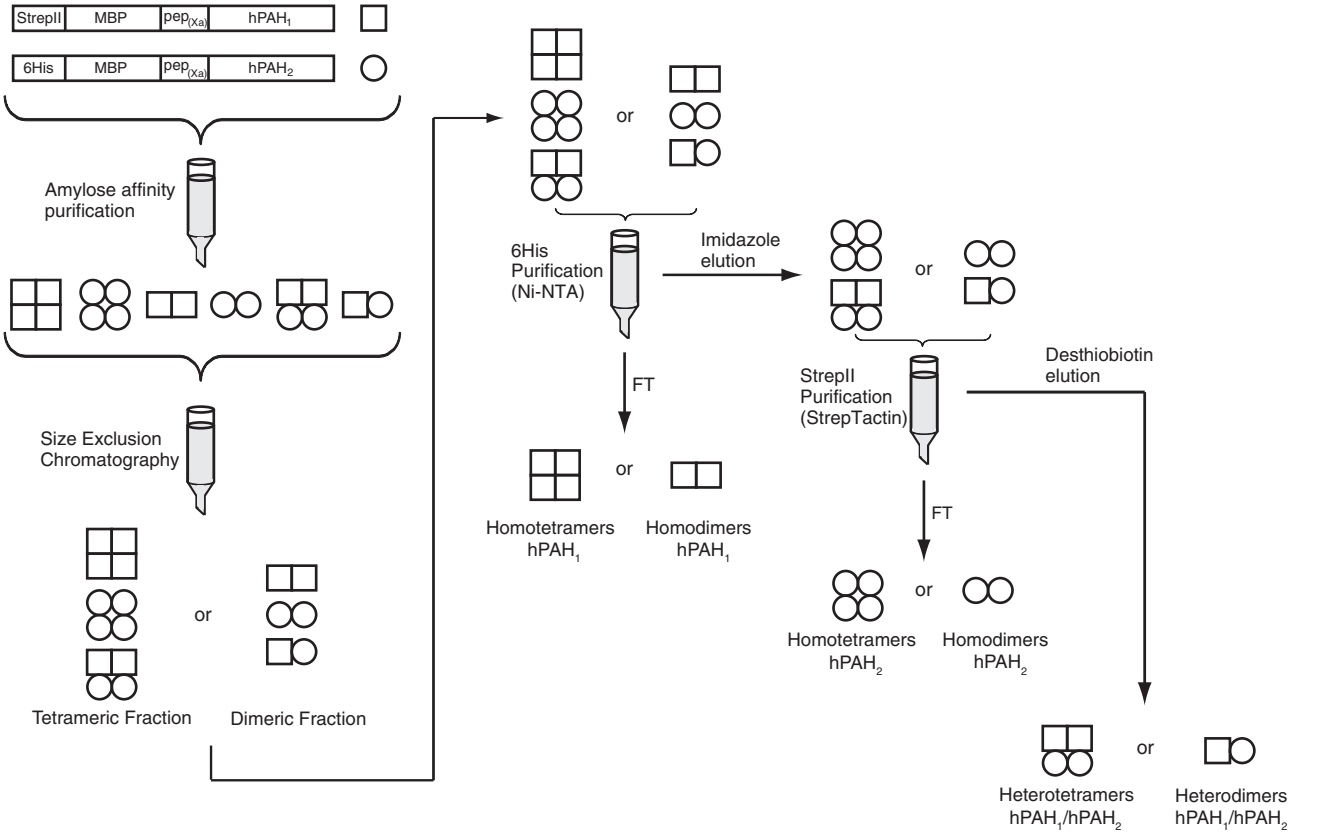

Fig. 2. Flow-chart of the purification procedure of recombinantly co-expressed hPAH polypeptide chains ($hPAH_1$ and $hPAH_2$). The supernatant of lysed bacteria co-expressing two different hPAH proteins was applied to an amylose resin in the first purification step. The MBP fusion proteins were eluted with maltose and applied to a size-exclusion column (SEC). The tetrameric (or dimeric) fraction recovered was applied to a Ni–NTA resin. The StrepII tagged homotetramers (or homodimers) were collected in the flow-through (FT) and the 6His tagged homotetramers (or homodimers) and StrepII/6His tagged heterotetramers (or heterodimers) bound to the resin were eluted with imidazole. In the last step, the eluted fraction was applied to a Strep-Tactin resin. The 6His tagged homotetramers (or homodimers) were obtained in the FT and the StrepII/6His tagged heterotetramers (or heterodimers) were eluted with desthiobiotin. This procedure resulted in the separation of three different hPAH protein species: homomeric StrepII tagged, homomeric 6His tagged and heteromeric StrepII/6His tagged.

proteins precluded the isolation of heteromeric recombinant enzymes for further biochemical and structural characterization. To overcome this problem, we developed here a bicistronic expression strategy, where in addition to two different purification tags (CBP or StrepII, and 6His), the putative molecular chaperone maltose binding protein was used as fusion partner, N-terminally to the hPAH protein, as outlined in Fig. 1A. The presence of two different purification tags offers the possibility to obtain pure hetero-oligomeric fractions by performing two affinity-chromatographic steps (Fig. 2). MBP was chosen as fusion partner (common to both polypeptides), as MBP has been shown to have a chaperone like effect [32,39], improving the yield of recombinant hPAH [30,33]. Using this strategy the WT-hPAH (~50 kDa subunit) was co-expressed with truncated forms of hPAH (Fig. 1B), namely the ΔN102-hPAH (~38.8 kDa subunit) which lacks the first 102 residues (corresponding to the N-regulatory domain) and is mainly expressed as a tetramer (96%) (Table 2); and the double truncated form ΔN102/ΔC24-hPAH (~36.2 kDa subunit) which also lacks the 24 C-terminal residues (corresponding to the tetramerization motif) and is mainly expressed as a dimer (81%) (Table 2). The rationale for co-expressing the WT-hPAH with the truncated forms was fourfold. First, co-expressing the WT-hPAH with the double truncated form (which is isolated mainly as dimer), will expectedly favor the assembly of a heterodimer and thus the presence/absence of these species will allow us to refute/validate our previous observations concerning the assembly of heterodimers (R. Almeida, J. Leandro et al., personal communication). Secondly, co-expressing the WT-hPAH with the N-terminally truncated form (which is isolated mainly as tetramer) will favor the assembly of a heterotetramer. Thirdly, due to the different catalytic properties of the wild-type and truncated forms [2,34] the impact of protomer interactions on the kinetic properties of the assembled heteromeric forms will be proficiently assessed. Fourthly, using SDS-PAGE analysis a clear distinction and quantification of the ratio of the different subunits will be possible since the truncated forms present molecular masses lower than the wild-type.

Small tags characterized by a high specificity and mild elution conditions (Supplementary Table S1) were selected. The polyhistidine tag was our first choice since we had already used it to express and purify recombinant hPAHs [40]. The choice of the second affinity tag was more challenging given the large number of alternatives [41,42]. As a first candidate we tested the CBP peptide. However, during the purification process the hPAH polypeptide, preceded by the CBP tag (CBP-MBP-pep$_{(Xa)}$-hPAH$_1$), suffered extensive aggregation as the result of the effect of a highly hydrophobic patch, present in the middle of the CBP tag (Supplementary Fig. S2). This aggregation was not overcome by the use of glycerol (10%), or by the mild non-ionic detergent n-octylglucoside (15 mM) nor by the use of the improved *E. coli* C41(DE3) strain [43,44] (data not shown). Hence, the CBP tag was replaced by the StrepII tag which allowed the recovery of soluble hPAH in high yields. Since the original pETDuet-1 vector presents only one T7 terminator after MCS2, a new T7 terminator was introduced after MCS1 (Fig. 1A), in order to guarantee the existence of just two mRNAs, each one corresponding to the transcribed sequence of the two different hPAH cDNAs.

The expression conditions (28 °C, 1 mM IPTG, 8 h) were chosen in a compromise between the maximum total recombinant protein produced, its amount in the soluble fraction and the minimization of hPAH deamidation that occurs with long induction times [45]. The expression of the recombinant hPAHs as MBP-fusion proteins resulted in high yields (~12 mg/L culture) when compared with the values obtained with the dual expression system used in our previous studies (~0.3 mg of fusion protein/L culture [14]). After the introduction of the new T7 terminator similar levels of the translated proteins were produced, as shown by SDS-PAGE analysis of the co-expressed proteins after amylose affinity purification (Supplementary Fig. S3). The double truncated dimer ΔN102/ΔC24-hPAH was an exception since it was recovered in the soluble (Supplementary Fig. S3B, lane 3) and dimeric fractions at higher levels due to its higher solubility. As expected, on size-exclusion chromatography the separately expressed StrepII-MBP-WT-hPAH and 6His-MBP-ΔN102-hPAH were recovered mainly in the tetrameric form whereas the double truncated 6His-MBP-ΔN102/ΔC24-hPAH was recovered as a dimer (Table 2). Accordingly, for the co-expressed StrepII-MBP-WT-hPAH and 6His-MBP-ΔN102/ΔC24-hPAH the dimer represented the major oligomeric form (Fig. 3A). SDS-PAGE of this fraction (peak 3) revealed one distinct band at ~96 kDa (StrepII-MBP-WT-hPAH) and another at ~82 kDa (6His-MBP-ΔN102/ΔC24-hPAH) of different intensities, as the double truncated form assembles as dimers with a higher solubility (Fig. 3A, inset, lane 3). SDS-PAGE of the tetrameric fraction (peak 2) gave a single band of ~96 kDa (Fig. 3A, inset, lane 2) corresponding to the StrepII-MBP-WT-hPAH protein. For the co-expressed StrepII-MBP-WT-hPAH and 6His-MBP-ΔN102-hPAH, the tetramers were the predominant species (Fig. 4A) with 96 and 84 kDa bands on SDS-PAGE (Fig. 4A, inset, lane 2), corresponding to the StrepII-MBP-WT-hPAH and 6His-MBP-ΔN102-hPAH, respectively. The dimeric fraction corresponding to the WT-hPAH (Fig. 4A, inset, lane 3), revealed a band corresponding to the truncated form, since the dimeric fraction (peak 3) was not completely resolved from the ΔN102-hPAH tetramer.

Table 2
Subunit molecular mass, major oligomeric forms, apparent molecular mass and relative amounts of the hPAH fusion protein forms used in this study.

Expressed or co-expressed fusion proteins	Subunit molecular mass (fusion protein)[a] (kDa)	Oligomeric state	Apparent molecular mass[b]	Relative amounts[b,c]
WT-hPAH	95.6	Aggregated	—	(40%)
		Tetramer	371 kDa	(52%)
		Dimer	205 kDa	(8%)
ΔN102-hPAH	84.4	Tetramer	310 kDa	(96%)[d]
ΔN102/ ΔC24-hPAH	81.8	Aggregated	—	(17%)[d]
		Dimer	156 kDa	(81%)[d]
(WT)/ (ΔN102)-hPAH	95.6/84.4	Aggregated	—	(9%)
		Tetramers	—[e]	(62%)
		Dimer	219 kDa	(12%)
(WT)/(ΔN102/ ΔC24)-hPAH	95.6/81.8	Aggregated	—	(20%)
		Tetramer	412 kDa	(14%)
		Dimers	—[e]	(55%)

[a] Subunit molecular mass calculated from the amino acid sequence.
[b] The apparent molecular mass of the oligomeric forms and their relative amounts were calculated by deconvolution analysis of the size-exclusion chromatograms using the PeakFit software (Systat Software Inc) of the MBP-fusions proteins before Ni–NTA and Strep-Tactin purification.
[c] Degradation products not included.
[d] Data from [34].
[e] Apparent molecular mass not determined, as the broad peak correspondent to 2 or more different species.

3.2. Study of the heterodimer and heterotetramer formation using WT and truncated forms of hPAH

3.2.1. (WT)/(ΔN102/ΔC24)-hPAH heterodimer is not formed

When the dimeric fraction of the co-expressed StrepII-MBP-WT-hPAH and 6His-MBP-ΔN102/ΔC24-hPAH was applied to the Ni–NTA resin, a protein with an apparent molecular mass of ~96 kDa, corresponding to the StrepII-MBP-WT-hPAH subunit, was recovered in the flow-through (Fig. 3B, lane 2). Only a trace amount of a ~82 kDa protein was observed, corresponding to the 6His-MBP-ΔN102/ΔC24-hPAH, indicating that homodimeric StrepII-MBP-WT-hPAH was mainly obtained in the flow-through. Elution of bound proteins with imidazole gave essentially one band at 82 kDa (Fig. 3B, lane 3), suggesting that only the 6His-MBP-ΔN102/ΔC24-hPAH species was recovered. In fact, when this fraction was applied to the Strep-Tactin resin (Fig. 3C) a band corresponding to the 6His-MBP-ΔN102/ΔC24-

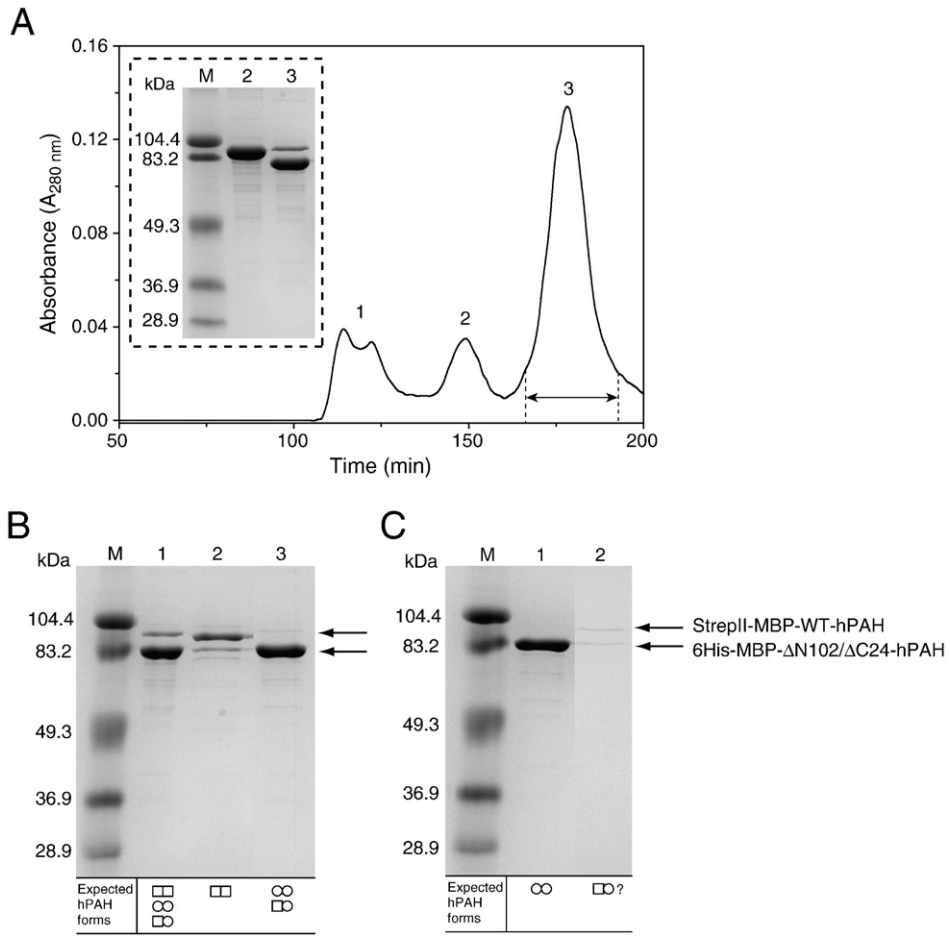

Fig. 3. Isolation and SDS-PAGE analysis of heterodimeric StrepII-MBP-WT-hPAH/6His-MBP-ΔN102/ΔC24-hPAH proteins. (A) Size-exclusion chromatography of the co-expressed StrepII-MBP-WT-hPAH and 6His-MBP-ΔN102/ΔC24-hPAH with three main peaks: (1) aggregated forms; (2) tetramers; and (3) dimers. The inset panel represents the SDS-PAGE analysis demonstrating the purity of the proteins eluted as tetramers (lane 2) and dimers (lane 3). The fraction with the double arrow between the two dashed lines indicates the collected dimers used in the further purification steps. (B) SDS-PAGE analysis of Ni–NTA purification. Lane 1, dimeric fraction from (A) applied on the Ni–NTA chelating resin; lane 2, flow-through containing StrepII-MBP-WT-hPAH homodimers (subunit M_r of ~96 kDa); lane 3, 150 mM imidazole eluted fraction containing 6His-MBP-ΔN102/ΔC24-hPAH homodimers (subunit M_r of ~82 kDa) and the potential StrepII-MBP-WT-hPAH/6His-MBP-ΔN102/ΔC24-hPAH heterodimers (subunits M_r of ~96 and ~82 kDa, respectively). (C) SDS-PAGE analysis of the Strep-Tactin purification. Lane 1, flow-through containing 6His-MBP-ΔN102/ΔC24-hPAH homodimers; lane 2, desthiobiotin eluted fraction after acetone-precipitation (see main text for further explanation — Results section). Lane M, low-molecular-mass marker (104.4, 83.2, 49.3, 36.9 and 28.9 kDa). At the bottom of each lane is indicated the expected hPAH forms as depicted in Fig. 2, with the StrepII-MBP-WT-hPAH polypeptide chain (□) and the 6His-MBP-ΔN102/ΔC24-hPAH polypeptide chain (○).

hPAH (82 kDa), which did not bind to the resin, was obtained in the flow-through (Fig. 3C, lane 1), and only negligible amounts of recombinant 82 kDa and 96 kDa fusion proteins were eluted with desthiobiotin (Fig. 3B, lane 2). This fraction was acetone-precipitated, and the recovered proteins, representing less than 1% of the homodimeric proteins, may correspond to proteins that remained bound to the column from the previous steps of purification. The results indicate that only StrepII-MBP-WT-hPAH and 6His-MBP-ΔN102/ΔC24-hPAH homodimers, but no StrepII-MBP-WT-hPAH/6His-MBP-ΔN102/ΔC24-hPAH heterodimers, were formed.

3.2.2. The (WT)/(ΔN102)-hPAH heterotetramer

The His-tag affinity purification of the co-expressed StrepII-MBP-WT-hPAH and 6His-MBP-ΔN102-hPAH proteins resulted in the recovery of the StrepII-MBP-WT-hPAH homotetramer (~96 kDa subunit) in the flow-through when applied to the Ni-chelating resin (Fig. 4B, lane 2), and the imidazole elution recovered the StrepII-MBP-WT-hPAH (~96 kDa) and 6His-MBP-ΔN102-hPAH (~84 kDa), in a ~1:3 ratio (Fig. 4B, lane 3). Subsequent StrepII-tag affinity purification of this fraction resulted in the recovery of the 6His-MBP-ΔN102-hPAH homotetramer (~84 kDa subunit) in the flow-through (Fig. 4C, lane 1), and the desthiobiotin elution recovered the heterotetramer StrepII-MBP-WT-hPAH/6His-MBP-ΔN102-hPAH, with two bands (~96 and ~84 kDa subunit) in a 1:1 ratio (Fig. 4C, lane 2).

3.3. Steady-state kinetic analysis of the (WT)/(ΔN102)-hPAH heterotetramers

After cleavage of the fusion tags the steady-state kinetic parameters of the tetrameric forms of WT-hPAH, ΔN102-hPAH and the (WT)/(ΔN102)-hPAH heterotetramer were determined (Tables 3 and 4). The factor Xa cleavage of the fusion proteins resulted in some unspecific cleavage that generated a mixture of WT-hPAH full-length and ΔN13-hPAH for the WT fusion protein [33]; and the cleavage of the ΔN102-hPAH fusion protein generated the truncated form ΔN112-hPAH [34]. However, the kinetic properties of the mixture of the full-length WT and ΔN13-hPAH enzymes were similar to those of the full-length enzyme in terms of cooperativity and substrate activation, with only the phosphorylation of S16 by cAMP-dependent protein kinase being affected [33]. The kinetic properties obtained for WT and ΔN102-hPAH are in line with the reported values in the literature [2,33,34]. Whereas relatively small differences in the K_m value for the cofactor were observed between the three species (Table 4), marked differences were observed for L-Phe in terms of concentration at half-maximal activity ($[S]_{0.5}$), catalytic efficiency, catalytic activation and cooperativity

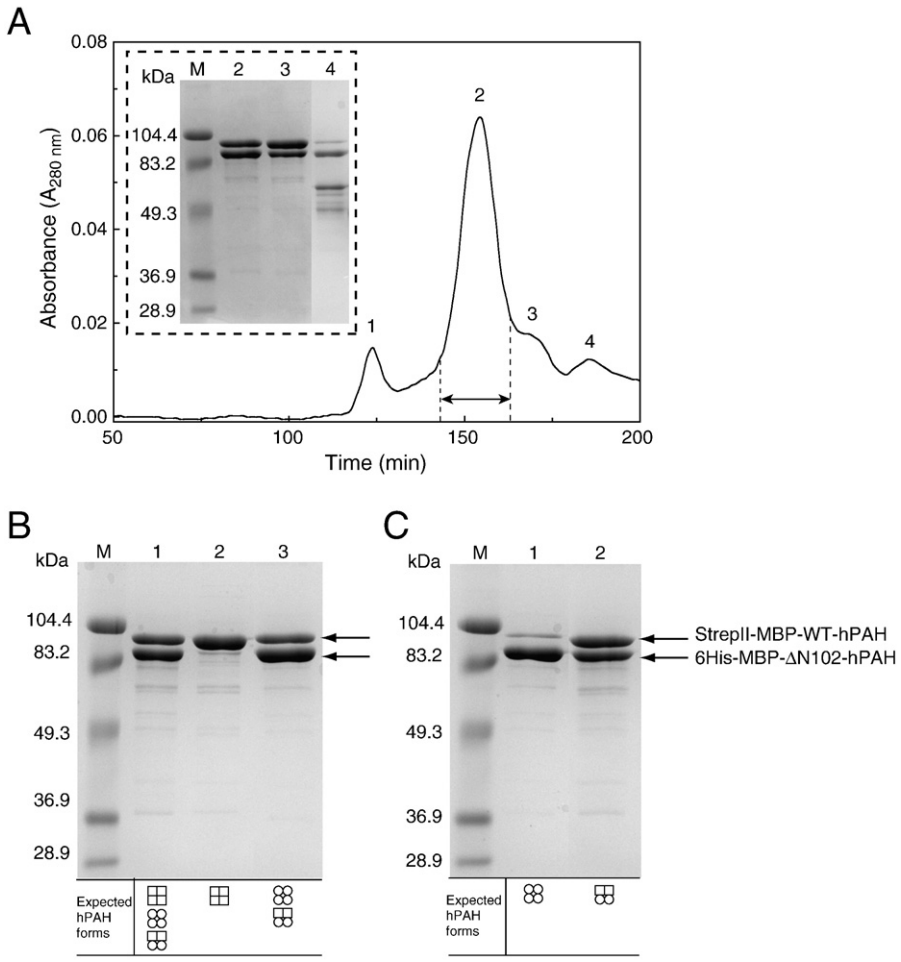

Fig. 4. Isolation and SDS-PAGE analysis of heterotetrameric StrepII-MBP-WT-hPAH/6His-MBP-ΔN102-hPAH proteins. (A) Size-exclusion chromatography of the co-expressed StrepII-MBP-WT-hPAH and 6His-MBP-ΔN102-hPAH with four main peaks: (1) aggregated forms, (2) tetramers, (3) dimers; and (4) low-molecular protein degradation products from the amylose purification (see Fig. 2). The inset panel represents the SDS-PAGE analysis of isolated protein from each peak in the elution profile, tetramers (lane 2), dimers (lane 3) and degradation products (lane 4). The fraction with the double arrow between the two dashed lines indicates the collected tetramers used in the further purification steps. (B) SDS-PAGE analysis of the Ni–NTA resin purification. Lane 1, tetrameric fraction from SEC applied on the Ni–NTA resin; lane 2, flow-through containing StrepII-MBP-WT-hPAH homotetramers (subunit M_r of ~96 kDa) (3); lane 3, 150 mM imidazole eluted fraction containing 6His-MBP-ΔN102-hPAH homotetramers (subunit M_r of ~84 kDa) and StrepII-MBP-WT-hPAH/6His-MBP-ΔN102-hPAH heterotetramers (subunits M_r of ~96 and ~84 kDa, respectively). (C) SDS-PAGE analysis of Strep-Tactin purification. Lane 1, flow-through containing 6His-MBP-ΔN102-hPAH homotetramers; lane 2, desthiobiotin eluted fraction containing StrepII-MBP-WT-hPAH/6His-MBP-ΔN102-hPAH heterotetramers. Lane M, low-molecular-mass marker (104.4, 83.2, 49.3, 36.9 and 28.9 kDa). At the bottom of each lane is indicated the expected hPAH forms as depicted in Fig. 2, with the StrepII-MBP-WT-hPAH polypeptide chain (□) and the 6His-MBP-ΔN102-hPAH polypeptide chain (○).

(Fig. 5 and Table 3). The (WT)/(ΔN102)-hPAH heterotetramer revealed a lower $[S]_{0.5}$ (L-Phe) value (76 ± 17 μM) than the WT-hPAH homotetramer ($[S]_{0.5} = 151 \pm 6$ μM), but only slightly higher than the truncated homotetramer ΔN102-hPAH ($[S]_{0.5} = 55 \pm 3$ μM) (Table 3). The heterotetramer is also characterized by a marked decrease in the k_{cat} ($0.34 \pm 0.03 \times 10^3$ nmol Tyr·min^{-1}· nmol tetramer^{-1}), a value lower than that predicted by averaging the k_{cat} of the homotetrameric counterparts ($k_{cat,PRA} = 1.12 \times 10^3$nmol Tyr·min^{-1}· nmol tetramer^{-1}) (Table 3). Moreover, the (WT)/(ΔN102)-hPAH heterotetramer revealed no kinetic cooperativity ($n_H = 1.0 \pm 0.1$) with respect to L-Phe and is not activated by L-Phe preincubation (1.1-fold), properties also observed for the truncated homotetramer ΔN102-hPAH ($n_H = 1.2 \pm 0.1$ and 1.0-fold, respectively). By contrast the WT-hPAH homotetramer revealed a kinetic positive cooperativity ($n_H = 2.1 \pm 0.1$) and a 3.6-fold activation

Table 3
Steady-state kinetic constants for the substrate (L-Phe) of WT-hPAH homotetramer, ΔN102-hPAH homotetramer and (WT)/(ΔN102)-hPAH heterotetramer.

hPAH	V_{max}	k_{cat}	k_{cat} (PRA)	V_i	$[S]_{0.5}$	K_i	$k_{cat}/[S]_{0.5}$	n_H	Fold activation $R(v_{+L\text{-Phe}}/v_{-L\text{-Phe}})$
	10^3 nmol Tyr·min^{-1}· mg^{-1}	10^3 nmol Tyr·min^{-1}· nmol^{-1}		10^3 nmol Tyr·min^{-1}· mg^{-1}	μM	mM	μM^{-1}· min^{-1}		
WT	2.79 ± 0.07	0.56 ± 0.01	–	1.55 ± 0.14	151 ± 6	2.20 ± 0.44	4	2.1 ± 0.1	3.6
ΔN102	10.4 ± 0.27	1.68 ± 0.04	–	4.53 ± 0.27	55 ± 3	1.56 ± 0.17	30	1.2 ± 0.1	1.0
(WT)/(ΔN102)	1.85 ± 0.18	0.34 ± 0.03	1.12	1.03 ± 0.05	76 ± 17	0.86 ± 0.23	4	1.0 ± 0.1	1.1

The catalytic activity was measured as described in the Materials and methods section at 25 °C, 75 μM BH_4 (L-Phe variable). $[S]_{0.5}$ represents the L-Phe concentration at half-maximal activity and $k_{cat}/[S]_{0.5}$ the catalytic efficiency which was calculated on the basis of the tetramer molecular mass of 200, 161.2 and 180.6 kDa for WT-hPAH, ΔN102-hPAH and (WT)/(ΔN102)-hPAH, respectively. PRA, predicted residual activity of the heterotetramer, is the mean of the k_{cat} of the corresponding homotetramers.

Table 4
Steady-state kinetic constants for the cofactor (BH_4) of WT-hPAH homotetramer, ΔN102-hPAH homotetramer and (WT)/(ΔN102)-hPAH heterotetramer.

hPAH	V_{max}	k_{cat}	k_{cat} (PRA)	K_m
	10^3 nmol Tyr·min^{-1}·mg^{-1}	10^3 nmol Tyr·min^{-1}·nmol^{-1}		μM
WT	2.83 ± 0.08	0.57 ± 0.02	–	27 ± 3
ΔN102	10.1 ± 0.44	1.63 ± 0.07	–	39 ± 5
(WT)/(ΔN102)	1.44 ± 0.05	0.26 ± 0.01	1.10	24 ± 3

The catalytic activity was measured as described in the Materials and methods section at 25 °C, 1 mM L-Phe (BH_4 variable). PRA, predicted residual activity.

on preincubation by L-Phe (Table 3). The catalytic efficiency ($k_{cat}/[S]_{0.5}$) was 4 μM^{-1}· min^{-1} for both the heterotetrameric form and WT-hPAH.

3.4. Limited proteolysis of (WT)/(ΔN102)-hPAH heterotetramer with trypsin

On limited proteolysis by trypsin, the WT-hPAH homotetramer (Fig. 6A) was found to be more resistant than the homotetrameric N-terminal truncated form both in the absence and presence of L-Phe (Fig. 6B). A small proteolytic fragment is rapidly cleaved off in the ΔN102-hPAH homotetramer, during the first 10 min of incubation, generating a core fragment of ~35 kDa resistant to further trypsin proteolysis. A core fragment of similar molecular mass was also obtained from the WT-hPAH trypsin proteolysis (data not shown). Whereas the WT-hPAH became markedly more susceptible to limited proteolysis in the presence of L-Phe, only a slight increase in the rate of proteolysis was observed for the truncated form (Fig. 6A and B). While the heterotetrameric (WT)/(ΔN102)-hPAH revealed no significant difference in the rate of proteolysis for the ΔN102-hPAH protomer (Fig. 6D), the WT protomer is more rapidly degraded (Fig. 6C).

4. Discussion

4.1. The developed bicistronic expression system is a valuable tool to produce and isolate heteromeric forms of hPAH

Co-expression of different proteins in *E. coli* can be achieved using three different strategies: (i) a multi-vector expression system (e.g. dual vector system with plasmids with different replication origins and selection markers and with identical or different promoters), (ii) a single polycistronic plasmid with a single promoter, encoding a long polycistronic mRNA, and (iii) a single polycistronic plasmid with individual promoters [46]. In our previous work [14] we followed the first strategy but the low yield preclude the isolation of the hybrid species. Since the use of the second strategy (one polycistronic vector with a single promoter) has been reported to lead to a lower expression of the more downstream encoded protein [47], we decided to follow the third strategy. Using a bicistronic vector with individual but identical promoters (T7 promoter) and two terminators, we obtained similar and high expression levels of both proteins. By using a single plasmid we also assured that the two proteins should localize within the same region of the cell, in contrast to replication from different plasmids which could have a different subcellular localization within the bacterium [48]. Additionally, due to expression from two similar sequences, verification of plasmid integrity is necessary to rule out homologous recombination, as *E. coli* BL21(DE3) (*recA*$^+$ strain) is one of the most commonly used expression strains. Alternatively, a *recA*$^-$ derivative of BL21 should be used (e.g. BLR (DE3) [49]).

In the present work the hPAH variants (WT and truncated forms) were recognized by their different molecular mass. In studies on missense mutations, the detection and quantification can readily be achieved by immuno-detection with monoclonal antibodies specific

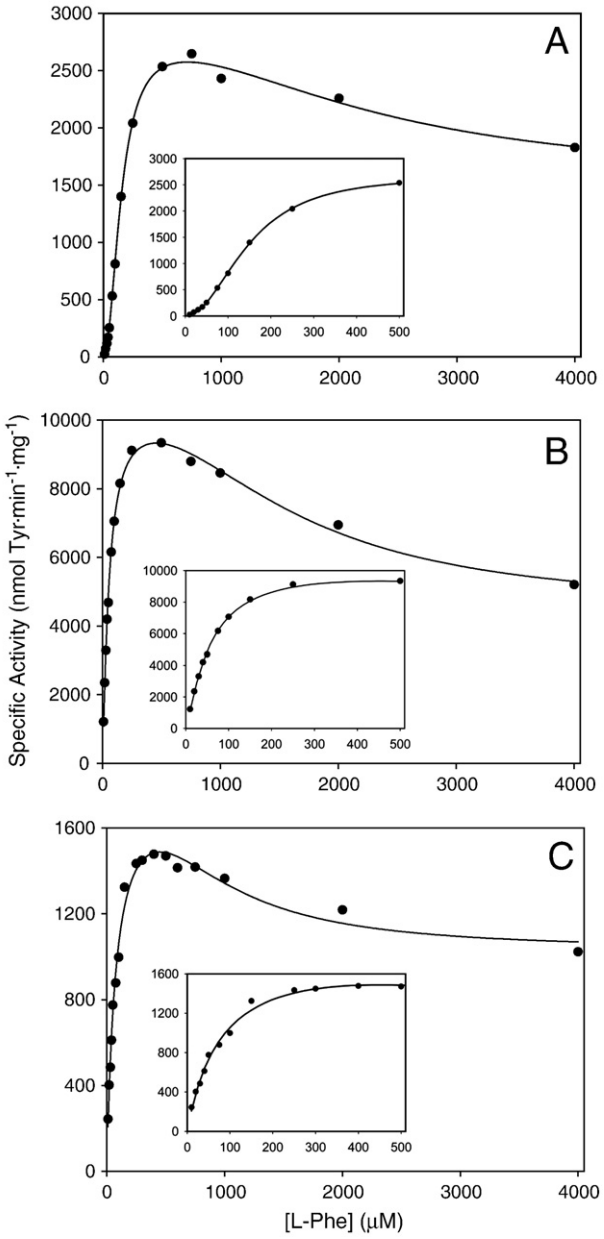

Fig. 5. The effect of substrate (L-Phe) concentration on the catalytic activity of the heterotetrameric (WT)/(ΔN102)-hPAH protein and homotetrameric counterparts. The hPAH activity was assayed at standard conditions (0–4 mM L-Phe, 75 μM BH_4 and 25 °C) for the isolated homotetrameric WT-hPAH (A), homotetrameric ΔN102-hPAH (B) and heterotetrameric (WT)/(ΔN102)-hPAH (C). The insets represent the data obtained in the concentration range 0–500 μM L-Phe. The kinetic constants are summarized in Table 3.

for the epitope tags (hexahistidyl peptide and StrepII peptide) and MS peptide analyses. Moreover, the depicted vector can be easily adapted to an *in vitro* transcription-translation system (the large tags can be removed and a consensus Kozak sequence introduced at the MCS2), as a potential tool to study the observed inconsistencies in BH_4 supplementation (see below).

4.2. The formation of hPAH heteromers occurs by a non-random assembly process

The C-terminal oligomerization domain of WT-hPAH (residues 412–452) consists of two short β-strands (Ser411-Tyr414 and Ile421-Leu424), connected by a loop (residues 415–420), and a 40 Å long α-helix (Gln428-Lys452). Dimerization is mediated by several van der

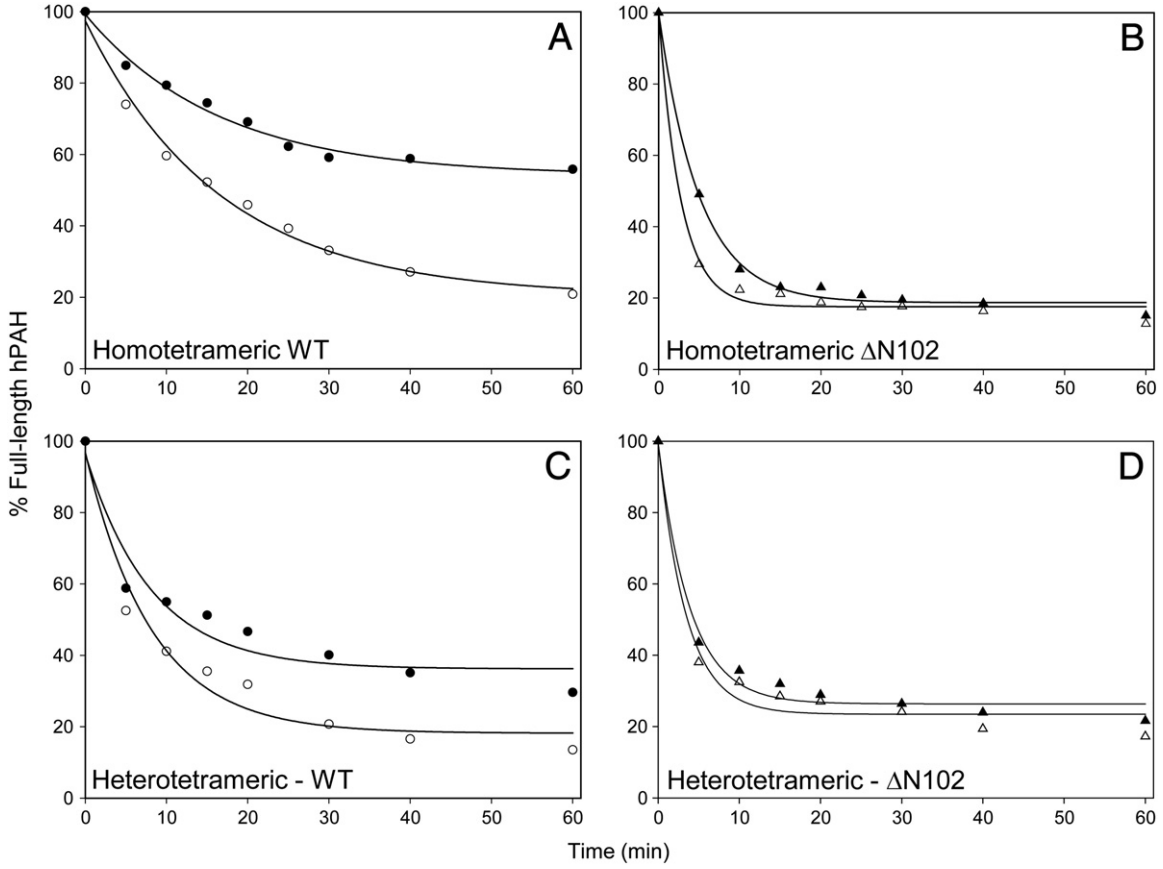

Fig. 6. Time-course for the limited proteolysis of the heterotetrameric (WT)/(ΔN102)-hPAH protein and homotetrameric counterparts by trypsin. The susceptibility to trypsin proteolysis of WT-hPAH homotetramer (● and ○) and ΔN102-hPAH homotetramer (▲ and △) is shown in panels A and B, respectively. In C and D, the proteolysis patterns of the WT (● and ○) and ΔN102 (▲ and △) protomers of the heterotetrameric (WT)/(ΔN102)-hPAH are shown, respectively. Limited proteolysis was performed in the absence (filled symbols, ● and ▲) or presence (open symbols, ○ and △) of 1 mM L-Phe at a protease/hPAH ratio of 1:200 (by mass). At time interval aliquots were mixed with soybean trypsin inhibitor and subjected to SDS-PAGE, and the band corresponding to the remaining full-length protein was quantified (WT subunit: ~50 kDa and ΔN102 subunit: ~38.8 kDa). The data were fitted to a single exponential decay curve. The recovery of the full-length WT-hPAH protomer in the heterotetramer at $t \sim 20$ min, in the absence of L-Phe, is practically the same as in the WT-hPAH homotetramer in the presence of L-Phe.

Waals and hydrogen bond interactions of the two symmetry-related loops (residues 415–420), one of each protomer [1,50], and through a relatively polar interface contributed by the regulatory domain in one protomer and the catalytic domain in the other protomer [51].

In the present study, the co-expression of WT-hPAH and truncated forms of the protein allowed the isolation of heterotetramers, resulting from the assembly of different homodimers ($2hPAH_1$/$2hPAH_2$), but no heterodimers were recovered. Thus, the absence of a random assortment of hPAH protomers suggests that hPAH dimerization, via the Asp415-Arg420 loop of the dimerization motif, is a co-translational process and that tetramer formation (dimer of dimers) occurs post-translationally. Tetramerization occurs from preformed dimers through domain swapping of the C-terminal α-helices (Gln428-Lys452) [1], and our data indicate that these interactions will not be affected by the presence of two different stable dimers with a WT like C-terminal α-helix structure. A co-translational assembly of dimers could explain why hPAH monomers were never found for WT-hPAH [34] or in mutant forms, except for Y417H mapped to the dimerization motif preventing the formation of dimers [52].

4.3. The WT protomer within the heterotetramer reveal conformational changes

Binding of L-Phe at the active site triggers reversible conformational changes in the catalytic domain [53], which are transmitted globally (dimer and tetramer) through several hinge-bending regions [53–56] resulting in a more open structure [54]. This conformational change results in an increased susceptibility to limited proteolysis by trypsin (Fig. 6A). The WT protomer revealed a higher susceptibility to limited proteolysis when present in the heterotetrameric (WT)/(ΔN102)-hPAH than in the homomeric form, both in the absence and presence of L-Phe, indicating that the WT protomer adopts a more open conformation. These results suggest that the assembly of the two different dimers (WT and ΔN102) induces a conformational change in the WT protomers mediated by the C-terminal 40-Å long α-helix (Gln428-Lys452), as the only contact between the two dimers in the assembled tetramer occurs by domain swapping of the four C-terminal helices (two from each dimer) [1].

4.4. Functional implications of the assembly of hPAH heterotetramers

A comparison of the steady-state kinetic parameters of the (WT)/(ΔN102)-hPAH heterotetramer with the homotetrameric counterparts (Table 3) revealed that the heterotetramer has acquired a catalytic efficiency similar to that of WT-hPAH. However, it has lost the cooperativity with respect to L-Phe and the ability to be activated by the substrate, which are characteristic properties of the ΔN102-hPAH tetramer. Moreover, the V_{max}-value was only ~30% of the predicted residual activity (PRA), thus demonstrating a negative interallelic complementation. However, it should be noted that the isolated WT-hPAH dimeric form revealed no kinetic cooperativity and only a minor fold activation by L-Phe when compared to the WT-hPAH tetramer [4], and the kinetic properties of the isolated ΔN102-hPAH

dimer are unknown as the truncated form is recovered mainly as tetramers (Table 2). If the two dimers in the heterotetramer were acting isolated, the lack of cooperativity and substrate activation in the hybrid could be explained. However, the L-Phe concentration at half-maximal activity ($[S]_{0.5}$) of the WT-hPAH dimeric form is much higher than the WT-hPAH tetramer [4], whereas the hybrid tetramer displays a $[S]_{0.5}$ (L-Phe) lower than the WT-hPAH tetramer. Taking these results into consideration and the ones obtained from the trypsin limited proteolysis, indicating that the WT dimer in the heterotetramer underwent a conformational change, it was not unexpected to find that the catalytic properties of the heterotetramer were consistently different from those obtained theoretically by averaging the homomeric counterparts. The fact that the presence of two homodimers with different kinetic parameters can alter the properties of resulting hybrid protein indicates that interactions are transmitted across the overall assembled protein and that the dimers are not acting isolated.

4.5. Implications of heterotetrameric assembly in PKU

Although the mutant partner used in the present study is a truncated protein and not a PKU-mutant enzyme, the results obtained in this work can give some insight into the mechanisms involved in PKU, as we report here the first isolation of a heterotetrameric form of hPAH with properties deviating significantly from the average of those of the parental enzymes. The developed expression/purification strategy provides the necessary experimental tools for studies on disease-associated hPAH mutations, notably those demonstrating inconsistencies both in genotype/phenotype correlations and in the response to BH_4 supplementation. The mechanisms underlying BH_4-responsiveness are multifactorial, including correction of catalytic defect (decreased affinity for BH_4) and stabilization of the mutant protein against degradation/inactivation *in vivo* and *in vitro* [57–59]. Until now, *in vitro* studies to unravel the mechanism of BH_4-responsiveness (e.g. steady-state kinetic analysis, isothermal titration calorimetry and thermostability followed by circular dichroism spectroscopy) have been limited to the study of homotetrameric proteins. However, they do not represent the hPAH protein population of a compound heterozygous patient. The isolation of the heterotetramers will allow the *in vitro* characterization of these species in terms of the cofactor effect. However, one limitation of the prokaryotic expression system is that it is not amenable to test the effect of precise BH_4 concentrations when the protein assembles *in vivo*. One alternative is to use the described system (with minor modifications) in an *in vitro* transcription–translation expression system. It will be important to understand how the mutations alter the observed $2hPAH_1$:$2hPAH_2$ association of hPAH dimers and if they also exert a dominant negative impact on the function of the heteromeric species. As a large fraction of PKU mutations affects stability and/or folding efficiency, this system will also be a valuable tool to understand how an aggregation-prone mutant (e.g. G46S [30,60]) affects the other mutant partner within the heteromeric protein.

The characterization of the interactions between wild-type and mutant dimers and between different mutant dimers (compound heterozygous) is clinically relevant, as they will contribute to a better understanding of the metabolic phenotype in the HPA/PKU patients and BH_4-responsiveness. It will also be essential in the development of new emerging therapies (e.g. pharmacological chaperones), as the hybrid proteins could respond differently from the parental enzymes.

Acknowledgements

This work was supported by Fundação para a Ciência e a Tecnologia, Portugal, grant SFRH/BD/19024/2004 and the University of Bergen, Norway. We thank Ali Sepulveda Munõz and Randi M. Svebak for expert technical assistance.

Appendix A. Supplementary data

Supplementary data to this article can be found online at doi:10.1016/j.bbadis.2011.02.001.

References

[1] T. Flatmark, R.C. Stevens, Structural insight into the aromatic amino acid hydroxylases and their disease-related mutant forms, Chem. Rev. 99 (1999) 2137–2160.
[2] A.J. Stokka, T. Flatmark, Substrate-induced conformational transition in human phenylalanine hydroxylase as studied by surface plasmon resonance analyses: the effect of terminal deletions, substrate analogues and phosphorylation, Biochem. J. 369 (2003) 509–518.
[3] F. Fusetti, H. Erlandsen, T. Flatmark, R.C. Stevens, Structure of tetrameric human phenylalanine hydroxylase and its implications for phenylketonuria, J. Biol. Chem. 273 (1998) 16962–16967.
[4] E. Bjørgo, R.M. de Carvalho, T. Flatmark, A comparison of kinetic and regulatory properties of the tetrameric and dimeric forms of wild-type and Thr427→Pro mutant human phenylalanine hydroxylase: contribution of the flexible hinge region Asp425-Gln429 to the tetramerization and cooperative substrate binding, Eur. J. Biochem. 268 (2001) 997–1005.
[5] S.W. Gersting, M. Staudigl, M.S. Truger, D.D. Messing, M.K. Danecka, C.P. Sommerhoff, K.F. Kemter, A.C. Muntau, Activation of phenylalanine hydroxylase induces positive cooperativity toward the natural cofactor, J. Biol. Chem. 285 (2010) 30686–30697.
[6] C.R. Scriver, The PAH gene, phenylketonuria, and a paradigm shift, Hum. Mutat. 28 (2007) 831–845.
[7] C.R. Scriver, M. Hurtubise, D. Konecki, M. Phommarinh, L. Prevost, H. Erlandsen, R. Stevens, P.J. Waters, S. Ryan, D. McDonald, C. Sarkissian, PAHdb 2003: what a locus-specific knowledgebase can do, Hum. Mutat. 21 (2003) 333–344.
[8] R. Surtees, N. Blau, The neurochemistry of phenylketonuria, Eur. J. Pediatr. 159 (Suppl 2) (2000) S109–S113.
[9] National Institutes of Health Consensus Development Panel, National Institutes of Health Consensus Development Conference statement: phenylketonuria: screening and management, October 16–18, 2000, Pediatrics 108 (2001) 972–982.
[10] H.L. Levy, A. Milanowski, A. Chakrapani, M. Cleary, P. Lee, F.K. Trefz, C.B. Whitley, F. Feillet, A.S. Feigenbaum, J.D. Bebchuk, H. Christ-Schmidt, A. Dorenbaum, Efficacy of sapropterin dihydrochloride (tetrahydrobiopterin, 6R-BH4) for reduction of phenylalanine concentration in patients with phenylketonuria: a phase III randomised placebo-controlled study, Lancet 370 (2007) 504–510.
[11] K. Michals-Matalon, Sapropterin dihydrochloride, 6-R-L-erythro-5, 6, 7, 8-tetrahydrobiopterin, in the treatment of phenylketonuria, Expert Opin. Investig. Drugs 17 (2008) 245–251.
[12] M.R. Zurflüh, J. Zschocke, M. Lindner, F. Feillet, C. Chery, A. Burlina, R.C. Stevens, B. Thöny, N. Blau, Molecular genetics of tetrahydrobiopterin-responsive phenylalanine hydroxylase deficiency, Hum. Mutat. 29 (2008) 167–175.
[13] S. Kaufman, E.E. Max, E.S. Kang, Phenylalanine hydroxylase activity in liver biopsies from hyperphenylalaninemia heterozygotes: deviation from proportionality with gene dosage, Pediatr. Res. 9 (1975) 632–634.
[14] J. Leandro, C. Nascimento, I.T. de Almeida, P. Leandro, Co-expression of different subunits of human phenylalanine hydroxylase: evidence of negative interallelic complementation, Biochim. Biophys. Acta, Mol. Basis Dis. 1762 (2006) 544–550.
[15] P.L. Howell, M.A. Turner, J. Christodoulou, D.C. Walker, H.J. Craig, L.R. Simard, L. Ploder, R.R. McInnes, Intragenic complementation at the argininosuccinate lyase locus: reconstruction of the active site, J. Inherit. Metab. Dis. 21 (Suppl 1) (1998) 72–85.
[16] R.R. McInnes, V. Shih, S. Chilton, Interallelic complementation in an inborn error of metabolism: genetic heterogeneity in argininosuccinate lyase deficiency, Proc. Natl Acad. Sci. U. S. A. 81 (1984) 4480–4484.
[17] B. Yu, G.D. Thompson, P. Yip, P.L. Howell, A.R. Davidson, Mechanisms for intragenic complementation at the human argininosuccinate lyase locus, Biochemistry 40 (2001) 15581–15590.
[18] Y. Ohgari, M. Sawamoto, M. Yamamoto, H. Kohno, S. Taketani, Ferrochelatase consisting of wild-type and mutated subunits from patients with a dominant-inherited disease, erythropoietic protoporphyria, is an active but unstable dimer, Hum. Mol. Genet. 14 (2005) 327–334.
[19] N.C. Christacos, J.L. Fridovich-Keil, Impact of patient mutations on heterodimer formation and function in human galactose-1-P uridylyltransferase, Mol. Genet. Metab. 76 (2002) 319–326.
[20] J.P. Elsevier, J.L. Fridovich-Keil, The Q188R mutation in human galactose-1-phosphate uridylyltransferase acts as a partial dominant negative, J. Biol. Chem. 271 (1996) 32002–32007.
[21] P. Hammarström, R.L. Wiseman, E.T. Powers, J.W. Kelly, Prevention of transthyretin amyloid disease by changing protein misfolding energetics, Science 299 (2003) 713–716.
[22] C.A. Keetch, E.H. Bromley, M.G. McCammon, N. Wang, J. Christodoulou, C.V. Robinson, L55P transthyretin accelerates subunit exchange and leads to rapid formation of hybrid tetramers, J. Biol. Chem. 280 (2005) 41667–41674.

[23] W. Dridi, R. Fetni, J. Lavoie, M.F. Poupon, R. Drouin, The dominant-negative effect of p53 mutants and p21 induction in tetraploid G1 arrest depends on the type of p53 mutation and the nature of the stimulus, Cancer Genet. Cytogenet. 143 (2003) 39–49.
[24] C.D. Nicholls, K.G. McLure, M.A. Shields, P.W. Lee, Biogenesis of p53 involves cotranslational dimerization of monomers and posttranslational dimerization of dimers. Implications on the dominant negative effect, J. Biol. Chem. 277 (2002) 12937–12945.
[25] C.R. Scriver, P.J. Waters, Monogenic traits are not simple: lessons from phenylketonuria, Trends Genet. 15 (1999) 267–272.
[26] P. Guldberg, F. Rey, J. Zschocke, V. Romano, B. Francois, L. Michiels, K. Ullrich, G.F. Hoffmann, P. Burgard, H. Schmidt, C. Meli, E. Riva, I. Dianzani, A. Ponzone, J. Rey, F. Güttler, A European multicenter study of phenylalanine hydroxylase deficiency: classification of 105 mutations and a general system for genotype-based prediction of metabolic phenotype, Am. J. Hum. Genet. 63 (1998) 71–79.
[27] E. Kayaalp, E. Treacy, P.J. Waters, S. Byck, P. Nowacki, C.R. Scriver, Human phenylalanine hydroxylase mutations and hyperphenylalaninemia phenotypes: a metanalysis of genotype–phenotype correlations, Am. J. Hum. Genet. 61 (1997) 1309–1317.
[28] I. Rivera, A. Cabral, M. Almeida, P. Leandro, C. Carmona, F. Eusébio, T. Tasso, L. Vilarinho, E. Martins, M.C. Lechner, I.T. de Almeida, D.S. Konecki, U. Lichter-Konecki, The correlation of genotype and phenotype in Portuguese hyperphenylalaninemic patients, Mol. Genet. Metab. 69 (2000) 195–203.
[29] F.K. Trefz, D. Scheible, H. Götz, G. Frauendienst-Egger, Significance of genotype in tetrahydrobiopterin-responsive phenylketonuria, J. Inherit. Metab. Dis. 32 (2009) 22–26.
[30] J. Leandro, N. Simonsen, J. Saraste, P. Leandro, T. Flatmark, Phenylketonuria as a protein misfolding disease: the mutation pG46S in phenylalanine hydroxylase promotes self-association and fibril formation, Biochim. Biophys. Acta 1812 (2011) 106–120.
[31] P.J. Waters, C.R. Scriver, M.A. Parniak, Homomeric and heteromeric interactions between wild-type and mutant phenylalanine hydroxylase subunits: evaluation of two-hybrid approaches for functional analysis of mutations causing hyperphenylalaninemia, Mol. Genet. Metab. 73 (2001) 230–238.
[32] R.B. Kapust, D.S. Waugh, Escherichia coli maltose-binding protein is uncommonly effective at promoting the solubility of polypeptides to which it is fused, Protein Sci. 8 (1999) 1668–1674.
[33] A. Martínez, P.M. Knappskog, S. Olafsdottir, A.P. Døskeland, H.G. Eiken, R.M. Svebak, M. Bozzini, J. Apold, T. Flatmark, Expression of recombinant human phenylalanine hydroxylase as fusion protein in *Escherichia coli* circumvents proteolytic degradation by host cell proteases. Isolation and characterization of the wild-type enzyme, Biochem. J. 306 (1995) 589–597.
[34] P.M. Knappskog, T. Flatmark, J.M. Aarden, J. Haavik, A. Martínez, Structure/function relationships in human phenylalanine hydroxylase. Effect of terminal deletions on the oligomerization, activation and cooperativity of substrate binding to the enzyme, Eur. J. Biochem. 242 (1996) 813–821.
[35] M.M. Bradford, A rapid and sensitive method for the quantitation of microgram quantities of protein utilizing the principle of protein-dye binding, Anal. Biochem. 72 (1976) 248–254.
[36] A. Martínez, S. Olafsdottir, J. Haavik, T. Flatmark, Inactivation of purified phenylalanine hydroxylase by dithiothreitol, Biochem. Biophys. Res. Commun. 182 (1992) 92–98.
[37] V.J. LiCata, N.M. Allewell, Is substrate inhibition a consequence of allostery in aspartate transcarbamylase? Biophys. Chem. 64 (1997) 225–234.
[38] T. Solstad, T. Flatmark, Microheterogeneity of recombinant human phenylalanine hydroxylase as a result of nonenzymatic deamidations of labile amide containing amino acids. Effects on catalytic and stability properties, Eur. J. Biochem. 267 (2000) 6302–6310.
[39] J.D. Fox, R.B. Kapust, D.S. Waugh, Single amino acid substitutions on the surface of *Escherichia coli* maltose-binding protein can have a profound impact on the solubility of fusion proteins, Protein Sci. 10 (2001) 622–630.
[40] P. Leandro, I. Rivera, M.C. Lechner, I.T. de Almeida, D. Konecki, The V388M mutation results in a kinetic variant form of phenylalanine hydroxylase, Mol. Genet. Metab. 69 (2000) 204–212.
[41] J. Arnau, C. Lauritzen, G.E. Petersen, J. Pedersen, Current strategies for the use of affinity tags and tag removal for the purification of recombinant proteins, Protein Expr. Purif. 48 (2006) 1–13.
[42] D.S. Waugh, Making the most of affinity tags, Trends Biotechnol. 23 (2005) 316–320.
[43] L. Dumon-Seignovert, G. Cariot, L. Vuillard, The toxicity of recombinant proteins in *Escherichia coli*: a comparison of overexpression in BL21(DE3), C41(DE3), and C43 (DE3), Protein Expr. Purif. 37 (2004) 203–206.
[44] B. Miroux, J.E. Walker, Over-production of proteins in *Escherichia coli*: mutant hosts that allow synthesis of some membrane proteins and globular proteins at high levels, J. Mol. Biol. 260 (1996) 289–298.
[45] R.N. Carvalho, T. Solstad, E. Bjørgo, J.F. Barroso, T. Flatmark, Deamidations in recombinant human phenylalanine hydroxylase. Identification of labile asparagine residues and functional characterization of Asn→Asp mutant forms, J. Biol. Chem. 278 (2003) 15142–15152.
[46] S. Gräslund, P. Nordlund, J. Weigelt, B.M. Hallberg, J. Bray, O. Gileadi, S. Knapp, U. Oppermann, C. Arrowsmith, R. Hui, J. Ming, S. dhe-Paganon, H.W. Park, A. Savchenko, A. Yee, A. Edwards, R. Vincentelli, C. Cambillau, R. Kim, S.H. Kim, Z. Rao, Y. Shi, T.C. Terwilliger, C.Y. Kim, L.W. Hung, G.S. Waldo, Y. Peleg, S. Albeck, T. Unger, O. Dym, J. Prilusky, J.L. Sussman, R.C. Stevens, S.A. Lesley, I.A. Wilson, A. Joachimiak, F. Collart, I. Dementieva, M.I. Donnelly, W.H. Eschenfeldt, Y. Kim, L. Stols, R. Wu, M. Zhou, S.K. Burley, J.S. Emtage, J.M. Sauder, D. Thompson, K. Bain, J. Luz, T. Gheyi, F. Zhang, S. Atwell, S.C. Almo, J.B. Bonanno, A. Fiser, S. Swaminathan, F.W. Studier, M.R. Chance, A. Sali, T.B. Acton, R. Xiao, L. Zhao, L.C. Ma, J.F. Hunt, L. Tong, K. Cunningham, M. Inouye, S. Anderson, H. Janjua, R. Shastry, C.K. Ho, D. Wang, H. Wang, M. Jiang, G.T. Montelione, D.I. Stuart, R.J. Owens, S. Daenke, A. Schütz, U. Heinemann, S. Yokoyama, K. Büssow, K.C. Gunsalus, Protein production and purification, Nat. Methods 5 (2008) 135–146.
[47] C. Scheich, D. Kümmel, D. Soumailakakis, U. Heinemann, K. Büssow, Vectors for co-expression of an unrestricted number of proteins, Nucleic Acids Res. 35 (2007) e43.
[48] N.H. Tolia, L. Joshua-Tor, Strategies for protein coexpression in *Escherichia coli*, Nat. Methods 3 (2006) 55–64.
[49] M. Schmidt, L. Romer, M. Strehle, T. Scheibel, Conquering isoleucine auxotrophy of *Escherichia coli* BLR(DE3) to recombinantly produce spider silk proteins in minimal media, Biotechnol. Lett. 29 (2007) 1741–1744.
[50] H. Erlandsen, F. Fusetti, A. Martínez, E. Hough, T. Flatmark, R.C. Stevens, Crystal structure of the catalytic domain of human phenylalanine hydroxylase reveals the structural basis for phenylketonuria, Nat. Struct. Biol. 4 (1997) 995–1000.
[51] B. Kobe, I.G. Jennings, C.M. House, B.J. Michell, K.E. Goodwill, B.D. Santarsiero, R.C. Stevens, R.G. Cotton, B.E. Kemp, Structural basis of autoregulation of phenylalanine hydroxylase, Nat. Struct. Biol. 6 (1999) 442–448.
[52] S.W. Gersting, K.F. Kemter, M. Staudigl, D.D. Messing, M.K. Danecka, F.B. Lagler, C.P. Sommerhoff, A.A. Roscher, A.C. Muntau, Loss of function in phenylketonuria is caused by impaired molecular motions and conformational instability, Am. J. Hum. Genet. 83 (2008) 5–17.
[53] O.A. Andersen, A.J. Stokka, T. Flatmark, E. Hough, 2.0 Å resolution crystal structures of the ternary complexes of human phenylalanine hydroxylase catalytic domain with tetrahydrobiopterin and 3-(2-thienyl)-L-alanine or L-norleucine: substrate specificity and molecular motions related to substrate binding, J. Mol. Biol. 333 (2003) 747–757.
[54] J. Li, L.J. Dangott, P.F. Fitzpatrick, Regulation of phenylalanine hydroxylase: conformational changes upon phenylalanine binding detected by hydrogen/deuterium exchange and mass spectrometry, Biochemistry 49 (2010) 3327–3335.
[55] A.J. Stokka, R.N. Carvalho, J.F. Barroso, T. Flatmark, Probing the role of crystallographically defined/predicted hinge-bending regions in the substrate-induced global conformational transition and catalytic activation of human phenylalanine hydroxylase by single-site mutagenesis, J. Biol. Chem. 279 (2004) 26571–26580.
[56] M. Thórólfsson, K. Teigen, A. Martínez, Activation of phenylalanine hydroxylase: effect of substitutions at Arg68 and Cys237, Biochemistry 42 (2003) 3419–3428.
[57] C. Aguado, B. Pérez, M. Ugarte, L.R. Desviat, Analysis of the effect of tetrahydrobiopterin on PAH gene expression in hepatoma cells, FEBS Lett. 580 (2006) 1697–1701.
[58] H. Erlandsen, A.L. Pey, A. Gámez, B. Pérez, L.R. Desviat, C. Aguado, R. Koch, S. Surendran, S. Tyring, R. Matalon, C.R. Scriver, M. Ugarte, A. Martínez, R.C. Stevens, Correction of kinetic and stability defects by tetrahydrobiopterin in phenylketonuria patients with certain phenylalanine hydroxylase mutations, Proc. Natl Acad. Sci. U. S. A. 101 (2004) 16903–16908.
[59] A.L. Pey, B. Pérez, L.R. Desviat, M.A. Martínez, C. Aguado, H. Erlandsen, A. Gámez, R.C. Stevens, M. Thórólfsson, M. Ugarte, A. Martínez, Mechanisms underlying responsiveness to tetrahydrobiopterin in mild phenylketonuria mutations, Hum. Mutat. 24 (2004) 388–399.
[60] H.G. Eiken, P.M. Knappskog, J. Apold, T. Flatmark, PKU mutation G46S is associated with increased aggregation and degradation of the phenylalanine hydroxylase enzyme, Hum. Mutat. 7 (1996) 228–238.

Supporting data for

Heterotetrameric Forms of Human Phenylalanine Hydroxylase: Co-expression of Wild-type and Mutant Forms in a Bicistronic System

João Leandro[a,b]*, Paula Leandro[b] and Torgeir Flatmark[a]

[a]Department of Biomedicine, University of Bergen, Jonas Lies vei 91, N-5009 Bergen, Norway and [b]Metabolism and Genetics Group, Research Institute for Medicines and Pharmaceutical Sciences (iMed.UL), Faculty of Pharmacy, University of Lisbon, Av. Prof. Gama Pinto, 1649-003 Lisbon, Portugal

*Corresponding author: João Leandro, Metabolism and Genetics Group, iMed.UL, Faculty of Pharmacy, University of Lisbon, Av. Prof. Gama Pinto, 1649-003 Lisbon, Portugal. Telephone: +351 217946400; Fax: +351 217946491; E-mail: jptleandro@ff.ul.pt

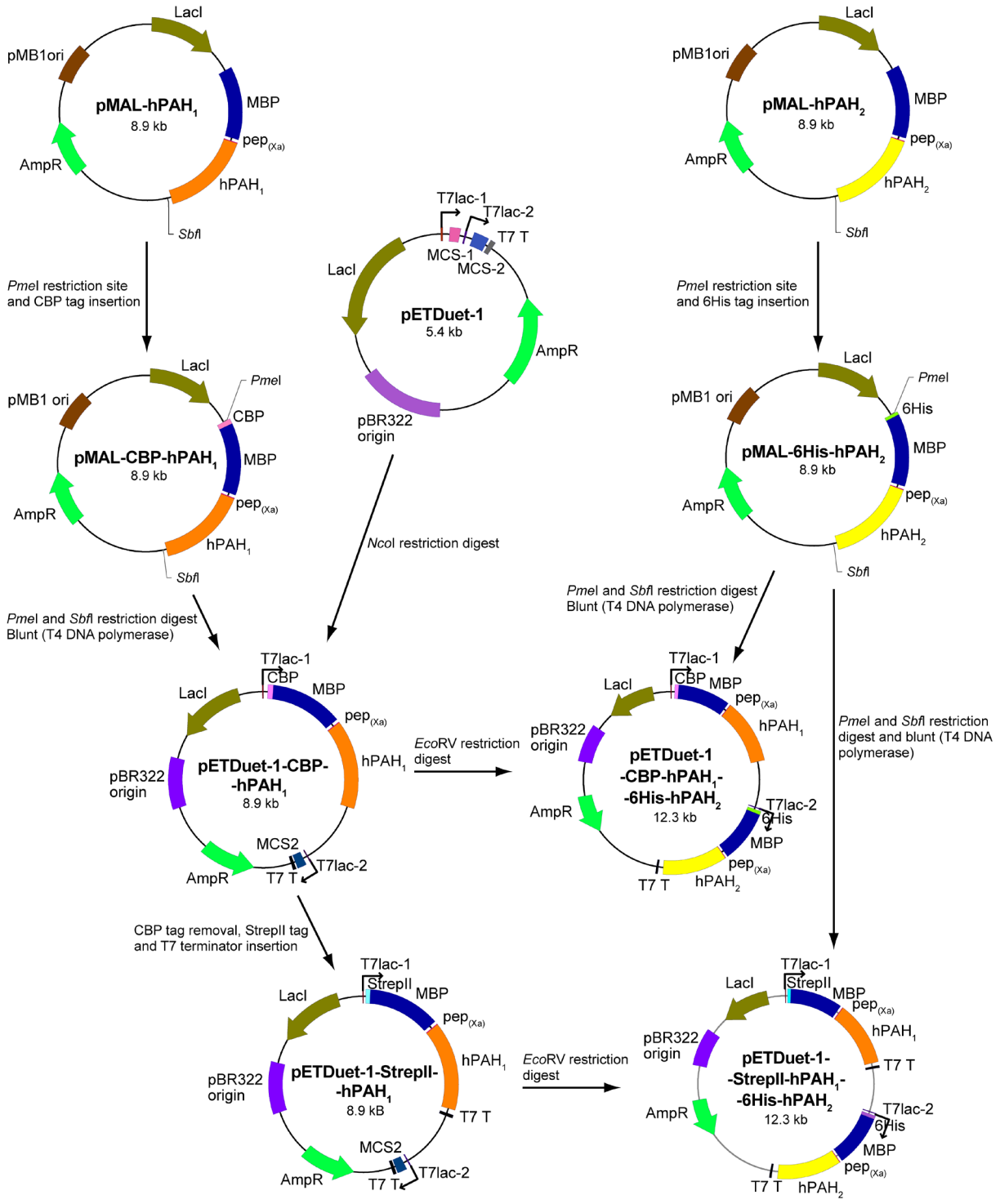

Supplementary Fig. S1. Schematic representation of the development of the bicistronic expression constructs to isolate recombinant heteromeric hPAH proteins. MBP, maltose binding protein; CBP, calmodulin binding peptide; StrepII, StrepII tag; 6His, hexa-histidyl tag; LacI, *lac* repressor; Amp^r, ampicillin resistance; T7 lac, T7 *lac* promoter; $pep_{(Xa)}$, sequence encoding the Factor Xa protease cleavage site; T7T, T7 terminator; MCS, multiple cloning site; $hPAH_1$, hPAH WT or $mutant_1$; $hPAH_2$, hPAH $mutant_2$.

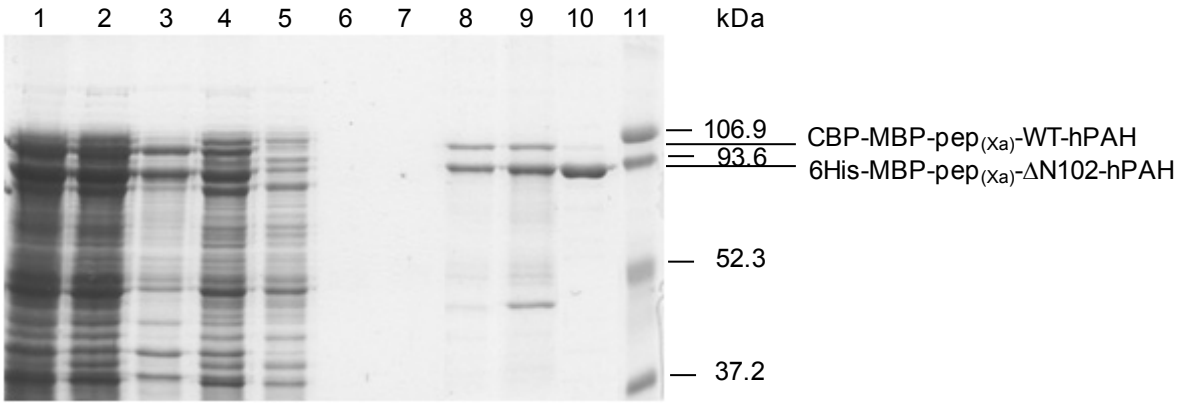

Supplementary Fig. S2. Effect of the calmodulin binding peptide on the co-expression of (WT)/(ΔN102)-hPAH fusion proteins. 10 % SDS-PAGE analysis of the purification of recombinant (WT)/(ΔN102)-hPAH. *Lane* 1, total cell lysate after 8h induction of recombinant hPAH by 1 mM IPTG at 28 ºC; *lane* 2, soluble fraction; *lane* 3, insoluble fraction, *lane* 4, flow-through from the amylose column; *lanes* 5–7, washing of amylose column; *lane* 8, elution of the isolated CBP-MBP-WT-hPAH/6His-MBP-ΔN102-hPAH fusion proteins from the amylose column; *lane* 9, isolated fusion proteins after concentration; *lane* 10, isolated tetrameric fusion proteins after size-exclusion chromatography; *lane* 11, low-molecular-mass marker. Co-expression using the construct pETDuet-1-[CBP-MBP-pep$_{(Xa)}$-WT-hPAH/6His-MBP-pep$_{(Xa)}$-ΔN102-hPAH].

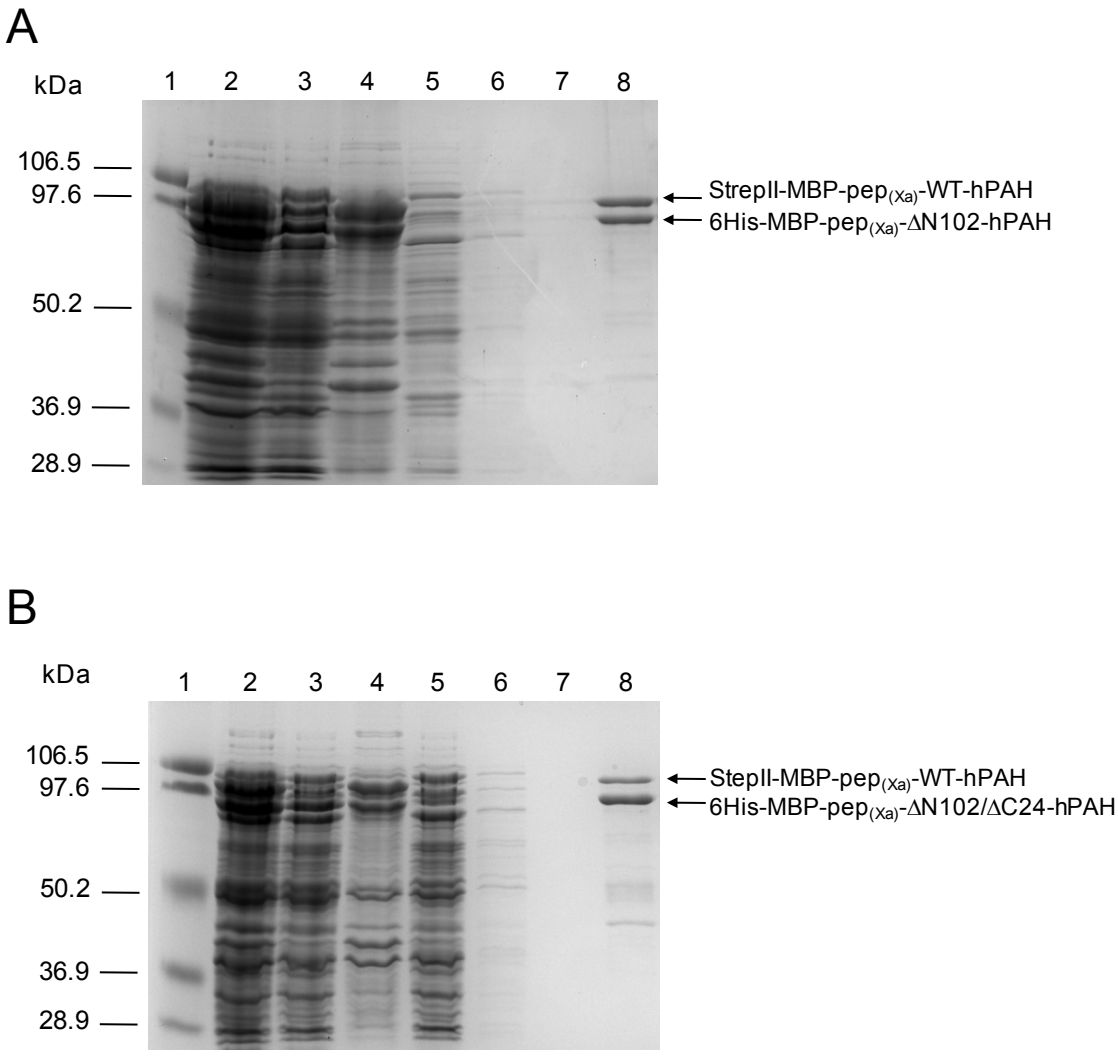

Supplementary Fig. S3. SDS-PAGE analysis of the amylose affinity purification of the recombinant (WT)/(ΔN102)-hPAH (A) and (WT)/(ΔN102/ΔC24)-hPAH (B) proteins. *Lane* 1, low-molecular-mass marker; *lane* 2, total cell lysate after 8h induction of recombinant hPAH by 1 mM IPTG at 28 ºC; *lane* 3, soluble fraction; *lane* 4, insoluble fraction, *lane* 5, flow-through from the amylose column; *lanes* 6 and 7, washing of amylose column; *lane* 8, elution of the isolated recombinant hPAH fusion proteins from the amylose column. Co-expressions using the constructs pETDuet-1-[StrepII-MBP-pep$_{(Xa)}$-WT-hPAH/6His-MBP-pep$_{(Xa)}$-ΔN102-hPAH] (A) and pETDuet-1-[StrepII-MBP-pep$_{(Xa)}$-WT-hPAH/6His-MBP-pep$_{(Xa)}$-ΔN102/ΔC24-hPAH] (B), respectively.

Supplementary Table S1
Properties of the affinity tags used in this study.

Affinity tag	Sequence	Residues	Size (kDa)	Resin	Elution Conditions
MBP	Protein	396	40.0	Amylose	10 mM maltose
CBP	KRRWKKNFIAVSAANRFKKISSSGAL	26	3.0	Calmodulin	2 mM EGTA
6His	HHHHHH	6	0.8	Ni^{2+}-NTA	150 mM imidazole
StrepII	WSHPQFEK	8	1.1	Strep-Tactin	2.5 mM desthiobiotin

Part IV

Phenylketonuria:
A Protein Misfolding Disease

1. Phenylketonuria as a protein misfolding disease: The mutation pG46S in phenylalanine hydroxylase promotes self-association and fibril formation

João Leandro, Nina Simonsen, Jaakko Saraste, Paula Leandro, Torgeir Flatmark

Biochimica et Biophysica Acta (Molecular Basis of Disease), 1812 (2011) 106–120.

Biochimica et Biophysica Acta 1812 (2011) 106–120

Contents lists available at ScienceDirect

Biochimica et Biophysica Acta

journal homepage: www.elsevier.com/locate/bbadis

Phenylketonuria as a protein misfolding disease: The mutation pG46S in phenylalanine hydroxylase promotes self-association and fibril formation

João Leandro [a,b], Nina Simonsen [a], Jaakko Saraste [a], Paula Leandro [b], Torgeir Flatmark [a,*]

[a] Department of Biomedicine, University of Bergen, Jonas Lies vei 91, N-5009 Bergen, Norway
[b] Metabolism and Genetics Group, iMed.UL, Faculty of Pharmacy, University of Lisbon, Av. Prof. Gama Pinto, 1649-003 Lisbon, Portugal

ARTICLE INFO

Article history:
Received 7 July 2010
Received in revised form 2 September 2010
Accepted 21 September 2010
Available online 16 October 2010

Keywords:
Phenylketonuria
Phenylalanine hydroxylase
pG46S
Polymerization
Fibril formation
Chaperone

ABSTRACT

The missense mutation pG46S in the regulatory (R) domain of human phenylalanine hydroxylase (hPAH), associated with a severe form of phenylketonuria, generates a misfolded protein which is rapidly degraded on expression in HEK293 cells. When overexpressed as a MBP-G46S fusion protein, soluble and fully active tetrameric/dimeric forms are assembled and recovered in a metastable conformational state. When MBP is cleaved off, G46S undergoes a conformational change and self-associates with a lag phase and an autocatalytic growth phase (tetramers ≫ dimers), as determined by light scattering. The self-association is controlled by pH, ionic strength, temperature, protein concentration and the phosphorylation state of Ser16; the net charge of the protein being a main modulator of the process. A superstoichiometric amount of WT dimers revealed a 2-fold enhancement of the rate of G46S dimer self-association. Electron microscopy demonstrates the formation of higher-order oligomers and linear polymers of variable length, partly as a branching network, and partly as individual long and twisted fibrils (diameter ~145–300 Å). The heat-shock proteins Hsp70/Hsp40, Hsp90 and a proposed pharmacological PAH chaperone (3-amino-2-benzyl-7-nitro-4-(2-quinolyl)-1,2-dihydroisoquinolin-1-one) partly inhibit the self-association process. Our data indicate that the G46S mutation results in a N-terminal extension of α-helix 1 which perturbs the wild-type α–β sandwich motif in the R-domain and promotes new intermolecular contacts, self-association and non-amyloid fibril formation. The metastable conformational state of G46S as a MBP fusion protein, and its self-association propensity when released from MBP, may represent a model system for the study of other hPAH missense mutations characterized by misfolded proteins.

1. Introduction

The human inborn error of metabolism phenylketonuria (PKU; OMIM# 261600) is caused by a dysfunction of the liver enzyme phenylalanine hydroxylase (hPAH; EC 1.14.16.1), inherited in an autosomal recessive fashion. At present > 500 disease causing mutations have been identified in the human *PAH* gene (see PAH Mutation Analysis Consortium database: http://www.pahdb.mcgill.ca/) [1]. Most of them are associated with PKU, and a smaller number has been identified among non-PKU hyperphenylalaninemia (HPA) patients. The current spectrum of alleged PKU/HPA mutations consists of ~60% missense substitutions, ~13% splice variants, ~13% deletions, ~6% nonsense (termination) mutations, and a few insertions, representing a broad spectrum of clinical, metabolic and enzymatic phenotypes [2]. Expression analyses of ~100 missense mutations in complementary *in vitro* systems (for review, see the PAH Mutation Analysis Consortium database) [1] have identified at least three main groups of enzymatic phenotypes which differ in their kinetic behavior and/or stability [3,4], i.e. (i) structurally stable mutations with altered kinetic properties, e.g. mutations at residues involved in substrate (L-phenylalanine, L-Phe) or the pterin cofactor ((6R)-L-*erythro*-5,6,7,8-tetrahydrobiopterin, BH_4) binding; (ii) mutations with normal or almost normal kinetic properties, but reduced stability both *in vitro* and *in vivo*; and (iii) mutations affecting both kinetic and stability properties of the enzyme.

Since a majority of the mutations results in enzyme forms with a propensity to self-associate when expressed as recombinant proteins in *E. coli* or in an *in vitro* transcription–translation system, PKU is often considered as a protein misfolding disease [5]. These mutations are located in different regions of the three-domain structure [4,6–9], and the mechanism of self-association may therefore have a variable structural basis. When overexpressed in *E. coli* several misfolding mutations result in both soluble and insoluble "aggregates", even when expressed and purified as MBP fusion proteins. Although MBP has been shown to have a chaperone like effect [10,11], the soluble mutant

Abbreviations: hPAH, human phenylalanine hydroxylase; rPAH, rat phenylalanine hydroxylase; PKU, phenylketonuria; L-Phe, L-phenylalanine; BH_4, (6R)-L-*erythro*-5,6,7,8-tetrahydrobiopterin; IPTG, isopropyl-thio-β-D-galactoside; MBP, maltose binding protein; SEC, size-exclusion chromatography; WT, wild-type; TM, tetramer; DM, dimer; ANS, 8-anilino-1-naphthalenesulfonic acid; DMSO, dimethyl sulfoxide; EM, electron microscopy

* Corresponding author. Tel.: +47 55586428; fax: +47 55586360.
E-mail address: torgeir.flatmark@biomed.uib.no (T. Flatmark).

0925-4439/$ – see front matter © 2010 Elsevier B.V. All rights reserved.
doi:10.1016/j.bbadis.2010.09.015

proteins are often recovered mostly as higher-order oligomers [4,6,9]. However, in some mutations, e.g. the missense mutation pG46S in the regulatory (R) domain, the expressed protein is assembled and recovered as stable tetrameric/dimeric forms, in addition to some soluble higher-order oligomers [12]. The MBP-G46S-hPAH tetramer is characterized by a near normal catalytic efficiency, but when the tetramer is cleaved by the restriction protease factor Xa, the G46S tetramer is destabilized and self-associates [12]. When expressed in eukaryotic cells as a non-fusion protein the enzyme is unstable and is rapidly degraded [12], thus explaining the severe PKU phenotype. However, the molecular mechanism of the self-association and the structural properties of the higher-order oligomers remain to be determined.

In the present study, the pG46S mutation was carefully analyzed. This mutation belongs to the second group of enzymatic phenotypes previously defined, with reduced stability both *in vitro* and *in vivo* that results in a severe form of PKU [12]. This group represents a large proportion of the PKU mutations, with a loss-of-function pathogenesis due to reduce stability [13]. The mutation pG46S is also located in the regulatory domain of hPAH, and there is growing evidence that the R-domain of hPAH is largely involved in the instability of hPAH mutant proteins [9]. Therefore, the recombinant WT-hPAH and the G46S-hPAH mutant form were isolated as MBP-$(pep)_{Xa}$-PAH fusion proteins with the goal to: (i) characterize the self-association process of G46S-hPAH induced *in vitro* by factor Xa cleavage and how the solvent conditions affect its propensity to self-associate; (ii) examine the effect of substrates (L-Phe and BH_4), phosphorylation of Ser16 (Ser16 is, together with substrate and cofactor, one of the main regulators of hPAH function, involved in the activation of the enzyme [14] and causing conformational changes in the regulatory domain [15,16]) and molecular/pharmacological/chemical chaperones on the propensity to self-associate; (iii) investigate if the self-association results in the formation of any stable polymeric structures such as fibrils, and (iv) gain some insight into the molecular mechanism by which such structures are formed. To answer these questions, we used a combined approach of real-time light-scattering, thioflavin-T and ANS fluorescence and structural analyses by electron microscopy (EM). Additionally, complementary studies on a MBP fusion protein with the regulatory domain, comprising residues 2–120, were performed on the WT and G46S mutant form.

2. Material and methods

2.1. Materials

TB1 cells, the prokaryotic expression vector pMAL-c2/pMAL-hPAH and the amylose resin were obtained from New England Biolabs (USA). The restriction protease factor Xa was obtained from Protein Engineering Technology ApS (Aarhus, Denmark). The catalytic *C*-subunit of cAMP-dependent protein kinase (PKA) was from Biaffin GmBH & Co KG (Kassel, Germany). SDS molecular mass standard (low M_r range) was delivered by Bio-Rad. The pterin cofactor tetrahydrobiopterin (BH_4) was obtained from Schircks Laboratories (Jona, Switzerland) and glycerol, trimethylamine *N*-oxide (TMAO) and (−)-epigallocatechin gallate (EGCG) were from Sigma-Aldrich (St. Louis, MO, USA). 3-amino-2-benzyl-7-nitro-4-(2-quinolyl)-1,2-dihydroisoquinolin-1-one was purchased from Maybridge (Tintagel, Cornwall, UK). The recombinant human molecular chaperones Hsp40 (catalog number SPP-400), Hsp70 (catalog number ESP-555) and Hsp90 (catalog number SPP-776) were provided by Assay Designs (Ann Arbor, MI, USA).

2.2. Site-specific mutagenesis

The WT regulatory domain (WT-hPAH (2–120)) and the mutant G46S regulatory domain (G46S-hPAH (2–120)) were obtained by introducing a stop signal in codon 121 of hPAH, by site-directed mutagenesis (QuikChange^R II, Stratagene), using the pMAL-WT-hPAH vector [17] and pMAL-G46S-hPAH vector [12] as template, respectively. Primers 5′-GACACAGTGCCCTGGT**AA**CCAAGAACCATTCAAGAGC-3′ (forward) and 5′-GCTCTTGAATGGTTCTTGG**TT**ACCAGGGCACTGTGTC-3′ (reverse) used for mutagenesis were provided by Eurogentec, Seraing, Belgium (the mismatch nucleotides are shown in bold type). The authenticity of the mutagenesis was verified by DNA sequencing as described previously [12].

2.3. Expression and isolation of fusion proteins

Expression of both the WT and the mutated form G46S of hPAH and the R-domain of hPAH (residues 2–120) was performed in *E. coli* as fusion proteins (MBP-$(pep)_{Xa}$-hPAH) [17]. The bacteria were grown at 37 °C and the induction of hPAH by 1 mM isopropyl-thio-β-D-galactoside (IPTG) was performed for 24 h at 28 °C. The fusion proteins were purified by affinity chromatography (amylose resin) and centrifuged in a TL-100 Ultracentrifuge (Beckman, USA) for 20 min at 50,000 *g* before size-exclusion chromatography (SEC) as described [17]. SEC was performed at 4 °C using a HiLoad Superdex 200 HR column (1.6 cm × 60 cm) prepacked from Amersham Biosciences (GE Healthcare, Uppsala, Sweden). The mobile phase consisted of 20 mM Na-Hepes and 0.2 M NaCl, pH 7.0 and the flow rate was 0.38 ml min^{-1}. The tetrameric/dimeric hPAH fusion proteins and the R-domain of hPAH also as a fusion protein were collected and concentrated by Centriplus 30 filter (Amicon, MA, USA). The concentration of purified fusion proteins was measured by the absorption coefficient A_{280} (1 mg ml^{-1} cm^{-1}) = 1.63 [17] for the full-length enzymes and A_{280} (1 mg ml^{-1} cm^{-1}) = 1.34 for the truncated form hPAH (2–120). A colorimetric method [18] was also used in some cases to measure enzyme concentrations, with bovine serum albumin as the standard.

T427P-hPAH [19] and ΔC24-hPAH [20] were expressed as fusion proteins with MBP in *E. coli* and isolated essentially as the G46S mutant protein, except that before SEC the proteins were cleaved for 4 h at 4 °C by factor Xa protease, using a protease to substrate ratio of 1:200 (by mass) to remove the MBP partner.

2.4. Phosphorylation of hPAH fusion protein

The phosphorylation of the fusion protein (tetrameric form) was performed in a reaction mixture containing 0.1 mM ethylene glycol bis-(α-amino ether)-N,N,N′N′-tetraacetic acid, 0.03 mM EDTA, 1 mM DTT, 10 mM MgAc, 60 μM ATP in 15 mM Na-Hepes, pH 7.0, at 30 °C for 1 h [21]. The enzyme concentrations were 20 μM (hPAH) and 100 nM (catalytic subunit) of PKA. The degree of phosphorylation was measured by the electrophoretic mobility shift [6]. The non-phosphorylated fusion protein control was obtained by incubating the enzyme in the absence of added PKA catalytic subunit, under otherwise identical conditions.

2.5. Cleavage of MBP-hPAH fusion proteins and assay of self-association by light scattering

In order to study the time-course for the cleavage of the tetrameric and dimeric MBP-hPAH fusion proteins and the self-association of the released enzyme, the fusion proteins were incubated in a medium containing 20 mM Na-Hepes, 0.1 M NaCl, pH 7.0 at 25 °C, except when stated otherwise. Before assay the tetrameric or dimeric fusion proteins were subjected to high-speed ultracentrifugation at 210,000 *g* for 15 min at 4 °C. In the standard assay the concentration of the fusion protein was 0.74 mg ml^{-1} and the concentration of factor Xa was adjusted to give a final ratio (by weight) of 1:150 relative to the fusion protein. Parameters as pH, neutral salt concentration, temperature, protein concentration and the presence of substrates (L-Phe and BH_4) varied in different experiments as described in the Results section. Self-association of the factor Xa released enzyme was followed in real-time by light scattering, as measured by the increase in apparent absorbance

at 350 nm ($A'_{350} = \log [I_o/(I_p + f \cdot I_d)]$ using an Agilent 8453 Diode Array Spectrophotometer with a Peltier temperature control unit. The change in light scattering was expressed as $\Delta A'_{350}$ by subtracting the background absorbance in the absence of added factor Xa. $\Delta A'_{350}/\Delta t$ is the rate of formation of higher-order oligomers/polymers obtained from the slope of the linear growth phase of each light scattering curve. For every self-association experiment a parallel time-course cleavage analysis was conducted to rule out any change in the cleavage rate of the fusion protein.

2.6. SDS-PAGE analyses

SDS-PAGE analyses were performed in a 10% (w/v) polyacrylamide gel [22]. The gels were stained by Coomassie Brilliant Blue R-250, scanned using VersaDoc 4000 (Bio-Rad) and quantification of the protein bands was obtained by using the Quantity One 1-D Analysis Software (Bio-Rad Laboratories, Hercules, CA, USA).

2.7. Cleavage of G46S-hPAH fusion protein in the presence of chaperones

In order to study the influence of chaperones on the self-association process following cleavage of the mutant enzyme, tetrameric MBP-G46S-hPAH and chaperone were added (together with the factor Xa protease) at a variable molar ratio as described in Results. The experimental conditions were the same as in the cleavage experiments without chaperone, except in the case of the pharmacological chaperone that was dissolved in DMSO and used at a final concentration of 100 μM and 0.83% DMSO. In this case controls were included with 0.83% DMSO.

2.8. Negative staining electron microscopy

For negative staining EM of unpolymerized and polymerized G46S-hPAH Formvar-coated 200 mesh nickel grids (Electron Microscopy Sciences, Fort Washington, USA) were used. The grids were further coated with carbon, stored dust-free in Petri dishes kept at low humidity, and glow-discharged for 15 s prior to use. Negative staining was carried out by first applying 5 μl of a protein solution on the specimen grid. Following absorption for 60 s, the sample drop was removed by blotting with filter paper and the grid was stained twice with 2% aqueous uranyl acetate. After application, the first drop (10 μl) was blotted off immediately, whereafter a fresh drop of the stain was added to the grid for 15 s. After final blotting and drying, the specimens were observed in a Jeol 1230 Electron Microscope operated at 80 kV.

2.9. Thioflavin-T fluorescence assay

The assay was performed according to a standard protocol [23]. Briefly, the thioflavin-T (ThT, Sigma-Aldrich) measurements were made by taking reaction aliquots and diluting them to 1.3 μM hPAH in 20 mM Na-Hepes, 0.1 M NaCl, pH 7.0 containing 20 μM ThT. Immediately following sample preparation the fluorescence was measured in a Perkin-Elmer LS-50B instrument (Perkin-Elmer, Waltham, MA, USA) at 25 °C (constant temperature cell holder) using an excitation of 440 nm and emission of 482 nm, with slit widths for excitation and emission of 3 and 7 nm, respectively, and by averaging four scans. The reported values were corrected by subtracting the background fluorescence of ThT in the absence of protein oligomers and controls with the protein oligomers in the absence of ThT (light scattering).

2.10. ANS fluorescence assay

Binding of 8-anilino-1-naphthalenesulfonic acid (ANS, Sigma-Aldrich) was performed as described by Aukrust et al. [24]. Briefly, 1.3 μM hPAH was incubated with 60 μM ANS in 20 mM Na-Hepes, 0.1 M NaCl, pH 7.0 at room temperature for 5 min in the dark. The fluorescence emission spectra were recorded between 400 and 600 nm (6 nm slit width) at 25 °C using an excitation wavelength of 385 nm (6 nm slit width) on a Perkin-Elmer LS-50B luminescence spectrometer and by averaging four scans.

2.11. Assay of hPAH activity

The hPAH activity was assayed at 25 °C in a standard reaction mixture containing a 0.4 μM subunit (unless otherwise stated) of tetrameric WT or G46S mutant fusion protein forms of hPAH, 1 mM L-Phe, 0.5 mg ml^{-1} bovine serum albumin, 5 mM dithiothreitol, 0.1 mg ml^{-1} catalase, 100 μM ferrous ammonium sulfate in 100 mM Na-Hepes, pH 7.0 [17]. After preincubation (5 min) with L-Phe the reaction was started by adding 75 μM (unless stated otherwise) BH_4 to the reaction mixture. The amount of L-Tyr formed after 1 min was measured by high pressure liquid chromatography and fluorimetric detection [25]. The steady-state kinetic data were analyzed by nonlinear regression analysis using the SigmaPlot® Technical Graphing Software and the modified Hill equation of LiCata and Allewel [26] for cooperative substrate binding as well as substrate inhibition [27]. In some experiments, 1 mM L-Phe was added either at the start of the preincubation period or together with 75 μM BH_4 at the initiation of the hydroxylation reaction. In this case a 3 min time-course was then followed in order to study the effect of preincubation with L-Phe on the specific activity.

2.12. Computational analysis

An estimation of the free energy of unfolding of the mutant protein was predicted using the CUPSAT server (http://cupsat.tu-bs.de/) [28] and the free energy of folding was predicted using the Concoord/PBSA server (http://ccpbsa.bioinformatik.uni-saarland.de/ccpbsa/) [29]. In order to evaluate the effect on G46S mutation on the secondary structure of the hPAH protein an algorithm based on helix–coil transition theory, AGADIR, was used to predict helical propensity (http://agadir.crg.es/) [30]. To identify the location of hinges in PAH we subjected the apo-rPAH crystal structure (PDB ID: 2PHM) to further analysis using the HingeMaster software program that predicts the hinge location in a protein by integrating existing hinge predictors (TLSMD, StoneHinge, FlexOracle and HingeSeq) with a family of novel hinge predictors based on grouping residues with correlated normal mode motions (http://molmovdb.org/cgi-bin/submit-flexoracle.cgi) [31].

2.13. Statistical analyses

Data obtained from independent measurements are presented as mean ± SD and Student's *t*-test was conducted for statistic analysis of quantitative data ($P<0.01$ was considered significant).

3. Results

3.1. Structural effects of the G46S mutation

The ~50 kDa monomer of WT mammalian PAH assembles *in vivo* and on overexpression in bacteria to form tetramers (TMs) and dimers (DMs). Atomic resolution structures of hPAH and rPAH have revealed that the monomer consists of three structural and functional domains, i.e. a regulatory (R), a catalytic (C) and a tetramerization (T) domain [32–34]. On the basis of the 3D structures of the C–T domains of hPAH and the R–C domains of rPAH a composite full-length model has been assembled for the PAH tetramer [8] (Fig. 1A and B). It is organized as an asymmetric dimer of dimers, and the model has the approximate dimensions of 85 Å × 100 Å × 75 Å. The R-domain has an α–β sandwich (βαββαβ) motif composed of a four-stranded antiparallel β-sheet flanked on one side by two short α-helices and the other side by the C-domain (Fig. 1C). Using the HingeMaster software program [31] (see

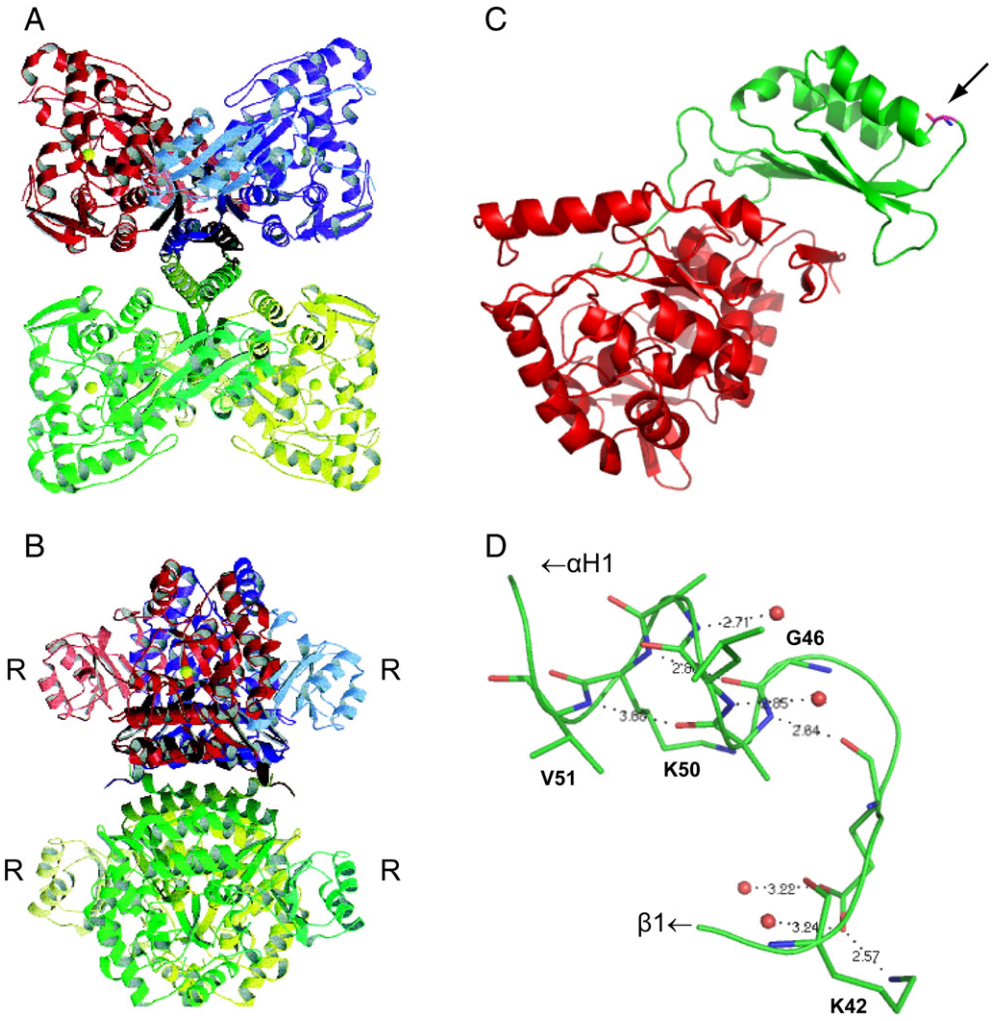

Fig. 1. 3D structure of PAH and the localization/interactions of the G46 residue in the N-terminal regulatory domain. (A) Structure of a composite model of full-length tetrameric hPAH. Cα-trace ribbon of the model created by combining the regulatory/catalytic domain crystal structure of rPAH (PDB ID: 1PHZ) and the catalytic/tetramerization domain structure of hPAH (PDB ID: 2PAH). Each monomer is colored separately, with the lightest color representing the regulatory domain (R) and the darkest color representing the tetramerization domain. (B) Side view 90° rotation from the view in A, with the position of the four regulatory domains indicated by a R. (C) Ribbon representation of the regulatory/catalytic domain crystal structure of rPAH in the monomeric form with the regulatory domain shown in green, the catalytic domain in red and G46 in stick model (pointed arrow). (D) Close-up of the location of G46 in the regulatory domain of rPAH, at the end of the loop between β-strand 1 and α-helix 1, where it H-bonds to K50. The Cα-atom trace is shown in green ribbon, with the relevant residues in stick model and water molecules as red spheres. The figures were created using MOLSCRIPT [76] (A and B) and PyMOL, version 1.1 (DeLano Scientific) [77] (C and D).

Materials and methods) our analysis revealed major hinges in the R–C domain structure around the interdomain residues 118–119 and around the intradomain residues 26–27 (Fig. 2A).

The residue G46 is positioned at the entry of α-helix 1 (A47–E57) in a five residue (L41–G46) loop structure (loop 1), with a relatively low crystallographic *B*-factor (Fig. 2B), linking β-strand 1 and α-helix 1 (Fig. 1D), and is stabilized by H-bonds and a salt-bridge (K42–E44) (Fig. 1D). The α-helix 1 is stabilized at the C-terminal end by forming a hydrophobic interphase with α-helix 2 (not shown). Using the coordinates of the R–C domains (PDB ID: 1PHZ) and two structure-based methods for the estimation of the free energy of unfolding [28] and folding [29] of mutant proteins, substitutions of G46 with any amino acid were found to be destabilizing, and for the G46S mutation the folding free energy was calculated to $\Delta\Delta G = 4.1$ kcal mol^{-1} with a major electrostatic contribution ($\Delta\Delta G_{es} = 4.7$ kcal mol^{-1}). Since Gly is known to have a large destabilizing effect on α-helices [35], whereas a substituted Ser and the preceding residues (V45, E44, E43, K42 and L41) in loop 1 have all a relatively high α-helix-forming propensity [35], the G46 substitution is predicted to promote a N-terminal extension of α-helix 1 by four residues or one turn using the AGADIR algorithm [30] (Fig. 2C).

3.2. Expression and isolation of the MBP fusion proteins

On expression of WT and the mutant form G46S as fusion proteins (MBP-$(pep)_{Xa}$-hPAH) the proteins were obtained in high yields and separated into their oligomeric forms by SEC (Fig. 3A and B). The chromatogram of both forms revealed a comparable elution pattern in which peak 1 represented higher-order oligomeric forms (eluted at or near the void volume), and peak 3 and peak 4 represented the TM and DM forms, respectively [12,17].

3.3. Catalytic properties of MBP-WT-hPAH and MBP-G46S-hPAH fusion proteins

Determination of the steady-state catalytic properties of the tetrameric MBP-G46S-hPAH fusion protein revealed that it has a higher specific activity than the WT protein, and a slightly higher

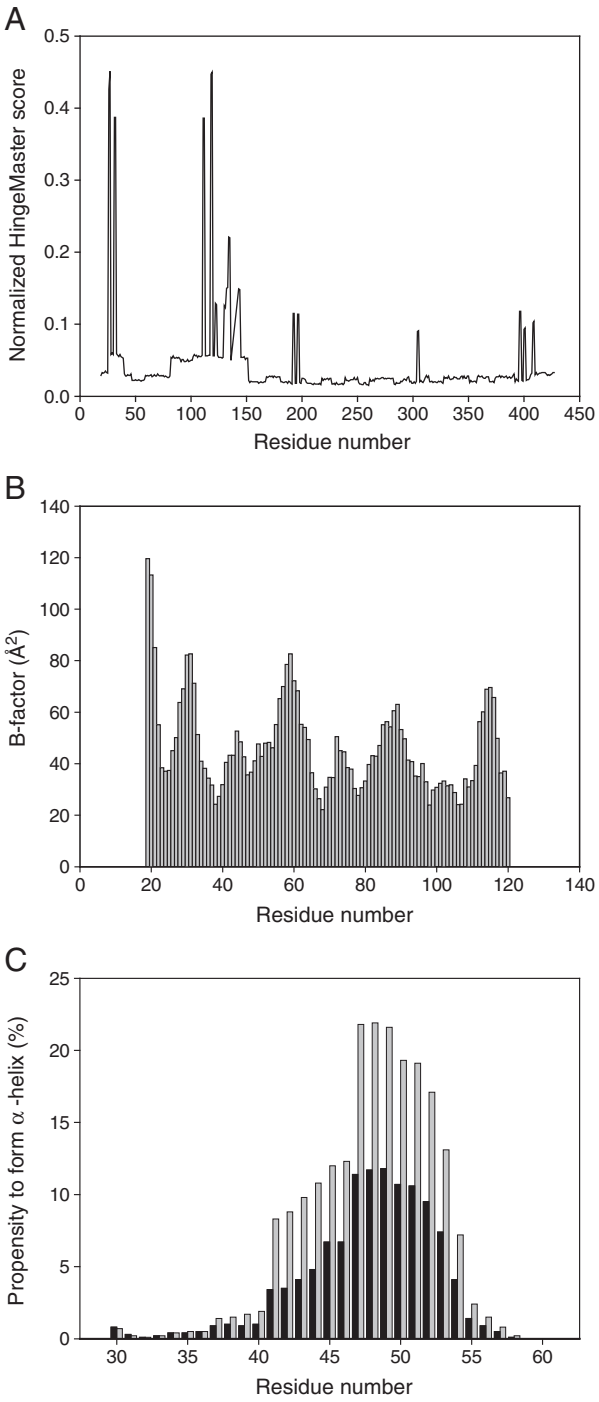

Fig. 2. Structural properties of the regulatory domain. (A) Combined hinge prediction scores of the R–C domain structure in the non-phosphorylated form of rPAH (PDB ID: 2PHM) using the HingeMaster server [31] as a function of amino acid residue number. A similar score profile was obtained for the phosphorylated form (PDB ID: 1PHZ). (B) The crystallographic *B*-factor values *vs.* residue numbers in the regulatory domain (PDB ID: 1PHZ). (C) Prediction of the effect of the G46→S substitution on the propensity to form an α-helix in the sequence comprising residues 30 to 58 using the AGADIR algorithm [30]. The black bars represent the propensity to form an α-helix in the WT-PAH protein and the gray bars correspond to the α-helix propensity in the mutant G46S-hPAH.

affinity for the substrate L-Phe ($[S]_{0.5} = 74 \pm 5$ μM for the mutant and $[S]_{0.5} = 106 \pm 2$ μM for MBP-WT-hPAH) (Table 1). The affinity for the cofactor BH_4 was unaffected. The mutant fusion protein revealed a low kinetic cooperativity with respect to L-Phe ($n_H = 1.2 \pm 0.1$) and was already in an activated conformational state. Both proteins showed an inhibition at higher substrate concentrations.

3.4. Cleavage of the MBP fusion proteins

In the standard assay conditions the cleavage reaction was similar for the tetrameric WT (not shown) and the mutant fusion protein (Fig. 4A), with $t_{1/2}$ (time at 50% cleavage) of ~11 min. The half-time and the end point of the cleavage reaction varied to some extent with the solvent conditions, notably with the ionic strength (Supplementary Fig. S1A) and the temperature (Supplementary Fig. S1B).

3.5. Self-association of tetrameric and dimeric forms of G46S-hPAH

At the selected standard assay conditions (pH 7.0, 0.1 M NaCl and 25 °C) the cleavage of the MBP-WT-hPAH tetramer (0.74 mg ml^{-1}) did not result in any change in light scattering (Fig. 4B). By contrast, the G46S-hPAH mutant form revealed a propensity to self-associate (Fig. 4B). A sigmoidal time-course was observed for the increase in light scattering with three relatively distinct phases, i.e. a delay period (lag phase), a growth phase of increasing light scattering ($\Delta A'_{350}/\Delta t$ (AU min^{-1}) $= 0.026 \pm 0.003$) and a final phase with a decrease in light scattering. In the absence of added factor Xa no change in light scattering of the MBP-G46S-hPAH fusion protein was observed within the time-scale of 3 h. A comparison of the TM and DM mutant fusion proteins (Fig. 7A) revealed that the DM displayed a similar lag phase but a 2-fold lower $\Delta A'_{350}/\Delta t$ value than the TM (at equal protein concentration) at pH 7.0.

3.6. Effects of pH and ionic strength

WT-hPAH and the R-domain (residues 1–120) have theoretical p*I*s of ~pH 6.2 and ~pH 6.1, respectively. Whereas no significant difference was observed in the cleavage rate of the fusion protein in the pH interval of 6.4 to 8.0 (Supplementary Fig. S2A), a large effect of pH was observed on the self-association (Fig. 5). Thus, by lowering the pH towards the p*I*, the lag phase was reduced and the $\Delta A'_{350}/\Delta t$ value greatly increased. At pH 8.0, with a theoretical net charge of ~−9.2 no measurable $\Delta A'_{350}/\Delta t$ value was observed within the time-scale of 3 h.

The ionic strength (range 0.1 M and 0.4 M NaCl) has a certain effect on the rate of cleavage of MBP-G46S-hPAH (Supplementary Fig. S1A), but a more dramatic effect on the lag phase and the $\Delta A'_{350}/\Delta t$ value of G46S-hPAH self-association (Table 2), demonstrating the importance of the global charge in the process.

3.7. Effect of temperature and protein concentration

Whereas the rate of the cleavage was only slightly slower at 15 °C ($t_{1/2}$ of 13.3 min) than at 25 °C ($t_{1/2}$ of 11.3 min) (Supplementary Fig. S1B), the self-association was largely affected by the reaction temperature. Thus, on increasing the temperature the lag phase decreases and the rate of self-association ($\Delta A'_{350}/\Delta t$) increases (Table 2) with an apparent activation energy (E_a) of 134 kJ mol^{-1}.

When the cleavage reaction was followed at the standard assay conditions, but with variable concentrations of fusion protein at a constant ratio of factor Xa:G46S-hPAH = 1:150 (by weight), the half-time was almost the same in the range of 0.37 to 0.74 mg ml^{-1} (Supplementary Fig. S2B). A more pronounced effect was observed on the lag phase and the rate of self-association ($\Delta A'_{350}/\Delta t$) (Table 2).

3.8. The effect of substrates and phosphorylation of Ser16

The binding of L-Phe or the pterin cofactor BH_4 at the active site triggers global conformational changes in the WT tetramer, including the R-domain [8]. Here, however, we observed no significant modulation of the self-association of G46S-hPAH in the presence of 75 μM BH_4, whereas 1 mM L-Phe slightly reduced the lag phase and increased the $\Delta A'_{350}/\Delta t$ value (Table 2). When the fusion protein was phosphorylated

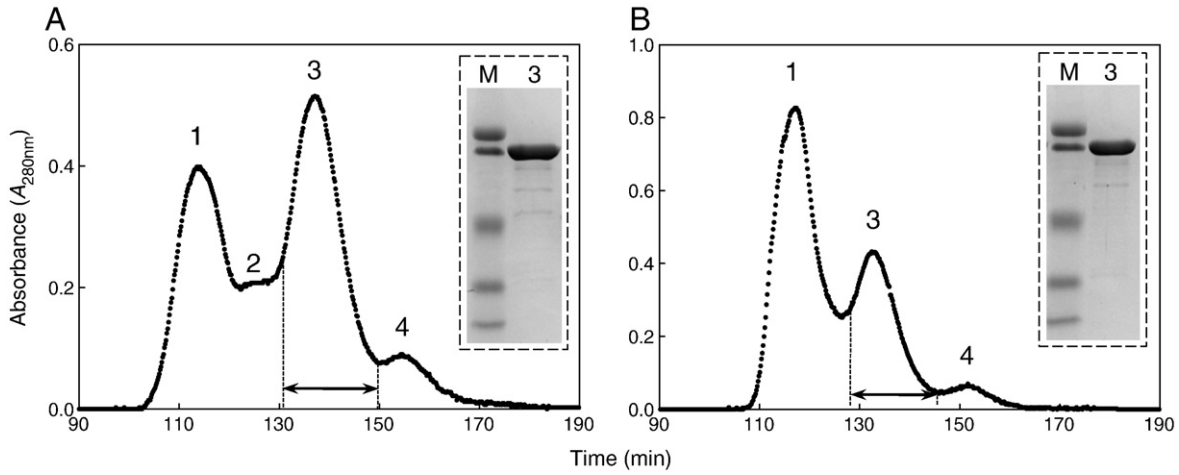

Fig. 3. Size-exclusion chromatography of WT-hPAH and the mutant G46S-hPAH. (A) The chromatogram of WT-hPAH with 4 main peaks, where peak 1 represents higher-order oligomeric forms (eluted in the void volume), peak 2 a presumably octameric form, peak 3 the tetramer (~365 kDa) and peak 4 the dimer (~209 kDa). (B) The chromatogram of the mutant form G46S-hPAH where the broad peak 1 represents higher-order oligomeric forms, peak 3 and 4 the tetramer and dimer, respectively. The apparent molecular mass of the enzyme forms were estimated using the elution position of standard molecular mass markers as a reference (not shown). The two dashed lines indicate the collected tetramers used in further experiments. The proteins were expressed as MBP fusion proteins in *E. coli* under identical expression conditions (24 h, 28 °C). The chromatography was performed on a HiLoad Superdex 200 HR column (1.6 cm × 60 cm), equilibrated and eluted with 20 mM Na-Hepes, 0.2 M NaCl, pH 7.0 at a flow rate of 0.38 ml ml^{-1} at 4 °C; detection was at 280 nm. The *inset* in panels A and B represent the SDS-PAGE analyses demonstrating the purity of the tetrameric fusion proteins. *Lane* M, low-molecular-mass standard (106.5, 97.6, 50.2, 36.9 and 28.9 kDa); *lane* 3, the respective tetrameric form enzymes (peak 3) of the size-exclusion chromatography.

at Ser16 to >95%, the self-association of G46S-hPAH was markedly inhibited, with a longer lag phase and a decreased $\Delta A'_{350}/\Delta t$ value (Fig. 6A). The time-courses for the cleavage of the phosphorylated and non-phosphorylated MBP-G46S-hPAH were essentially identical (Supplementary Fig. S2C), and the substrates were without effect on the cleavage of MBP-G46S-hPAH (Supplementary Fig. S2D).

3.9. Effects of heat-shock proteins

Molecular chaperones facilitate the proper folding of many newly synthesized proteins as well as rescue proteins that are misfolded, e.g. due to mutations. Chaperone proteins also exhibit the unique property to inhibit self-association of certain client proteins [36]. From Fig. 6 it is seen that the Hsp70/Hsp40 chaperone system inhibits the self-association of G46S-hPAH in a dose-dependent manner. At the lowest molar ratio (1:20) of Hsp70/Hsp40 there is no effect on the $\Delta A'_{350}/\Delta t$ value, whereas at the higher ratio (1:2) the heat-shock proteins markedly prolong the lag phase and decrease the $\Delta A'_{350}/\Delta t$ value (Fig. 6B). A similar effect was observed for Hsp90 at a molar ratio of 1:2 (Fig. 6C). In control experiments with ovalbumin, no such effects were observed. Moreover, for both chaperones the addition of ATP did not further enhance the modulatory effects observed in the absence of nucleotide (data not shown). The chaperones did not contain cleavage sites for factor Xa restriction protease and were without effect on the cleavage of MBP-G46S-hPAH (Supplementary Fig. S2E).

3.10. Effects of pharmacological and chemical chaperones

The pterin cofactor BH_4 has been shown to increase the stability *versus* limited proteolysis by trypsin of WT-hPAH [37], as well as of a number of PKU mutant proteins *in vitro*, and to make them less vulnerable to degradation pathways when expressed in cells [38]. Since the structural basis of the stabilizing effect is quite well understood [37–39] the cofactor is currently used as a pharmacological chaperone in the treatment of a subgroup of PKU/HPA patients [40]. However, as seen from Table 2, BH_4 did not have any protective effect on the self-association of G46S-hPAH.

A recent screening of over 1000 pharmacological agents has identified two small-molecule binders (3-amino-2-benzyl-7-nitro-4-(2-quinolyl)-1,2-dihydroisoquinolin-1-one and 5,6-dimethyl-3-(4-methyl-2-pyridinyl)-2-thioxo-2,3-dihydrothieno[2,3-d]pyrimidin-4(1H)-one) as potential therapeutic agents to treat PKU [41]. Here we have found that only 3-amino-2-benzyl-7-nitro-4-(2-quinolyl)-1,2-dihydroisoquinolin-1-one, at a comparable concentration (100 μM), partly inhibits the *in vitro* self-association of G46S-hPAH (Fig. 6D).

The use of osmolytes can produce a chemical chaperoning effect *in vitro* and thus be able to rescue folding defects in proteins involved in conformational disorders [42,43]. In this study we have tested glycerol, trimethylamine N-oxide (TMAO) and (−)-epigallocatechin gallate (EGCG), but only glycerol showed a protective effect, while the other two compounds promoted the self-association (Table 2). The

Table 1
Kinetic properties of tetrameric wild-type hPAH (MBP-WT-hPAH) and G46S-hPAH (MBP-G46S-hPAH) fusion proteins.

	BH_4		L-Phe						
	V_{max} (nmol Tyr min^{-1} mg^{-1})	K_m (μM)	V_{max} (nmol Tyr min^{-1} mg^{-1})	$[S]_{0.5}$ (μM)	$k_{cat}/[S]_{0.5}$ (μM^{-1} min^{-1})	n_H	V_i (nmol Tyr min^{-1} mg^{-1})	K_i (μM)	Fold activation $R(_{v+\text{L-Phe}/v-\text{L-Phe}})$
MBP-WT-hPAH	3346 ± 151	43 ± 5	2360 ± 33	106 ± 2	2.09	2.5 ± 0.1	1072 ± 218	3190 ± 644	3.9
MBP-G46S-hPAH	4227 ± 187	42 ± 5	3677 ± 104	74 ± 5	4.67	1.2 ± 0.1	1521 ± 131	1911 ± 241	1.1

The catalytic activity was measured as described in the Materials and methods section at 25 °C; the substrate concentrations were 1 mM L-Phe (BH_4 variable) and 75 μM BH_4 (L-Phe variable). $[S]_{0.5}$ represents the L-Phe concentration at half-maximal activity and $k_{cat}/[S]_{0.5}$ the "catalytic efficiency". The "catalytic efficiency" was calculated on the basis of a subunit molecular mass of 94 kDa.

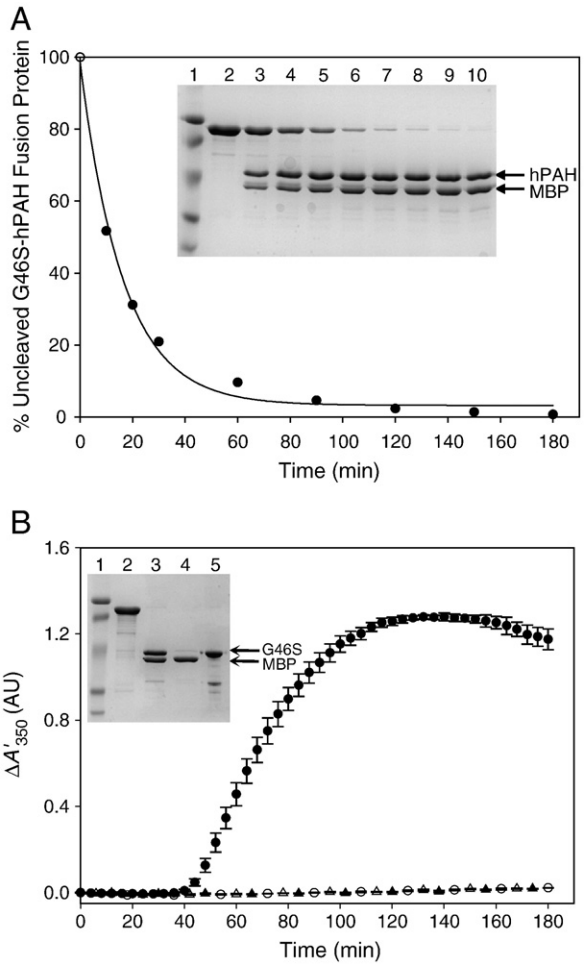

Fig. 4. The self-association of tetrameric G46S-hPAH following cleavage of the MBP fusion protein by factor Xa. (A) Time-course for the cleavage of tetrameric MBP-G46S-hPAH by the restriction protease factor Xa. The cleavage was performed at standard assay conditions (0.74 mg ml^{-1} fusion protein, 5.0 μg ml^{-1} factor Xa, 20 mM Na-Hepes, 0.1 M NaCl, pH 7.0 and 25 °C). 50% cleavage was obtained at ~11 min ($t_{1/2}$). The data was fitted to a single exponential decay curve. The *inset* represents a 10% SDS-PAGE analysis of the cleavage reaction. Aliquots (4 μg protein) were withdrawn at 0, 10, 20 and 30 min (*lanes* 2–5, respectively), and at 1, 1.30, 2, 2.30 and 3 h (*lanes* 6–10, respectively). *Lane* 1, low-molecular-mass marker (104.4, 83.2, 49.3, 36.9 and 28.9 kDa). (B) Self-association of the released enzyme was followed in real-time by light scattering, as measured by the increase in the apparent absorbance at 350 nm ($A'_{350} = \log [I_o/(I_p + f \cdot I_d)]$) using an Agilent 8453 Diode Array Spectrophotometer. The change in light scattering was expressed as $\Delta A'_{350}$ by subtracting the background absorbance in the absence of the added factor Xa. The data points correspond to G46S-hPAH fusion protein following cleavage by factor Xa (●), and in the absence of factor Xa (○); WT-hPAH fusion protein following cleavage by factor Xa (▲) and in the absence of factor Xa (Δ). Some data points were omitted for clarity. The reactions were performed at standard assay conditions. Error bars represent mean ± SD, $n = 3–5$ independent experiments. The *inset* represents SDS-PAGE analysis of the G46S-hPAH fusion protein at $t = 0$ (*lane* 2), and following its cleavage by factor Xa at $t = 180$ min (*lane* 3). The reaction mixture (after 180 min) was subjected to ultracentrifugation at 200,000 *g* and both the supernatant (*lane* 4) and pellet (*lane* 5) were recovered and analyzed by 10% SDS-PAGE. *Lane* 1, low-molecular-mass marker (104.4, 83.2, 49.3, 36.9 and 28.9 kDa).

pharmacological and chemical chaperones at the concentrations tested were without effect on the cleavage of MBP-G46S-hPAH (Supplementary Fig. S2D and F).

3.11. Effects of WT-hPAH dimer and ΔC24-hPAH dimer on the self-association of G46S-hPAH dimer

Since the G46S-hPAH tetramer self-associates to higher-order oligomers at a 2-fold higher rate than the dimer (Fig. 7A), it was of interest to see if a molar excess of the WT-hPAH dimer, which does not self-associate beyond the tetramer (data not shown), has any effect on the

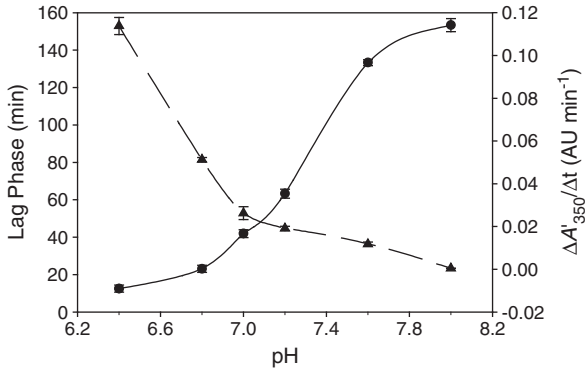

Fig. 5. The effect of pH. The effect of pH on the lag phase (●) and the rate of self-association ($\Delta A'_{350}/\Delta t$) (▲) of G46S-hPAH tetramer at otherwise standard assay conditions. Error bars represent mean ± SD.

self-association of G46S-hPAH dimer. From Fig. 7B it is seen that the WT-hPAH dimer at a 5-fold molar excess markedly shortens the lag phase and increases the $\Delta A'_{350}/\Delta t$ value about 2-fold, presumably by promoting the formation of G46S-WT heterotetramers (see Discussion). By contrast, a 5-fold molar excess of the truncated ΔC24-hPAH dimer, lacking the tetramerization domain, only slightly shortens the lag phase, whereas the rate of self-association ($\Delta A'_{350}/\Delta t$) is almost the same as for the G46S-hPAH dimer alone or in the presence of a 5-fold molar excess of ovalbumin (Fig. 7B). A dimeric mutant form (T427P-hPAH), with a reduced tendency to form tetramer [19], promotes a lower rate of self-association of the G46S-hPAH dimer than the WT-hPAH dimer (Fig. 7B). Moreover, the G46S-hPAH dimer in the presence of a 5-fold molar excess WT-hPAH dimer and 1 mM L-Phe, displayed almost the same lag phase as for the G46S-hPAH dimer alone and only a slightly increased $\Delta A'_{350}/\Delta t$ value (Fig. 7C). In this case the presence of L-Phe promotes the formation of WT tetramer [17]. The presence of 1 mM L-Phe has a negligible effect on the self-association pattern of the G46S-hPAH dimer alone (Fig. 7C) indicating that the G46S dimer ↔ G46S tetramer equilibrium is less responsive to L-Phe than that of WT-hPAH.

Table 2
The effect of solvent conditions, protein concentration, substrates and chemical chaperones on the self-association of tetrameric G46S-hPAH.

		Lag phase (min)	$\Delta A'_{350}/\Delta t$[a] (AU min^{-1})	$(\Delta A'_{350})_{max}$ (AU)
[NaCl]	100	41.9 ± 2.1	0.026 ± 0.003	1.24 ± 0.04
(mM)	200	112.1 ± 3.3	0.007 ± 0.001	0.49 ± 0.09
	400	118.5 ± 2.1	0.000 ± 0.000	0.03 ± 0.01
Temperature	15	87.5 ± 8.0	0.006 ± 0.002	0.49 ± 0.17
(°C)	25	41.9 ± 2.1	0.026 ± 0.003	1.24 ± 0.04
[G46S-hPAH fusion protein]	0.37	79.5[b]	0.014[b]	0.85[b]
(mg ml^{-1})	0.49	44.3[b]	0.017[b]	0.91[b]
	0.74	41.9 ± 2.1	0.026 ± 0.003	1.24 ± 0.04
L-Phe	0	41.9 ± 2.1	0.026 ± 0.003	1.24 ± 0.04
(mM)	1	38.7 ± 4.3	0.035 ± 0.009	1.30 ± 0.14
BH_4	0	41.9 ± 2.1	0.026 ± 0.003	1.24 ± 0.04
(μM)	75	45.7 ± 4.0	0.021 ± 0.008	1.22 ± 0.15
Glycerol	0	41.9 ± 2.1	0.026 ± 0.003	1.24 ± 0.04
(%)	1	49.6 ± 3.3	0.020 ± 0.004	1.13 ± 0.16
	2.5	55.9 ± 1.3	0.011 ± 0.001	0.84 ± 0.04
	5	95.3 ± 5.1	0.004 ± 0.001	0.33 ± 0.08
Trimethylamine *N*-oxide	0	41.9 ± 2.1	0.026 ± 0.003	1.24 ± 0.04
(TMAO)	5	39.8[b]	0.032[b]	1.35[b]
(mM)	150	31.8[b]	0.039[b]	1.59[b]
	250	30.5 ± 3.5	0.048 ± 0.008	1.68 ± 0.19
(−)-Epigallocatechin gallate	1:0	41.9 ± 2.1	0.026 ± 0.003	1.24 ± 0.04
(EGCG)	1:0.1	28.6 ± 1.3	0.038 ± 0.001	1.27 ± 0.01
(G46S-hPAH:EGCG)	1:1	23.3 ± 2.4	0.113 ± 0.014	2.37 ± 0.14

[a] $\Delta A'_{350}/\Delta t$ is the rate of formation of higher-order oligomers/polymers as obtained from the slope of the linear growth phase of each light scattering curve. Values are shown as mean±SD (n=3–5).
[b] SD not determined.

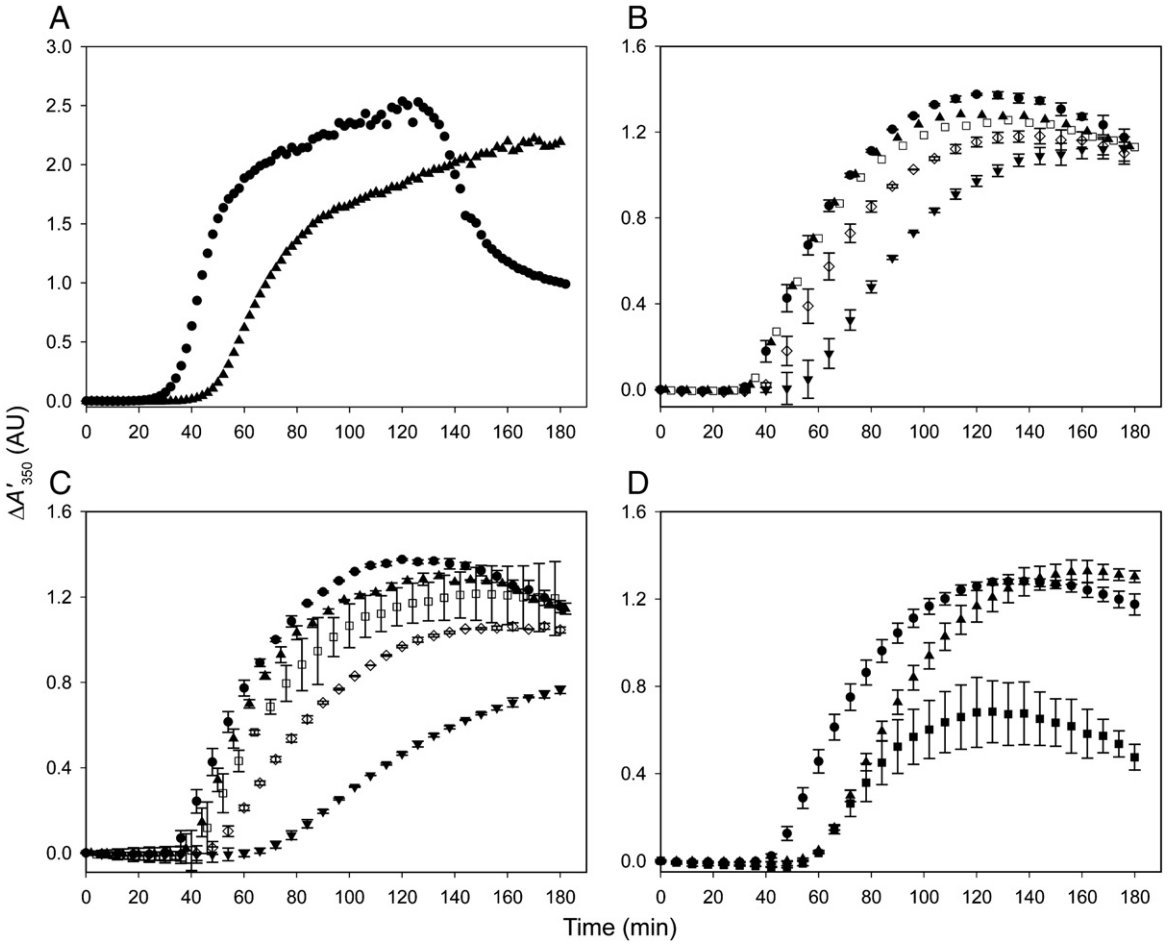

Fig. 6. Effect of phosphorylation at Ser16 and chaperones on the self-association of tetrameric G46S-hPAH. (A) The time-course for the self-association of phosphorylated enzyme (▲) and non-phosphorylated enzyme (●). The non-phosphorylated fusion protein control was obtained by incubating the enzyme in the absence of added PKA catalytic subunit, under otherwise identical conditions of the phosphorylated enzyme. Results are representative of two independent experiments. (B) The effect of Hsp70/Hsp40 (molar ratio 100:1) on the self-association of G46S-hPAH at different concentrations (expressed as molar ratios of chaperone:G46S-hPAH fusion protein): 0:1 (●), 1:20 (▲), 1:10 (□), 1:5 (◊) and 1:2 (▼). (C) The effect of Hsp90 on the self-association of G46S-hPAH at different concentrations (expressed as molar ratios of chaperone:G46S-hPAH fusion protein): 0:1 (●), 1:20 (▲), 1:10 (□),1:5 (◊) and 1:2 (▼). (D) The effect of a pharmacological chaperone on the time-course of the self-association. The data points represent G46S-hPAH in the absence of any added compound (●), in the presence of 0.83% DMSO (▲) or of 100 μM 3-amino-2-benzyl-7-nitro-4-(2-quinolyl)-1,2-dihydroisoquinolin-1-one (in 0.83% DMSO) (■). The self-association reactions were performed at standard assay conditions (0.74 mg ml^{-1} fusion protein (7.85 μM monomer), 5.0 μg ml^{-1} factor Xa, 20 mM Na-Hepes, 0.1 M NaCl, pH 7.0 and 25 °C). Some data points were omitted for clarity. Error bars represent mean ± SD, ($n = 3$).

3.12. Binding of thioflavin-T and ANS

Thioflavin-T (ThT) is a dye that when bound to amyloid fibrils displays an enhanced fluorescence at 482 nm, but nonspecific binding to some non-amyloid proteins has also been reported [23]. Binding of ThT to MBP-WT-hPAH results in a fluorescence enhancement (ΔThT) beyond that of MBP alone, but did not significantly increase ($P = 0.13$) upon cleavage by factor Xa (Fig. 8A). The MBP-G46S-hPAH fusion protein revealed a significantly higher ΔThT-value than MBP-WT-hPAH ($p < 0.01$), and factor Xa cleavage further increased the fluorescence enhancement ($p < 0.01$). About 50% of the total ΔThT-value (at 3 h) was observed during the lag period (~42 min) in which no light scattering (and fibril formation) was observed (Fig. 8B). Moreover, during the period of exponential increase in light scattering the ΔThT represented only 37% of the total fluorescence response. Thus, the ThT fluorescence enhancement of G46S-hPAH *vs* the WT-hPAH protein is dominated by the cleavage of the fusion protein and a related conformational change.

ANS is a spectroscopic probe that has affinity for hydrophobic clusters which are not tightly packed in a fully folded structure, or become exposed in partially unfolded structures [44]. ANS binds to G46S-hPAH fusion protein (Fig. 8C, *trace* 5) with an increase in the fluorescence intensity and a maximum at ~478 nm (blue shift). Since this fluorescence response is higher than that observed for the WT-hPAH fusion protein (Fig. 8C, *trace* 3), the mutant form has more hydrophobic clusters exposed than the WT-hPAH. However, after cleavage the fluorescence intensity of the mutant form G46S-hPAH (Fig. 8C, *trace* 7) is only slightly higher than that of the fusion protein (Fig. 8C, *trace* 5). The MBP fusion partner has a negligible contribution to the ANS fluorescence (Fig. 8C, *trace* 2).

3.13. Self-association of the isolated regulatory domain

To further assess the importance of the R-domain for the self-association of full-length G46S-hPAH, we generated WT and G46S truncated forms including the N-terminal residues 2–120 (R-domain) and examined their oligomeric state as MBP fusion proteins and propensity to self-associate on factor Xa cleavage. On bacterial expression as MBP fusion proteins and affinity purification the WT form was recovered in high yield as a mixture of dimer and monomer (Supplementary Fig. S3A), whereas the recovery of the mutant form was very low with higher-order oligomers as the predominating species (Supplementary Fig. S3B). Moreover, SDS-PAGE revealed that the mutant form was significantly more proteolysed than the WT form (Supplementary Fig. S3A and B, *inset*). On cleavage of the dimeric fusion proteins by factor Xa both proteins self-associate with a similar time-

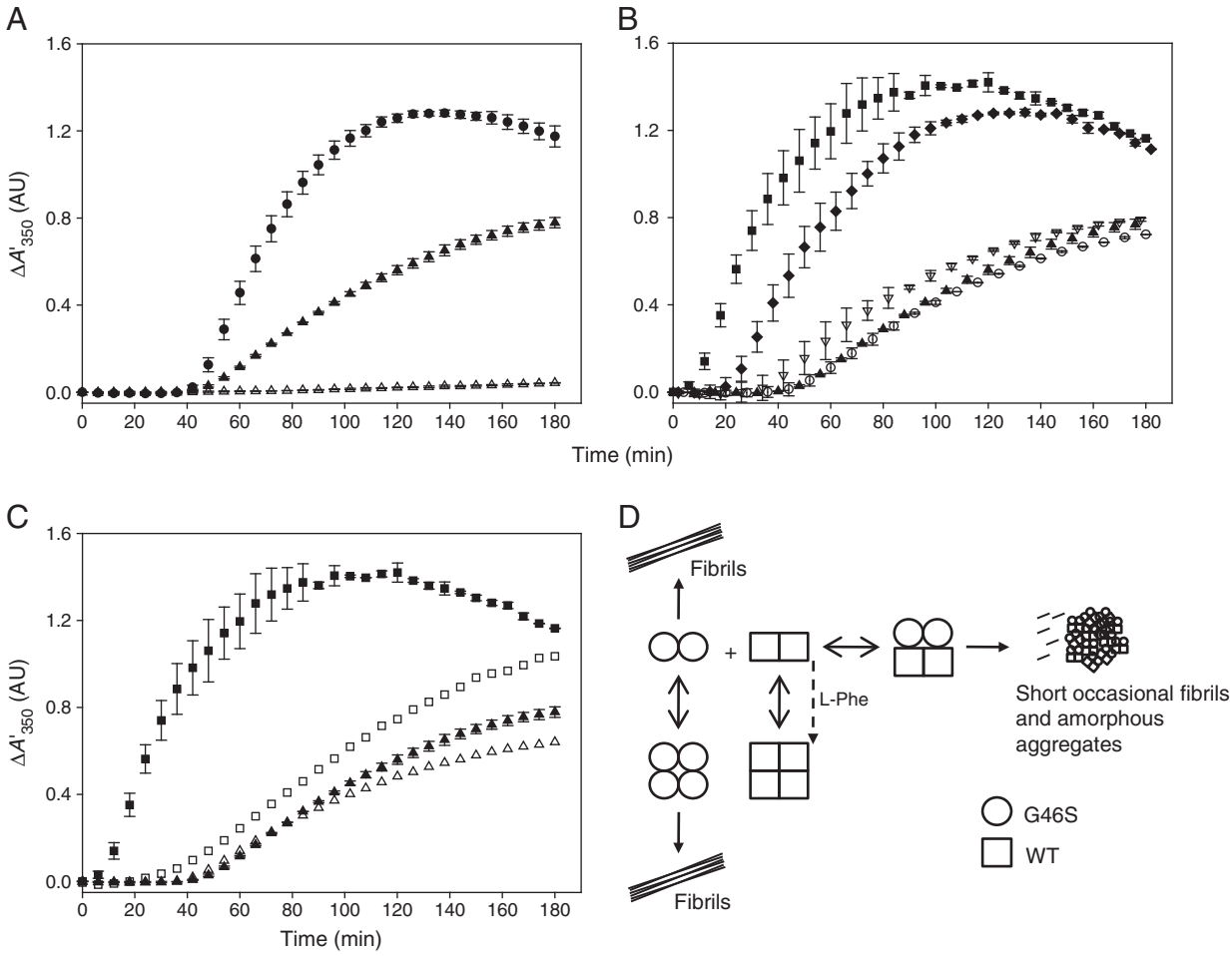

Fig. 7. The self-association of G46S-hPAH dimers and the effect of WT-hPAH dimers and L-Phe. (A) The time-course for the self-association of G46S-hPAH tetramers (●) and dimers (▲) following cleavage of the respective fusion proteins by factor Xa. (Δ) G46S-hPAH dimer fusion protein in the absence of factor Xa. (B) The self-association of G46S-hPAH dimers in the absence of any added protein (▲), and in the presence of a 5-fold molar excess (5×) of WT-hPAH dimer (■), or of 5×ΔC24-hPAH dimer (▽), or of 5×T427P-hPAH dimer (♦) or of 5×ovalbumin (○). (C) The effect of L-Phe on the self-association of G46S-hPAH dimers in the absence and presence of WT-hPAH dimers. G46S-hPAH dimers in the absence of any added protein and L-Phe (▲) or with 1 mM L-Phe (Δ); G46S-hPAH dimers in the presence of a 5-fold molar excess of WT-hPAH dimers with no L-Phe (■) or with 1 mM L-Phe (□). (D) Schematic presentation of the G46S-WT homo- and heterotetramer formation. The reactions in (A–C) were performed at standard assay conditions (0.74 mg ml^{-1} fusion protein, 5.0 μg ml^{-1} factor Xa, 20 mM Na-Hepes, 0.1 M NaCl, pH 7.0 and 25 °C) and the WT-hPAH, ΔC24-hPAH and T427P-hPAH enzyme forms were added as already factor Xa cleaved forms. Some data points were omitted for clarity. Error bars represent mean ± SD, ($n = 3$).

course, including a lag period and an exponential phase of increasing light scattering (Fig. 8D). Self-association of the WT protein was inhibited by both substrates (L-Phe > BH_4), whereas self-association of the G46S mutant R-domain remained unaffected. In both conditions the L-Phe substrate had no effect on the cleavage by factor Xa (Supplementary Fig. S3C and D). The formation of higher-order oligomers gave only a minor enhancement of the ThT fluorescence (Fig. 8A) and no fibrils were detected on EM (data not shown).

3.14. Ultrastructure of G46S-hPAH polymers

In order to get information on the structure of the higher-order oligomers that are formed after cleavage of the G46S-hPAH fusion protein, negative staining EM was performed. For the WT-hPAH no significant difference was observed in the EM pattern when comparing time points 0 and 180 min (data not shown). By contrast, the G46S-hPAH (Fig. 9A–E) revealed a variety of higher-order structures in a time-dependent fashion. At the end of the delay period small clusters of higher-order oligomeric structures of tetrameric G46S-hPAH were observed (Fig. 9B), followed in time by the appearance of linear polymers (Fig. 9C) (correlating with increased light scattering). These fibrils can bundle together and form branches thereby forming extensive network structures (Fig. 9D). EM also revealed that some of the long fibrils display an apparent twisted configuration (Fig. 9E). Using high magnification images (*inset* of panel Fig. 9E and Supplementary Fig. S4) the diameters of the fibrils were determined as ~145 Å (the narrowest region) and ~300 Å (the broadest region), using a correction of 15% for the flattening on the electron microscope grid [45]. Interestingly, dimeric G46S-hPAH also generates fibrils with a pronounced tendency to network formation (Fig. 9D), which is inhibited by a 5-fold molar excess of WT-hPAH dimer (Fig. 9F). Additionally, the pharmacological chaperone 3-amino-2-benzyl-7-nitro-4-(2-quinolyl)-1,2-dihydroisoquinolin-1-one inhibits the formation of fibrils by tetrameric G46S-hPAH (Fig. 9G).

4. Discussion

4.1. Self-association of G46S-hPAH in vitro

The isolated tetrameric/dimeric MBP-$(pep)_{Xa}$-G46S-hPAH fusion protein is recovered in a soluble metastable form, stabilized by MBP as a chaperone. When cleaved by the restriction protease factor Xa the released free enzyme is destabilized and forms different types of higher-order oligomers and polymers (fibrils), as determined by

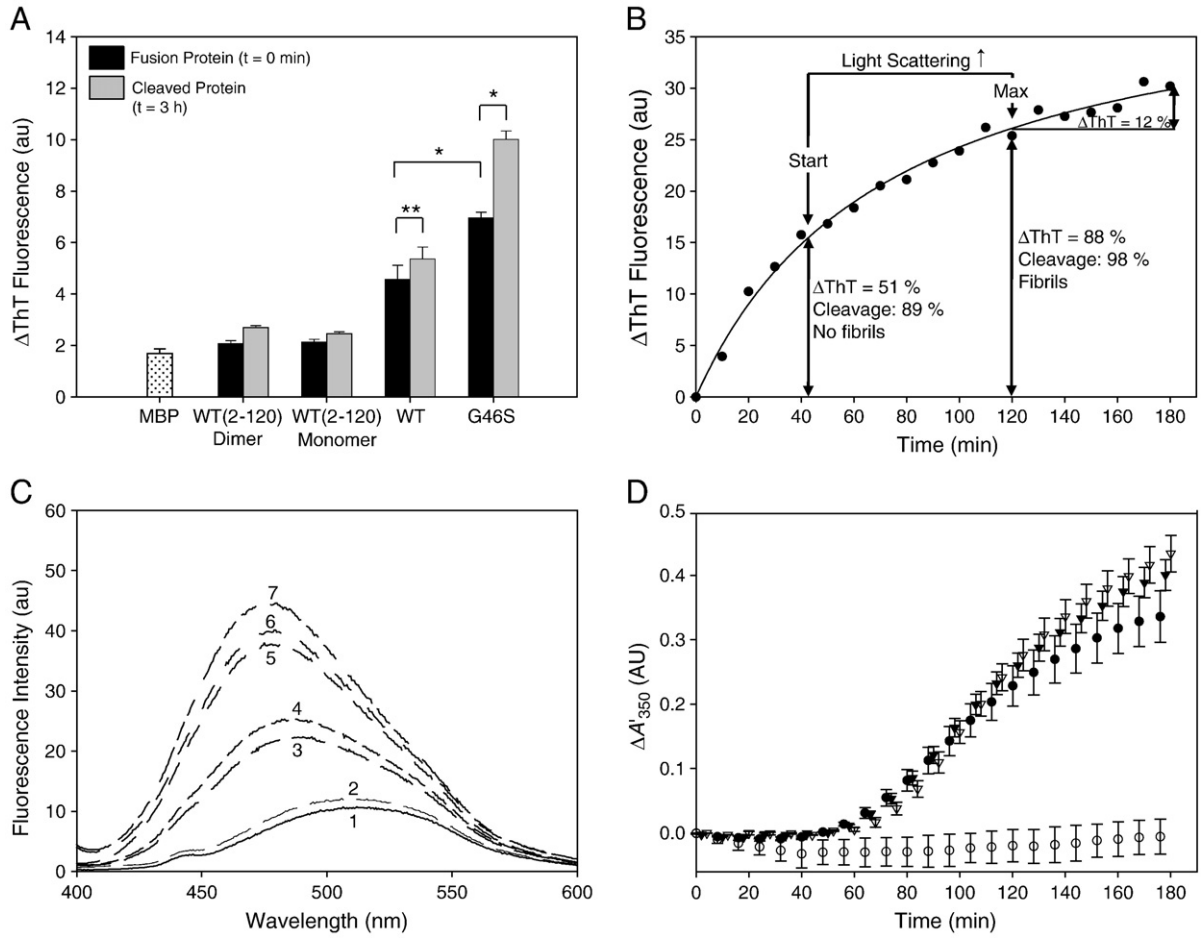

Fig. 8. The binding of thioflavin-T (ThT) and ANS. The binding of ThT and ANS to the uncleaved and cleaved MBP fusion proteins of truncated (residues 2–120, R-domain) and full-length forms of WT and G46S mutant hPAH. (A) ThT fluorescence enhancement (ΔThT) was measured on samples at the beginning of the cleavage reaction of the respective fusion proteins by factor Xa and at the end point ($t = 3$ h). The response was normalized by subtracting the background fluorescence of ThT and light scattering contribution, and the values represent means ± SD of three independent experiments (*$P<0.01$, **$P=0.13$). (B) Time-course of the ThT fluorescence enhancement following cleavage of the MBP-G46S-hPAH, including the lag phase (~42 min) and the exponential self-association (78 min), as measured by light scattering and EM (78 min). The start and maximum of light scattering from Fig. 4B is indicated, as well as the change in ThT fluorescence (ΔThT) at selected time points, with the percentage of cleavage specified (Fig. 4A). (C) ANS fluorescence emission spectra observed during the cleavage of MBP-G46S-hPAH fusion protein by factor Xa, i.e. at $t = 0$ min (*trace* 5), at t~42 min (*trace* 6) and at $t = 3$ h (*trace* 7). The corresponding spectra for the cleavage of MBP-WT-hPAH fusion protein are shown for comparison at $t = 0$ min (*trace* 3) and $t = 3$ h (*trace* 4). The MBP protein was used as a control (*trace* 2) and the emission spectrum of buffer with ANS is shown (*trace* 1). The excitation wavelength was 385 nm. (D) The self-association of a truncated form (residues 2–120, R-domain) of WT-hPAH and its G46S mutant form and the effect of the substrate (L-Phe). The time-course of the self-association of WT-hPAH (2–120) dimeric protein following cleavage of the fusion protein by factor Xa in the absence (●) and presence of 150 μM L-Phe (○); G46S-hPAH (2–120) dimer fusion protein following cleavage by factor Xa in the absence (▼) and presence of 150 μM L-Phe (▽). The assays were performed at standard assay conditions and error bars represent mean ± SD, $n = 3$ independent experiments.

light scattering (Fig. 4B) and negative staining EM (Fig. 9B–E). The formation of polymers involves at least three elementary processes: (i) the cleavage of the fusion protein with release of the free enzyme tetramer/dimer,

$$\begin{array}{l} \mathrm{MBP{-}(pep)_{Xa}{-}G46S{-}hPAH} \\ \quad\quad \downarrow \text{ Factor Xa} \\ \mathrm{G46S{-}hPAH + MBP} \end{array} \quad (1)$$

and (ii) self-association with the formation of higher-order oligomers/short polymers [$(\mathrm{G46S\text{-}hPAH})_n$], detectable by EM (Fig. 9B) and to some extent by light scattering at 350 nm,

$$\begin{array}{l} \mathrm{n{\cdot}G46S{-}hPAH} \\ \quad\quad \downarrow \\ \mathrm{(G46S{-}hPAH)_n} \end{array} \quad (2)$$

and (iii) the autocatalytic formation of larger structures [$(\mathrm{G46S\text{-}hPAH})_{m\cdot n}$], detectable by light scattering and EM (Fig. 9C and E),

$$\begin{array}{l} \mathrm{m{\cdot}(G46S{-}hPAH)_n} \\ \quad\quad \downarrow \\ \mathrm{(G46S{-}hPAH)_{m{\cdot}n}} \end{array} \quad (3)$$

On cleavage, the light-scattering *versus* time profile (Fig. 4B) can be divided into a delay period (lag phase) and a growth phase with an autocatalytic formation of higher-order oligomers/polymers that is expressed as $\Delta A'_{350}/\Delta t$ in the relatively linear part of the light scattering increase. At the end point a decrease in light scattering was observed at acidic pH, low ionic strength and temperature >15 °C, caused by the sedimentation of protein at 1 *g*. By comparing the time-course for the cleavage (Fig. 4A) with the delay time (Fig. 4B), it can be concluded that the cleavage is not rate-limiting in the overall reaction leading to the formation of hPAH polymers, most clearly seen at a low temperature (Supplementary Fig. S1B and Table 2). The delay time

and the rate $\Delta A'_{350}/\Delta t$ were both found to be very sensitive to pH, neutral salt ionic strength and temperature (Fig. 5 and Table 2). Moreover, the experimental conditions which favor a short delay time also promote a high rate of the autocatalytic process.

4.2. The effects of chaperones

Since the first report on PKU patients responding to oral administration of BH_4 by lowering their blood Phe levels [46], the cofactor has been successfully used for the long-term treatment of HPA patients as an alternative to dietary treatment [47,48]. Based on the BIOPKUdb database (www.bh4.org/BH4DatabasesBiopku.asp) [48] BH_4-responsiveness is expected in about 50% of all patients with PAH deficiency [48]. Interestingly, the responsive mutations are preferentially located to the R-domain, possibly related to its structural and physico-chemical properties (see below), and the effect on its stability by the specific interaction with the 1′,2′-dihydroxypropyl side-chain of BH_4, when bound at the active site of WT-hPAH [16,37]. A positive clinical response to BH_4 has been reported even in a patient with severe PKU and the genotype G46S/S303A [47], but it was concluded that the S303A allele was responsible for the observed decrease in plasma Phe level caused by oral BH_4. The present *in vitro* study (Table 2) further supports the conclusion that the G46S allele is non-responsive to BH_4.

Due to the mutant selectivity and the high cost of BH_4 alternative pharmacological chaperones have been explored. A recent screening of over 1000 pharmacological agents has identified a small-molecule binder (3-amino-2-benzyl-7-nitro-4-(2-quinolyl)-1,2-dihydroisoquinolin-1-one) that efficiently enhances the thermal stability of WT-PAH and misfolded mutant forms in the R-domain (I65T and R68S), and significantly increases the activity and steady-state PAH protein levels in transiently transfected cells [41]. Here we have found that this small-molecule binder, used at a comparable concentration (100 μM), partly inhibits the self-association of G46S-hPAH, as measured by light scattering (Fig. 6D) and completely inhibits the fibril formation (Fig. 9G).

Glycerol and trimethylamine *N*-oxide (TMAO) have been shown to correct folding/assembly defects of some neurodegenerative and metabolic conformational disorders [49–53]. In this study glycerol had a protective effect, with a delayed lag phase and decreased $\Delta A'_{350}/\Delta t$ value, whereas TMAO promoted the self-association (Table 2). A similar promotive effect was observed for (−)-epigallocatechin gallate (EGCG) (Table 2), the major polyphenol in green tea that was recently shown to inhibit the fibrillogenesis of amyloidogenic polypeptides [54].

4.3. The self-association of G46S-hPAH generates non-amyloid fibrils

With reference to the ThT fluorescence response (Fig. 8A and B) and the ultrastructures observed by EM (Fig. 9), three lines of evidence point to the formation of non-amyloid fibrils. First, in the self-association of G46S-hPAH the initial part (~51%) of the hyperbolic time-course for ThT fluorescence enhancement occurs in the lag phase (~42 min) where no increase in light scattering or formation of fibrils was observed. In the self-association of proteins forming amyloid-like fibrils the ThT fluorescence enhancement is related to the fibril formation [55]. Thus, the initial fluorescence enhancement of G46S-hPAH is related to the main cleavage of the fusion protein (~89%), presumably reflecting a conformational change in its R-domain, since no fluorescence enhancement was observed on cleavage of the WT-hPAH fusion protein (Fig. 8A). Such unspecific binding of ThT has been observed for some other proteins [23,55]. In addition, studies on amyloid-like peptides revealed a poor correlation between ThT fluorescence enhancement and the formation of amyloid-like structures [56]. Secondly, the ΔThT value increased by only 37% during the autocatalytic formation of fibrils (Fig. 8B), partly explained by the residual cleavage of the fusion protein. Thirdly, the fibrils generated by G46S-hPAH are highly branched (Fig. 9 and Supplementary Fig. S4A) forming networks, and the diameters of individual fibrils range from ~145 to 300 Å, whereas amyloid and amyloid-like fibrils appear by EM as rigid, nonbranching structures from ~60 to 130 Å in diameter [57].

The self-association of G46S-hPAH demonstrates some apparent similarities with that of sickle cell hemoglobin (deoxy-HbS). Deoxy-HbS and G46S-hPAH are both misfolded tetrameric proteins, and their self-association is caused by mutations affecting a single surface exposed amino acid (E6V in the β-chain of HbS and G46S in the R-domain of hPAH). The two mutant proteins also display similar kinetic patterns of the self-association process, as measured by light scattering, and they polymerize into a number of ultrastructures as a function of time, initiated by factor Xa cleavage of MBP-G46S-hPAH and by deoxygenation of HbS, respectively [58]. The G46S-hPAH fibrils and those derived from deoxy-HbS also share common properties. At the present resolution (160,000×) the typical fibrillar structures formed by tetrameric G46S-hPAH (Fig. 9E, *inset* and Supplementary Fig. S4A) show the above described periodic variation in apparent diameter, i.e. from ~145 Å (the narrowest region) to ~300 Å (the broadest region). Some of the structures have the appearance of twisted fibrils (Fig. 9C and Supplementary Fig. S4A). By comparison, the corresponding dimensions of the deoxy-HbS fibrils were reported to be 180 and 230 Å [45,59]. However, the self-association of the two proteins involves different molecular mechanisms.

4.4. Structural insight into the self-association of G46S-hPAH

In WT-PAH the R-domain has some unique structural and physico-chemical properties, which may explain why mutations in this domain affect the stability of the enzyme. First, the 3D structure [34] has demonstrated an overall high crystallographic *B*-factor of the R-domain (Fig. 2B). In the full-length enzyme the R-domain is also characterized by a particularly low thermal stability, as compared to the C-domain [60,61]. The R-domain is partly stabilized by its interaction with the 1′,2′-dihydroxypropyl side-chain of the pterin cofactor BH_4 when bound at the active site [16,37]. Secondly, by using the TANGO algorithm for sequence-dependent prediction of the propensity to aggregate [62], the β1-strand (residues I35–L41) and the β2-strand (residues E76–T81) were predicted to promote aggregation, whereas the G46S substitution did not change this prediction. However, since the WT-hPAH tetramer/dimer, in contrast to the G46S-hPAH tetramer/dimer, does not self-associate at standard experimental conditions (Fig. 4B), the predicted aggregation propensity cannot explain the difference. Of more importance is the prediction (Fig. 2C) that the G46S mutation results in an extension of α-helix 1 by four residues. Such a change of the C_α backbone conformation and the α–β sandwich structure of the WT enzyme may promote new intermolecular contacts and self-association via the mutually misfolded regions of their R-domains (Supplementary Fig. S4B). Thirdly, the inhibitory effect of phosphorylation of Ser16 (Fig. 6A) also indicates that the C_α backbone conformation of the R-domain is important for the self-association process. Moreover, MD simulations of WT-hPAH have revealed that this phosphorylation

Fig. 9. Electron micrographs of negatively stained G46S-hPAH before and after cleavage of its MBP fusion protein by factor Xa. (A) The tetrameric MBP-G46S-hPAH fusion protein before cleavage, and (B) after cleavage for 42 min (~ the end of lag phase, as shown in Fig. 4B), and (C) for 2 h (~ maximum light scattering, Fig. 4B). (D and F) The result of cleavage of the dimeric MBP-G46S-hPAH in the absence (D) and presence of a 5-fold molar excess of dimeric WT-hPAH (F). (E) The twisted fibrils and a single fibril of tetrameric G46S-hPAH (*inset*) at high resolution. (G) The effect of the pharmacological chaperone 3-amino-2-benzyl-7-nitro-4-(2-quinolyl)-1,2-dihydroisoquinolin-1-one on the self-association of tetrameric G46S-hPAH at $t = 3$ h of cleavage. The proteins were negatively stained with aqueous uranyl acetate and analyzed in Jeol 1230 Electron Microscope operated at 80 kV. Short fibrils in B and F are indicated by arrows. Scale bars: 500 nm (A–C, F and G), 1 μm (D) and 100 nm (E).

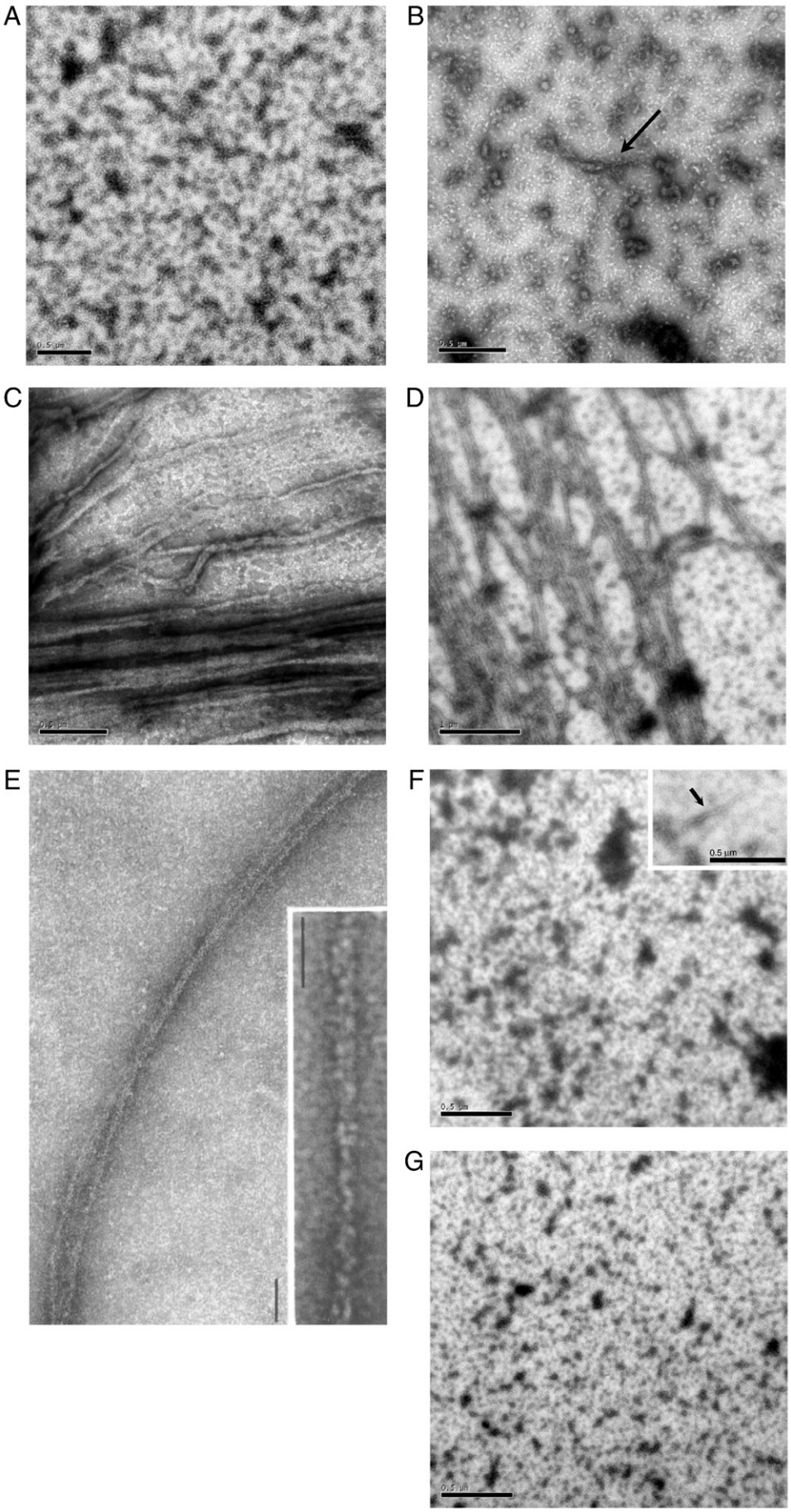
A
B
C
D
E
F
G
0.5 µm

causes local conformational changes in the autoregulatory sequence (residues 1–33) [16], and FT-IR spectroscopy of the isolated WT R-domain (residues 2–110) has suggested that it induces an apparent increase in the α-helix content [15]. In addition, deamidation of labile asparagine residues in hPAH — notably Asn32 in the R-domain [63] — also affects the G46S-hPAH self-association. Accordingly, the non-deamidated form of G46S-hPAH (2 h induction) showed a higher tendency to self-associate (with a slightly shorter lag phase and a higher rate of self-association), as compared with the deamidated G46S-hPAH form (24 h induction) (Supplementary Fig. S5). Studies on the isolated R-domain (residues 2–120) (Fig. 8D) further emphasize the importance of its conformation in the self-association process. The dimeric and monomeric forms of this truncated protein display a high propensity to self-associate, even in their WT forms, and the G46S mutation slightly increased this propensity.

The finding that the G46S-hPAH dimer also self-associates beyond the tetrameric state, although at a slower rate than the tetramer (Fig. 7A), requires a special comment. Since the WT-PAH exists in a two-state TM ↔ DM equilibrium [8], it is likely that a similar equilibrium exists for the G46S-hPAH mutant. As seen from Fig. 7B, the presence of a superstoichiometric amount of WT dimer during the cleavage of the MBP-G46S-hPAH dimer supports the formation of hybrid WT–G46S heterotetramer, which self-associates at an enhanced rate compared to G46S-hPAH dimer alone. In this case, however, EM studies demonstrated predominantly amorphous aggregates (Figs. 7D and 9F). Based on these results one might expect that in a heterozygous WT/G46S genotype, the fraction of the G46S-hPAH dimer could form WT–G46S heterotetramers that would promote the self-association and the degradation of the WT subunit. However, in WT-hPAH the TM ↔ DM equilibrium is shifted towards the tetrameric form in the presence of L-Phe [17], whereas in G46S-hPAH the TM ↔ DM equilibrium is less responsive to L-Phe, as there is only a minor enhancement of the self-association of the G46S-hPAH dimer in the presence of 1 mM L-Phe (Fig. 7C). Because the two equilibria respond differently to L-Phe, the WT-hPAH dimer will form WT-hPAH tetramers in the presence of L-Phe and will not be available to form WT–G46S heterotetramers that were responsible for the observed enhancement of the self-association of the G46S-hPAH dimer in the presence of the WT-hPAH dimer. The concentration of L-Phe (50–100 μM in the hepatocyte of normal individuals), depends on the metabolic state and extracellular concentration of L-Phe in the blood [64]. In a homozygous G46S phenotype the L-Phe will not have any significant effect on the TM ↔ DM equilibrium (Fig. 7C). Thus, our results suggest that the self-association of G46S-hPAH is favored by the tetrameric structure, and the propensity of the G46S-WT hybrids to self-associate is defined by the conformational state of the G46S subunits.

The relation between self-association of a protein, its fundamental physico-chemical intrinsic properties (e.g. hydrophobicity, secondary structure propensity, charge and hydrophobic/ hydrophilic patterns), and extrinsic factors have been extensively studied [65–67]. All the data presented in this study (pH, ionic strength, phosphorylation state of Ser16) indicate that the net charge of the protein, or its R-domain, is a main modulator of the self-association of G46S-hPAH *in vitro*, as measured by light scattering (Table 2).

4.5. Potential in vivo implications

In our previous transfection studies in HEK293 cells the expression level of G46S-hPAH was only ~3% of WT-hPAH (immunoreactive PAH protein) when related to the mRNA levels, compatible with the severe form of PKU observed in the homozygous patient [12]. The present *in vitro* studies offer an explanation for the accelerated degradation of the mutant protein, although we do not know how G46S self-associates in the complex and crowded macromolecular environment of the hepatocyte. Since there is no reported link between any liver dysfunction or amyloid pathology and severe forms of PKU, it is unlikely that self-associated, misfolded hPAH mutant proteins exert a toxic effect on the liver. Based on inhibition of the self-association of tetrameric G46S-hPAH *in vitro* by substoichiometric concentrations of the heat-shock protein Hsp90 (Fig. 6C), and to some extent by Hsp70/Hsp40 (Fig. 6B), the mutant is a likely client protein of the molecular chaperone systems *in vivo*, as observed for the chaperonins GroESL on co-expression with several PKU/HPA mutant proteins in *E. coli* [5,68,69]. However, the accelerated degradation of G46S-hPAH in HEK293 cells [12] indicates that the physiological level of chaperones in these cells (and in hepatocytes) is not sufficient to rescue this misfolded protein. Therefore, the main question to be answered relates to the mechanism by which G46S-hPAH and related misfolded and unstable hPAH proteins are degraded *in vivo*. Although WT-hPAH is poly/multi-ubiquitinated *in vitro* [70], no significant stabilizing effect of proteasome inhibitors have been observed in cases of selected missense mutations [4]. Therefore, the accelerated turnover observed upon their expression in eukaryotic cells may be explained by an alternative quality control mechanism. Previous studies on the turnover of WT-hPAH in cultured hepatoma cells gave an estimated half-life of 8.2 h [71], i.e. similar to that of a number of other cytosolic liver proteins with a slow turnover, which are considered to be degraded by autophagosome pathway [72]. Intracellular self-association of a number of misfolded proteins has been connected with the formation of aggresomes, which are ultimately degraded by autophagolysosomes, in a process that also involves ubiquitination [73].

4.6. Relevance for the study of misfolding PKU/HPA mutations

The tetrameric form of recombinant WT-hPAH has a small margin of stability. Even a low concentration of a mild denaturant (urea) allows the enzyme to explore a range of different structural states and induces its self-association [74]. Therefore, it is not unexpected to find a high frequency of misfolding hPAH mutations associated with PKU/HPA, resulting in a variety of molecular subtypes showing different conformational and stability properties. Thus, these misfolded hPAH proteins represent a phenotypically heterogeneous group which often has a propensity to self-associate and to form higher-order oligomers when overexpressed in prokaryotic systems, and are rapidly degraded when expressed in eukaryotic cells. Upon overexpression in *E. coli*, these misfolded mutant proteins are often stabilized by MBP as a fusion partner, and the metastable fusion proteins are frequently used in *in vitro* studies to elucidate the molecular basis of the functional impairment in PAH deficiency [9,68,69]. However, the present study shows that the physico-chemical properties of the metastable MBP-mutant-hPAH fusion protein are not representative for those of the mutant protein. Our current experimental approach, therefore, should be a useful supplement in systematic *in vitro* studies of misfolded PAH/HPA-associated mutant proteins, as well as for the assessment of the capability of molecular and pharmacological chaperones to prevent their self-association and stabilize their native states. This experimental approach may also provide valuable mechanistic insights into the frequently observed and poorly understood compound heterozygous forms of PKU/HPA [75].

Acknowledgements

This work was supported by Fundação para a Ciência e a Tecnologia, Portugal, grant SFRH/BD/19024/2004 and the University of Bergen, Norway. We thank Ali Sepulveda Munõz for French press preparation of recombinant protein and Randi M. Svebak for expert technical assistance.

Appendix A. Supplementary data

Supplementary data to this article can be found online at doi:10.1016/j.bbadis.2010.09.015.

References

[1] L. Hoang, S. Byck, L. Prevost, C.R. Scriver, PAH Mutation Analysis Consortium Database: a database for disease-producing and other allelic variation at the human PAH locus, Nucleic Acids Res. 24 (1996) 127–131.

[2] C.R. Scriver, P.J. Waters, Monogenic traits are not simple: lessons from phenylketonuria, Trends Genet. 15 (1999) 267–272.

[3] T. Flatmark, P.M. Knappskog, E. Bjørgo, A. Martínez, Molecular characterization of disease related mutant forms of human phenylalanine hydroxylase and tyrosine hydroxylase, in: W. Pfleiderer, H. Rokos (Eds.), Chemistry and Biology of Pteridines and Folates, vol. 8, Blackwell Science, Berlin, 1997, pp. 503–508.

[4] P.J. Waters, How PAH gene mutations cause hyper-phenylalaninemia and why mechanism matters: insights from in vitro expression, Hum. Mutat. 21 (2003) 357–369.

[5] N. Gregersen, P. Bross, B.S. Andresen, C.B. Pedersen, T.J. Corydon, L. Bolund, The role of chaperone-assisted folding and quality control in inborn errors of metabolism: protein folding disorders, J. Inherit. Metab. Dis. 24 (2001) 189–212.

[6] E. Bjørgo, P.M. Knappskog, A. Martinez, R.C. Stevens, T. Flatmark, Partial characterization and three-dimensional-structural localization of eight mutations in exon 7 of the human phenylalanine hydroxylase gene associated with phenylketonuria, Eur. J. Biochem. 257 (1998) 1–10.

[7] H. Erlandsen, R.C. Stevens, The structural basis of phenylketonuria, Mol. Genet. Metab. 68 (1999) 103–125.

[8] T. Flatmark, R.C. Stevens, Structural insight into the aromatic amino acid hydroxylases and their disease-related mutant forms, Chem. Rev. 99 (1999) 2137–2160.

[9] S.W. Gersting, K.F. Kemter, M. Staudigl, D.D. Messing, M.K. Danecka, F.B. Lagler, C.P. Sommerhoff, A.A. Roscher, A.C. Muntau, Loss of function in phenylketonuria is caused by impaired molecular motions and conformational instability, Am. J. Hum. Genet. 83 (2008) 5–17.

[10] J.D. Fox, R.B. Kapust, D.S. Waugh, Single amino acid substitutions on the surface of *Escherichia coli* maltose-binding protein can have a profound impact on the solubility of fusion proteins, Protein Sci. 10 (2001) 622–630.

[11] R.B. Kapust, D.S. Waugh, *Escherichia coli* maltose-binding protein is uncommonly effective at promoting the solubility of polypeptides to which it is fused, Protein Sci. 8 (1999) 1668–1674.

[12] H.G. Eiken, P.M. Knappskog, J. Apold, T. Flatmark, PKU mutation G46S is associated with increased aggregation and degradation of the phenylalanine hydroxylase enzyme, Hum. Mutat. 7 (1996) 228–238.

[13] A.L. Pey, F. Stricher, L. Serrano, A. Martinez, Predicted effects of missense mutations on native-state stability account for phenotypic outcome in phenylketonuria, a paradigm of misfolding diseases, Am. J. Hum. Genet. 81 (2007) 1006–1024.

[14] F.F. Miranda, K. Teigen, M. Thorolfsson, R.M. Svebak, P.M. Knappskog, T. Flatmark, A. Martinez, Phosphorylation and mutations of Ser(16) in human phenylalanine hydroxylase. Kinetic and structural effects, J. Biol. Chem. 277 (2002) 40937–40943.

[15] R. Chehin, M. Thorolfsson, P.M. Knappskog, A. Martinez, T. Flatmark, J.L. Arrondo, A. Muga, Domain structure and stability of human phenylalanine hydroxylase inferred from infrared spectroscopy, FEBS Lett. 422 (1998) 225–230.

[16] K. Teigen, A. Martinez, Probing cofactor specificity in phenylalanine hydroxylase by molecular dynamics simulations, J. Biomol. Struct. Dyn. 20 (2003) 733–740.

[17] A. Martinez, P.M. Knappskog, S. Olafsdottir, A.P. Døskeland, H.G. Eiken, R.M. Svebak, M. Bozzini, J. Apold, T. Flatmark, Expression of recombinant human phenylalanine hydroxylase as fusion protein in *Escherichia coli* circumvents proteolytic degradation by host cell proteases. Isolation and characterization of the wild-type enzyme, Biochem. J. 306 (1995) 589–597.

[18] M.M. Bradford, A rapid and sensitive method for the quantitation of microgram quantities of protein utilizing the principle of protein–dye binding, Anal. Biochem. 72 (1976) 248–254.

[19] E. Bjørgo, R.M. de Carvalho, T. Flatmark, A comparison of kinetic and regulatory properties of the tetrameric and dimeric forms of wild-type and Thr427–>Pro mutant human phenylalanine hydroxylase: contribution of the flexible hinge region Asp425-Gln429 to the tetramerization and cooperative substrate binding, Eur. J. Biochem. 268 (2001) 997–1005.

[20] P.M. Knappskog, T. Flatmark, J.M. Aarden, J. Haavik, A. Martinez, Structure/function relationships in human phenylalanine hydroxylase. Effect of terminal deletions on the oligomerization, activation and cooperativity of substrate binding to the enzyme, Eur. J. Biochem. 242 (1996) 813–821.

[21] A.P. Døskeland, A. Martinez, P.M. Knappskog, T. Flatmark, Phosphorylation of recombinant human phenylalanine hydroxylase: effect on catalytic activity, substrate activation and protection against non-specific cleavage of the fusion protein by restriction protease, Biochem. J. 313 (Pt 2) (1996) 409–414.

[22] U.K. Laemmli, Cleavage of structural proteins during the assembly of the head of bacteriophage T4, Nature 227 (1970) 680–685.

[23] R. Eisert, L. Felau, L.R. Brown, Methods for enhancing the accuracy and reproducibility of Congo red and thioflavin T assays, Anal. Biochem. 353 (2006) 144–146.

[24] I. Aukrust, L. Evensen, H. Hollås, F. Berven, R.A. Atkinson, G. Travé, T. Flatmark, A. Vedeler, Engineering, biophysical characterisation and binding properties of a soluble mutant form of annexin A2 domain IV that adopts a partially folded conformation, J. Mol. Biol. 363 (2006) 469–481.

[25] A.P. Døskeland, S.O. Døskeland, D. Øgreid, T. Flatmark, The effect of ligands of phenylalanine 4-monooxygenase on the cAMP-dependent phosphorylation of the enzyme, J. Biol. Chem. 259 (1984) 11242–11248.

[26] V.J. LiCata, N.M. Allewell, Is substrate inhibition a consequence of allostery in aspartate transcarbamylase? Biophys. Chem. 64 (1997) 225–234.

[27] T. Solstad, T. Flatmark, Microheterogeneity of recombinant human phenylalanine hydroxylase as a result of nonenzymatic deamidations of labile amide containing amino acids. Effects on catalytic and stability properties, Eur. J. Biochem. 267 (2000) 6302–6310.

[28] V. Parthiban, M.M. Gromiha, D. Schomburg, CUPSAT: prediction of protein stability upon point mutations, Nucleic Acids Res. 34 (2006) W239–W242.

[29] A. Benedix, C.M. Becker, B.L. de Groot, A. Caflisch, R.A. Bockmann, Predicting free energy changes using structural ensembles, Nat. Methods 6 (2009) 3–4.

[30] E. Lacroix, A.R. Viguera, L. Serrano, Elucidating the folding problem of alpha-helices: local motifs, long-range electrostatics, ionic-strength dependence and prediction of NMR parameters, J. Mol. Biol. 284 (1998) 173–191.

[31] S.C. Flores, K.S. Keating, J. Painter, F. Morcos, K. Nguyen, E.A. Merritt, L.A. Kuhn, M.B. Gerstein, HingeMaster: normal mode hinge prediction approach and integration of complementary predictors, Proteins 73 (2008) 299–319.

[32] H. Erlandsen, F. Fusetti, A. Martinez, E. Hough, T. Flatmark, R.C. Stevens, Crystal structure of the catalytic domain of human phenylalanine hydroxylase reveals the structural basis for phenylketonuria, Nat. Struct. Biol. 4 (1997) 995–1000.

[33] F. Fusetti, H. Erlandsen, T. Flatmark, R.C. Stevens, Structure of tetrameric human phenylalanine hydroxylase and its implications for phenylketonuria, J. Biol. Chem. 273 (1998) 16962–16967.

[34] B. Kobe, I.G. Jennings, C.M. House, B.J. Michell, K.E. Goodwill, B.D. Santarsiero, R.C. Stevens, R.G. Cotton, B.E. Kemp, Structural basis of autoregulation of phenylalanine hydroxylase, Nat. Struct. Biol. 6 (1999) 442–448.

[35] K.T. O'Neil, W.F. DeGrado, A thermodynamic scale for the helix-forming tendencies of the commonly occurring amino acids, Science 250 (1990) 646–651.

[36] C.G. Evans, S. Wisen, J.E. Gestwicki, Heat shock proteins 70 and 90 inhibit early stages of amyloid beta-(1–42) aggregation in vitro, J. Biol. Chem. 281 (2006) 33182–33191.

[37] T. Solstad, A.J. Stokka, O.A. Andersen, T. Flatmark, Studies on the regulatory properties of the pterin cofactor and dopamine bound at the active site of human phenylalanine hydroxylase, Eur. J. Biochem. 270 (2003) 981–990.

[38] C. Aguado, B. Perez, M. Ugarte, L.R. Desviat, Analysis of the effect of tetrahydrobiopterin on PAH gene expression in hepatoma cells, FEBS Lett. 580 (2006) 1697–1701.

[39] B. Perez, L.R. Desviat, P. Gomez-Puertas, A. Martinez, R.C. Stevens, M. Ugarte, Kinetic and stability analysis of PKU mutations identified in BH4-responsive patients, Mol. Genet. Metab. 86 (Suppl 1) (2005) S11–S16.

[40] C.R. Scriver, The PAH gene, phenylketonuria, and a paradigm shift, Hum. Mutat. 28 (2007) 831–845.

[41] A.L. Pey, M. Ying, N. Cremades, A. Velazquez-Campoy, T. Scherer, B. Thöny, J. Sancho, A. Martinez, Identification of pharmacological chaperones as potential therapeutic agents to treat phenylketonuria, J. Clin. Invest. 118 (2008) 2858–2867.

[42] P. Leandro, C.M. Gomes, Protein misfolding in conformational disorders: rescue of folding defects and chemical chaperoning, Mini Rev. Med. Chem. 8 (2008) 901–911.

[43] A. Martinez, A.C. Calvo, K. Teigen, A.L. Pey, Rescuing proteins of low kinetic stability by chaperones and natural ligands phenylketonuria, a case study, Prog. Mol. Biol. Transl. Sci. 83 (2008) 89–134.

[44] G.V. Semisotnov, N.A. Rodionova, O.I. Razgulyaev, V.N. Uversky, A.F. Gripas, R.I. Gilmanshin, Study of the "molten globule" intermediate state in protein folding by a hydrophobic fluorescent probe, Biopolymers 31 (1991) 119–128.

[45] G.W. Dykes, R.H. Crepeau, S.J. Edelstein, Three-dimensional reconstruction of the 14-filament fibers of hemoglobin S, J. Mol. Biol. 130 (1979) 451–472.

[46] S. Kure, D.C. Hou, T. Ohura, H. Iwamoto, S. Suzuki, N. Sugiyama, O. Sakamoto, K. Fujii, Y. Matsubara, K. Narisawa, Tetrahydrobiopterin-responsive phenylalanine hydroxylase deficiency, J. Pediatr. 135 (1999) 375–378.

[47] M.D. Boveda, M.L. Couce, D.E. Castineiras, J.A. Cocho, B. Perez, M. Ugarte, J.M. Fraga, The tetrahydrobiopterin loading test in 36 patients with hyperphenylalaninaemia: evaluation of response and subsequent treatment, J. Inherit. Metab. Dis. 30 (2007) 812.

[48] M.R. Zurfluh, J. Zschocke, M. Lindner, F. Feillet, C. Chery, A. Burlina, R.C. Stevens, B. Thöny, N. Blau, Molecular genetics of tetrahydrobiopterin-responsive phenylalanine hydroxylase deficiency, Hum. Mutat. 29 (2008) 167–175.

[49] P. Leandro, M.C. Lechner, I. Tavares de Almeida, D. Konecki, Glycerol increases the yield and activity of human phenylalanine hydroxylase mutant enzymes produced in a prokaryotic expression system, Mol. Genet. Metab. 73 (2001) 173–178.

[50] C. Nascimento, J. Leandro, I. Tavares de Almeida, P. Leandro, Modulation of the activity of newly synthesized human phenylalanine hydroxylase mutant proteins by low-molecular-weight compounds, Protein J. 27 (2008) 392–400.

[51] J.L. Song, D.T. Chuang, Natural osmolyte trimethylamine N-oxide corrects assembly defects of mutant branched-chain alpha-ketoacid decarboxylase in maple syrup urine disease, J. Biol. Chem. 276 (2001) 40241–40246.

[52] V.N. Uversky, J. Li, A.L. Fink, Trimethylamine-N-oxide-induced folding of alpha-synuclein, FEBS Lett. 509 (2001) 31–35.

[53] D.S. Yang, C.M. Yip, T.H. Huang, A. Chakrabartty, P.E. Fraser, Manipulating the amyloid-beta aggregation pathway with chemical chaperones, J. Biol. Chem. 274 (1999) 32970–32974.

[54] D.E. Ehrnhoefer, J. Bieschke, A. Boeddrich, M. Herbst, L. Masino, R. Lurz, S. Engemann, A. Pastore, E.E. Wanker, EGCG redirects amyloidogenic polypeptides into unstructured, off-pathway oligomers, Nat. Struct. Mol. Biol. 15 (2008) 558–566.

[55] R. Khurana, C. Coleman, C. Ionescu-Zanetti, S.A. Carter, V. Krishna, R.K. Grover, R. Roy, S. Singh, Mechanism of thioflavin T binding to amyloid fibrils, J. Struct. Biol. 151 (2005) 229–238.

[56] M.I. Ivanova, M.J. Thompson, D. Eisenberg, A systematic screen of beta(2)-microglobulin and insulin for amyloid-like segments, Proc. Natl. Acad. Sci. U. S. A. 103 (2006) 4079–4082.
[57] M.J. Bennett, M.R. Sawaya, D. Eisenberg, Deposition diseases and 3D domain swapping, Structure 14 (2006) 811–824.
[58] F.A. Ferrone, J. Hofrichter, W.A. Eaton, Kinetics of sickle hemoglobin polymerization. I. Studies using temperature-jump and laser photolysis techniques, J. Mol. Biol. 183 (1985) 591–610.
[59] G. Dykes, R.H. Crepeau, S.J. Edelstein, Three-dimensional reconstruction of the fibres of sickle cell haemoglobin, Nature 272 (1978) 506–510.
[60] A.J. Stokka, R.N. Carvalho, J.F. Barroso, T. Flatmark, Probing the role of crystallographically defined/predicted hinge-bending regions in the substrate-induced global conformational transition and catalytic activation of human phenylalanine hydroxylase by single-site mutagenesis, J. Biol. Chem. 279 (2004) 26571–26580.
[61] M. Thorolfsson, B. Ibarra-Molero, P. Fojan, S.B. Petersen, J.M. Sanchez-Ruiz, A. Martinez, L-phenylalanine binding and domain organization in human phenylalanine hydroxylase: a differential scanning calorimetry study, Biochemistry 41 (2002) 7573–7585.
[62] A.M. Fernandez-Escamilla, F. Rousseau, J. Schymkowitz, L. Serrano, Prediction of sequence-dependent and mutational effects on the aggregation of peptides and proteins, Nat. Biotechnol. 22 (2004) 1302–1306.
[63] T. Solstad, R.N. Carvalho, O.A. Andersen, D. Waidelich, T. Flatmark, Deamidation of labile asparagine residues in the autoregulatory sequence of human phenylalanine hydroxylase, Eur. J. Biochem. 270 (2003) 929–938.
[64] A.L. Pey, A. Martinez, The activity of wild-type and mutant phenylalanine hydroxylase and its regulation by phenylalanine and tetrahydrobiopterin at physiological and pathological concentrations: an isothermal titration calorimetry study, Mol. Genet. Metab. 86 (Suppl 1) (2005) S43–S53.
[65] A.K. Buell, G.G. Tartaglia, N.R. Birkett, C.A. Waudby, M. Vendruscolo, X. Salvatella, M.E. Welland, C.M. Dobson, T.P. Knowles, Position-dependent electrostatic protection against protein aggregation, Chembiochem 10 (2009) 1309–1312.
[66] F. Chiti, M. Stefani, N. Taddei, G. Ramponi, C.M. Dobson, Rationalization of the effects of mutations on peptide and protein aggregation rates, Nature 424 (2003) 805–808.
[67] K.F. DuBay, A.P. Pawar, F. Chiti, J. Zurdo, C.M. Dobson, M. Vendruscolo, Prediction of the absolute aggregation rates of amyloidogenic polypeptide chains, J. Mol. Biol. 341 (2004) 1317–1326.
[68] A. Gamez, B. Perez, M. Ugarte, L.R. Desviat, Expression analysis of phenylketonuria mutations. Effect on folding and stability of the phenylalanine hydroxylase protein, J. Biol. Chem. 275 (2000) 29737–29742.
[69] A.L. Pey, L.R. Desviat, A. Gamez, M. Ugarte, B. Perez, Phenylketonuria: genotype–phenotype correlations based on expression analysis of structural and functional mutations in PAH, Hum. Mutat. 21 (2003) 370–378.
[70] A.P. Døskeland, T. Flatmark, Conjugation of phenylalanine hydroxylase with polyubiquitin chains catalysed by rat liver enzymes, Biochim. Biophys. Acta 1547 (2001) 379–386.
[71] R.E. Baker, R. Shiman, Measurement of phenylalanine hydroxylase turnover in cultured hepatoma cells, J. Biol. Chem. 254 (1979) 9633–9639.
[72] J. Kopitz, G.O. Kisen, P.B. Gordon, P. Bohley, P.O. Seglen, Nonselective autophagy of cytosolic enzymes by isolated rat hepatocytes, J. Cell Biol. 111 (1990) 941–953.
[73] V. Kirkin, D.G. McEwan, I. Novak, I. Dikic, A role for ubiquitin in selective autophagy, Mol. Cell 34 (2009) 259–269.
[74] R. Kleppe, K. Uhlemann, P.M. Knappskog, J. Haavik, Urea-induced denaturation of human phenylalanine hydroxylase, J. Biol. Chem. 274 (1999) 33251–33258.
[75] J. Leandro, C. Nascimento, I.T. de Almeida, P. Leandro, Co-expression of different subunits of human phenylalanine hydroxylase: evidence of negative interallelic complementation, Biochim. Biophys. Acta 1762 (2006) 544–550.
[76] P.J. Kraulis, Molscript — a program to produce both detailed and schematic plots of protein structures, J. Appl. Crystallogr. 24 (1991) 946–950.
[77] W.L. Delano, The PyMOL Molecular Graphics System, DeLano Scientific, San Carlos, USA, 2002.

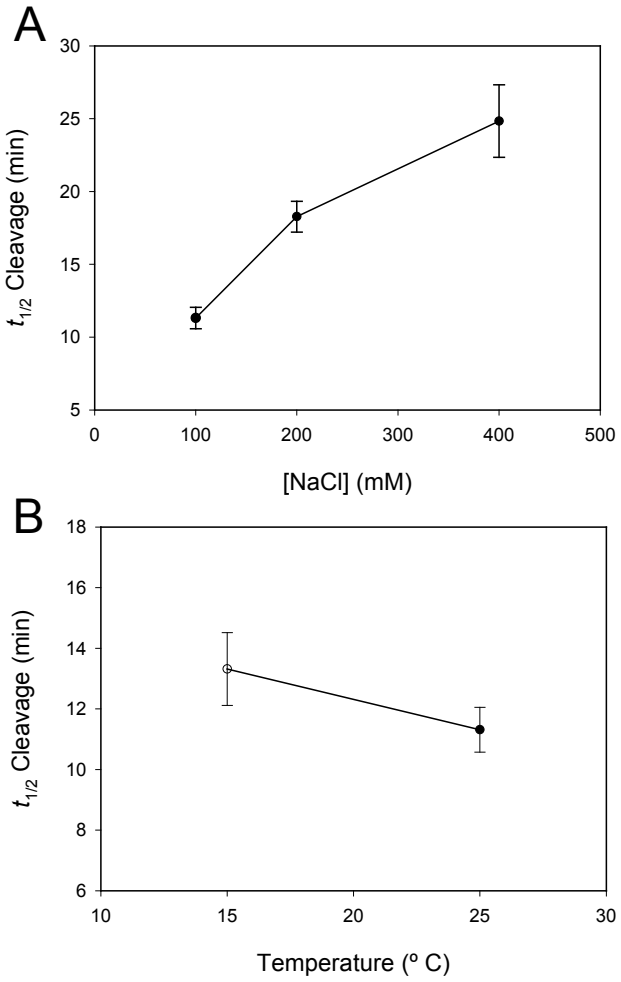

Supplementary Fig. S1. The effect of NaCl concentration (A) and temperature (B) on $t_{1/2}$ cleavage of tetrameric MBP-G46S-hPAH fusion protein by the restriction protease factor Xa. Error bars represent standard mean ± SD.

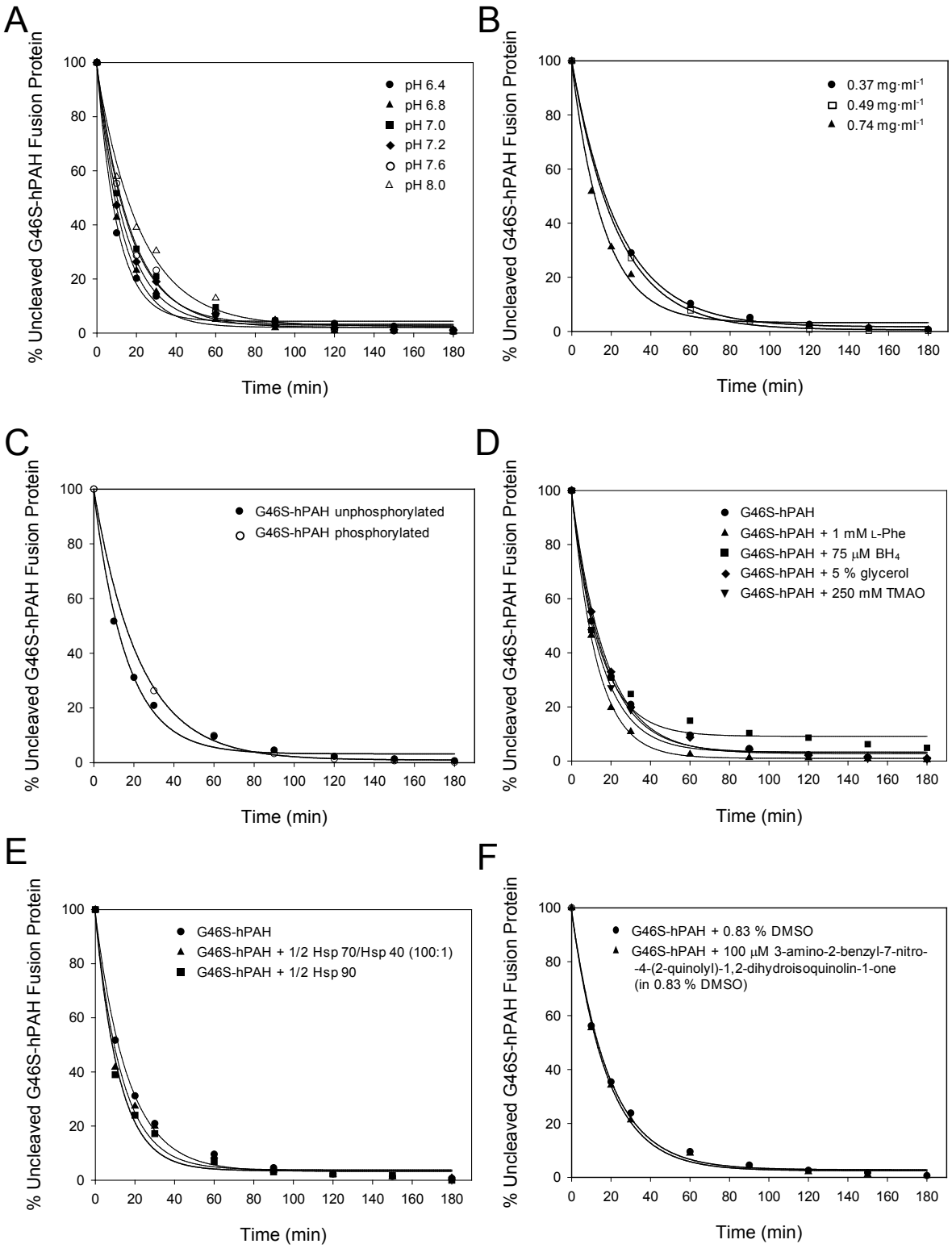

Supplementary Fig. S2. Time-course for the cleavage of tetrameric MBP-G46S-hPAH fusion

protein by the restriction protease factor Xa at different pH values (A) or different fusion protein concentrations (B). In addition, the effects of phosphorylation (C), the presence of substrate (L-Phe), cofactor (BH_4), glycerol and TMAO (D), molecular chaperones (E), and pharmacological chaperones (F) are shown. The data were fitted to a single exponential decay curve. The time-course of cleavage was performed at standard assay conditions (0.74 $mg \cdot ml^{-1}$ fusion protein, 5.0 $\mu g \cdot ml^{-1}$ factor Xa, 20 mM Na-Hepes, 0.1 M NaCl, pH 7.0 and 25 ^{o}C).

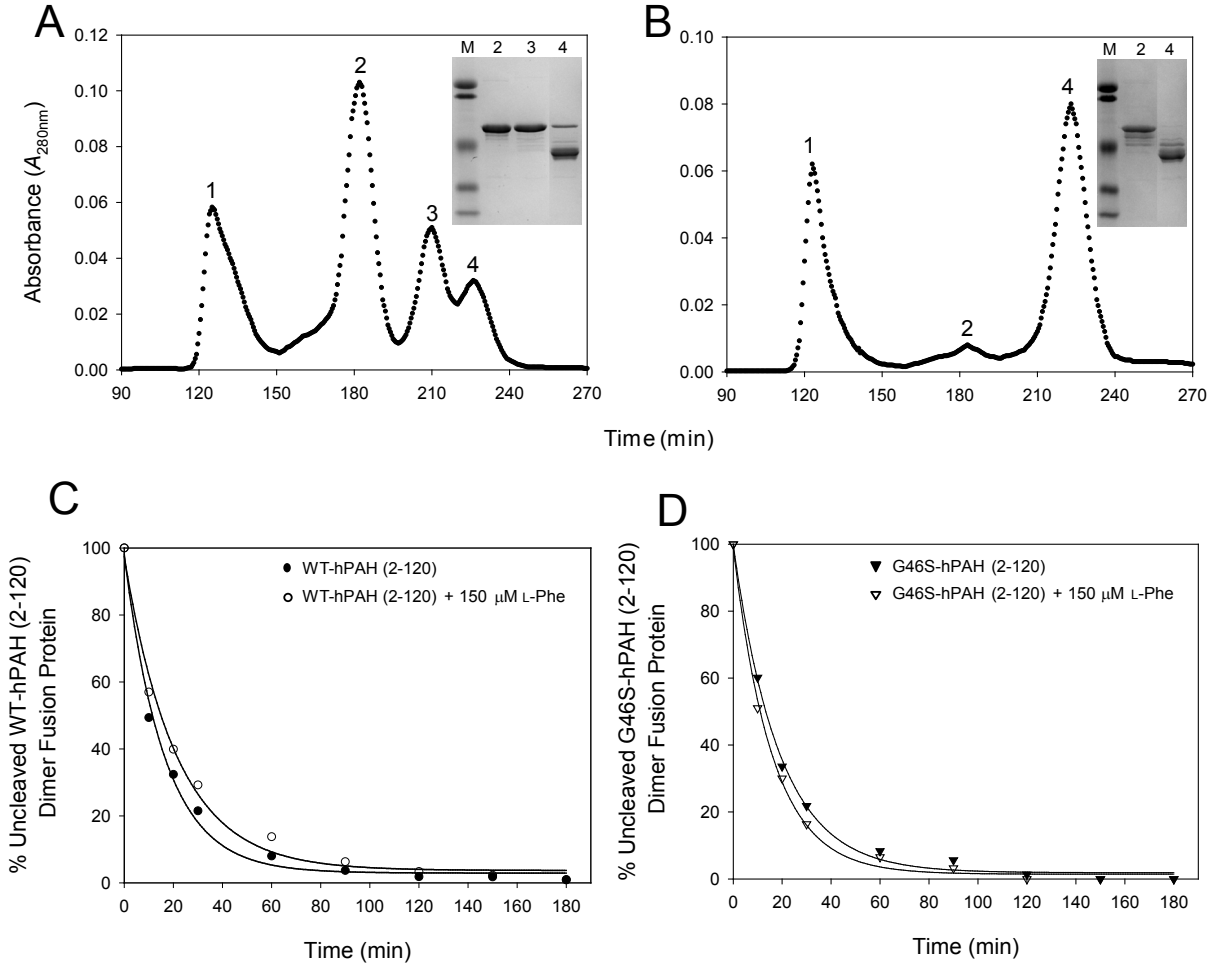

Supplementary Fig. S3. The WT and G46S truncated forms (residues 2-120, R-domain). (A) Size exclusion chromatography of WT-hPAH (2-120) expressed as a MBP fusion protein in *E. coli*. Peak 1, higher-order oligomeric forms (eluted in the void volume); peak 2, dimeric form (~ 156 kDa); peak 3, monomeric form (~ 65 kDa) and peak 4, degradation products (~ 39 kDa). (B) Size exclusion chromatography of G46S-hPAH (2-120) expressed as a MBP fusion protein in *E. coli*. Peak 1, higher-order oligomeric forms (eluted in the void volume); peak 2, dimeric form (~ 148 kDa) and peak 4, degradation products (~ 39 kDa). The molecular mass of the enzyme forms

were estimated using the elution position of standard molecular mass markers as a reference (not shown). 10.7 mg and 9.3 mg fusion protein were applied to the column in (A) and (B), respectively. The chromatography was performed on a HiLoad Superdex 200 HR column (1.6 cm × 60 cm), equilibrated and eluted with 20 mM Na-Hepes, 0.2 M NaCl, pH 7.0 at a flow rate of 0.38 $ml \cdot min^{-1}$ at 4 °C and detection was at 280 nm. The inset in panels (A) and (B) represent a SDS-PAGE analysis demonstrating the purity of the fusion proteins after two steps of purification (amylose affinity chromatography and size-exclusion chromatography). *Lane* M, low-molecular-mass standard (106.5, 97.6, 50.2, 36.9 and 28.9 kDa); *lane* 2, the respective dimeric form enzymes (peak 2); *lane* 3, monomeric form (peak 3) and *lane* 4, degradation products (peak 4) after the size-exclusion chromatography. (C) Time-course for the cleavage of dimeric WT-hPAH (2-120) in the absence (●) and presence of 150 μM L-Phe (○) by the restriction protease factor Xa. (D) Time-course for the cleavage of dimeric G46S-hPAH (2-120) in the absence (▼) and presence of 150 μM L-Phe (▽) by the restriction protease factor Xa. Data were fitted to a single exponential decay curve. The time-course of cleavage was performed at standard assay conditions (0.74 $mg \cdot ml^{-1}$ fusion protein, 5.0 $\mu g \cdot ml^{-1}$ factor Xa, 20 mM Na-Hepes, 0.1 M NaCl, pH 7.0 and 25 ^{o}C).

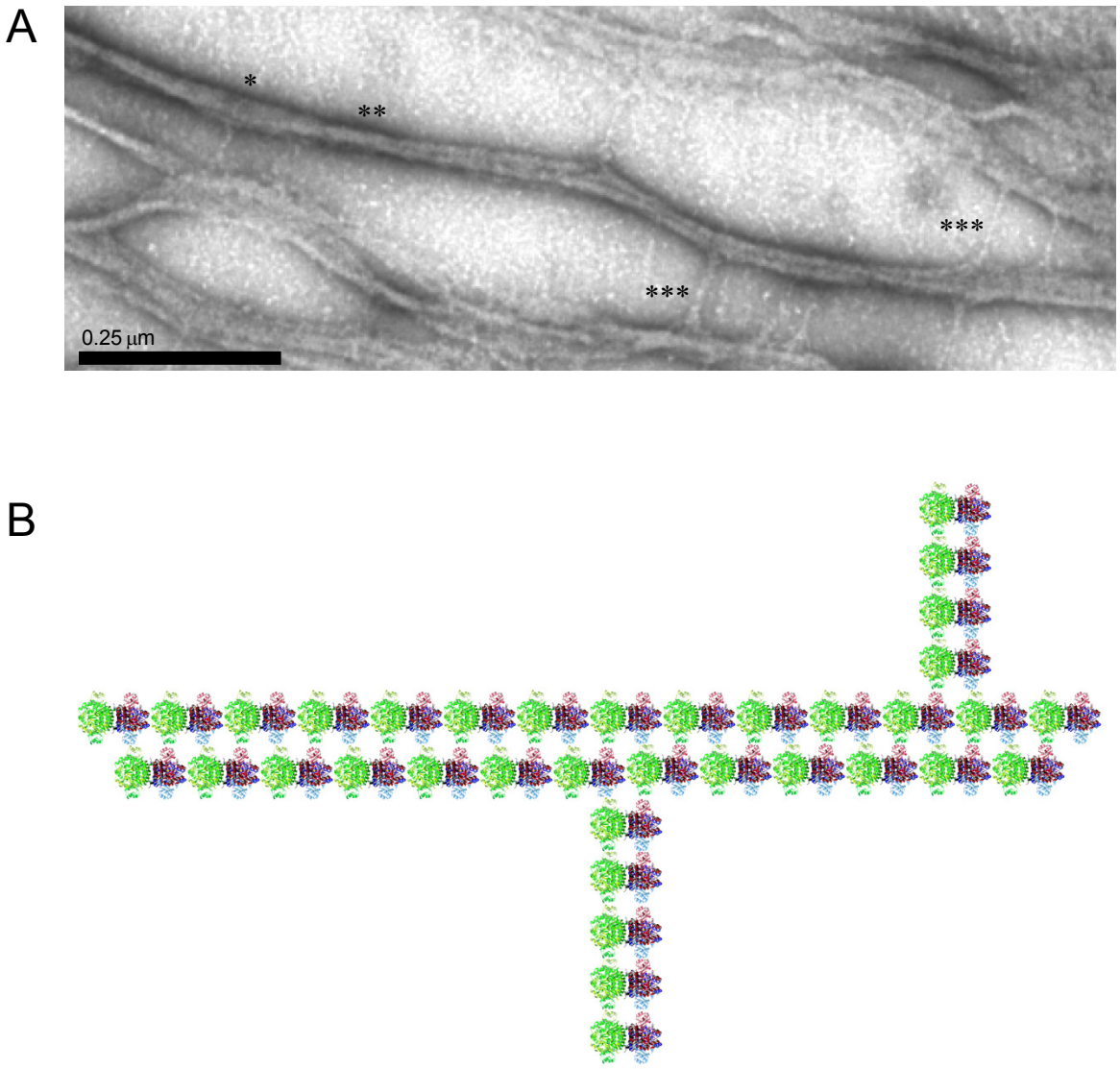

Supplementary Fig. S4. G46S-hPAH fibril formation. (A) Electron micrograph of a negatively stained twisted fibril of G46S-hPAH. The broadest part (∗), narrowest part (∗∗), and branching (∗∗∗) of the fibril are indicated. (B) Schematic representation of a potential mechanism of self-association resulting in the formation of branched fibrils.

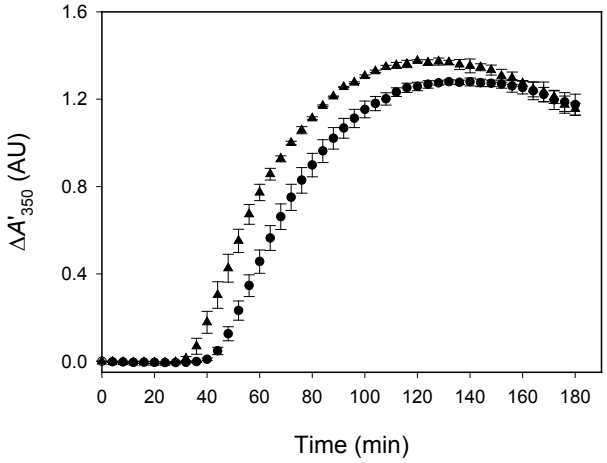

Supplementary Fig. S5. Effect of deamidation on the self-association of tetrameric G46S-hPAH. The time-course for the self-association of a non-deamidated (2 h induction) (▲) and a deamidated (24 h induction) (●) tetrameric G46S-hPAH. The self-association reactions were performed at standard assay conditions (0.74 mg·ml^{-1} fusion protein (7.85 μM monomer), 5.0 μg·ml^{-1} factor Xa, 20 mM Na-Hepes, 0.1 M NaCl, pH 7.0 and 25 ºC). Some data points were omitted for clarity. Error bars represent mean ± SD, (n = 3).

2. Stereospecific binding of L-phenylalanine to the isolated regulatory domain of human phenylalanine hydroxylase

João Leandro, Jaakko Saraste, Paula Leandro, Torgeir Flatmark

Submitted

Stereospecific binding of L-phenylalanine to the isolated regulatory domain of human phenylalanine hydroxylase

João Leandro[a,b] , Jaakko Saraste[a], Paula Leandro[b] and Torgeir Flatmark[a]*

[a]Department of Biomedicine, University of Bergen, Jonas Lies vei 91, N-5009 Bergen, Norway and [b]Metabolism and Genetics Group, Research Institute for Medicines and Pharmaceutical Sciences (iMed.UL), Faculty of Pharmacy, University of Lisbon, Av. Prof. Gama Pinto, 1649-003 Lisbon, Portugal

Abstract

The proposal that mammalian phenylalanine hydroxylase (PAH) has an allosteric regulatory binding site for L-phenylalanine (L-Phe), in addition to the catalytic site, has been a controversial issue for 30 years. In the present study a truncated maltose binding protein tagged construct of the human enzyme (MBP-(pep_{Xa})-$hPAH^{2-120}$), comprising the regulatory (*R*) domain, was expressed in *E. coli* and recovered in a metastable state as a dimer and monomer. Upon cleavage of the fusion proteins by factor Xa both forms of $hPAH^{2-120}$ self-associate and form unstructured oligomers as observed by electron microscopy. This self-association revealed a stereospecific inhibition (> 95%) by L-Phe with a $[L]_{0.5}$ value of 23.3 ± 0.5 μM L-Phe for the dimer and 15.1 ± 2.4 μM L-Phe for the monomer. Interestingly, the self-association of the dimer of a conformationally variant mutant form (G46S) revealed no inhibition by L-Phe, indicating that the L-Phe binding site in the *R*-domain is sensitive to the conformation of its $\beta\alpha\beta\beta\alpha\beta$ motif (ACT domain). Moreover, several independent lines of direct experimental evidence from recent studies support the conclusion that the binding site is not available in the native full-length tetrameric/dimeric enzyme, as a result of a conformational change in the *R*-domain and/or a steric hindrance due to interdomain interactions.

Keywords: ACT domain; phenylalanine hydroxylase; regulatory domain; self-association; L-phenylalanine

Running Title: Stereospecific binding of L-Phe to the isolated *R*-domain of hPAH

*Corresponding author. Department of Biomedicine, University of Bergen, Jonas Lies vei 91, N-5009 Bergen, Norway. Tel.: +47 55586428; Fax.: +47 55586360
Email: torgeir.flatmark@biomed.uib.no

Introduction

The ~ 50 kDa monomer of wild-type (WT) mammalian phenylalanine hydroxylase (PAH) assembles *in vivo* and on overexpression in bacteria to form tetramers and dimers, in equilibrium. The 3D structures of human phenylalanine hydroxylase (hPAH) and rat phenylalanine hydroxylase (rPAH) have revealed that the protomer consists of three structural and functional domains, i.e. a regulatory (*R*, residues 1-117), a catalytic (*C*, residues 118-410) and an oligomerization (*O*, residues 411-452) domain with a tetramerization motif (Erlandsen et al. 1997; Fusetti et al. 1998; Kobe et al. 1999). On the basis of the 3D structures of the *C*+*O* domains of hPAH and the *R*+*C* domains of rPAH a composite full-length (*R*+*C*+*O*) model has been assembled for the PAH tetramer (Flatmark and Stevens 1999) organized as an asymmetric dimer of dimers. The N-terminal *R*-domain

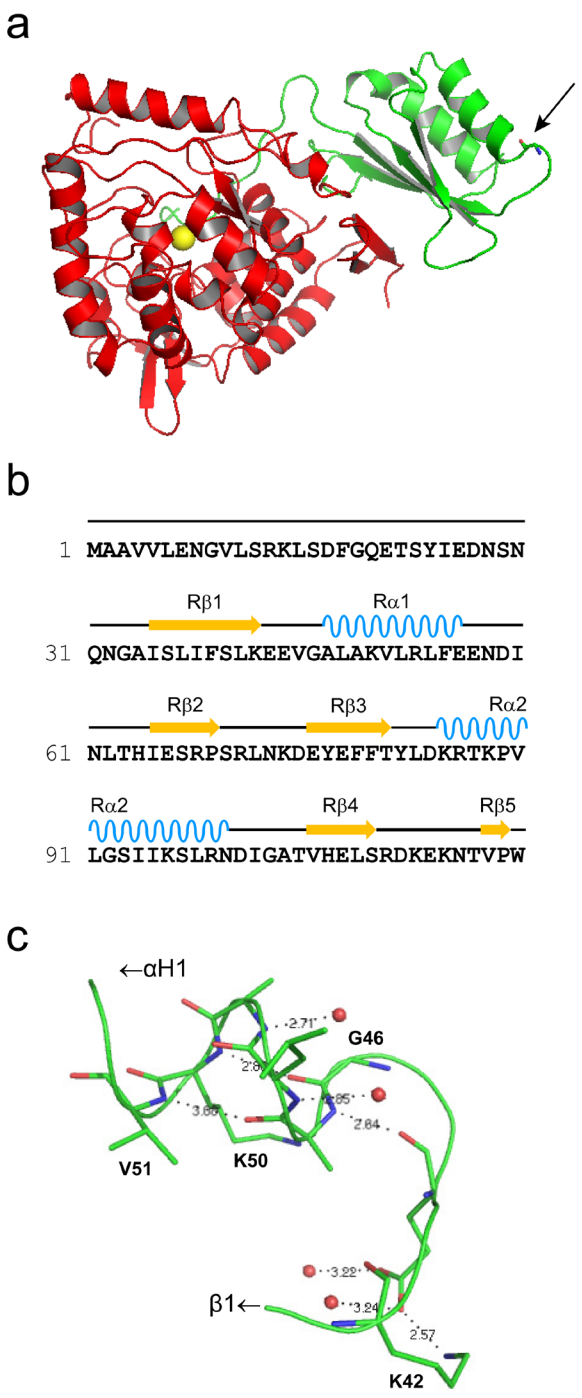

Fig. 1 3D structure of PAH protomer (rPAH$^{1-429}$), sequence and secondary structure assignment of the N-terminal regulatory domain (*R*-domain) of hPAH and the localization/interactions of the G46 residue in the *R*-domain. **a** Ribbon representation of the regulatory/catalytic domain crystal structure of rPAH (PDB ID: 1PHZ) in the monomeric form with the regulatory domain shown in green, the catalytic domain in red, the iron as a yellow sphere and G46 in stick model (pointed arrow). **b** Sequence of the N-terminal regulatory domain of hPAH (SwissProt P00439) with elements of secondary structure (determined from the coordinates of the combined PAH structures (Flatmark and Stevens 1999) with the program DSSP (Kabsch and Sander 1983)) indicated above the sequence and numbered sequentially from the N-terminus (Kobe et al. 1999). **c** Close-up of the location of G46 in the regulatory domain of rPAH, at the end of the loop between *β*-strand 1 and *α*-helix 1, where it H-bonds to K50. The Cα-atom trace is shown in green ribbon, with the relevant residues in stick model and water molecules as red spheres. The figures were created using PyMOL, version 1.1 (DeLano Scientific) (Delano 2002) (a and c).

has an *α*-*β* sandwich (*βαββαβ*) motif composed of a four-stranded antiparallel *β*-sheet flanked on one side by two short *α*-helices and the other side by the *C*-domain (Fig. 1a, b), and the motif has been classified as an ACT domain (Aravind and Koonin 1999; Kobe et al. 1999). However, PAH differs from other archetypical ACT domains in proteins binding regulatory amino acids, since there are no contacts between the ACT domains in the dimeric and tetrameric structures of mammalian PAH (Flatmark and Stevens 1999). As seen from Table 1 the possible regulatory function of a second L-phenylalanine (L-Phe) binding site in mammalian PAH has over the years been a controversial issue. Among the supportive evidence was the demonstration of an *in vitro* binding of [^{14}C]-L-Phe to recombinant WT and mutant forms (G46S, A47V, T63P/H64N, I65T and R68S) of the isolated *R*-domain (hPAH$^{2-120}$), expressed as maltose binding protein (MBP) fusion proteins (Gjetting et al. 2001). More recently ^{1}H-^{15}N heteronuclear single-quantum coherence (HSQC) NMR studies of a dimeric isolated *R*-domain (rPAH$^{1-117}$) revealing chemical shift perturbations in the presence of L-Phe, that are consistent with its binding at a specific site (Li et al. 2010b). Some of these binding studies have been challenged (Liberles et al. 2005; Siltberg-Liberles and Martínez 2009), partly due to the fact that the MBP fusion proteins utilized (Gjetting et al. 2001) were predominantly dimers, and therefore not considered

representative for the situation in the full-length enzyme where no contacts between the proposed binding sites in the ACT domain of the different protomers occurs (Flatmark and Stevens 1999).

In the present study, therefore, the *R*-domain (residues 2-120) of the recombinant WT and a conformationally variant mutant form (G46S) (Leandro et al. 2011) were isolated as MBP-$(pep)_{Xa}$-$hPAH^{2-120}$ fusion proteins with the goal to: (i) isolate their oligomeric forms; (ii) demonstrate that the *R*-domain is in a metastable state as fusion protein and self-associates upon cleavage of the fusion protein forming unstructured higher-order oligomers; (iii) show that L-Phe inhibits the propensity of WT, but not a G46S mutant form, to self-associate; (iv) demonstrate that the inhibition of self-association by L-Phe of the monomeric form is stereospecific and of relatively high affinity. To address these aspects, we used a combined approach of real-time light-scattering, thioflavin-T and ANS fluorescence-based binding assays and electron microscopy (EM) structural analyses.

Materials and Methods

Materials

TB1 cells, the prokaryotic expression vector pMAL-c2/pMAL-hPAH and the amylose resin were obtained from New England Biolabs (USA). The restriction protease factor Xa was obtained from Protein Engineering Technology ApS (Aarhus, Denmark). Thioflavin-T (ThT) and 8-anilino-1-naphthalenesulfonic acid (ANS) were obtained from Sigma-Aldrich.

Site-specific mutagenesis

The WT regulatory (*R*) domain (WT-$hPAH^{2-120}$) and its G46S mutant form (G46S-$hPAH^{2-120}$) were obtained by introducing a stop signal in codon 121 of hPAH, by site-directed mutagenesis (QuikChange^{R} II, Stratagene), using the pMAL-WT-hPAH (Martínez et al. 1995) and pMAL-G46S-hPAH constructs (Eiken et al. 1996) as template, respectively. Primers 5′-GACACAGTGCCCTGGT**AA**CCAAGAACCATTCA AGAGC-3′ (forward) and 5′-GCTCTTGAATGGTTCTTGG**TT**ACCAGGGCACTG TGTC-3′ (reverse) used for mutagenesis were provided by Eurogentec, Seraing, Belgium (the mismatch nucleotides are shown in bold type). The authenticity of the mutagenesis was verified by DNA sequencing as described previously (Eiken et al. 1996).

Expression and isolation of fusion proteins

The WT and G46S mutant form were expressed in *E. coli* as fusion proteins (MBP-$(pep)_{Xa}$-$hPAH^{2-120}$) (Martínez et al. 1995). The bacteria were grown at 37 ºC and the induction by 1 mM isopropyl-thio-*β*-D-galactoside was performed for 8 h at 28 ºC. The fusion proteins were purified by affinity chromatography (amylose resin) and centrifuged in a TL-100 Ultracentrifuge (Beckman, USA) for 20 min at 50,000*g* before size-exclusion chromatography (SEC) as described (Martínez et al. 1995). SEC was performed at 4 ºC using a HiLoad Superdex 200 HR column (1.6 cm×60 cm) prepacked from Amersham Biosciences (GE Healthcare, Uppsala, Sweden). The mobile phase consisted of 20 mM Na-Hepes and 0.2 M NaCl, pH 7.0 and the flow rate was 0.38 ml·min^{-1}. The dimeric and monomeric fusion proteins were concentrated by Centriplus 30 filter (Amicon, MA, USA). The concentration of purified fusion proteins was measured using the absorption coefficient A_{280} (1 mg·ml^{-1}·cm^{-1}) = 1.34. A colorimetric method (Bradford 1976) was in some cases also used to measure enzyme concentrations, with bovine serum albumin as the standard.

Table 1 Experimental evidence interpreted as supportive and non supportive of a second regulatory binding site for L-Phe in mammalian PAH.

Evidence	*Reference*
Supportive	
1. Tryptophan is a substrate, but does not activate the rPAH-TM [a]	(Shiman 1980)
2. Equilibrium binding of [^{14}C]-L-Phe to rPAH-TM giving a stoichiometry of L-Phe:subunit ~ 1.5:1	(Parniak and Kaufman 1981; Phillips et al. 1984)
3. *R*-domain of rPAH$^{19-428}$-DM has a $\beta\alpha\beta\beta\alpha\beta$ motif (ACT domain) similar to its distant homolog prephanate hydratase [b]	(Kobe et al. 1999)
4. Equilibrium binding of [^{14}C]-L-Phe to MBP-hPAH$^{2-120}$-DM giving half maximal binding at ~ 130 µM [b]	(Gjetting et al. 2001)
5. Gel filtration and ^{1}H-^{15}N HSQC NMR studies of rPAH$^{2-117}$ in the presence of L-Phe reveal changes in peak elution and chemical shift perturbations, respectively, consistent with L-Phe binding at a specific site	(Li et al. 2010b)
Non supportive	
1. Equilibrium binding of [^{14}C]-L-Phe to rPAH-TM giving a stoichiometry of L-Phe:subunit ~ 0.8:1	(Shiman 1980)
2. Equilibrium binding of [^{3}H]-L-noradrenaline to hPAH-TM giving a stoichiometry of L-noradrenaline:subunit of ~ 0.5:1 and a Hill coefficient of 1.9 [c]	(Martínez et al. 1990)
3. Differential scanning calorimetry supports the binding of L-Phe to the catalytic domain of hPAH-TM with a stoichiometry of L-Phe:subunit ~ 1:1	(Thórólfsson et al. 2002)
4. 3D structural analysis of hPAH$^{121-427}$-DM, lacking the *R*-domain, demonstrates a global conformation change on binding L-Phe at the active site	(Andersen et al. 2003)
5. Full-length hPAH-DM is not activated by L-Phe [a]	(Bjørgo et al. 2001)
6. Isothermal titration calorimetry demonstrates the binding of L-Phe to hPAH-TM with a stoichiometry of L-Phe:subunit 1.2 ± 0.1:1 and a k_D = 13.6 µM	(Flydal et al. 2010)

[a]Preincubation with L-Phe activates the tetrameric enzyme several fold. The abbreviations TM and DM represent tetrameric and dimeric forms of the enzyme, respectively.
[b]The ACT domain of prephenate hydratase binds L-Phe with high affinity at its dimer interphase, involving the sequence motifs G^{191}LLV and E^{218}SRP (Tan et al. 2008); the corresponding sequence motifs in rPAH(hPAH) are G^{46}AL and E^{66}SRP.
[c]The analog binds at the active site iron with positive cooperativity (n_H = 1.9), forming a charge transfer complex (Martínez et al. 1990), and induces a global conformational change (Solstad et al. 2003).

Cleavage of MBP-hPAH$^{2-120}$ fusion proteins and assay of self-association by light scattering

Before cleavage of the MBP-hPAH$^{2-120}$ fusion proteins by factor Xa they were subjected to high-speed ultracentrifugation at 210,000*g* for 15 min at 4 ºC. In the standard assay at 20 mM Na-Hepes, 0.1 M NaCl, pH 7.0 and 25 °C the concentration of the fusion protein was 0.74 mg·ml^{-1}, and the concentration of factor Xa was adjusted to give a final ratio (by weight) of 1:150 relative to the fusion protein. Self-association of the factor Xa released *R*-domain was followed in real-time by light scattering, as measured by the increase in the apparent absorbance at 350 nm ($A'_{350} = \log [I_o/(I_p + f \cdot I_d)]$ using an Agilent 8453 Diode Array

Spectrophotometer with a Peltier temperature control unit. The change in light scattering was expressed as $\Delta A'_{350}$ by subtracting the background absorbance in the absence of added factor Xa. The rate of forming higher-order oligomers was expressed as $\Delta A'_{350}/\Delta t$ and was obtained from the slope of the linear growth phase of each light scattering curve. In each experiment a parallel time-course cleavage analysis was conducted to rule out any effect of the cleavage rate.

In order to study the inhibitory effect of L-Phe on the self-association of WT-hPAH$^{2-120}$ and the mutant form G46S-hPAH$^{2-120}$, the fusion proteins were preincubated for 5 min at standard assay conditions with L-Phe (0-1 mM) before the cleavage was initiated with factor Xa. The inhibition of the self-association was analyzed by nonlinear regression analysis using the SigmaPlot® Technical Graphing Software and a reverse Hill equation (four parameter logistic equation): $\upsilon = V_{min} + ((V_{max} - V_{min})/(1 + (L/[L]_{0.5})^s)$, (DeLean et al. 1978; Oz-Gleenberg et al. 2007; Prinz 2010) where υ is the rate of formation of higher-order oligomers ($\Delta A'_{350}/\Delta t$); L, the ligand (L-Phe) concentration; V_{max}, the rate of self-association when the ligand is absent; V_{min}, the rate of self-association for infinite concentration of the ligand; $[L]_{0.5}$ is the apparent equilibrium dissociation constant ~ IC_{50} (50 % inhibition), and s, a pseudo-Hill coefficient (sigmoid factor) that determines the steepness of the curve.

SDS-PAGE analyses

The purification of the fusion proteins and the efficiency of its cleavage by factor Xa, was analyzed by SDS-PAGE in a 10 % (w/v) polyacrylamide gel (Laemmli 1970). The gels were stained by Coomassie Brilliant Blue R-250, scanned using VersaDoc 4000 (Bio-Rad) and quantification of the protein bands was obtained by using the Quantity One 1-D Analysis Software (Bio-Rad, Hercules, CA, USA).

ANS binding assay

Fluorescence-based 8-anilino-1-naphthalenesulfonic acid (ANS) binding studies were performed as described by Aukrust et al (Aukrust et al. 2006). Briefly, 1.3 μM hPAH$^{2-120}$ was incubated with 60 μM ANS in 20 mM Na-Hepes, 0.1 M NaCl, pH 7.0 at room temperature for 5 min in the dark. The fluorescence emission spectra were recorded between 400 and 600 nm (6 nm slit width) at 25 ºC using an excitation wavelength of 385 nm (6 nm slit width) on a Perkin-Elmer LS-50B luminescence spectrometer (Perkin-Elmer, Waltham, MA, USA) and by averaging four scans.

Thioflavin-T binding assay

Fluorescence-based thioflavin-T (ThT) binding studies were performed according to a standard protocol (Eisert et al. 2006). Briefly, the ThT measurements were made by taking reaction aliquots and diluting them to 1.3 μM hPAH$^{2-120}$ in 20 mM Na-Hepes, 0.1 M NaCl, pH 7.0 containing 20 μM ThT. Immediately following sample preparation the fluorescence was measured on a Perkin-Elmer LS-50B luminescence spectrometer at 25 ºC using an excitation wavelength of 440 nm and emission of 482 nm, with slit widths of 3 and 7 nm for excitation and emission, respectively, and by averaging four scans. The reported values (ΔThT) have been corrected by subtracting the background fluorescence of ThT in the absence of protein and with the protein in the absence of ThT (light scattering).

Negative staining of WT-hPAH$^{2-120}$ oligomers and electron microscopy

For the negative staining EM of WT-hPAH$^{2-120}$ oligomers, Formvar-coated 200 mesh nickel grids (Electron Microscopy Sciences, Fort Washington, USA) were used. The grids were further coated with carbon, stored dust-free in Petri dishes kept at low humidity, and glow-discharged for 15 s prior to use. Negative staining was carried out by first applying 5 µl of a protein solution on the specimen grid. Following absorption for 60 s, the sample drop was removed by blotting with filter paper, and the grid was stained twice with 2 % (w/v) aqueous uranyl acetate. After application, the first drop (10 µl) was blotted off immediately, whereafter a fresh drop of the stain was added to the grid for 15 s. After final blotting and drying, the specimens were observed in a Jeol 1230 Electron Microscope operated at 80 kV.

Computational Analysis

The effect of the G46S mutation on the free energy of folding (ΔΔG) was predicted using the structural coordinates of (ΔC428-452)-rPAH (PDB ID: 1PHZ) and the Concoord/PBSA server (http://ccpbsa.biologie.uni-erlangen.de/ccpbsa/index.php) (Benedix et al. 2009). In order to assess the effect on G46S mutation on the secondary structure of the hPAH protein an algorithm based on helix-coil transition theory, AGADIR, was used to predict helical propensity (http://agadir.crg.es/) (Lacroix et al. 1998). WT-hPAH$^{2-120}$ predicted isoelectric point (p*I*) is 6.1 and a global net charge of -1.7 at pH 7 (calculated using the EMBL IEP Service, http://www3.embl.de/cgi/pi-wrapper.pl).

Results

Expression and isolation of the MBP-hPAH$^{2-120}$ fusion proteins

On expression of WT MBP-(pep)$_{Xa}$-hPAH$^{2-120}$ and its mutant form G46S, the affinity purified fusion proteins were separated into their oligomeric forms by SEC. The chromatogram of the WT-hPAH$^{2-120}$ form (Fig. 2) revealed four peaks where peak 1 represented higher-order oligomeric forms (eluted at or near the void volume), and peak 2 and peak 3 represented the dimeric and monomeric forms, respectively. For the G46S-hPAH$^{2-120}$ fusion protein only the dimeric form was recovered at sufficiently high yield for further analyses. Moreover, SDS-PAGE revealed that the mutant form was more partly proteolysed than the WT form (data not shown).

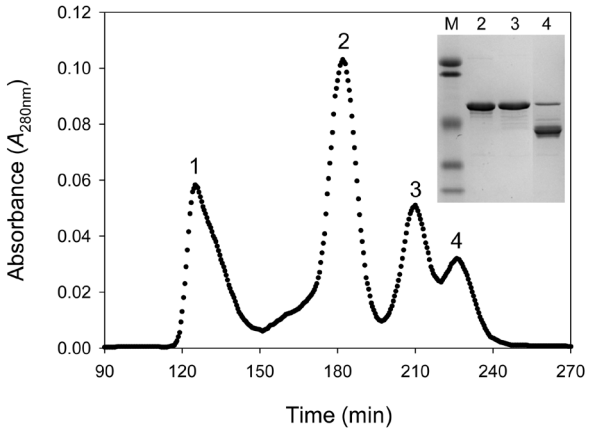

Fig. 2 Size-exclusion chromatography of the WT *R*-domain (WT-hPAH$^{2-120}$) expressed as a MBP fusion protein in *E. coli*. Peak 1, higher-order oligomeric forms (eluted in the void volume); peak 2, dimeric form (~ 156 kDa); peak 3, monomeric form (~ 65 kDa) and peak 4, degradation products (~ 39 kDa). The molecular mass of the enzyme forms were estimated using the elution position of standard molecular mass markers as a reference (not shown). 10.7 mg of fusion protein were applied to the column. The chromatography was performed on a HiLoad Superdex 200 HR column (1.6 cm×60 cm), equilibrated and eluted with 20 mM Na-Hepes, 0.2 M NaCl, pH 7.0 at a flow rate of 0.38 ml·min^{-1} at 4 °C and detection was at 280 nm. The *inset* represents a SDS-PAGE analysis demonstrating the purity of the fusion proteins after two steps of purification. *Lane* M, low-molecular-mass standard (106.5, 97.6, 50.2, 36.9 and 28.9 kDa); *lane* 2, dimeric form (peak 2); *lane* 3, monomeric form (peak 3) and *lane* 4, degradation products (peak 4) after the size-exclusion chromatography.

The hPAH$^{2-120}$ fusions proteins comprising the hPAH regulatory domain (residues 2-117) and including also residue W120 were used, as this residue has been used as a valuable conformational probe for the full-length WT and truncated forms of enzyme (Knappskog and Haavik 1995; Stokka and Flatmark 2003). However, no change in tryptophan fluorescence was detected in absence and presence of L-Phe. The hPAH$^{2-120}$ fusions proteins were also used in order to compare the results of the cleaved forms obtained here with the results of the fusion proteins obtained by Gjetting et al. that comprise residues 2-120 (Gjetting et al. 2001).

Cleavage of the MBP fusion proteins

At the standard assay conditions the cleavage of the WT-hPAH$^{2-120}$ fusion protein by factor Xa was very similar for the dimeric (Supplementary Fig. S1) and the monomeric fusion protein, with $t_{1/2}$ (time at 50 % cleavage) of ~ 11 min. The presence of L-Phe had no significant effect on the cleavage reaction of WT-hPAH$^{2-120}$ by factor Xa (Supplementary Fig. S1), as well as on the cleavage of G46S-hPAH$^{2-120}$ (data not shown).

Self-association of dimeric and monomeric forms of WT-hPAH$^{2-120}$

On cleavage of the dimeric and monomeric MBP-hPAH$^{2-120}$ fusion proteins by factor X_a (pH 7.0, 0.1 M NaCl and 25 ^{o}C) the proteins self-associate (Fig. 3) with a similar time-course, including a delay period (lag phase), a growth phase of increasing light scattering ($\Delta A'_{350}/\Delta t$) of 3.9 ± 0.1 × 10^{-3} and 1.3 ± 0.1 × 10^{-3} AU·min^{-1}, for dimeric (Fig. 3a) and monomeric (Fig. 3b) forms, respectively. In the absence of added factor Xa no change in light scattering was observed within the time scale of 3 h.

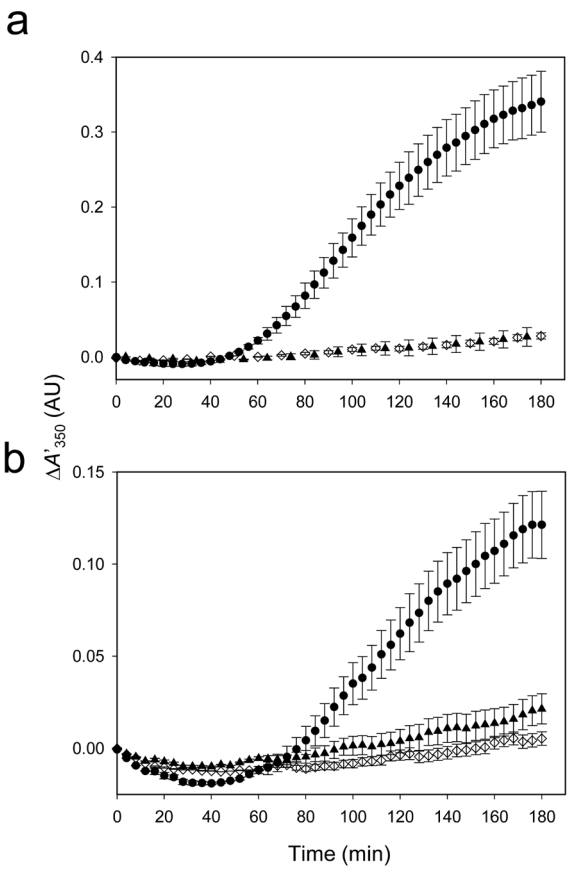

Fig. 3 The self-association of dimeric **(a)** and monomeric **(b)** WT-hPAH$^{2-120}$ following cleavage of the MBP fusion protein by factor Xa, and the effect of L-Phe. **a** The time-course of the self-association of dimeric WT-hPAH$^{2-120}$ protein following cleavage of the fusion protein by factor Xa was followed in real-time by light scattering, as measured by the increase in the apparent absorbance at 350 nm ($\Delta A'_{350}$). The data points correspond to cleavage in the absence of any added compound (●) and in the presence of 1 mM L-Phe (▲). (◇) represents dimeric WT-hPAH$^{2-120}$ fusion protein in the absence of factor Xa. **b** The time-course of the self-association of monomeric WT-hPAH$^{2-120}$ protein following cleavage of the fusion protein by factor Xa in the absence of any added compound (●) and in the presence of 1 mM L-Phe (▲). (◇) represents monomeric WT-hPAH$^{2-120}$ fusion protein in the absence of factor Xa. The reactions were performed at standard assay conditions (0.74 mg·ml^{-1} fusion protein, 5.0 µg·ml^{-1} factor Xa, 20 mM Na-Hepes, 0.1 M NaCl, pH 7.0 and 25 ^{o}C). Some data points were omitted for clarity. Error bars represent mean ± SD, (n = 3).

Inhibition of self-association by L-Phe and stereospecificity

The self-association of the dimeric WT-hPAH$^{2-120}$ is inhibited in a stereospecific manner by phenylalanine;

100 μM L-Phe almost completely inhibited the self-association of the dimeric *R*-domain whereas 100 μM D-Phe revealed almost no effect (Fig. 4a). A similar relation was observed for the monomeric form (data not shown). Whereas the inhibition of the dimeric form (Fig. 5a) revealed a $[L]_{0.5}$ value of 23.3 ± 0.5 μM L-Phe, that of the monomeric form (Fig. 5b) was 15.1 ± 2.4 μM L-Phe (Table 2). By contrast, the self-association of the dimeric form of the G46S mutant revealed no inhibition by L-Phe (Fig. 4b). The effect of other hydrophobic L-amino acids (e.g. L-alanine) were test, but no inhibition of the self-association of WT-hPAH$^{2-120}$ was observed, even at higher concentrations of the amino acids (1 mM) (data not shown).

Binding of ANS and ThT

ANS is a spectroscopic probe that has affinity for hydrophobic clusters which are not tightly packed in a fully folded structure or become exposed in partially unfolded structures (Semisotnov et al. 1991). ANS binds to dimeric WT MBP-hPAH$^{2-120}$ fusion protein (Fig. 6a) and its factor Xa cleaved form (t = 3 h) (Fig. 6b) with an increase in the fluorescence intensity and a blue shift (maximum at ~ 478 nm). Similar spectra were obtained in the absence and presence of 1 mM D-Phe whereas L-Phe revealed a concentration dependent decrease and red shift of the fluorescence spectra (Fig. 6a, b). Similar results were obtained for the monomeric WT-hPAH$^{2-120}$ as a fusion protein (Fig. 6c) and after its cleavage by factor Xa (Fig. 6d). The MBP fusion partner alone has a negligible contribution to the ANS fluorescence, and there was no additional effect of L-Phe (Fig. 6a). At the standard assay conditions the higher-order oligomers, related to the increase in light-scattering, revealed only a minor enhancement of the ThT fluorescence (Supplementary Fig. S2).

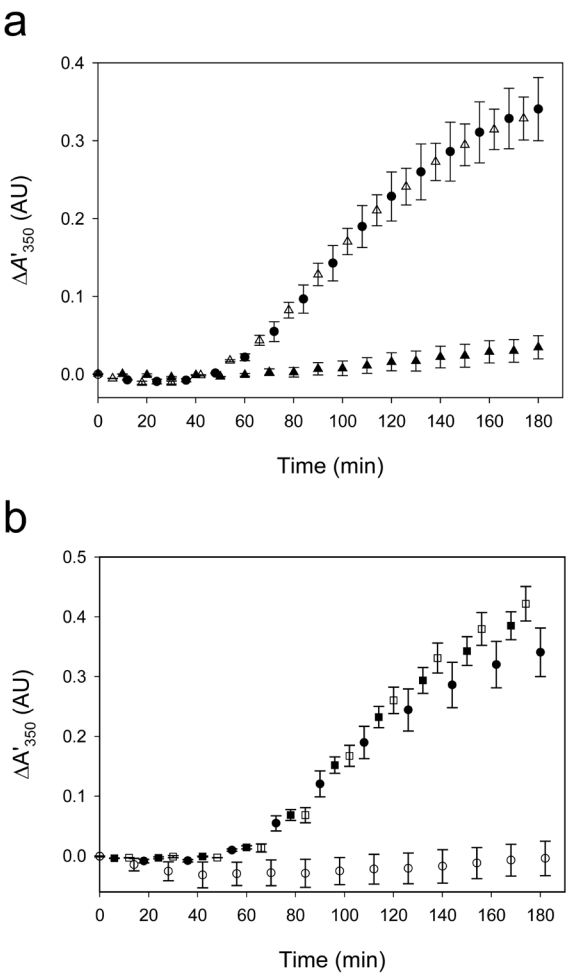

Fig. 4 a The stereospecific inhibition of the self-association of WT-hPAH$^{2-120}$ by phenylalanine. The time-course of the self-association of dimeric WT-hPAH$^{2-120}$ protein following cleavage of the fusion protein by factor Xa in the absence (●) and presence of 100 μM L-Phe (▲) or 100 μM D-Phe (△). **b** The self-association of dimeric WT-hPAH$^{2-120}$ and its G46S mutant form and the effect of L-Phe. The time-course of the self-association of WT-hPAH$^{2-120}$ dimeric protein following cleavage of the fusion protein by factor Xa in the absence (●) and presence of 150 μM L-Phe (○); G46-hPAH$^{2-120}$ dimer fusion protein following cleavage by factor Xa in the absence (■) and presence of 150 μM L-Phe (□). Some data points were omitted for clarity. The assays were performed at standard assay conditions and error bars represent mean ± SD, n = 3 independent experiments.

Ultrastructure of WT hPAH$^{2-120}$ oligomers

In order to get information on the morphology of the higher-order oligomers of dimeric WT hPAH$^{2-120}$ that are formed on factor Xa cleavage of the fusion protein,

Table 2 L-Phe inhibition of the self-association of dimeric and monomeric WT-hPAH$^{2-120}$.

Enzyme	V_{max}[a] ($\times 10^{-3}$ AU·min^{-1})	V_{min} ($\times 10^{-3}$ AU·min^{-1})	$[L]_{0.5}$[b] (μM)	Pseudo-Hill Coefficient (s)
WT-hPAH$^{2-120}$ dimer	3.6 ± 0.1	0.06 ± 0.05	23.3 ± 0.5	4.8 ± 0.5
WT-hPAH$^{2-120}$ monomer	1.3 ± 0.1	0.04 ± 0.05	15.1 ± 2.4	1.3 ± 0.2

The effect of L-Phe concentration on the rate of forming higher-order oligomers ($\Delta A'_{350}/\Delta t$) was determined as described in the Materials and methods section at standard conditions (0.74 mg·ml^{-1} fusion protein, 5.0 μg·ml^{-1} factor Xa, 20 mM Na-Hepes, 0.1 M NaCl, pH 7.0 and 25 °C) with varying concentrations of L-Phe (0–1 mM).

[a] V represents the rate of forming higher-order oligomers ($\Delta A'_{350}/\Delta t$). [b] $[L]_{0.5}$ corresponds to IC_{50} (50 % inhibition).

negative staining EM was performed on aliquots removed during the cleavage reaction. At the final time point (t = 180 min) the EM micrographs (Fig. 7) revealed that the self-association of the WT protein generated unstructured higher-order oligomers, but no fibrils were observed.

Discussion

In a previous study (Gjetting et al. 2001), the binding of [^{14}C]-L-Phe to the isolated *R*-domain (hPAH$^{2-120}$), expressed as a MBP fusion protein was performed on dimeric fusion proteins stabilized by MBP as a chaperone. Whereas the WT form revealed an apparent half maximal binding at ~ 130 μM L-Phe, five mutants (G46S, A47V, T63P/H64N, I65T and R68S) were reported to bind L-Phe with a variably reduced affinity. Since the semi-quantitative binding data were obtained only on dimeric fusion proteins, the interpretation of the data and their relevance for the full-length enzyme has later been questioned (Liberles et al. 2005; Siltberg-Liberles and Martínez 2009). In the present study, we have found (Figs. 3a, 5a) that L-Phe also binds to the MBP-free dimeric form of WT *R*-domain (hPAH$^{2-120}$), by inhibiting its self-association to higher-order oligomeric forms. The affinity ($[L]_{0.5}$ = 23.3 ± 0.5 μM L-Phe) was higher than previously reported for the dimeric fusion protein (Gjetting et al. 2001). More important was the finding that L-Phe binds to the monomeric form (Figs. 3b, 5b), with an even

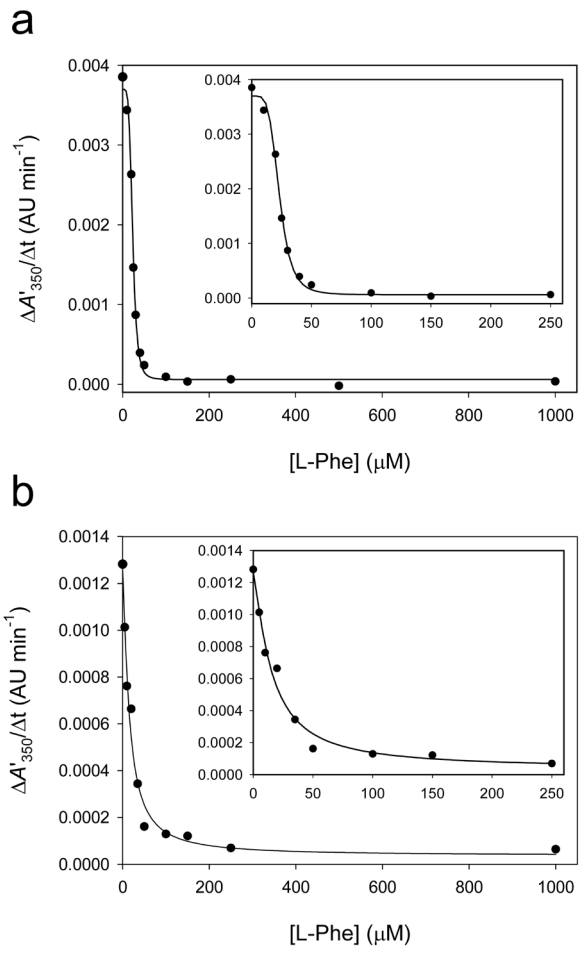

Fig. 5 The effect of L-Phe concentration on the inhibition of the self-association of dimeric **(a)** and monomeric **(b)** WT-hPAH$^{2-120}$. The inhibitory effect of L-Phe on the self-association of WT-hPAH$^{2-120}$ was assayed at standard conditions (0.74 mg·ml^{-1} fusion protein, 5.0 μg·ml^{-1} factor Xa, 20 mM Na-Hepes, 0.1 M NaCl, pH 7.0 and 25 °C) with varying concentrations of L-Phe (0–1 mM) and the rate of forming higher-order oligomers ($\Delta A'_{350}/\Delta t$) was obtained from the slope of the linear growth phase of each light scattering curve. The L-Phe dose-dependent inhibition curves of the self-association were generated by nonlinear regression analysis of the experimental data using the four parameter logistic equation (see Materials and methods). The insets represent the data obtained in the concentration range 0–250 μM L-Phe.

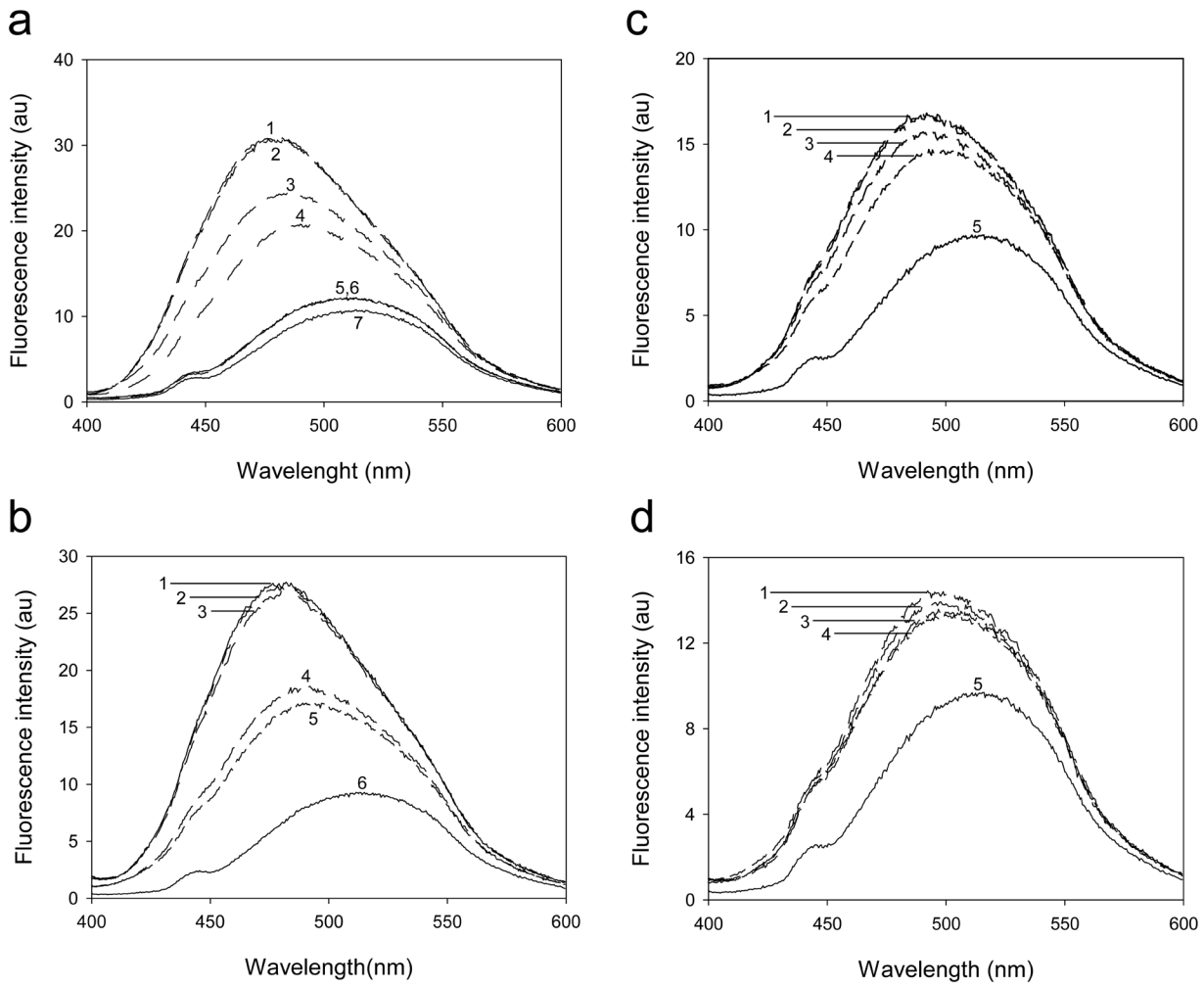

Fig. 6 The binding of ANS to dimeric and monomeric WT-hPAH$^{2\text{-}120}$. **a** ANS fluorescence emission spectra of the dimeric WT-hPAH$^{2\text{-}120}$ fusion protein in the absence of ligand (*trace* 1), with 100 μM L-Phe (*trace* 3), 1 mM L-Phe (*trace* 4), and 1 mM D-Phe (*trace* 2). The MBP protein was used as a control in the absence (*trace* 5) and in the presence of 1 mM L-Phe (*trace* 6) and the emission spectrum of buffer with ANS is shown (*trace* 7). **b** ANS fluorescence emission spectra observed after cleavage of the dimeric WT-hPAH$^{2\text{-}120}$ fusion protein by factor Xa (t = 3 h) in the absence of ligand (*trace* 1), with 100 μM L-Phe (*trace* 4), 1 mM L-Phe (*trace* 5), 100 μM D-Phe (*trace* 2), 1 mM D-Phe (*trace* 3) and the emission spectrum of buffer with ANS (*trace* 6). **c** ANS fluorescence emission spectra of the monomeric WT-hPAH$^{2\text{-}120}$ fusion protein in the absence of ligand (*trace* 1), with 100 μM L-Phe (*trace* 3), 1 mM L-Phe (*trace* 4), 1 mM D-Phe (*trace* 2) and the emission spectrum of buffer with ANS (*trace* 5). **d** ANS fluorescence emission spectra observed after cleavage of the monomeric WT-hPAH$^{2\text{-}120}$ fusion protein by factor Xa (t = 3 h) in the absence of ligand (*trace* 1), with 100 μM L-Phe (*trace* 3), 1 mM L-Phe (*trace* 4), 1 mM D-Phe (*trace* 2) and the emission spectrum of buffer with ANS (*trace* 5). The excitation wavelength was 385 nm.

higher affinity ($[L]_{0.5}$ = 15.1 ± 2.4 μM L-Phe). Thus, an interaction between two *R*-domains in a dimer is not required for the binding of L-Phe as is the case for the binding of this amino acid to the archetypical regulatory ACT domain of the distant homologous enzyme prephenate dehydratase (Aravind and Koonin 1999; Tan et al. 2008). That L-Phe binds to hPAH$^{2\text{-}120}$ also in the fusion protein (before factor Xa cleavage) was shown by its quenching of the ANS fluorescence enhancement observed on binding the hydrophobic fluorescence probe to the fusion protein (Fig. 6). Moreover, in both assay systems the measured responses to L-Phe were stereospecific (Figs. 4a, 6), and also specific for

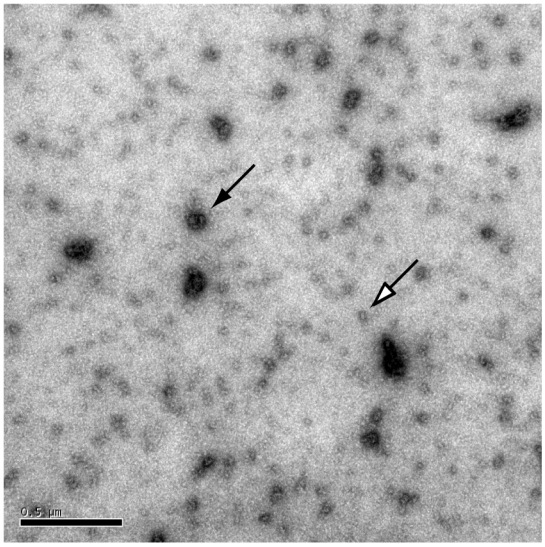

Fig. 7 Electron micrograph of negatively stained dimeric WT-hPAH$^{2-120}$ after cleavage of its MBP fusion protein by factor Xa (t = 3 h). The proteins were negatively stained with aqueous uranyl acetate and analyzed in Jeol 1230 Electron Microscope operated at 80 kV. The dark arrow points to large unstructured oligomers and the light arrow to small roughly spherical structures. Scale bar: 500 nm.

phenylalanine in a physiological concentration range (data not shown).

In contrast to the WT-hPAH$^{2-120}$, a conformationally variant mutant form (G46S) revealed no inhibition by L-Phe of its self-association induced by factor Xa cleavage, indicating that the binding site in the *R*-domain is sensitive to the conformation of its $\beta\alpha\beta\beta\alpha\beta$ sandwich motif (ACT domain). The residue G46 is positioned at the entry of α-helix 1 (A47-E57) in a five residue (L41-G46) loop structure (loop 1), linking β-strand 1 and α-helix 1 (Fig. 1c). The substitution G46→S was found to be destabilizing ($\Delta\Delta G$ = 4.1 kcal·mol^{-1}), using a structure-based method for the estimation of the free energy of folding (Benedix et al. 2009), and predicted to promote a N-terminal extension of α-helix 1 by four residues, or one turn, using the AGADIR algorithm (Lacroix et al. 1998). Thus, the change of the C_α backbone conformation and the α-β sandwich structure of the WT *R*-domain, induced by the G46→S mutation, are likely to promote the formation of new intermolecular contacts of the domain, including its binding of L-Phe. It may also partly explain why L-Phe does not bind to this site in the full-length oligomeric WT enzyme.

Comparing the 3D structural data of the *R*+*C* domains of rPAH (PDB ID: 1PHZ) (Kobe et al. 1999) with the data obtained from infrared spectroscopy analyses of the hPAH *R*-domain (comprising residues 2-110) (Chehin et al. 1998), suggests that the degree of ordered structure in the isolated *R*-domain is slightly different from that in the intact phenylalanine hydroxylase, by a decrease in the α-helix content. This structure is able to bind L-Phe, in contrast to the G46S mutant form that is predicted to extend the α-helix 1, impairing the L-Phe binding.

Recent studies on a dimeric *R*-domain (rPAH$^{1-117}$) involving gel filtration and ^{1}H-^{15}N HSQC NMR analyses also support a binding site for phenylalanine in the *R*-domain (Li et al. 2010b). However, as seen from Table 1, there is mounting experimental evidence supporting the conclusion that the L-Phe binding site in the isolated *R*-domain is not available in the native full-length tetrameric/dimeric enzyme. The strongest evidence is the isothermal titration calorimetry measurements demonstrating that L-Phe binds to full-length hPAH tetramer with a stoichiometry of L-Phe:subunit = 1.2 ± 0.1:1 and a k_D of 13.6 µM (Flydal et al. 2010). By contrast, full-length PAH tetramer isolated from *C. elegans* (cePAH) demonstrated two binding sites (L-Phe:subunit = 2.1 ± 0.05:1) with slightly different affinities, interpreted as a potential binding site in the *R*-domain (k_D of 8.2 µM) in addition to the active site (k_D of 15.0 µM) (Flydal et al. 2010). Although the modeled tetrameric structures of cePAH and hPAH are very similar, a unique pocket and putative L-Phe binding site was found only in cePAH

close to the interface between an *R*-domain and an adjacent *C*-domain, lined by the ACT-domain motifs $G^{41}AL/E^{61}SRP$ (Flydal et al. 2010). In the modeled tetrameric structures the accessibility of this site in hPAH was found to be sterically hindered by the large side-chains of K^{215} and Y^{216} in the adjacent *C*-domain, in contrast to cePAH where the corresponding residues are Q^{215} and N^{216} (Flydal et al. 2010). The functional significance of the second binding site of L-Phe in cePAH and its absence in full-length mammalian PAH is, however, an evolutionary challenging issue. Whereas cePAH has a major anabolic function, related to the synthesis of a melanin-like pigment (Calvo et al. 2008), mammalian PAH has an essential catabolic function in the regulation of the L-Phe homeostasis.

L-Phe plays a major role in the regulation of the catalytic activity of tetrameric mammalian PAH which is activated several-fold by preincubation with the substrate (Shiman and Gray 1980). The related hysteretic conformational isomerization is an intrinsically complex process (Andersen et al. 2003; Flatmark and Stevens 1999; Li et al. 2010a), and the molecular mechanism of substrate activation is not fully understood. We consider that the experimental evidence presented in Table 1 (namely the recent isothermal titration calorimetry data) do not support a separate allosteric binding site for L-Phe as originally proposed by Shiman and Gray (Shiman and Gray 1980), but the conclusion that the conformational isomerization and catalytic activation is initiated by binding of L-Phe to the active site, as the "epicentre" of the related conformational hysteresis. Our previous 3D structural analyses of a truncated form (ΔN1-102/ΔC428-452)-hPAH, lacking the *R*-domain, have demonstrated that binding of the analog 3-(2-thienyl)-L-alanine and L-norleucine at the active site triggers structural changes throughout the entire catalytic domain (Andersen et al. 2003), which partly activates the enzyme (Stokka and Flatmark 2003). This truncated form is in its unliganded form already highly activated (Knappskog et al. 1996), due to removal of the autoinhibitory sequence of the *R*-domain (Jennings et al. 2001). The 3D structural conformational changes observed in the isolated *C*-domain upon substrate binding, has recently been confirmed by hydrogen/deuterium exchange and mass spectrometry analyses of rPAH (Li et al. 2010a). In the full-length tetrameric hPAH the substrate analog L-noradrenaline binds covalently at the active site, with positive cooperativity (n_H = 1.9), and it is associated with a conformational change (Martínez et al. 1990).

hPAH is an enzyme that demonstrates a low stability towards chemical denaturation (Kleppe et al. 1999) and a low thermal stability, even at physiological temperature, in the absence of its stabilizing natural pterin cofactor (6*R*)-L-*erythro*-5,6,7,8-tetrahydrobiopterin (BH_4) (Martínez et al. 2008). By differential scanning calorimetry it has been shown that the thermal unfolding of the full-length tetramer occurs with two transition temperatures, i.e. T_m ~ 45°C assigned to the unfolding of the four *R*-domains and T_m ~ 54 °C assigned to the unfolding of two *C*-domains, followed by an irreversible protein denaturation (Thórólfsson et al. 2002). Disease causing missense mutations in hPAH, distributed by the overall structure of the protomer (http://www.pahdb.mcgill.ca/) (Scriver et al. 2003), often results in misfolded proteins and have an additional destabilizing effect both *in vitro* and *in vivo* (Erlandsen and Stevens 1999; Pey et al. 2007). It has been suggested (Gersting et al. 2008) that these mutations, independent of their position, have a major impact on the folding of the inherently unstable *R*-domain. Here we have found that L-Phe binding to the isolated *R*-domain has a stabilizing effect, and a loss of

this ability in the full-length WT enzyme may contribute to explain its low stability.

Acknowledgements
This work was supported by Fundação para a Ciência e a Tecnologia, Portugal, grant SFRH/BD/19024/2004 and the University of Bergen, Norway.

References

Andersen OA, Stokka AJ, Flatmark T, Hough E (2003) 2.0 Å resolution crystal structures of the ternary complexes of human phenylalanine hydroxylase catalytic domain with tetrahydrobiopterin and 3-(2-thienyl)-L-alanine or L-norleucine: substrate specificity and molecular motions related to substrate binding. J Mol Biol 333:747-757

Aravind L, Koonin EV (1999) Gleaning non-trivial structural, functional and evolutionary information about proteins by iterative database searches. J Mol Biol 287:1023-1040

Aukrust I, Evensen L, Hollås H, Berven F, Atkinson RA, Travé G, Flatmark T, Vedeler A (2006) Engineering, biophysical characterisation and binding properties of a soluble mutant form of annexin A2 domain IV that adopts a partially folded conformation. J Mol Biol 363:469-481

Benedix A, Becker CM, de Groot BL, Caflisch A, Böckmann RA (2009) Predicting free energy changes using structural ensembles. Nat Methods 6:3-4

Bjørgo E, de Carvalho RM, Flatmark T (2001) A comparison of kinetic and regulatory properties of the tetrameric and dimeric forms of wild-type and Thr427→Pro mutant human phenylalanine hydroxylase: contribution of the flexible hinge region Asp425-Gln429 to the tetramerization and cooperative substrate binding. Eur J Biochem 268:997-1005

Bradford MM (1976) A rapid and sensitive method for the quantitation of microgram quantities of protein utilizing the principle of protein-dye binding. Anal Biochem 72:248-254

Calvo AC, Pey AL, Ying M, Loer CM, Martínez A (2008) Anabolic function of phenylalanine hydroxylase in *Caenorhabditis elegans*. FASEB J 22:3046-3058

Chehin R, Thórólfsson M, Knappskog PM, Martínez A, Flatmark T, Arrondo JL, Muga A (1998) Domain structure and stability of human phenylalanine hydroxylase inferred from infrared spectroscopy. FEBS Lett 422:225-230

Delano WL (2002) The PyMOL Molecular Graphics System. DeLano Scientific, San Carlos, USA

DeLean A, Munson PJ, Rodbard D (1978) Simultaneous analysis of families of sigmoidal curves: application to bioassay, radioligand assay, and physiological dose-response curves. Am J Physiol 235:E97-102

Eiken HG, Knappskog PM, Apold J, Flatmark T (1996) PKU mutation G46S is associated with increased aggregation and degradation of the phenylalanine hydroxylase enzyme. Hum Mutat 7:228-238

Eisert R, Felau L, Brown LR (2006) Methods for enhancing the accuracy and reproducibility of Congo red and thioflavin T assays. Anal Biochem 353:144-146

Erlandsen H, Fusetti F, Martínez A, Hough E, Flatmark T, Stevens RC (1997) Crystal structure of the catalytic domain of human phenylalanine hydroxylase reveals the structural basis for phenylketonuria. Nat Struct Biol 4:995-1000

Erlandsen H, Stevens RC (1999) The structural basis of phenylketonuria. Mol Genet Metab 68:103-125

Flatmark T, Stevens RC (1999) Structural Insight into the Aromatic Amino Acid Hydroxylases and Their Disease-Related Mutant Forms. Chem Rev 99:2137-2160

Flydal MI, Mohn TC, Pey AL, Siltberg-Liberles J, Teigen K, Martínez A (2010) Superstoichiometric binding of L-Phe to phenylalanine hydroxylase from *Caenorhabditis elegans*: evolutionary implications. Amino Acids (in press), doi:10.1007/s00726-010-0611-6

Fusetti F, Erlandsen H, Flatmark T, Stevens RC (1998) Structure of tetrameric human phenylalanine hydroxylase and its implications for phenylketonuria. J Biol Chem 273:16962-16967

Gersting SW, Kemter KF, Staudigl M, Messing DD, Danecka MK, Lagler FB, Sommerhoff CP, Roscher AA, Muntau AC (2008) Loss of function in phenylketonuria is caused by impaired molecular motions and conformational instability. Am J Hum Genet 83:5-17

Gjetting T, Petersen M, Guldberg P, Güttler F (2001) Missense mutations in the N-terminal domain of human phenylalanine hydroxylase interfere with binding of regulatory phenylalanine. Am J Hum Genet 68:1353-1360

Jennings IG, Teh T, Kobe B (2001) Essential role of the N-terminal autoregulatory sequence in the regulation of phenylalanine hydroxylase. FEBS Lett 488:196-200

Kabsch W, Sander C (1983) Dictionary of protein secondary structure: pattern recognition of hydrogen-bonded and geometrical features. Biopolymers 22:2577-2637

Kleppe R, Uhlemann K, Knappskog PM, Haavik J (1999) Urea-induced denaturation of human phenylalanine hydroxylase. J Biol Chem 274:33251-33258

Knappskog PM, Flatmark T, Aarden JM, Haavik J, Martínez A (1996) Structure/function relationships in human phenylalanine hydroxylase. Effect of terminal deletions on the oligomerization, activation and cooperativity of substrate binding to the enzyme. Eur J Biochem 242:813-821

Knappskog PM, Haavik J (1995) Tryptophan fluorescence of human phenylalanine hydroxylase produced in *Escherichia coli*. Biochemistry 34:11790-11799

Kobe B, Jennings IG, House CM, Michell BJ, Goodwill KE, Santarsiero BD, Stevens RC, Cotton RG, Kemp BE (1999) Structural basis of autoregulation of phenylalanine hydroxylase. Nat Struct Biol 6:442-448

Lacroix E, Viguera AR, Serrano L (1998) Elucidating the folding problem of alpha-helices: local motifs, long-

range electrostatics, ionic-strength dependence and prediction of NMR parameters. J Mol Biol 284:173-191

Laemmli UK (1970) Cleavage of structural proteins during the assembly of the head of bacteriophage T4. Nature 227:680-685

Leandro J, Simonsen N, Saraste J, Leandro P, Flatmark T (2011) Phenylketonuria as a protein misfolding disease: The mutation pG46S in phenylalanine hydroxylase promotes self-association and fibril formation. Biochim Biophys Acta 1812:106-120

Li J, Dangott LJ, Fitzpatrick PF (2010a) Regulation of phenylalanine hydroxylase: conformational changes upon phenylalanine binding detected by hydrogen/deuterium exchange and mass spectrometry. Biochemistry 49:3327-3335

Li J, Ilangovan U, Daubner SC, Hinck AP, Fitzpatrick PF (2010b) Direct Evidence for a Phenylalanine Site in the Regulatory Domain of Phenylalanine Hydroxylase. Arch Biochem Biophys (in press), doi:10.1016/j.abb.2010.10.009

Liberles JS, Thórólfsson M, Martínez A (2005) Allosteric mechanisms in ACT domain containing enzymes involved in amino acid metabolism. Amino Acids 28:1-12

Martínez A, Calvo AC, Teigen K, Pey AL (2008) Rescuing proteins of low kinetic stability by chaperones and natural ligands phenylketonuria, a case study. Prog Mol Biol Transl Sci 83:89-134

Martínez A, Haavik J, Flatmark T (1990) Cooperative homotropic interaction of L-noradrenaline with the catalytic site of phenylalanine 4-monooxygenase. Eur J Biochem 193:211-219

Martínez A, Knappskog PM, Olafsdottir S, Døskeland AP, Eiken HG, Svebak RM, Bozzini M, Apold J, Flatmark T (1995) Expression of recombinant human phenylalanine hydroxylase as fusion protein in *Escherichia coli* circumvents proteolytic degradation by host cell proteases. Isolation and characterization of the wild-type enzyme. Biochem J 306:589-597

Oz-Gleenberg I, Herschhorn A, Goldgur Y, Hizi A (2007) Inhibition of human immunodeficiency virus type-1 reverse transcriptase by a novel peptide derived from the viral integrase. Arch Biochem Biophys 458:202-212

Parniak MA, Kaufman S (1981) Rat liver phenylalanine hydroxylase. Activation by sulfhydryl modification. J Biol Chem 256:6876-6882

Pey AL, Stricher F, Serrano L, Martínez A (2007) Predicted effects of missense mutations on native-state stability account for phenotypic outcome in phenylketonuria, a paradigm of misfolding diseases. Am J Hum Genet 81:1006-1024

Phillips RS, Parniak MA, Kaufman S (1984) The interaction of aromatic amino acids with rat liver phenylalanine hydroxylase. J Biol Chem 259:271-277

Prinz H (2010) Hill coefficients, dose-response curves and allosteric mechanisms. J Chem Biol 3:37-44

Scriver CR, Hurtubise M, Konecki D, Phommarinh M, Prevost L, Erlandsen H, Stevens R, Waters PJ, Ryan S, McDonald D, Sarkissian C (2003) PAHdb 2003: what a locus-specific knowledgebase can do. Hum Mutat 21:333-344

Semisotnov GV, Rodionova NA, Razgulyaev OI, Uversky VN, Gripas AF, Gilmanshin RI (1991) Study of the "molten globule" intermediate state in protein folding by a hydrophobic fluorescent probe. Biopolymers 31:119-128

Shiman R (1980) Relationship between the substrate activation site and catalytic site of phenylalanine hydroxylase. J Biol Chem 255:10029-10032

Shiman R, Gray DW (1980) Substrate activation of phenylalanine hydroxylase. A kinetic characterization. J Biol Chem 255:4793-4800

Siltberg-Liberles J, Martínez A (2009) Searching distant homologs of the regulatory ACT domain in phenylalanine hydroxylase. Amino Acids 36:235-249

Solstad T, Stokka AJ, Andersen OA, Flatmark T (2003) Studies on the regulatory properties of the pterin cofactor and dopamine bound at the active site of human phenylalanine hydroxylase. Eur J Biochem 270:981-990

Stokka AJ, Flatmark T (2003) Substrate-induced conformational transition in human phenylalanine hydroxylase as studied by surface plasmon resonance analyses: the effect of terminal deletions, substrate analogues and phosphorylation. Biochem J 369:509-518

Tan K, Li H, Zhang R, Gu M, Clancy ST, Joachimiak A (2008) Structures of open (R) and close (T) states of prephenate dehydratase (PDT) - implication of allosteric regulation by L-phenylalanine. J Struct Biol 162:94-107

Thórólfsson M, Ibarra-Molero B, Fojan P, Petersen SB, Sanchez-Ruiz JM, Martínez A (2002) L-phenylalanine binding and domain organization in human phenylalanine hydroxylase: a differential scanning calorimetry study. Biochemistry 41:7573-7585

Supplementary material

Stereospecific binding of L-phenylalanine to the isolated regulatory domain of human phenylalanine hydroxylase

João Leandro[a,b], Jaakko Saraste[a], Paula Leandro[b] and Torgeir Flatmark[a]*

[a]Department of Biomedicine, University of Bergen, Jonas Lies vei 91, N-5009 Bergen, Norway and [b]Metabolism and Genetics Group, Research Institute for Medicines and Pharmaceutical Sciences (iMed.UL), Faculty of Pharmacy, University of Lisbon, Av. Prof. Gama Pinto, 1649-003 Lisbon, Portugal

Running Title: Stereospecific binding of L-Phe to the isolated *R*-domain of hPAH

*Corresponding author. Department of Biomedicine, University of Bergen, Jonas Lies vei 91, N-5009 Bergen, Norway. Tel.: +47 55586428; Fax.: +47 55586360

Email: torgeir.flatmark@biomed.uib.no

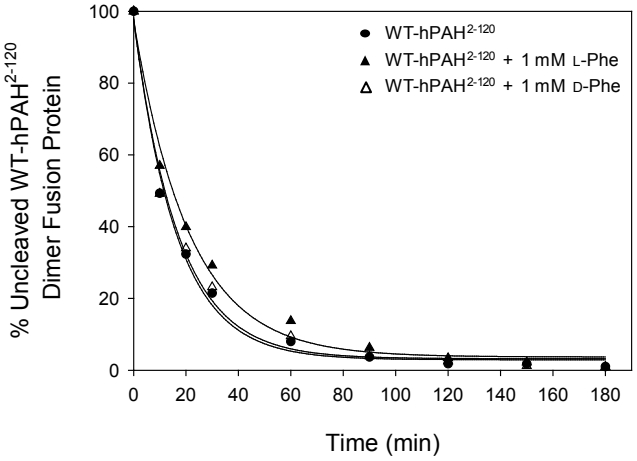

Supplementary Fig. S1 Time-course for the cleavage of dimeric WT-hPAH$^{2-120}$ fusion protein by the restriction protease factor Xa in the absence of any compound (●), with 1 mM L-Phe (▲) and 1 mM D-Phe (△).The data were fitted to a single exponential decay curve. The time-course of cleavage was performed at standard assay conditions (0.74 mg·ml^{-1} fusion protein, 5.0 μg·ml^{-1} factor Xa, 20 mM Na-Hepes, 0.1 M NaCl, pH 7.0 and 25 ^{o}C).

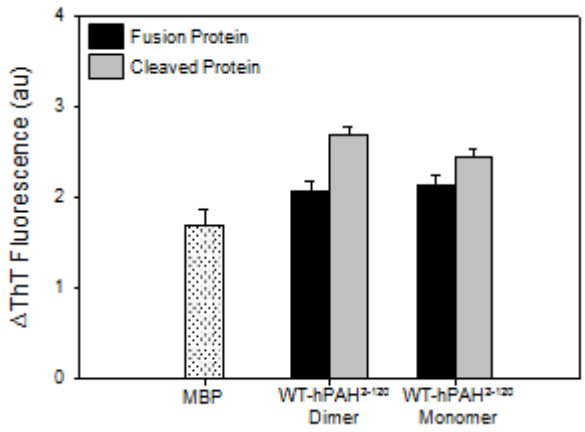

Supplementary Fig. S2 The binding of ANS to the uncleaved and cleaved MBP fusion proteins of dimeric and monomeric WT-hPAH$^{2\text{-}120}$. The ThT fluorescence enhancement (ΔThT) was measured on samples at the beginning of the cleavage reaction of the respective fusion proteins by factor Xa and at the end point (t = 3 h). The MBP protein was included as a control. The response was normalized by subtracting the background fluorescence of ThT and light scattering contribution, and the values represent means ± SD of three independent experiments.

Part V

Insights into the Mechanism of Catalytic Activation of human Phenylalanine Hydroxylase

1. Structure-function analysis of human phenylalanine hydroxylase: The functional role of Tyr138 in the flexible surface/active site loop

Anne J. Stokka, João Leandro , Ole A. Andersen, Paula Leandro, Torgeir Flatmark

Submitted

Structure-function analysis of human phenylalanine hydroxylase - The functional role of Tyr138 in the flexible surface/active site loop

Anne J. Stokka[a], João Leandro[a,b] , Ole A. Andersen[a], Paula Leandro[b] and Torgeir Flatmark[a]*

[a]Department of Biomedicine, University of Bergen, Jonas Lies vei 91, N-5009 Bergen, Norway and [b]Metabolism and Genetics Group, Research Institute for Medicines and Pharmaceutical Sciences (iMed.UL), Faculty of Pharmacy, University of Lisbon, Av. Prof. Gama Pinto, 1649-003 Lisbon, Portugal

Abstract

The mononuclear non-heme iron(II)-containing enzyme phenylalanine hydroxylase (PAH) catalyzes the conversion of L-phenylalanine (L-Phe) to L-tyrosine in the presence of the pterin cofactor (6*R*)-L-*erythro*-5,6,7,8-tetrahydrobiopterin and dioxygen as co-substrates. The high-resolution structure of the dimeric catalytic core domain (ΔN102/ΔC24-hPAH) have revealed that substrate binding triggers a conformational isomerization including a Cα displacement of ~10 Å for Y138 and ~21 Å of its side-chain hydroxyl group from a surface position in a flexible loop to a partially buried position within a hydrophobic core at the active site. In this study, we have compared the tolerance for substitutions of Y138 in the dimeric catalytic core domain and the full-length tetrameric enzyme. The catalytic efficiency ($k_{cat}/[S]_{0.5,Phe}$) of the Y138F/A/E/K substitutions was found to be equally reduced (38 – 95 %) in the two enzyme forms ($r^2 = 0.99$), whereas the coupling efficiency was slightly affected only in the Y138E/K substitutions of the full-length enzyme. Our data lend support to the conclusion that the repositioning of the flexible loop and Y138, as observed in the 3D structure of the catalytic core domain, is representative for the full-length enzyme. Moreover, in the full-length tetramer the L-Phe-triggered conformational isomerization, as measured by surface plasmon resonance spectroscopy, revealed an increased equilibrium signal amplitude in the Y138A mutation and a correlated fold increase in catalytic activation, whereas both were slightly reduced by the K and E substitutions. Thus, Y138 plays a regulatory role both in the L-Phe triggered conformational isomerization related to catalytic activation and in positioning the substrates for catalysis.

Keywords: phenylalanine hydroxylase, mutations, conformational transition, flexible loop, isomerization, hysteresis, substrate activation.

Running Title: Functional role of Tyr138 in human phenylalanine hydroxylase

*Corresponding author. Department of Biomedicine, University of Bergen, Jonas Lies vei 91, N-5009 Bergen, Norway. Tel.: +47 55586428; Fax.: +47 55586360
Email: torgeir.flatmark@biomed.uib.no

Introduction

Phenylalanine hydroxylase (PAH, phenylalanine 4-monooxygenase, EC 1.14.16.1) catalyzes the stereospecific hydroxylation of L-phenylalanine (L-Phe) to L-tyrosine, the first and rate-limiting step in the

Abbreviations : 6-MPH_4, 6-methyl-5,6,7,8-tetrahydropterin; BH_4, (6*R*)-L-*erythro*-5,6,7,8-tetrahydrobiopterin; CvPAH, *Chromobacterium violaceum* PAH; hPAH, human phenylalanine hydroxylase; MBP, maltose binding protein; L-Phe, L-phenylalanine; L-Tyr, L-tyrosine; n_H, Hill coefficient; rPAH, rat phenylalanine hydroxylase; RU, resonance units; SEC, size-exclusion chromatography; SPR, surface plasmon resonance; THA, 3-(2-thienyl)-L-alanine; WT, wild-type.

catabolism of L-Phe (for reviews, see [1-4]). The enzyme uses a five-coordinated Fe(II) to activate dioxygen in the tightly coupled hydroxylation of L-Phe with the pterin cofactor (6*R*)-L-*erythro*-5,6,7,8-tetrahydrobiopterin (BH_4) as the electron donor. Mammalian PAH is a homotetramer (in equilibrium with a dimeric form) with the protomer (452 residues) consisting of three structural and functional subdomains: a N-terminal regulatory domain (residues 1-117), a catalytic core domain (residues 118-410), and a C-terminal oligomerization domain (residues 411-452), with a dimerization and a tetramerization motif (for review, see [1]). The full-length enzyme has been resistant to crystallization, but high-resolution structures of a truncated tetrameric form (ΔN102-hPAH) lacking the N-terminal regulatory domain [5] and a truncated dimeric form (ΔC24-rPAH) lacking 24 C-terminal residues of the tetramerization motif [6], have allowed the generation of a modeled structure of the ligand-free tetrameric full-length hPAH [1]. Moreover, the structures have indicated a functional role of the conformational changes which occur at the active site upon substrate binding, by an apparently induced-fit mechanism [7-10]. Thus, upon L-Phe binding to the binary cofactor complex (ΔN102/ΔC24-hPAH-Fe(II)·BH_4) hinge-bending motions results in a displacement of a flexible surface loop (Fig. 1A and B) [8,9] and a relocation of the side-chain of Y138 to a partially buried position at the active site (Fig. 1C). Additionally, these structures have provided insights into the roles of active site residues and conformational changes in substrate recognition and catalysis, leading to the proposal of a catalytic mechanism for PAH [8]. This functional model has more recently been extended to the full-length form of the structurally and functionally related enzyme rat tyrosine hydroxylase (rTH) in a structure-based mutagenesis study [11]. The 3D structure of a tetrameric N-terminal truncated form of rTH (ΔN155/158-rTH), lacking residues 1-155/158, has also revealed a flexible loop structure, comprising residues 177-191 [12,13], where residues 180-185 correspond to residues 134-139 in the homologous loop of PAH. Mutation of F184 in rTH (~ Y138 in hPAH) in the center of the loop to an A resulted in a ~ 6-fold reduction in both catalytic and coupling efficiency, and it was proposed that a motion of the flexible loop may be involved in the rate-limiting step of the TH reaction [11]. The functional importance of the L-Phe-induced displacement observed for the flexible surface loop in hPAH (conserved in mammalian PAHs) and relocation of the Y138 hydroxyl group to a partially buried position at the active site [8,9] has, however, yet to be addressed experimentally.

To further probe the functional role of Y138 we have generated mutations of this residue (Y138F/A/E/K) in the dimeric catalytic core domain (ΔN102/ΔC24-hPAH) and in the full-length tetrameric hPAH. The functional impact was assessed by steady-state kinetic analysis, by measuring the coupling efficiency of the hydroxylation reaction and by monitoring the substrate-induced conformational isomerization (hysteresis) of the full-length tetramer in real-time by surface plasmon resonance (SPR) spectroscopy. A comparison of the functional perturbations of the two enzyme forms lends support to the conclusion that Y138 in the flexible loop has an equally important catalytic function in the dimeric catalytic core domain and in the full-length tetrameric enzyme. Moreover, in the full-length tetramer Y138 also plays a regulatory role in the L-Phe triggered conformational isomerization of the enzyme, related to its catalytic activation.

Experimental Procedures

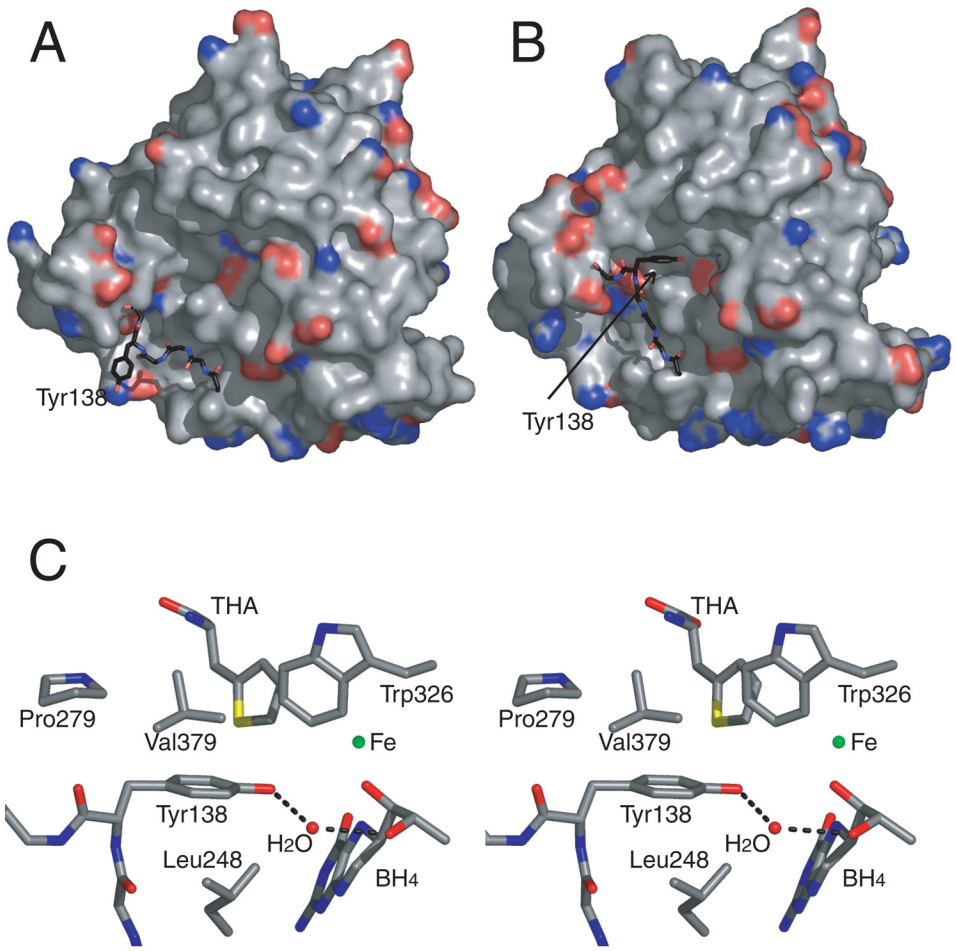

Fig. 1. The localization and interactions of the Y138 residue in the catalytic core domein of human phenylalanine hydroxylase. (A) Electrostatic surface potential of the binary ΔN102/ΔC24-hPAH-Fe(II)·BH_4 complex (PDB i.d. 1j8u) and (B) electrostatic surface potential of the ternary ΔN102/ΔC24-hPAH-Fe(II)·BH_4·THA complex (PDB i.d. 1kw0). The C_α backbone of the loop surrounding Y138 (residues 134-139) and the Y138 side-chain is shown in stick model. Red and blue represent negative and positive potentials, respectively. (C) A stereo view of the Y138 interactions in the hydrophobic core at the active site of the ternary complex ΔN102/ΔC24-hPAH-Fe(II)·BH_4·THA (PDB i.d. 1kw0), where it forms an intramolecular hydrogen bond to a water molecule (Wat 2, red sphere), which is also hydrogen bonded to O2' of the dihydroxypropyl side chain of BH_4. The figures were created using PyMOL, version 1.1 (DeLano Scientific) [29].

Materials

The primers for site-directed mutagenesis were obtained from Eurogentec (Seraing, Belgium) and MWG-Biotech AG (Ebersberg, Germany). The QuikChange® II site-directed mutagenesis kit was from Stratagene (La Jolla, CA, USA). The BigDye® Terminator v3.1 Cycle Sequencing Kit used to prepare DNA for sequencing was delivered by Applied Biosystems, and the DNA sequencing was carried out on an ABI 3730xl DNA Analyzer (Applied Biosystems). The restriction protease factor Xa was obtained from Protein Engineering ApS (Aarhus, Denmark). The reagents and the sensor chip CM5 used in the surface plasmon resonance (SPR) analyses were purchased from Biacore AB (Uppsala, Sweden). (6*R*)-L-*erythro*-5,6,7,8-tetrahydrobiopterin was delivered by Dr. B. Schircks Laboratory (Jona, Switzerland).

Site-specific mutagenesis

The mutations Y138 → F/A/K/E were introduced into the cDNAs of the WT-hPAH and double truncated form ΔN102/ΔC24-hPAH using the QuikChange® II site-directed mutagenesis kit. The pMAL-hPAH [14] and the pMAL-ΔN102/ΔC24-hPAH plasmids [15], containing a cleavage site for factor Xa, were used as the template and the specific oligonucleotides primers listed in Supplementary Table S1 were used for mutagenesis. The constructs were sequenced in both directions to verify the introduction of the desired mutations.

Expression and purification of hPAH

The WT-hPAH, the double truncated form ΔN102/ΔC24-hPAH and respective mutant fusion proteins were expressed in *Escherichia coli* (TB1 cells) with maltose binding protein (MBP) as the fusion partner [14]. The bacteria were harvested after 8 h of induction with 1 mM isopropyl-thio-*β*-D-galactoside (IPTG) at 28 ºC, and the tetrameric and dimeric fusion proteins were purified by affinity chromatography to homogeneity as previously described [14]. The fusions proteins were cleaved for 4 h at 4 ºC by the restriction protease factor Xa (Protein Engineering Technology ApS, Aarhus, Denmark) using a protease to substrate ratio of 1:200 (by mass) followed by size-exclusion chromatography (SEC) at 4 ºC using a Hiload Superdex 200 HR column (1.6 cm×60 cm), prepacked from Amersham Biosciences (GE Healthcare, Uppsala, Sweden), equilibrated and eluted with 20 mM Na-Hepes, 0.2 M NaCl, pH 7.0 at a flow rate of 0.38 $ml \cdot min^{-1}$. The isolated WT-hPAH tetramers (and corresponding full-length tetrameric mutants) and ΔN102/ΔC24-hPAH dimers (and corresponding double truncated dimeric mutants) were collected. Protein concentrations were determined using the absorption coefficient A_{280} (1 $mg \cdot ml^{-1} \cdot cm^{-1}$) of 1.0 for the WT-hPAH [14] and of 1.24 for the ΔN102/ΔC24-hPAH, determined according to the method of Gill and von Hippel [16] in 20 mM Na-Hepes, 200 mM NaCl, pH 7.0, with and without 6 M guanidium chloride. For the isolated Y138F/A/K/E-hPAH full-length mutants, A_{280} (1 $mg \cdot ml^{-1} \cdot cm^{-1}$) of 0.92 was used and for the isolated ΔN102/ΔC24-Y138F/A/K/E-hPAH double truncated mutants, A_{280} (1 $mg \cdot ml^{-1} \cdot cm^{-1}$) of 1.19 was used, both determined by the method of Gill and von Hippel [16].

Protein purity was analyzed by SDS-PAGE in a 10 % (w/v) polyacrylamide gel [17]. The gels were stained by Coomassie Brilliant Blue R-250, scanned using VersaDoc 4000 (Bio-Rad) and quantification of the protein bands was obtained by using the Quantity One 1-D Analysis Software (Bio-Rad, Hercules, CA, USA).

Assay of enzymatic activity and coupling efficiency

The catalytic activity was assayed at 25 ºC in a medium containing 100 mM Na-Hepes, pH 7.0, 5 mM DTT, 0.04 $mg \cdot ml^{-1}$ catalase, 100 μM ferrous ammonium sulfate, 0.5 $mg \cdot ml^{-1}$ bovine serum albumin, 0.3–0.9 μM subunit of tetrameric hPAH or dimeric ΔN102/ΔC24-hPAH and variable concentrations of L-Phe and pterin cofactor BH_4. After 5-min preincubation with L-Phe, the reaction was initiated by adding BH_4 with DTT, and allowed to proceed as described [18]. The amount of L-Tyr formed after one minute (standard), or other selected time points, was measured by HPLC with fluorimetric detection [14]. The steady-state kinetic parameters were calculated by non-linear regression analysis using the SigmaPlot® Technical Graphing Software and the modified Hill equation of LiCata and Allewel [19] for cooperative substrate binding as well as substrate inhibition [18], i.e. the velocity $v = \{V_{max} + V_i([S]^x/K^x_i)\}/\{1 + (K^h/[S]^h) + ([S]^x/K^x_i)\}$ [19]. The exponent x is a second Hill coefficient which allows for the possibility that the

substrate inhibition may also be cooperative, and by varying the value of x between 1 and 3, $x = 2$ gave the best fit for our values. $[S]_{0.5}$ is taken as the concentration of substrate at one-half the calculated V_{max}. In order to study the effect of preincubation with L-Phe on the specific activity (fold activation), 1 mM L-Phe was added either at the start of the preincubation period or together with 75 μM BH_4 at the initiation of the hydroxylation reaction.

The coupling efficiency of the hydroxylation reaction was measured in a mixture containing 0.3–1.5 μM hPAH, 200 μM NADH, 0.05 $\mu g \cdot \mu l^{-1}$ catalase, 10 units superoxide dismutase, 10 μM ferrous ammonium sulfate, 1 mM L-Phe, excess dihydropteridine reductase in 187 mM Hepes buffer, pH 7 at 25 ºC [9]. The reaction was started by adding 100 μM BH_4, and the oxidation of NADH was followed in real-time at 340 nm, using an Agilent 8453 Diode Array spectrophotometer with a Peltier temperature control unit. At selected time points aliquots of the reaction mixture were mixed with acidic ethanol (stop solution), and the amount of L-Tyr formed was measured by HPLC with fluorimetric detection [20]. The degree of coupling was expressed as the molar ratio of L-Tyr formation to BH_4 oxidation (measured as oxidized NADH, using the molar extinction coefficient, $\varepsilon = 6220$ $M^{-1} \cdot cm^{-1}$).

Surface plasmon resonance analysis

Real-time interaction analysis between immobilized enzyme and L-Phe was measured by surface plasmon resonance (SPR) spectroscopy [21-23] using the Biacore 3000 biosensor system (BiaCore AB, Uppsala, Sweden). The full-length enzymes, diluted in 10 mM sodium acetate buffer (pH 5.5) to a final concentration of 0.23 $mg \cdot ml^{-1}$, were immobilized covalently to the hydrophilic carboxymethylated dextran matrix of a CM5 sensor chip by the standard primary amine coupling reaction. The system was equilibrated with HBS-EP (10 mM Hepes, 150 mM NaCl, 3.4 mM EDTA and 0.005 % (v/v) of the surfactant P20, pH 7.4) at a flow rate of 5 $\mu l \cdot min^{-1}$ at 25 ºC [21]. Various concentrations of L-Phe in HBS-EP buffer were injected over immobilized hPAH, and the sensorgrams were analyzed by simple Langmuir response isotherms [21,23]. The equilibrium responses (ΔRU_{eq} at $t = 3$ min) as a function of the free analyte (L-Phe) concentration was used to determine the concentration at half maximal response ($[L]_{0.5}$) and the maximum ΔRU_{eq}-value by nonlinear regression analysis using the SigmaPlot® Technical Graphing Software. The experimental error for replicate injections of the analyte was < 4%. The SPR responses were expressed as $\Delta RU/(ng\ protein/mm^2)$ where 1000 RU corresponds to ~ 1 ng protein/mm^2 of immobilized protein [24].

Computational and structural analysis

The effect of Y138F/A/E/K mutations in the catalytic core domain, ΔN102/ΔC24-hPAH, on the free energy of folding (ΔΔG) was predicted for its unliganded and substrate bound conformational states using the coordinates of Protein Data Bank codes PDB i.d. 1pah and 1kw0, respectively, and the algorithm Concoord/PBSA [25] available at (http://ccpbsa.biologie.uni-erlangen.de/ccpbsa/index.php). Experimental *B*-factors of C_α atoms in the truncated form ΔC24-rPAH (PDB i.d. 1phz) were obtained using the algorithm MolMovDB [26,27] (http://molmovdb.mbb.yale.edu/molmovdb/). To identify the location of potential hinge-bending regions in PAH we subjected the crystal structure of unliganded rPAH (PDB i.d. 2phm) to further analysis using the HingeMaster software program that predicts the

location of hinges in a protein by integrating existing hinge predictors (TLSMD, StoneHinge, FlexOracle and HingeSeq) with a family of novel hinge predictors based on grouping residues with correlated normal mode motions (http://molmovdb.org/cgi-bin/submit-flexoracle.cgi) [28]. Structural images were generated with PyMol [29] available at (http://www.pymol.org/).

Results

Expression and isolation of WT-hPAH and ΔN102/ΔC24-hPAH and their Y138F/A/E/K mutant forms

The fusion proteins of WT-hPAH and ΔN102/ΔC24-hPAH and their Y138F/A/E/K mutant forms were expressed at comparable high yields in *E. coli* and isolated by affinity chromatography and SEC. Cleavage of the fusion proteins and the subsequent isolation of their oligomeric forms by SEC resulted in mg quantities of soluble tetrameric and dimeric forms, respectively, with identical electrophoretic mobilities on SDS-PAGE for the WT and mutant forms (Supplementary Fig. S1A and B).

The effect of Y138F/A/E/K mutations on the free energy of folding

Using the coordinates of the ligand-free double truncated ΔN102/ΔC24-hPAH-Fe(II) dimeric form (PDB i.d. 1pah) and the structure based method for prediction of the free energy of folding [25] of mutant proteins, substitutions of the surface located Y138 (solvent accessibility ~80%) with F (aromatic without the hydroxyl group), A (small, uncharged), E (acidic) and K (basic) residues were found not to have any significant effect on its stability (Fig. 2A). By contrast, using the coordinates of its ternary complex ΔN102/ΔC24-hPAH-Fe(II)·BH_4·THA (PDB i.d. 1kw0)

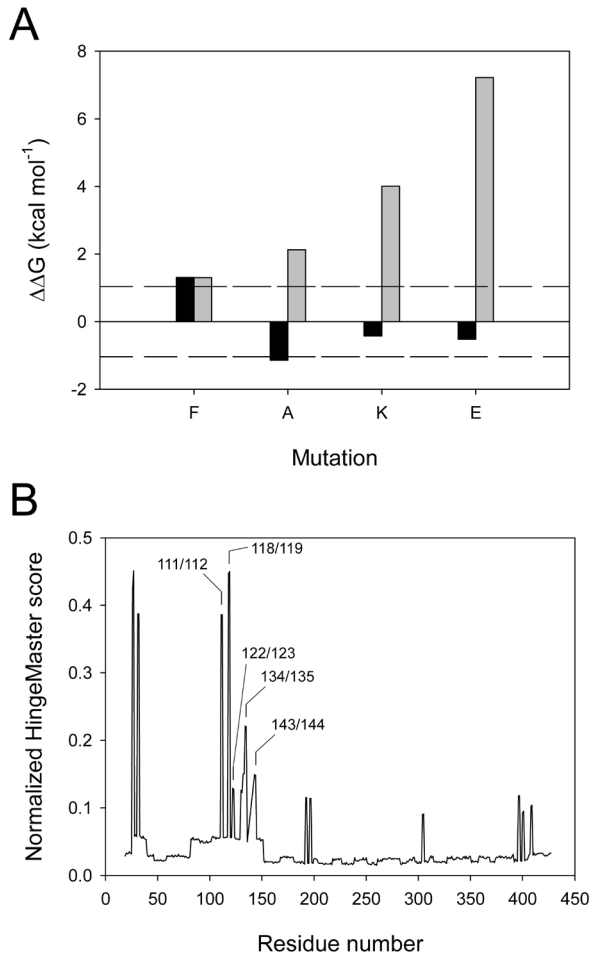

Fig. 2. (A) Estimation of the free energy of folding (ΔΔG) of the mutant proteins (Y138F/A/E/K) using the Concoord/PBSA algorithm [25] with the coordinates of the unliganded double truncated ΔN102/ΔC24-hPAH dimeric form (PDB i.d. 1pah) (black bars), and the coordinates of the ternary complex ΔN102/ΔC24-hPAH-Fe(II)·BH_4·THA (PDB i.d. 1kw0) (gray bars). The two horizontal dashed lines represent the standard deviation of the method (σ = 1.04 kcal·mol^{-1}). (B) Combined hinge prediction scores of the *R-C* domain structure in the non-phosphorylated form of rPAH (PDB i.d. 2phm) using the HingeMaster server [28] as a function of amino acid residue number with particular hinge bending regions indicated.

the A, K and E substitutions of the active site located Y138 (solvent accessibility ~22%) were predicted to have an increasingly (A<K<E) destabilizing effect (Fig. 2A). A similar comparison could, however, not be made for the two truncated forms ΔC24-rPAH-Fe(III) (PDB i.d. 1phz) and ΔN102-hPAH-Fe(III) (PDB i.d. 2pah), since no electron density was observed for the residues

Table 1. Steady-state kinetic properties of dimeric double truncated form ΔN102/ΔC24-hPAH, dimeric Y138 double truncated mutant forms, tetrameric wild-type and tetrameric Y138 mutant forms of hPAH (full-length).

	L-Phe						BH_4	
hPAH	V_{max} (nmol Tyr·min^{-1}·mg^{-1})	$[S]_{0.5}$ (μM)	h	$k_{cat}/[S]_{0.5}$[a] (μM^{-1}·min^{-1})	Substrate inhibition	Fold activation	V_{max} (nmol Tyr·min^{-1}·mg^{-1})	K_m (μM)
ΔN102/ΔC24	7948 ± 339	46 ± 4	1.47 ± 0.13	6.50	yes (pronounced)	0.9	4804 ± 222	25 ± 4
ΔN102/ΔC24-Y138F	4995 ± 346	47 ± 6	1.47 ± 0.16	4.00	yes (pronounced)	0.9	4638 ± 214	62 ± 7
ΔN102/ΔC24-Y138A	2385 ± 118	36 ± 3	1.64 ± 0.17	2.49	yes (pronounced)	0.8	1267 ± 70	27 ± 5
ΔN102/ΔC24-Y138E	2068 ± 70	63 ± 4	1.28 ± 0.07	1.23	yes	1.0	2336 ± 94	60 ± 6
ΔN102/ΔC24-Y138K	2174 ± 53	128 ± 7	1.03 ± 0.03	0.64	yes	0.9	2384 ± 73	58 ± 4
Wild-type	5056 ± 222	170 ± 10	1.95 ± 0.17	1.49	yes	5.3	5840 ± 262	39 ± 5
Y138F	2869 ± 145	172 ± 7	1.70 ± 0.11	0.83	yes	5.2	1939 ± 83	35 ± 5
Y138A	1653 ± 57	144 ± 9	1.80 ± 0.15	0.57	yes	9.2	1924 ± 119	47 ± 8
Y138E	856 ± 13	203 ± 9	1.47 ± 0.06	0.21	no	2.2	752 ± 19	32 ± 3
Y138K	702 ± 16	459 ± 27	1.20 ± 0.07	0.08	no	3.9	668 ± 29	44 ± 5

The specific activity and kinetic properties were determined at 25 ºC; the substrate concentrations were 1 mM L-Phe (BH_4 variable) and 75 μM BH_4 (L-Phe variable).
[a] The catalytic efficiency was calculated on the basis of a subunit molecular mass of 50 kDa for the full-length forms and 37.6 kDa for the double truncated forms of hPAH. $[S]_{0.5}$ represents the L-Phe concentration at half-maximal activity and $k_{cat}/[S]_{0.5}$ the catalytic efficiency.

137-142 of the flexible loop in these structures (Supplementary Fig. S2).

The effect of Y138F/A/E/K mutations on the steady-state kinetic parameters

The steady-state kinetic parameters of the dimeric catalytic core domain and the tetrameric WT-hPAH and their Y138F/A/E/K mutant forms were determined with L-Phe and BH_4 as the variable substrates (Table 1). The dimeric WT catalytic core domain revealed a 4-fold higher catalytic efficiency ($k_{cat}/[S]_{0.5,L\text{-}Phe}$) than the WT full-length tetrameric enzyme, and was not further activated by preincubation with L-Phe. Moreover, it demonstrated a more pronounced substrate inhibition than the tetrameric enzyme (Fig. 3A and B), which complicated the determination of the kinetic cooperativity with respect to L-Phe (see Methods section). The substitutions Y138F/A/E/K reduced the catalytic efficiency to 62, 38, 19 and 10 % of WT, respectively, and except for the Y→A substitution the K_m value for BH_4 was increased (Table 1).

L-Phe plays a major role in the regulation of the catalytic activity of the full-length tetrameric PAH which is activated several-fold by preincubation with the substrate and displays a positive kinetic cooperativity with respect to L-Phe (for review, see [1-4]). The tetrameric WT-hPAH revealed a Hill coefficient of n_H = 1.95 ± 0.17 and a $[S]_{0.5}$-value of 170 ± 10 μM with a 5.3-fold enhancement of the catalytic activity (activation) on a 5-min preincubation with 1 mM L-Phe at 25 ºC (Table 1). The substitutions Y138F/A/E/K lowered the catalytic efficiency ($k_{cat}/[S]_{0.5,L\text{-}Phe}$) to 56, 38, 18 and 5 % of WT, respectively, but the K_m value for BH_4 did not change significantly (Table 1). Interestingly, the Y138A tetramer revealed a slightly decreased $[S]_{0.5}$ value (144 ± 9 μM) for L-Phe and a higher fold activation (9.2-fold) on preincubation with 1 mM L-Phe, whereas in the Y138E/K mutations the $[S]_{0.5,L\text{-}Phe}$ value increased and the fold activation by substrate was reduced (Table 1). All the mutant tetramers revealed a lower Hill coefficient than WT-hPAH (Table 1), most pronounced for the Y138E/K mutant forms.

From Fig. 4 it is seen that a high correlation (r^2 = 0.99) was observed between the effect of the mutations on the catalytic efficiency ($k_{cat}/[S]_{0.5,Phe}$) of the catalytic core domain and the full-length tetrameric enzyme. Moreover, as seen from Table 2 the hydroxylation reaction was fully coupled in the catalytic core domain mutants whereas a slight uncoupling was observed for the Y138A/E/K mutations of the full-length tetrameric enzyme.

Table 2. The degree of coupling of the hydroxylation reaction catalyzed by dimeric double truncated form ΔN102/ΔC24-hPAH, dimeric Y138 double truncated mutant forms, tetrameric wild-type and tetrameric Y138 mutant forms of hPAH (full-length). The data represent the mean values of 3-6 independent assays.

hPAH	Coupling efficiency (mol Tyr formed/mol BH_4 oxidized)
ΔN102/ΔC24	0.97 ± 0.07
ΔN102/ΔC24-Y138F	1.08 ± 0.05
ΔN102/ΔC24-Y138A	0.96 ± 0.05
ΔN102/ΔC24-Y138E	1.03 ± 0.02
ΔN102/ΔC24-Y138K	1.00 ± 0.02
Wild-type	0.97 ± 0.03
Y138F	0.92 ± 0.03
Y138A	0.82 ± 0.11
Y138E	0.78 ± 0.07
Y138K	0.87 ± 0.05

The Y138F/A/E/K mutations perturb the L-Phe-induced conformational isomerization of the full-length tetrameric enzyme

The L-Phe triggered activation of the tetrameric enzyme is characterized by a reversible conformational isomerization, a characteristic feature of this hysteretic enzyme. Surface plasmon resonance (SPR) and intrinsic tryptophan fluorescence spectroscopy have previously been used to monitor in real-time this process which occurs on a *s*-to-*min* time scale [21-23,30]. Here, the full-length tetrameric WT-hPAH and its mutant forms were immobilized at high ΔRU-values in the range of 32000-38000 RU, i.e. 32-38 ng bound tetramer/mm^2. As previously described [22,23] a time-dependent increase in the SPR signal response to L-Phe injection was observed for the full-length WT-hPAH tetramer and in all the mutant forms, with ΔRU_{eq} reached at ~3 min (individual sensorgrams not shown). However, the maximum ΔRU_{eq} value (ΔRU_{max}), calculated from the respective L-Phe *vs* ΔRU_{eq} response isotherms varied (Fig. 5A). Thus, the ΔRU_{max} was increased in the Y138A mutant form whereas it was slightly reduced in the Y138E/K mutants. Moreover, from Fig. 5B it is seen that the fold increase in the catalytic activity on preincubation with 1 mM L-Phe (fold activation) (Table 1) correlates (r^2 = 0.96) with the ΔRU_{eq} of the SPR signal response at the same L-Phe concentration.

Since the catalytic core domain ΔN102/ΔC24-hPAH is already in an activated state, it did not demonstrate any hysteresis, but only a minor time independent SPR response to L-Phe binding (~0.05 RU/ng subunit/mm^2) [23].

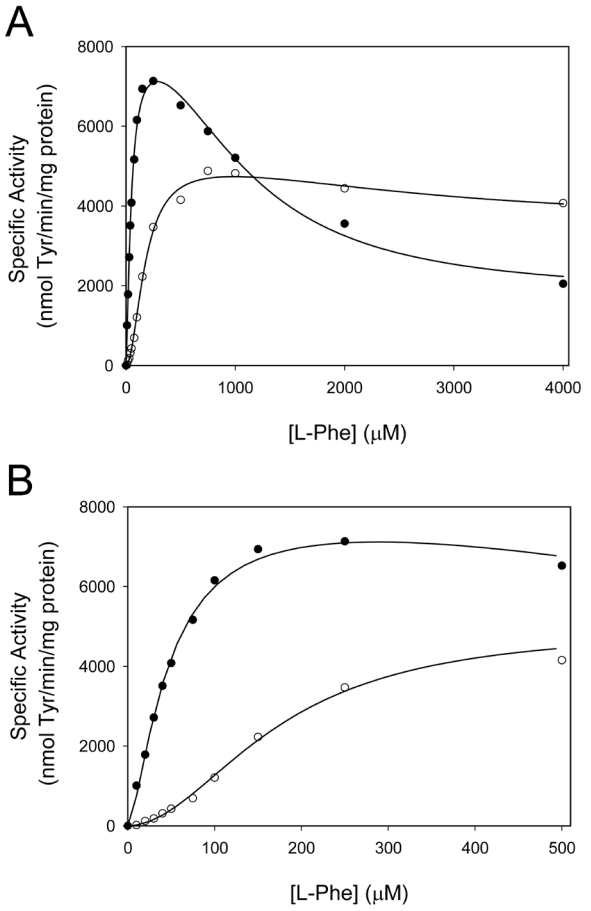

Fig. 3. The effect of substrate (L-Phe) concentration on the catalytic activity of the dimeric catalytic core domain ΔN102/ΔC24-hPAH (●) and of the full-length tetrameric WT-hPAH (○). The hPAH activity was assayed at standard conditions (0–4 mM L-Phe, 75 μM BH_4 and 25 ºC). (B) Close-up of the data shown in A obtained in the concentration range 0–500 μM L-Phe, demonstrating a positive cooperativity for the full-length tetrameric WT-hPAH.

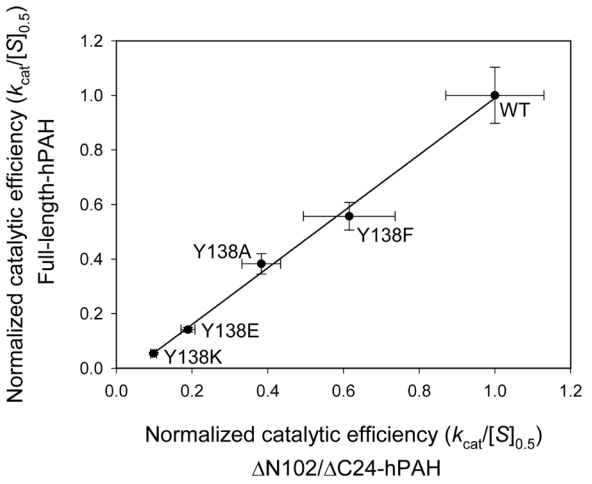

Fig. 4. Secondary plot demonstrating the positive correlation between the catalytic efficiency ($k_{cat}/[S]_{0.5}$) of the Y138F/A/E/K mutations in the dimeric catalytic core domain (ΔN102/ΔC24-hPAH) and the full-length tetrameric WT-hPAH. The primary data are given in Table 1. The values for the catalytic efficiency were normalized with the WT full-length and WT catalytic core domain as a reference (1.0). Error bars represent SD; the correlation coefficient was r^2 = 0.99.

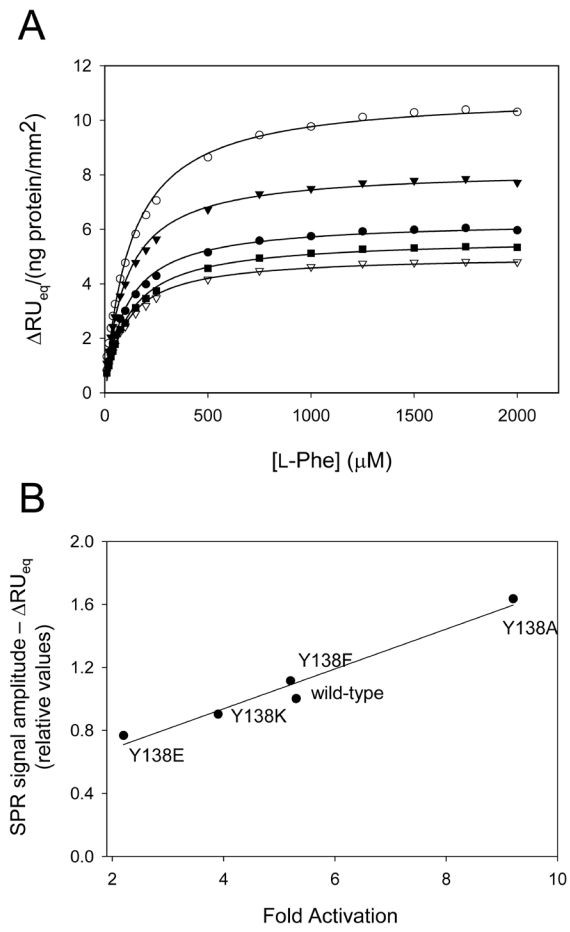

Fig. 5. The equilibrium L-Phe binding isotherm of full-length tetrameric WT-hPAH and respective mutant forms as measured by surface plasmon resonance (SPR). (A) The SPR response isotherm for immobilized full-length tetrameric WT-hPAH (●), Y138F-hPAH (▼), Y138A-hPAH (○), Y138E-hPAH (▽) and Y138K-hPAH (■) to increased concentrations of L-Phe. The truncated form ΔN102/ΔC24-hPAH (catalytic core enzyme) was immobilized to the reference cell. The experiments were performed at 25 ºC in HBS-EP buffer (10 mM Hepes, 150 mM NaCl, 3.4 mM EDTA and 0.005 % (v/v) of the surfactant P20, pH 7.4). The experimental error for replicate injections of the analyte was < 4%. The curve fitting of the binding isotherms was calculated by non-linear regression analysis using SigmaPlot® Technical Graphing Software with a r^2 = 0.99. (B) Secondary plot demonstrating the relationship between the fold activation and the substrate-induced global conformational change (ΔR_{eq}) of full-length tetrameric WT-hPAH and respective mutant forms as measured by SPR. The primary data are given in Table 1 and Fig. 5A. The fold activation was measured with and without a 5-min preincubation step of the enzyme with the substrate L-Phe (1 mM). The relative values of the SPR signal amplitude corresponds to the ΔRU_{eq} values for the equilibrium L-Phe binding isotherms at 1 mM L-Phe, with the wild-type as a reference (1.0). A strong positive correlation (r^2 = 0.96) between the fold activation and the global conformational change is observed.

Discussion

The existence of coupled residue motions on various time scales in enzymes is now well accepted, and their detailed characterization has become an essential element in understanding the role of protein dynamics in catalysis. So far, only a small number of enzymes have been shown to rely on essential coupled residue motions for catalysis (for reviews, see [31] and [32]). Based on combined enzyme kinetic and biophysical studies on the full-length tetrameric mammalian PAH there is broad agreement that its catalytic activation by L-Phe, preceding the chemical steps of the reaction, can be presented by the following equation,

$$\text{PAH} + \text{Phe} \overset{k_1}{\leftrightarrow} \text{PAH}\cdot\text{Phe} \overset{k_2}{\leftrightarrow} \text{PAH}^*\cdot\text{Phe} \qquad (1)$$

where PAH represents the ligand-free state of the enzyme, PAH·Phe its low-activity binary enzyme-

substrate complex and PAH*·Phe the binary complex of the high-activity state in which a relatively slow (*s*-to-*min* time scale) conformational isomerization has occurred [21-23,33], with $k_{2,obs} << k_{1,obs}$, characteristic of a hysteretic enzyme. The substrate triggered isomerization has been followed in real-time by intrinsic tryptophan fluorescence and SPR spectroscopy [21-23], and found to be correlated (r^2 = 0.93 - 0.96) to the degree of catalytic activation [22,33]. Moreover, the high-resolution structures of the ligand-free form, the binary (with BH_4) and the ternary (with BH_4 and 3-(2-thienyl)-L-alanine (THA)) substrate complexes of its catalytic core domain (ΔN102/ΔC24-hPAH-Fe(II)) have provided insights into potentially catalytically related motions [7-9]. In this enzyme form substrate binding triggers structural changes throughout the entire catalytic domain [8,9], including the active site (Fig. 1), which is considered to represent the "epicenter" of the conformational transition [8,9]. Substrate binding also results in a change in the co-ordination of the catalytic ferrous iron and a reorientation of residues lining the active site [7-9], representing major contributions to catalysis [8,9,34]. One of the most prominent motions is observed for the flexible surface loop (residues 131-155) with a maximum Cα displacement of ~10 Å for Y138 [8,9], bringing its hydroxyl group ~21 Å closer to the iron atom (O^{η} only 6.5 Å away) (Fig. 1 A and B). The phenolic group packs (interactions within 4.0 Å) within a hydrophobic pocket consisting of the side-chains of L248, W326, V379 as well as the main-chain of P279 and the aromatic group of the substrate (Fig. 1C), and its position stabilized by hydrogen bonding to the pterin cofactor and hydrophobic contacts (Fig. 1C). The question is, however, to what extent this relocation of the mobile surface loop and Y138 is representative for the full-length enzyme.

The 3D structure of the ligand-free truncated dimeric form ΔC24-rPAH-Fe(III), with an intact regulatory domain but lacking 24 residues of the C-terminal tetramerization motif [6] (PDB i.d. 1phz), is the closest representative for the ligand-free full-length dimeric WT-PAH, also with respect to catalytic activity and regulatory properties [23]. Thus, L-Phe triggers a similar reversible conformational isomerization as in the full-length enzyme and demonstrates a catalytic activation by L-Phe preincubation [23]. The 3D structure of ΔC24-rPAH-Fe(III) also identified the flexible surface loop (residues 131-155) with a high crystallographic *B*-factor (Supplementary Fig. S2), as in the catalytic core domain structure, but with an unassigned electron density for the center residues 137-142. Moreover, two potential hinge-bending regions are predicted within the loop (Fig. 2B). These structural properties imply that the Y138 loop in ΔC24-hPAH-(Fe(III) has the flexibility required for its relocation to the active site on substrate binding, as observed in the ΔN102/ΔC24-hPAH-Fe(II) catalytic core domain (Fig. 1A-C), which may be extended to include the full-length enzyme. This conclusion is further supported by the kinetic analyses of the Y138F/A/E/K mutations in the full-length tetrameric hPAH (Table 1 and Fig. 4) demonstrating, with minor differences, similar kinetic effects as observed for the dimeric catalytic core domain. Additionally, Y138 shows a regulatory role in the L-Phe triggered conformational isomerization and catalytic activation of the tetrameric enzyme.

In the structurally and functionally related enzyme tyrosine hydroxylase (rTH), the mutation F184A (~ Y138 in hPAH) in the homologous 14 residue flexible loop structure (residues 177-191) of the full-length enzyme was found to result in a 95 % reduction in V_{max} and 84 % reduction in the coupling efficiency, using the pterin cofactor analog 6-MPH_4 as the electron donor,

and it was concluded that the F184 loop controls the coupling of L-Tyr hydroxylation to tetrahydropterin oxidation [11]. Thus, the reported kinetic effects of the F184A mutation in rTH are far more dramatic than those observed here for the Y138A substitution in hPAH using the natural cofactor BH_4 (Tables 1 and 2), the preferred electron donor in studies on coupling efficiency [35]. Although the catalytic mechanism of PAH and TH is considered to be essentially the same, the regulatory properties of the two enzymes are quite different [1,36,37]. In striking contrast to PAH no catalytic activation of TH is observed on preincubation with its substrate, and a potential conformational change upon substrate (L-Tyr) binding has not been demonstrated experimentally [37]. Here, our mutation analyses have revealed a regulatory role of Y138 also in the catalytic activation of the full-length enzyme (Fig. 5) since its substitution with F/A/E/K perturbs the L-Phe induced isomerization equilibrium. Thus, the propensity to adopt to its catalytically most active isomeric conformation (~PAH*·L-Phe in eqn. 1), as measured by ΔRU_{max} of the equilibrium SPR signal response, is promoted by the Y→A substitution (Fig. 5A), and the related fold catalytic activation [22] is enhanced in a proportional way (Fig. 5B). These effects of the Y138A mutation indicate that the substitution of the bulky aromatic side-chain may allow an easier access of this residue to the hydrophobic active site pocket (Fig. 1C), and thus promote the substrate-induced conformational isomerization (Fig. 5), although it simultaneously negatively impacting the catalytic reaction (Table 1). In the Y138F substitution no significant change was observed in the $[S]_{0.5,Phe}$ value, the K_m for the cofactor and the fold activation by substrate preincubation, but the V_{max} value decreased by 38 % (truncated form) and 34 % (full-length form) with L-Phe as the variable substrate (Table 1). In this case a loss of the water (WAT2) mediated hydrogen bond (2.7 Å), linking the side-chain of Y138 with BH_4 O2' (Fig. 1C and Fig. S3) [8,9], may cause a structural destabilization of the active site interactions. Although WAT2 in the WT structure may have a stabilizing effect on the active site structure, this iron co-ordinated water does not seem to be of importance in the catalytic reaction [8,38]. As expected from the computed ΔΔG values for the mutations (Fig. 2) the most perturbing effects on substrate activation and catalytic efficiency was observed when Y138 is substituted with the hydrophilic and charged amino acids (K and E), presumably explained by an unfavorable polarity/charge effect and steric conflict with the side-chains of residues lining the active site.

The catalytic mechanism of PAH is sequential and all three substrates (BH_4, L-Phe and O_2) are bound at the active site before any L-Tyr is released [35,39]. Our crystal structure analyses of the binary hPAH-Fe(II)·BH_4 and ternary hPAH-Fe(II)·BH_4·THA complexes of the catalytic core domain [7,8] have demonstrated that an open co-ordination position on the iron becomes available for dioxygen only in the presence of both reduced pterin cofactor (BH_4) and substrate (THA). The proposed reaction scheme [8] has later been supported by steady-state kinetic analyses using a monomeric bacterial enzyme (CvPAH) which is devoid of the complex regulatory properties of the mammalian enzyme [1]. The catalytic mechanism was found to be fully ordered, with reduced pterin cofactor binding the active site first, L-Phe second and O_2 last [39]. Interestingly, the overall fold of CvPAH resembles the catalytic domain in hPAH [40], and has a ~ 10-fold higher specific activity [39,40]. The finding that the hydroxylation of L-Phe catalyzed by the Y138F/A/E/K mutant forms of the catalytic core enzyme are all fully coupled (Table 2), and almost fully

coupled in the full-length enzyme, indicates that the reduced pterin cofactor is protected from oxidation as in the WT form. The Y138 loop behaves like a "lid" domain, whose proper closure restricts the accessibility of bulk solvent. Our data suggest that the reduced catalytic efficiency (k_{cat} /$[S]_{0.5,Phe}$) measured for all the mutant forms (Table 1) reflect a perturbation of the precise positioning of active site residues (Fig. 1C), and a destabilization of the transition state complex.

A destabilization of the active site structure which involves Y138 may also occur in some mutations associated with phenylketonuria (PKU). Past magnetic circular dichroism and X-ray absorption spectroscopy of the full-length tetrameric WT-rPAH have confirmed the 3D structure analyses of the catalytic core enzyme [8,9] that the substrate triggered conformational isomerization brings the catalytic ferrous iron and the substrates in proper position for activation of dioxygen and catalysis [34]. One PKU mutant (E280K) was found to result in a destabilization of the active site structure, leading to a partly uncoupled hydroxylation reaction and a 60-fold reduction of the specific activity [34]. Interestingly, in our 3D structure of the ternary complex of the WT catalytic core enzyme, the side-chain of E280 forms a stabilizing hydrogen bond with the amide N of Y138 (Supplementary Fig. S3). The E280K substitution may abolish this hydrogen bond which at least partly explains the kinetic effects of the mutation.

In summary, the high-resolution crystal structures of mammalian PAH have revealed a unique active-site design, and together with biochemical/biophysical data indicated the importance of conformational changes in the mechanism of PAH catalysis. Here, our Y138F/A/E/K mutations in the catalytic domain have provided functional insights into the crystallographically observed substrate triggered repositioning of a flexible surface loop with the center residue Y138 moving from a surface position to a partially buried position at the active site. In the full-length tetrameric enzyme the mutations perturb both the L-Phe triggered global conformational isomerization (catalytic activation), including the repositioning of the loop, and the formation of a precise orientation of catalytic groups and residues necessary for catalysis.

Acknowledgements

This work was supported by Fundação para a Ciência e a Tecnologia, Portugal, grant SFRH/BD/19024/2004 and the University of Bergen, Norway. We thank Ali Sepulveda Munõz and Randi M. Svebak for expert technical assistance.

References

[1] T. Flatmark, R.C. Stevens, Structural Insight into the Aromatic Amino Acid Hydroxylases and Their Disease-Related Mutant Forms, Chem. Rev. 99 (1999) 2137-2160.
[2] S.E. Hufton, I.G. Jennings, R.G. Cotton, Structure and function of the aromatic amino acid hydroxylases, Biochem. J. 311 (Pt 2) (1995) 353-366.
[3] T.J. Kappock, J.P. Caradonna, Pterin-Dependent Amino Acid Hydroxylases, Chem. Rev. 96 (1996) 2659-2756.
[4] S. Kaufman, The phenylalanine hydroxylating system, Adv. Enzymol. Relat. Areas Mol. Biol. 67 (1993) 77-264.
[5] F. Fusetti, H. Erlandsen, T. Flatmark, R.C. Stevens, Structure of tetrameric human phenylalanine hydroxylase and its implications for phenylketonuria, J. Biol. Chem. 273 (1998) 16962-16967.
[6] B. Kobe, I.G. Jennings, C.M. House, B.J. Michell, K.E. Goodwill, B.D. Santarsiero, R.C. Stevens, R.G. Cotton, B.E. Kemp, Structural basis of autoregulation of phenylalanine hydroxylase, Nat. Struct. Biol. 6 (1999) 442-448.
[7] O.A. Andersen, T. Flatmark, E. Hough, High resolution crystal structures of the catalytic domain of human phenylalanine hydroxylase in its catalytically active Fe(II) form and binary complex with tetrahydrobiopterin, J. Mol. Biol. 314 (2001) 279-291.
[8] O.A. Andersen, T. Flatmark, E. Hough, Crystal structure of the ternary complex of the catalytic domain of human phenylalanine hydroxylase with tetrahydrobiopterin and 3-(2-thienyl)-L-alanine, and its implications for the mechanism of catalysis and substrate activation, J. Mol. Biol. 320 (2002) 1095-1108.
[9] O.A. Andersen, A.J. Stokka, T. Flatmark, E. Hough, 2.0 Å resolution crystal structures of the ternary complexes of human phenylalanine hydroxylase catalytic domain with tetrahydrobiopterin and 3-(2-thienyl)-L-alanine or L-

norleucine: substrate specificity and molecular motions related to substrate binding, J. Mol. Biol. 333 (2003) 747-757.
[10] H. Erlandsen, E. Bjørgo, T. Flatmark, R.C. Stevens, Crystal structure and site-specific mutagenesis of pterin-bound human phenylalanine hydroxylase, Biochemistry 39 (2000) 2208-2217.
[11] S.C. Daubner, J.T. McGinnis, M. Gardner, S.L. Kroboth, A.R. Morris, P.F. Fitzpatrick, A flexible loop in tyrosine hydroxylase controls coupling of amino acid hydroxylation to tetrahydropterin oxidation, J. Mol. Biol. 359 (2006) 299-307.
[12] K.E. Goodwill, C. Sabatier, C. Marks, R. Raag, P.F. Fitzpatrick, R.C. Stevens, Crystal structure of tyrosine hydroxylase at 2.3 Å and its implications for inherited neurodegenerative diseases, Nat. Struct. Biol. 4 (1997) 578-585.
[13] K.E. Goodwill, C. Sabatier, R.C. Stevens, Crystal structure of tyrosine hydroxylase with bound cofactor analogue and iron at 2.3 Å resolution: self-hydroxylation of Phe300 and the pterin-binding site, Biochemistry 37 (1998) 13437-13445.
[14] A. Martínez, P.M. Knappskog, S. Olafsdottir, A.P. Døskeland, H.G. Eiken, R.M. Svebak, M. Bozzini, J. Apold, T. Flatmark, Expression of recombinant human phenylalanine hydroxylase as fusion protein in *Escherichia coli* circumvents proteolytic degradation by host cell proteases. Isolation and characterization of the wild-type enzyme, Biochem. J. 306 (1995) 589-597.
[15] P.M. Knappskog, T. Flatmark, J.M. Aarden, J. Haavik, A. Martínez, Structure/function relationships in human phenylalanine hydroxylase. Effect of terminal deletions on the oligomerization, activation and cooperativity of substrate binding to the enzyme, Eur. J. Biochem. 242 (1996) 813-821.
[16] S.C. Gill, P.H. von Hippel, Calculation of protein extinction coefficients from amino acid sequence data, Anal. Biochem. 182 (1989) 319-326.
[17] U.K. Laemmli, Cleavage of structural proteins during the assembly of the head of bacteriophage T4, Nature 227 (1970) 680-685.
[18] T. Solstad, T. Flatmark, Microheterogeneity of recombinant human phenylalanine hydroxylase as a result of nonenzymatic deamidations of labile amide containing amino acids. Effects on catalytic and stability properties, Eur. J. Biochem. 267 (2000) 6302-6310.
[19] V.J. LiCata, N.M. Allewell, Is substrate inhibition a consequence of allostery in aspartate transcarbamylase?, Biophys. Chem. 64 (1997) 225-234.
[20] A. Martínez, S. Olafsdottir, J. Haavik, T. Flatmark, Inactivation of purified phenylalanine hydroxylase by dithiothreitol, Biochem. Biophys. Res. Commun. 182 (1992) 92-98.
[21] T. Flatmark, A.J. Stokka, S.V. Berge, Use of surface plasmon resonance for real-time measurements of the global conformational transition in human phenylalanine hydroxylase in response to substrate binding and catalytic activation, Anal. Biochem. 294 (2001) 95-101.
[22] A.J. Stokka, R.N. Carvalho, J.F. Barroso, T. Flatmark, Probing the role of crystallographically defined/predicted hinge-bending regions in the substrate-induced global conformational transition and catalytic activation of human phenylalanine hydroxylase by single-site mutagenesis, J. Biol. Chem. 279 (2004) 26571-26580.
[23] A.J. Stokka, T. Flatmark, Substrate-induced conformational transition in human phenylalanine hydroxylase as studied by surface plasmon resonance analyses: the effect of terminal deletions, substrate analogues and phosphorylation, Biochem. J. 369 (2003) 509-518.
[24] U. Jönsson, L. Fägerstam, B. Ivarsson, B. Johnsson, R. Karlsson, K. Lundh, S. Löfås, B. Persson, H. Roos, I. Rönnberg, S. Sjölander, E. Stenberg, R. Ståhlberg, C. Urbaniczky, H. Östlin, M. Malmqvist, Real-Time Biospecific Interaction Analysis Using Surface-Plasmon Resonance and a Sensor Chip Technology, Biotechniques 11 (1991) 620-627.
[25] A. Benedix, C.M. Becker, B.L. de Groot, A. Caflisch, R.A. Böckmann, Predicting free energy changes using structural ensembles, Nat. Methods 6 (2009) 3-4.
[26] N. Echols, D. Milburn, M. Gerstein, MolMovDB: analysis and visualization of conformational change and structural flexibility, Nucleic Acids Res. 31 (2003) 478-482.
[27] M. Gerstein, W. Krebs, A database of macromolecular motions, Nucleic Acids Res 26 (1998) 4280-4290.
[28] S.C. Flores, K.S. Keating, J. Painter, F. Morcos, K. Nguyen, E.A. Merritt, L.A. Kuhn, M.B. Gerstein, HingeMaster: normal mode hinge prediction approach and integration of complementary predictors, Proteins 73 (2008) 299-319.
[29] W.L. Delano, The PyMOL Molecular Graphics System, DeLano Scientific, San Carlos, USA. (2002).
[30] T. Solstad, A.J. Stokka, O.A. Andersen, T. Flatmark, Studies on the regulatory properties of the pterin cofactor and dopamine bound at the active site of human phenylalanine hydroxylase, Eur. J. Biochem. 270 (2003) 981-990.
[31] P.K. Agarwal, Enzymes: An integrated view of structure, dynamics and function, Microb Cell Fact 5 (2006) 2.
[32] A. Tousignant, J.N. Pelletier, Protein motions promote catalysis, Chem. Biol. 11 (2004) 1037-1042.
[33] R. Shiman, D.W. Gray, Substrate activation of phenylalanine hydroxylase. A kinetic characterization, J. Biol. Chem. 255 (1980) 4793-4800.
[34] J.N. Kemsley, E.C. Wasinger, S. Datta, N. Mitic, T. Acharya, B. Hedman, J.P. Caradonna, K.O. Hodgson, E.I. Solomon, Spectroscopic and kinetic studies of PKU-inducing mutants of phenylalanine hydroxylase: Arg158Gln and Glu280Lys, J. Am. Chem. Soc. 125 (2003) 5677-5686.
[35] T.J. Kappock, P.C. Harkins, S. Friedenberg, J.P. Caradonna, Spectroscopic and kinetic properties of unphosphorylated rat hepatic phenylalanine hydroxylase expressed in *Escherichia coli*. Comparison of resting and activated states, J. Biol. Chem. 270 (1995) 30532-30544.
[36] P.F. Fitzpatrick, Mechanism of aromatic amino acid hydroxylation, Biochemistry 42 (2003) 14083-14091.
[37] G.R. Sura, M. Lasagna, V. Gawandi, G.D. Reinhart, P.F. Fitzpatrick, Effects of ligands on the mobility of an active-site loop in tyrosine hydroxylase as monitored by fluorescence anisotropy, Biochemistry 45 (2006) 9632-9638.
[38] E. Olsson, A. Martínez, K. Teigen, V.R. Jensen, Water dissociation and dioxygen binding in phenylalanine hydroxylase, Eur. J. Inorg. Chem. 2010 (2010) 351-356.
[39] A. Volner, J. Zoidakis, M.M. Abu-Omar, Order of substrate binding in bacterial phenylalanine hydroxylase and its mechanistic implication for pterin-dependent oxygenases, J. Biol. Inorg. Chem. 8 (2003) 121-128.
[40] H. Erlandsen, J.Y. Kim, M.G. Patch, A. Han, A. Volner, M.M. Abu-Omar, R.C. Stevens, Structural comparison of

bacterial and human iron-dependent phenylalanine hydroxylases: similar fold, different stability and reaction rates, J. Mol. Biol. 320 (2002) 645-661.

Supplementary data for

Structure-function analysis of human phenylalanine hydroxylase - The functional role of Tyr138 in the flexible surface/active site loop

Anne J. Stokka[a], João Leandro[a,b] , Ole A. Andersen[a], Paula Leandro[b] and Torgeir Flatmark[a]*

[a]Department of Biomedicine, University of Bergen, Jonas Lies vei 91, N-5009 Bergen, Norway and [b]Metabolism and Genetics Group, Research Institute for Medicines and Pharmaceutical Sciences (iMed.UL), Faculty of Pharmacy, University of Lisbon, Av. Prof. Gama Pinto, 1649-003 Lisbon, Portugal

Running Title: Functional role of Tyr138 in human phenylalanine hydroxylase

*Corresponding author. Department of Biomedicine, University of Bergen, Jonas Lies vei 91, N-5009 Bergen, Norway. Tel.: +47 55586428; Fax.: +47 55586360

Email: torgeir.flatmark@biomed.uib.no

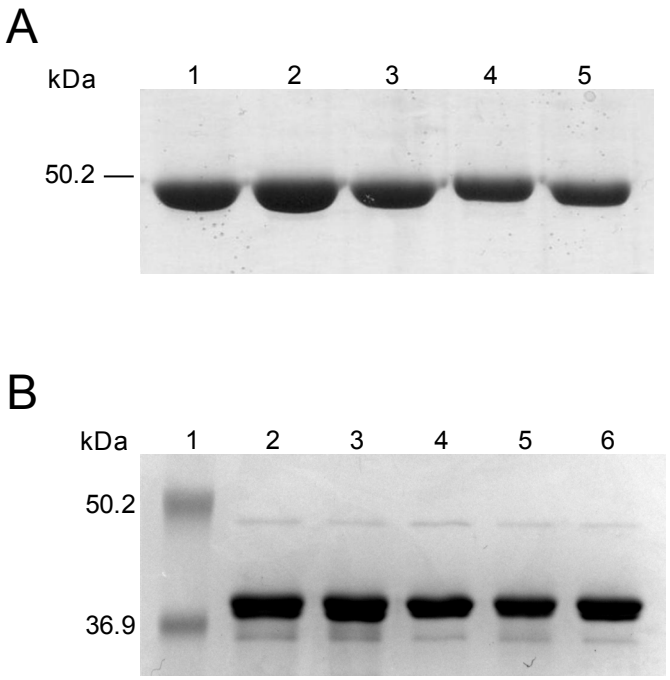

Supplementary Fig. S1. 10 % SDS-PAGE analysis of the purified recombinant hPAH proteins. (A) Full-length tetrameric WT-hPAH and respective tetrameric mutant forms. *Lane* 1, WT-hPAH; *lane* 2, Y138F-hPAH; *lane* 3, Y138A-hPAH; *lane* 4, Y138E-hPAH; *lane* 4, Y138K-hPAH. (B) Double truncated dimeric catalytic core ΔN102/ΔC24-hPAH and respective double truncated dimeric mutant forms. *Lane* 1, low-molecular-mass standard; *lane* 2, ΔN102/Δ24-hPAH; *lane* 3, ΔN102/ΔC24-hPAH-Y138F; *lane* 4, ΔN102/ΔC24-hPAH-Y138A; *lane* 5, ΔN102/ΔC24-hPAH-Y138E; *lane* 6, ΔN102/ΔC24-hPAH-Y138K.

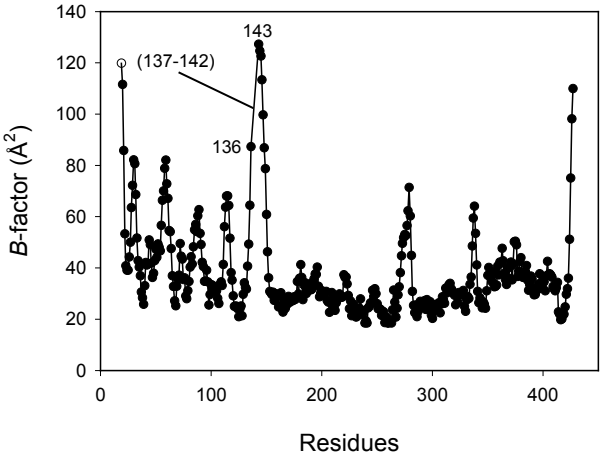

Supplementary Fig. S2. Crystallographic *B*-factor values of C_α carbons of the rPAH (PDB i.d. 1phz). No electron density was observed for the residues 137-142 in the 24-residue flexible loop structure.

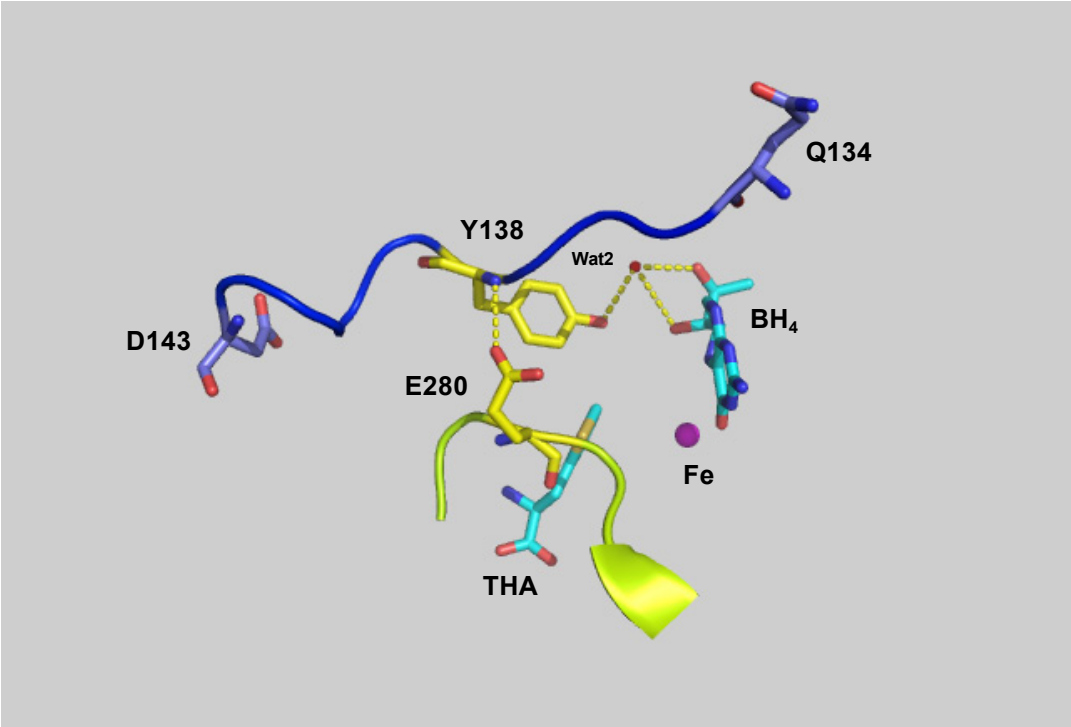

Supplementary Fig. S3. Potential stabilizing hydrogen bonds between Y138 and Wat 2 in the ternary complex hPAH-Fe(II)·BH_4·THA (PDB i.d. 1mmk) of the catalytic domain of hPAH. The C_α backbone of the loop surrounding Y138 and the loop surrounding E280 as well as the Y138 and E280 side-chains are shown in stick model. The water molecule Wat 2 and the iron are shown as red and magenta spheres, respectively. The figure was created using PyMOL version 1.1 (DeLano Scientific) [1].

Supplementary Table S1.
Oligonucleotides used for site-directed mutagenesis. Mismatch nucleotides are shown in boldface.

Primer	Sense	PAH cDNA position[a]	Sequence (5′→3′)
Y138F	Forward	628-648	CTCAGCT**T**TGGAGCGGAACTG
Y138F	Reverse	628-648	CAGTTCCGCTCCA**A**AGCTGAG
Y138A	Forward	628-648	CTCAGC**GC**TGGAGCGGAACTG
Y138A	Reverse	628-648	CAGTTCCGCTCCA**GC**GCTGAG
Y138K	Forward	622-653	CAGATTCTCAGC**A**AA**A**GGAGCGGAACTGGATGC
Y138K	Reverse	622-653	GCATCCAGTTCCGCTCC**T**TT**T**GCTGAGAATCTG
Y138E	Forward	622-653	CAGATTCTCAGC**G**A**G**GGAGCGGAACTGGATGC
Y138E	Reverse	622-653	GCATCCAGTTCCGCTCC**C**T**C**GCTGAGAATCTG

[a]Data are taken from [2].

Supplementary References

[1] W.L. Delano, The PyMOL Molecular Graphics System, DeLano Scientific, San Carlos, USA. (2002).

[2] S.C. Kwok, F.D. Ledley, A.G. DiLella, K.J. Robson, S.L. Woo, Nucleotide sequence of a full-length complementary DNA clone and amino acid sequence of human phenylalanine hydroxylase, Biochemistry 24 (1985) 556-561.

Part VI

Concluding Remarks and Perspectives

Phenylketonuria (PKU), the most common inborn error of metabolism, was one of the first genetic diseases to be explained at the metabolic level, and the first to provide a chemical explanation for mental retardation and a basis for an efficient dietary treatment (for review, see (Scriver 2007)). Since the first description of the disorder by Asbjørn Følling in the 1930s (Følling 1934), a large collection of data on the disease and the protein has been gathered, shifting the PKU paradigm from a biochemical enzyme deficiency to a protein misfolding disease with a loss of function. Thus, a large number of mutations result in a reduced folding efficiency and a reduced thermal/chemical stability of the enzyme, which leads to an increased turnover when expressed in mammalian cells (Eiken *et al.* 1996; Pey *et al.* 2007; Gersting *et al.* 2008; Martínez *et al.* 2008; Gersting *et al.* 2010; Muntau and Gersting 2010). Human PAH comprises a series of features that made it an excellent model system for studying the underlying causes and potential therapeutic tools of cytosolic misfolding diseases. It is an allosteric multimeric protein that is regulated by several mechanisms, including post-translational modifications, which may lead to functionally important conformational changes (Flatmark and Stevens 1999; Li *et al.* 2010). Human PAH has a small margin of stability *versus* chemical denaturation (Kleppe *et al.* 1999), which may explain the observed high frequency of misfolding of the mutant proteins. The large genotypic heterogeneity, together with the oligomerization equilibrium (between tetramers, dimers and higher-order oligomeric forms) of hPAH and its intrinsic property to form hybrid forms adds an additional dimension to the molecular heterogeneity that might have impact in the catalytic/regulatory properties and protein misfolding in the cell. Here, our current results contribute to elucidate specific aspects of PAH and PKU related to: (i) the phenomenon of interallelic complementation as observed in heterozygous and compound heterozygous patients when hybrid proteins are formed (heterotetramers); (ii) the misfolding of hPAH mutant forms characterized by a high tendency to self-associate (e.g. G46S), in particular the misfolding of the *R*-domain, an ACT domain module with a putative binding site for L-Phe and (iii) the role of a flexible surface/active site loop in the mechanisms of catalysis and catalytic activation of the enzyme.

Interallelic complementation (IC) in PKU was first suggested by Kaufman and collaborators (Kang *et al.* 1970; Kaufman *et al.* 1975) in parents of PKU patients (carriers), which demonstrated a lower hepatic PAH activity than expected from the average activity of the wild-type and mutant homozygous enzymes. In the following years IC has been considered as an

additional factor contributing to the high phenotypic diversity observed in PKU patients (Scriver and Waters 1999), and genotype-phenotype correlations have been difficult to predict in some compound heterozygous combinations (e.g. I65T, R158Q, R261Q, R270K, V388M, R408Q, Y414C) (Lichter-Konecki *et al.* 1994; Burgard *et al.* 1996; Kayaalp *et al.* 1997; Guldberg *et al.* 1998; Rivera *et al.* 2000). Compound heterozygous patients carrying these mutations revealed a more severe metabolic/clinical phenotype than expected from the predicted residual activity (PRA) of the homoallelic state. In these patients a negative IC phenomenon was proposed as a plausible contributing factor to the observed discrepancies, as the interactions between the different mutant protomers may result in hybrid enzymes with reduced enzymatic activity and/or stability. Although interactions between wild-type and some mutant subunits (F39L, K42I, L48S, I65T, A104D and R157N) have been shown by the yeast two-hybrid system (Waters *et al.* 2001), the enzymatic heteroallelic state was not evaluated and individual hybrid forms were not isolated.

Our studies concerning candidate mutations for negative IC in the Portuguese hyperphenylalaninemic (HPA) population (I65T, R261Q, R270K and V338M) (Part III, section 1) have revealed that combinations among them or with the WT (for the V388M mutation) showed a decrease in the enzymatic activity, when compared to the predicted values obtained in the homoallelic state (PRA). In these studies we were able to mimic the actual situation occurring in heterozygous and compound heterozygous individuals, where a mixture of hPAH homotetramers, heterotetramers and dimers is likely to exist. However, the isolation of individual hybrid proteins and the possible existence of heterodimers were still unresolved.

In studies of wild-type and truncated forms of hPAH (Part III, section 2) we were able to show that heterodimers were not formed, but only heterotetramers, if the mutant retains a WT-like C-terminal domain structure. This indicates a co-translational dimerization process, explaining why monomers have so far not been reported for WT-hPAH, and a post-translational formation of heterotetramers. This was corroborated by *in vitro* studies of pre-formed dimers of WT and a misfolding mutant G46S that self-associates *in vitro,* forming fibrils (Part IV, section 1). The presence of WT dimers resulted in an enhancement of the self-association of the G46S mutant dimers by forming WT/G46S heterotetramers that resulted in the formation of amorphous aggregates. However, the presence of L-Phe avoids this self-association, preventing a negative IC in this situation, in what might seem a paradox. This is because the tetramer $\leftrightarrow$ dimer

equilibrium of the G46S mutant does not respond to the L-Phe level, in contrast to the WT protein, and therefore the WT equilibrium is shifted towards the WT homotetramer. We also reported the first isolation of a hybrid hPAH protein, the WT/ΔN102-hPAH heterotetramer (Part III, section 2). The hybrid protein revealed kinetic and regulatory properties, as well as conformational changes that were influenced by interactions between the two homodimers within the heterotetramer, and therefore the dimers were not acting as isolated units.

Besides the restricted phenylalanine-free diet, BH_4 supplementation is currently approved for the treatment of a subset of mutations (BH_4-responsive) (Levy *et al.* 2007). The supplementation with the approved commercial form (sapropterin dihydrochloride) allows adjustments towards a less restrictive diet for these patients and in some of them the possibility of a normal diet (Blau 2010). However, a number of inconsistencies have been reported for BH_4 supplementation, where compound heterozygous patients carrying two known BH_4 responsive mutations revealed an absence or only a partial response to the cofactor (Muntau *et al.* 2002; Desviat *et al.* 2004; Erlandsen *et al.* 2004; Karačić *et al.* 2009). Negative IC was proposed as one possible explanation (Trefz *et al.* 2009), and a number of these inconsistencies in BH_4-responsive genotypes of compound heterozygous patients (e.g. I65T/R261Q, I65T/V388M) (Trefz *et al.* 2009) represent a combination of mutations where we have shown a negative IC at the level of enzymatic activity (Part III, section 1).

Nowadays, the full genotype is considered important to evaluate BH_4-responsiveness. Owing to the large number of compound heterozygous patients (~75% of the PKU patients) it will be interesting to extent these studies to determine the effect of BH_4 on hybrid assembly and stability properties, as until now these studies have been limited to homotetrameric enzymes. A mouse model for compound heterozygous BH_4-responsive mutations has been described (Lagler *et al.* 2010) and will also contribute to understand the mechanisms underlying BH_4-responsiveness in compound heterozygous patients.

Hybrid hPAH proteins should also be taken into account in the development of new therapeutic strategies, as the emerging pharmacological chaperones (Pey *et al.* 2008). They will also be important in studies on the genotype-phenotype correlations, elucidating the frequency of formation of these hybrid protein forms and their properties, with particular emphasis when one of the mutations is an aggregation-prone protein.

A large number of mutations result in the misfolding/aggregation/degradation of hPAH (Eiken *et al.* 1996; Bjørgo *et al.* 1998; Pey *et al.* 2007; Gersting *et al.* 2008). The small margin of stability of hPAH (Kleppe *et al.* 1999) is probably related to its high structural flexibility, which is of functional importance e.g. in terms of catalytic activation by its substrate (L-Phe), where large conformational changes are observed (Stokka and Flatmark 2003; Li *et al.* 2010). The high number of point mutations that lead to protein misfolding could also be related to the reduce thermal stability of the *R*-domain of the protein (an ACT module) (Thórólfsson *et al.* 2002).

Our studies on the missense mutation G46S in the *R*-domain (Part IV, section 1) have revealed a self-association which lead to the formation of large, twisted non-amyloid fibrils. The *in vitro* studies were made possible by the expression of the mutant as a maltose binding protein (MBP) fusion, which allowed its recovery in a metastable form. Removal of the MBP partner resulted in self-association of both the tetramer and the dimer, and we were thus able to study the modulation of the self-association process at a series of experimental conditions. The G46S self-association process is highly dependent on the net charge of the protein, and it could be modulated with an increased delay and/or a decrease in the level of self-association by chemical chaperones (glycerol), the proposed pharmacological chaperone 3-amino-2-benzyl-7-nitro-4-(2-quinolyl)-1,2-dihydroisoquinolin-1-one (Pey *et al.* 2007) and by the heat-shock proteins Hsp70/Hsp40 and Hsp90. As far as we know there are no reports on liver dysfunction or *in vivo* fibril formation in individuals with PKU/HPA, and although the mutant protein being a client protein for the molecular chaperone systems it is rapidly degraded when expressed in HEK293 cells (Eiken *et al.* 1996). However, the cellular mechanism by which G46S and other misfolded hPAH proteins are degraded *in vivo* remains to be further analyzed. Moreover, the experimental approach developed in this study can in the future be applied to the study of other mutant proteins, especially aggregation-prone mutations.

The *R*-domain has been implicated in the conformational instability of the hPAH protein, even when the mutations are localized in the other domains (Gersting *et al.* 2008). In the 3D structure, the *R*-domain of one subunit makes contacts with the catalytic domain of the neighbor subunit and with the active site of his own subunit, through the IARS sequence. Therefore, misfolding mutations in the catalytic domain can be transmitted to the intrinsically unstable *R*-domain. In our studies we expressed and isolated the WT *R*-domain and its G46S mutant form (residues 2-120) (Part IV, section 2), and observed that not only the mutant domain self-

associates but also the WT *R*-domain. However L-Phe inhibits in a stereospecific way the self-association of the WT, but not of the mutant G46S. These data lead us to revisit the controversial regulatory binding site for the substrate in human PAH.

The *R*-domain of PAH contains an ACT module which in other ACT domain-containing proteins is known to have a regulatory function by binding of small molecules (e.g. amino acids, pyrimidines), usually at ACT module dimer interface in proteins forming dimers or higher order oligomers (Siltberg-Liberles and Martínez 2009). In hPAH there are no contacts between the four *R*-domains in the tetrameric enzyme, and therefore the ACT module in hPAH exists as a monomeric entity. However, a second binding site (putatively at the interface between the *R*-domain and the adjacent catalytic domain) has been shown in PAHs from lower eukaryotes, e.g. in the *Caenorhabditis elegans* PAH (CePAH) tetrameric enzyme, which does not display a catalytic activation and a positive cooperativity in response to L-Phe binding (Flydal *et al.* 2010). However, all the data collected in our studies and from other groups (Flydal *et al.* 2010; Li *et al.* 2011 for latest developments), seem to support the conclusion that the *R*-domain of full-length hPAH has lost the regulatory binding site with the evolutionary emergence of the regulatory properties (activation and cooperativity), due to conformational changes in the *R*-domain and/or a steric hindrance due to interdomain interactions (Flydal *et al.* 2010). Nevertheless, the isolated *R*-domain of hPAH is able to bind L-Phe, and in our studies this binding has a stabilizing effect. Therefore, the gain of regulatory properties and the loss of ability to bind L-Phe may explain the low stability of the *R*-domain in the full-length WT human PAH. The function played by the ACT domain in the hPAH regulation, conformational changes upon L-Phe triggered catalytic activation at the active site and protein misfolding is an area that should deserve more attention in the following years.

PAH has been shown to undergo large conformational changes during the catalytic cycle, and catalytic activation by L-Phe binding is one of the main regulatory mechanisms in this enzyme (Flatmark and Stevens 1999). Binding of L-Phe at the active site triggers reversible molecular motions that are transmitted from this "epicenter" to the entire protein, resulting in an activation of the enzyme and a positive cooperativity of substrate binding to the tetrameric form (Bjørgo *et al.* 2001; Flatmark *et al.* 2001; Stokka and Flatmark 2003; Stokka *et al.* 2004). The lack of a full-length crystal structure has precluded a structural explanation of the activation mechanism, but the structures of a truncated form, representing the catalytically active *C*-domain, have

highlighted the conformational changes in the catalytic domain associated with substrate binding (Andersen *et al.* 2002; Andersen *et al.* 2003). Thus, the crystal structures of the substrate-free and the ternary enzyme-substrate complex have provided "snapshots" of the enzyme during the catalytic cycle. The largest molecular motion observed was a relocation of a flexible surface/active site loop, containing Tyr138 (large Cα displacement) to a partially buried position at the active site upon substrate binding. Our comparative steady-state kinetic analyses (Part V, section 1) of the truncated (*C*-domain) and full-length Y138X mutant forms support the conclusion that this conformational change and relocation of Tyr138 is representative also for the full-length enzyme, and that it participates in the positioning of substrates for catalysis. Our studies also revealed an additional role of the Tyr138 loop in the conformational isomerization of the full-length enzyme that lead to catalytic activation upon L-Phe binding. Substitution of Tyr with a small amino acid (Ala) at residue 138 may allow an easier access of this residue to the active site and thus promoting the conformational isomerization as measured by surface plasmon resonance, but it has a negative impact on catalysis. Our studies and those of other groups (Andersen *et al.* 2003; Stokka and Flatmark 2003; Thórólfsson *et al.* 2003; Stokka *et al.* 2004; Li *et al.* 2010) point to a mechanism for the catalytic activation which involves local conformational changes triggered at the active site ("epicenter") upon L-Phe binding, which propagate throughout the entire protein with repositioning of the *R*- and *C*-domains. However, the protein motions which occur during the catalytic cycle are far from being solved, both in terms of 3D structure and protein motions at the backbone and residue level.

References

Andersen O. A., Flatmark T. and Hough E. (2002) Crystal structure of the ternary complex of the catalytic domain of human phenylalanine hydroxylase with tetrahydrobiopterin and 3-(2-thienyl)-L-alanine, and its implications for the mechanism of catalysis and substrate activation. *J. Mol. Biol.* 320: 1095-1108.

Andersen O. A., Stokka A. J., Flatmark T. and Hough E. (2003) 2.0 Å resolution crystal structures of the ternary complexes of human phenylalanine hydroxylase catalytic domain with tetrahydrobiopterin and 3-(2-thienyl)-L-alanine or L-norleucine: substrate specificity and molecular motions related to substrate binding. *J. Mol. Biol.* 333: 747-757.

Bjørgo E., Knappskog P. M., Martínez A., Stevens R. C. and Flatmark T. (1998) Partial characterization and three-dimensional-structural localization of eight mutations in exon 7 of the human phenylalanine hydroxylase gene associated with phenylketonuria. *Eur. J. Biochem.* 257: 1-10.

Bjørgo E., de Carvalho R. M. and Flatmark T. (2001) A comparison of kinetic and regulatory properties of the tetrameric and dimeric forms of wild-type and Thr427→Pro mutant human phenylalanine hydroxylase: contribution of the flexible hinge region Asp425-Gln429 to the tetramerization and cooperative substrate binding. *Eur. J. Biochem.* 268: 997-1005.

Blau N. (2010) Sapropterin dihydrochloride for phenylketonuria and tetrahydrobiopterin deficiency. *Expert Rev. Endocrinol. Metab.* 5: 483-494.

Burgard P., Rupp A., Konecki D. S., Trefz F. K., Schmidt H. and Lichter-Konecki U. (1996) Phenylalanine hydroxylase genotypes, predicted residual enzyme activity and phenotypic parameters of diagnosis and treatment of phenylketonuria. *Eur. J. Pediatr.* 155 Suppl 1: S11-15.

Desviat L. R., Peréz B., Belanger-Quintana A., Castro M., Aguado C., Sánchez A., García M. J., Martínez-Pardo M. and Ugarte M. (2004) Tetrahydrobiopterin responsiveness: results of the BH_4 loading test in 31 Spanish PKU patients and correlation with their genotype. *Mol. Genet. Metab.* 83: 157-162.

Eiken H. G., Knappskog P. M., Apold J. and Flatmark T. (1996) PKU mutation G46S is associated with increased aggregation and degradation of the phenylalanine hydroxylase enzyme. *Hum. Mutat.* 7: 228-238.

Erlandsen H., Pey A. L., Gámez A., Pérez B., Desviat L. R., Aguado C., Koch R., Surendran S., Tyring S., Matalon R., Scriver C. R., Ugarte M., Martínez A. and Stevens R. C. (2004) Correction of kinetic and stability defects by tetrahydrobiopterin in phenylketonuria patients with certain phenylalanine hydroxylase mutations. *Proc. Natl. Acad. Sci. U. S. A.* 101: 16903-16908.

Flatmark T. and Stevens R. C. (1999) Structural insight into the aromatic amino acid hydroxylases and their disease-related mutant forms. *Chem. Rev.* 99: 2137-2160.

Flatmark T., Stokka A. J. and Berge S. V. (2001) Use of surface plasmon resonance for real-time measurements of the global conformational transition in human phenylalanine hydroxylase in response to substrate binding and catalytic activation. *Anal. Biochem.* 294: 95-101.

Flydal M. I., Mohn T. C., Pey A. L., Siltberg-Liberles J., Teigen K. and Martínez A. (2010) Superstoichiometric binding of L-Phe to phenylalanine hydroxylase from *Caenorhabditis elegans*: evolutionary implications. *Amino Acids* (*In press*), doi:10.1007/s00726-010-0611-6.

Følling A. (1934) Über ausscheidung von phenylbrenztraubensäure in den harn als stoffwechselanomalie in verbindung mit imbezillität. *Hoppe-Seylers Z. Physiol. Chem.* 277: 169-176.

Gersting S. W., Kemter K. F., Staudigl M., Messing D. D., Danecka M. K., Lagler F. B., Sommerhoff C. P., Roscher A. A. and Muntau A. C. (2008) Loss of function in phenylketonuria is caused by impaired molecular motions and conformational instability. *Am. J. Hum. Genet.* 83: 5-17.

Gersting S. W., Lagler F. B., Eichinger A., Kemter K. F., Danecka M. K., Messing D. D., Staudigl M., Domdey K. A., Zsifkovits C., Fingerhut R., Glossmann H., Roscher A. A. and Muntau A. C. (2010) Pah^{enu1} is a mouse model for tetrahydrobiopterin-responsive phenylalanine hydroxylase deficiency and promotes analysis of the pharmacological chaperone mechanism *in vivo*. *Hum. Mol. Genet.* 19: 2039-2049.

Guldberg P., Rey F., Zschocke J., Romano V., François B., Michiels L., Ullrich K., Hoffmann G. F., Burgard P., Schmidt H., Meli C., Riva E., Dianzani I., Ponzone A., Rey J. and Güttler F. (1998) A European multicenter study of phenylalanine hydroxylase deficiency: classification of 105 mutations and a general system for genotype-based prediction of metabolic phenotype. *Am. J. Hum. Genet.* 63: 71-79.

Kang E. S., Kaufman S. and Gerald P. S. (1970) Clinical and biochemical observations of patients with atypical phenylketonuria. *Pediatrics* 45: 83-92.

Karačić I., Meili D., Sarnavka V., Heintz C., Thöny B., Ramadža D. P., Fumić K., Mardešić D., Barić I. and Blau N. (2009) Genotype-predicted tetrahydrobiopterin (BH_4)-responsiveness and molecular genetics in Croatian patients with phenylalanine hydroxylase (PAH) deficiency. *Mol. Genet. Metab.* 97: 165-171.

Kaufman S., Max E. E. and Kang E. S. (1975) Phenylalanine hydroxylase activity in liver biopsies from hyperphenylalaninemia heterozygotes: deviation from proportionality with gene dosage. *Pediatr. Res.* 9: 632-634.

Kayaalp E., Treacy E., Waters P. J., Byck S., Nowacki P. and Scriver C. R. (1997) Human phenylalanine hydroxylase mutations and hyperphenylalaninemia phenotypes: a metanalysis of genotype-phenotype correlations. *Am. J. Hum. Genet.* 61: 1309-1317.

Kleppe R., Uhlemann K., Knappskog P. M. and Haavik J. (1999) Urea-induced denaturation of human phenylalanine hydroxylase. *J. Biol. Chem.* 274: 33251-33258.

Lagler F. B., Gersting S. W., Zsifkovits C., Steinbacher A., Eichinger A., Danecka M. K., Staudigl M., Fingerhut R., Glossmann H. and Muntau A. C. (2010) New insights into tetrahydrobiopterin pharmacodynamics from $Pah^{enu1/2}$, a mouse model for compound heterozygous tetrahydrobiopterin-responsive phenylalanine hydroxylase deficiency. *Biochem. Pharmacol.* 80: 1563-1571.

Levy H. L., Milanowski A., Chakrapani A., Cleary M., Lee P., Trefz F. K., Whitley C. B., Feillet F., Feigenbaum A. S., Bebchuk J. D., Christ-Schmidt H. and Dorenbaum A. (2007) Efficacy of sapropterin dihydrochloride (tetrahydrobiopterin, 6*R*-BH_4) for reduction of phenylalanine concentration in patients with phenylketonuria: a phase III randomised placebo-controlled study. *Lancet* 370: 504-510.

Li J., Dangott L. J. and Fitzpatrick P. F. (2010) Regulation of phenylalanine hydroxylase: conformational changes upon phenylalanine binding detected by hydrogen/deuterium exchange and mass spectrometry. *Biochemistry* 49: 3327-3335.

Li J., Ilangovan U., Daubner S. C., Hinck A. P. and Fitzpatrick P. F. (2011) Direct evidence for a phenylalanine site in the regulatory domain of phenylalanine hydroxylase. *Arch. Biochem. Biophys.* 505: 250-255.

Lichter-Konecki U., Rupp A., Konecki D. S., Trefz F. K., Schmidt H. and Burgard P. (1994) Relation between phenylalanine hydroxylase genotypes and phenotypic parameters of diagnosis and treatment of hyperphenylalaninaemic disorders. German Collaborative Study of PKU. *J. Inherit. Metab. Dis.* 17: 362-365.

Martínez A., Calvo A. C., Teigen K. and Pey A. L. (2008) Rescuing proteins of low kinetic stability by chaperones and natural ligands phenylketonuria, a case study. *Prog. Mol. Biol. Transl. Sci.* 83: 89-134.

Muntau A. C., Röschinger W., Habich M., Demmelmair H., Hoffmann B., Sommerhoff C. P. and Roscher A. A. (2002) Tetrahydrobiopterin as an alternative treatment for mild phenylketonuria. *N. Engl. J. Med.* 347: 2122-2132.

Muntau A. C. and Gersting S. W. (2010) Phenylketonuria as a model for protein misfolding diseases and for the development of next generation orphan drugs for patients with inborn errors of metabolism. *J. Inherit. Metab. Dis.* 33: 649-658.

Pey A. L., Stricher F., Serrano L. and Martínez A. (2007) Predicted effects of missense mutations on native-state stability account for phenotypic outcome in phenylketonuria, a paradigm of misfolding diseases. *Am. J. Hum. Genet.* 81: 1006-1024.

Pey A. L., Ying M., Cremades N., Velazquez-Campoy A., Scherer T., Thöny B., Sancho J. and Martínez A. (2008) Identification of pharmacological chaperones as potential therapeutic agents to treat phenylketonuria. *J. Clin. Invest.* 118: 2858-2867.

Rivera I., Cabral A., Almeida M., Leandro P., Carmona C., Eusébio F., Tasso T., Vilarinho L., Martins E., Lechner M. C., de Almeida I. T., Konecki D. S. and Lichter-Konecki U. (2000) The correlation of genotype and phenotype in Portuguese hyperphenylalaninemic patients. *Mol. Genet. Metab.* 69: 195-203.

Scriver C. R. and Waters P. J. (1999) Monogenic traits are not simple: lessons from phenylketonuria. *Trends Genet.* 15: 267-272.

Scriver C. R. (2007) The *PAH* gene, phenylketonuria, and a paradigm shift. *Hum. Mutat.* 28: 831-845.

Siltberg-Liberles J. and Martínez A. (2009) Searching distant homologs of the regulatory ACT domain in phenylalanine hydroxylase. *Amino Acids* 36: 235-249.

Stokka A. J. and Flatmark T. (2003) Substrate-induced conformational transition in human phenylalanine hydroxylase as studied by surface plasmon resonance analyses: the effect of terminal deletions, substrate analogues and phosphorylation. *Biochem. J.* 369: 509-518.

Stokka A. J., Carvalho R. N., Barroso J. F. and Flatmark T. (2004) Probing the role of crystallographically defined/predicted hinge-bending regions in the substrate-induced global conformational transition and

catalytic activation of human phenylalanine hydroxylase by single-site mutagenesis. *J. Biol. Chem.* 279: 26571-26580.

Thórólfsson M., Ibarra-Molero B., Fojan P., Petersen S. B., Sanchez-Ruiz J. M. and Martínez A. (2002) L-phenylalanine binding and domain organization in human phenylalanine hydroxylase: a differential scanning calorimetry study. *Biochemistry* 41: 7573-7585.

Thórólfsson M., Teigen K. and Martínez A. (2003) Activation of phenylalanine hydroxylase: effect of substitutions at Arg68 and Cys237. *Biochemistry* 42: 3419-3428.

Trefz F. K., Scheible D., Götz H. and Frauendienst-Egger G. (2009) Significance of genotype in tetrahydrobiopterin-responsive phenylketonuria. *J. Inherit. Metab. Dis.* 32: 22-26.

Waters P. J., Scriver C. R. and Parniak M. A. (2001) Homomeric and heteromeric interactions between wild-type and mutant phenylalanine hydroxylase subunits: evaluation of two-hybrid approaches for functional analysis of mutations causing hyperphenylalaninemia. *Mol. Genet. Metab.* 73: 230-238.